GEOLOGICAL SURVEY OF CANADA
MEMOIR 433

QUATERNARY GEOLOGY OF PRINCE OF WALES ISLAND, ARCTIC CANADA

Arthur S. Dyke, Thomas F. Morris, David E.C. Green, and John England

1992

Energy, Mines and Resources Canada
Énergie, Mines et Ressources Canada

Canada

GEOLOGICAL SURVEY OF CANADA
MEMOIR 433

QUATERNARY GEOLOGY OF PRINCE OF WALES ISLAND, ARCTIC CANADA

Arthur S. Dyke, Thomas F. Morris, David E. C. Green,
and John England

1992

Available in Canada through authorized
bookstore agents and other bookstores

or by mail from

Canada Communication Group – Publishing
Ottawa, Canada K1A 0S9

and from

Geological Survey of Canada offices:

601 Booth Street
Ottawa, Canada K1A 0E8

3303-33rd Street N.W.,
Calgary, Alberta T2L 2A7

A deposit copy of this publication is also available for
reference in public libraries across Canada

Cat. No. M46-433E
ISBN 0-660-14408-5

Price subject to change without notice

Front cover description

Transition Bay drumlin field and dispersal plume in relation to older bedforms.

Back cover description

See Figure 10, page 20.

Critical Reader

D.S. Lemmen

Authors' addresses

Arthur S. Dyke
Geological Survey of Canada
601 Booth Street
Ottawa, Ontario K1A 0E8

Thomas F. Morris
Engineering and Terrain Geology Division
Ontario Geological Survey
77 Grenville Street
Toronto, Ontario M7A 1W4

David E. C. Green
Consulting Geologist
373 Mayfair Avenue
Ottawa, Ontario K1Y 0K4

John England
Department of Geography
University of Alberta
Edmonton, Alberta T6G 2H4

Original manuscript received: 1990 - 04
Final version approved for publication: 1990 - 10

Preface

This report is the third of a series of regional geological studies of the central Arctic by the senior author. The initial stimulus for research in the region, which started in 1975, was the need for information on terrain conditions along a then-proposed pipeline corridor. Maps and reports were released to the public soon after the reconnaissance phase and a series of more detailed studies were pursued to address research opportunities identified during the reconnaissance. This report results from one of these, a study carried out co-operatively with the University of Alberta.

The report describes the surficial geology of a 38 000 km^2 island in Canada's central Arctic. Mapping and description of the surficial geology are the basis for reconstructing the preglacial evolution, glacial history, and postglacial history of the area. Large landscape elements are interpreted in terms of temperature conditions at the base of the former ice sheet that covered the area. The maps and interpretations are then shown to have direct and important environmental implications and potential uses in mineral exploration.

Elkanah A. Babcock
Assistant Deputy Minister
Geological Survey of Canada

Préface

Ce rapport est le troisième d'une série d'études géologiques régionales de la région arctique centrale. Le stimulant de la recherche entreprise dans la région dès 1975 a été le besoin d'information sur l'état du terrain le long du corridor alors proposé pour l'installation d'un pipeline. Des cartes et des rapports ont été diffusés au public peu après l'étape de reconnaissance du terrain; une série d'études plus détaillées ont été entreprises pour couvrir les possibilités en matière de recherche, identifiées au cours des travaux de reconnaissance. Le présent rapport est le produit de l'une de ces études, qui a été exécutée conjointement avec l'Université de l'Alberta.

Dans ce rapport, on décrit la géologie des formations en surface d'une île de 38 000 km^2 dans la région arctique centrale. On se base sur la cartographie et sur la description de la géologie des formations en surface pour reconstruire l'évolution préglaciaire, l'histoire glaciaire et l'histoire post-glaciaire de la région. Les grands éléments topographiques sont interprétés en fonction des conditions de température à la base de l'ancien inlandsis qui recouvrait la région. On montre ensuite que les cartes et interprétations ont des implications environnementales directes et notables et pourront sans doute servir à l'exploration minérale.

Elkanah A. Babcock
Sous-ministre adjoint
Commission géologique du Canada

CONTENTS

Appendices

Tables

Illustrations

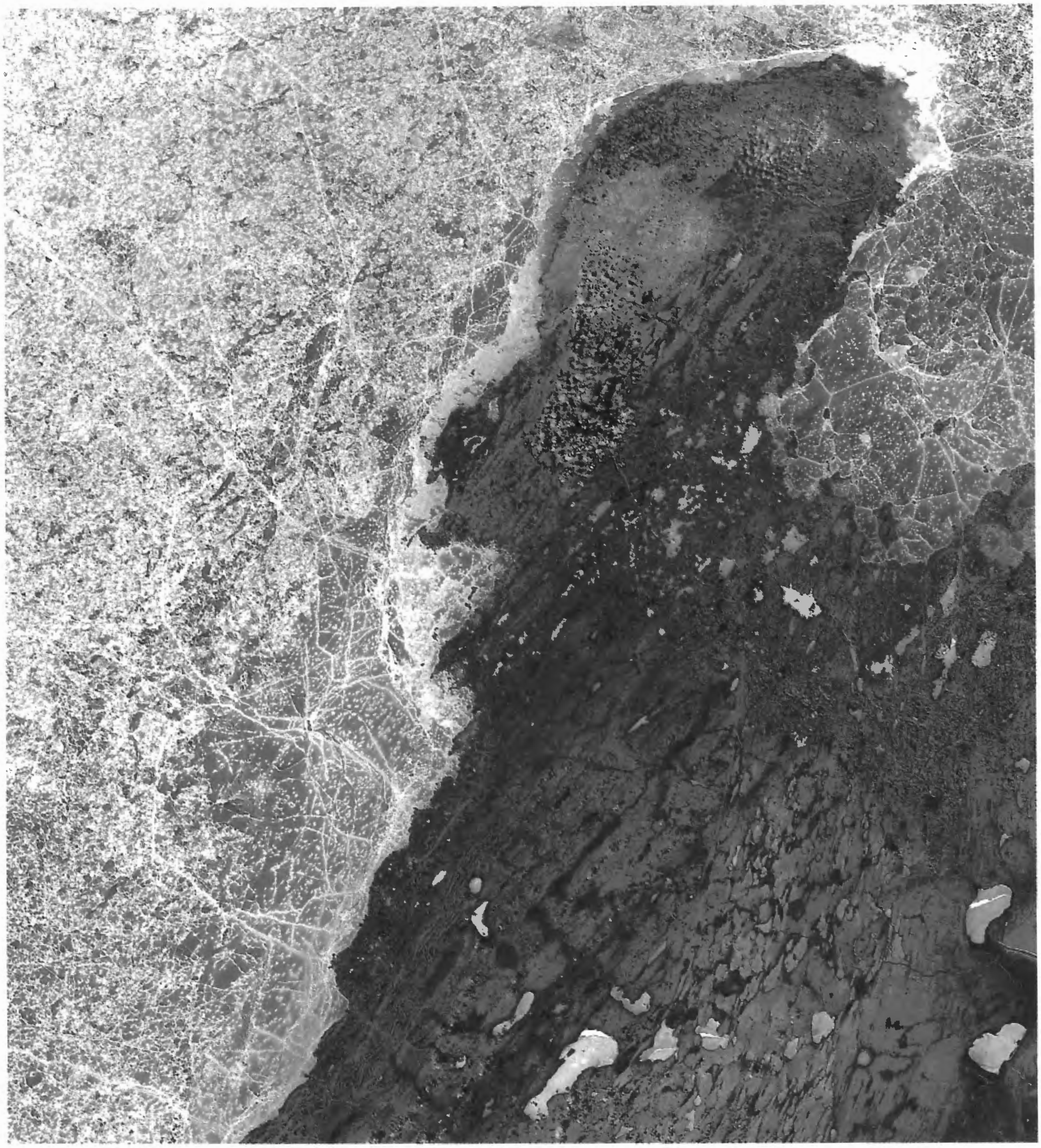

Frontispiece. Satellite image at a scale of 1:1 000 000 of western Prince of Wales Island showing megaflutes of Arrowsmith Plains crosscut in the east by the Crooked Lake drumlin field.

QUATERNARY GEOLOGY OF PRINCE OF WALES ISLAND, ARCTIC CANADA

Abstract

The large physiographic elements of Prince of Wales Island consist of several stepped planation surfaces incised by broad meandering fluvial channels that predate formation of the archipelago. Erosion surfaces likely correlate with Sverdrup Basin Mesozoic clastic fills.

Most of the island is covered by thick drift, largely till. A few subtill nonglacial deposits are likely Sangamonian. Wisconsin Glaciation left a single till sheet with three cross-cutting landscape assemblages, each recording a phase and direction of flow. Keewatin Ice flowed northwestward during phase 1 and was warm based except on the northern plateau; it formed megaflutes and a drumlin field. During phase 2, ice over phase 1 terrain was cold based but formed drumlin and ribbed moraine fields where warm based and a lateral shear moraine along the boundary, parallel to flow, between warm- and cold-based ice. During phase 3, the cold-based zone further encompassed phase 2 terrain and flow rotated suddenly by 90° and more because of capture of ice over the island by an ice stream in Gulf of Boothia. Where warm based, phase 3 and later ice formed drumlins and flutings under convergent flow across lower terrain; it formed ribbed moraine at the boundary of warm- and cold-based ice at the head of a drumlin field, where flow was normal to the boundary. Phase 3 flow was beheaded before 11 ka, when the oldest end moraines were forming.

The island occupies part of the tail of a zone of dispersion of shield debris, >700 km from source, perhaps resulting from phases 1 and 2. During phase 3, debris was dispersed >120 km eastward from the island, most strongly in plumes representing ice streams. Till granule lithology best indicates dispersion.

Postglacial sediments are mainly raised beaches with minor deltaic and alluvial sediment. Wetlands cap most fine glaciomarine and lacustrine deposits.

A range of environmental concerns can be addressed using the surficial geology, which also provides a basis for planning mineral exploration.

Résumé

Les grands éléments physiographiques de l'île du Prince-de-Galles se composent de plusieurs surfaces d'aplanissement étagées et entaillées par de vastes lits fluviaux à méandres qui se sont formés avant l'archipel. Il est probable que les surfaces d'érosion se laissent corréler avec les matériaux de remplissage clastiques d'âge mésozoïque du bassin de Sverdrup.

En majorité, l'île est recouverte par d'épais dépôts de drift, largements composés de till. Quelques dépôts non glaciaires sous-jacents au till sont probablement d'âge sangamonien. La glaciation Wisconsinienne a déposé une seule nappe de till avec trois assemblages topographiques qui se recoupent entre eux, et témoignent chacun d'une phase et d'une direction d'écoulement. Les glaces du Keewatin se sont écoulées vers le nord-ouest durant la phase 1 et avaient une base chaude, à l'exception du plateau septentrional; elles ont formé des mégacannelures et un champ de drumlins. Durant la phase 2, les glaces recouvrant le terrain de la phase 1 avaient une base froide, mais ont formé des champs de drumlins et de moraines côtelées là où elles avaient une base chaude, et une moraine de cisaillement latérale le long de la limite, parallèle à l'écoulement, entre les glaces à base chaude et celles à base froide. Durant la phase 3, la zone de glaces à base froide a englobé une plus grande partie du terrain de la phase 2 et l'écoulement y a soudainement subi une rotation de 90° et davantage en raison de la capture des glaces traversant l'île par une langue glaciaire qui circulait dans le golfe de Boothia. Là où elles avaient une base froide, les glaces de la phase 3 et des phases ultérieures ont donné naissance à des drumlins et à des cannelures au-dessous de l'écoulement convergent traversant les terrains bas; elles ont formé des moraines côtelées à la limite entre les glaces à base chaude et les glaces à base froide tout à fait en amont d'un champ de drumlins, où l'écoulement était perpendiculaire à cette limite. L'écoulement de la phase 3 a été interrompu il y a plus de 11 ka, au moment où se formaient les plus anciennes moraines frontales.

L'île occupe une partie de la traînée d'une zone de dispersion composée de débris du Bouclier précambrien, à plus de 700 km de la source de débris, peut-être comme conséquence des phases 1 et 2. Durant la phase 3, les débris se sont dispersés à plus 120 km vers l'est à partir de l'île, surtout suivant des traînées qui correspondent aux langues de glace. La lithologie des granules de till indique le mieux la dispersion.

Les sédiments post-glaciaires sont les constituants majeurs des plages soulevées, ils contiennent des quantités mineures de sédiments deltaïques et alluviaux. Des terres humides coiffent la plupart des sédiments glaciomarins et lacustres fins.

Divers problèmes environnementaux peuvent être abordés à partir d'une étude géologique des formations en surface, qui permettrait également de planifier l'exploration minérale.

SUMMARY

This report presents the results of field work during 1984, 1985, and 1986 and concurrent photo-geological mapping. Field work involved 25 000 km of ground and minor helicopter traverses. Hence, this mapping is the first regional Quaternary geology of the area that postdates the airphoto and airborne reconnaissance phases of investigation. Specialized aspects of the study are presented in two additional reports that deal with postglacial tectonic and sea level history (Dyke et al., 1991) and with postglacial changes in climate, sea ice extent, and ocean circulation patterns (Dyke and Morris, 1990).

The large physiographic elements predate formation of the inter-island channels and are only loosely dated and poorly understood. Current hypotheses of fluvial or tectonic origin of the inter-island channels can not be constrained or tested by data at hand but it is possible to outline appropriate tests. Prince of Wales Island has several large erosional planation surfaces at various levels and large meandering fluvial channels that cut across it. The oldest erosion surface cuts the Devonian Peel Sound Formation. The youngest predates the Beaufort Formation and may correlate with the Eureka Sound Group of Late Cretaceous and Early Tertiary age. Hence, the multiple erosion surfaces of Prince of Wales Island may, in general, correlate with the Sverdrup Basin clastic fills, which are mostly of Mesozoic age. A strong physiographic contrast between Prince of Wales and Somerset islands, both adjacent Peel Sound, may reflect a difference in tectonic history on either side of the sound.

A thick Wisconsinan drift sheet comprised dominantly of till underlies most of Prince of Wales Island except for its high eastern rim. The skimpy record of events before the last glaciation consists of pre-Wisconsinan weathered rock and colluvium on the northern plateau and a few exposures of fluvial, marine, and glacial deposits below the surface till. The

SOMMAIRE

Dans ce rapport, sont présentés les résultats des travaux de terrain entrepris en 1984, 1985 et 1986, et de la cartographie photogéologique réalisée conjointement. Les levés de terrain englobaient 25 000 km de lignes de cheminement parcourues au sol ou survolées en hélicoptère. Par conséquent, ce travail de cartographie représente la première étude géologique régionale du Quaternaire qui fasse suite aux phases préliminaires de l'étude, qui étaient l'examen de photographies aériennes et la reconnaissance aérienne du terrain. Les aspects spécialisés de cette étude sont expliqués dans deux rapports complémentaires traitant de l'évolution tectonique et des variations du niveau de la mer à l'époque post-glaciaire (Dyke et al., 1991) et aussi de variations post-glaciaires du climat, de l'étendue des glaces de mer et des schémas de circulation des courants océaniques (Dyke et Morris, 1990).

Les grands éléments physiographiques sont antérieurs à la formation des passages interinsulaires; ils ne sont que très approximativement datés et sont encore peu compris. Les hypothèses actuelles selon lesquelles ces passages interinsulaires auraient une origine fluviale ou tectonique ne peuvent être vérifiées dans certaines limites ou à partir des données accessibles, mais il est possible d'esquisser des modes adéquats de vérification. L'île du Prince-de-Galles comporte plusieurs surfaces d'aplanissement à divers niveaux et de grands chenaux fluviaux à méandres qui les traversent. La plus ancienne surface d'érosion recoupe la formation de Peel Sound d'âge dévonien. La plus récente surface d'érosion précède la formation de Beaufort et pourrait être corrélée avec le groupe d'Eureka Sound du Crétacé supérieur et du Tertiaire inférieur. Par conséquent, les multiples surfaces d'érosion de l'île du Prince-de-Galles se laissent en général corréler avec les matériaux de remplissage clastiques du bassin de Sverdrup qui datent surtout du Mésozoïque. Un contraste physiographique prononcé entre l'île du Prince-de-Galles et l'île Somerset, toutes deux jouxtant le détroit de Peel, traduit peut-être une différence d'évolution tectonique de part et d'autre du détroit.

Une épaisse nappe de drift wisconsinien, surtout composée de till, constitue la majeure partie de la subsurface de l'île du Prince-de-Galles, sauf sur la bordure orientale élevée de l'île. Les rares témoins des épisodes survenus avant l'ultime glaciation sont des roches altérées et des colluvions préwisconsiniennes sur le plateau septentrional et quelques affleurements de sédiments fluviatiles, marins et glaciaires au-dessous du till superficiel.

single exposure of older till indicates glaciation by northward flowing Laurentide ice, presumably during Illinoian isotopic stage 6. Known subtill nonglacial deposits are assigned to the Sangamonian, when the emergent island had a climate similar to present. Wisconsinan englaciation is recorded by subtill, ice-proximal, glaciomarine sediments that are uranium-series dated to the isotopic stage 5/4 transition at 80 ka.

A single till sheet represents Wisconsin Glaciation. Morphological facies of the till form three cross-cutting morphostratigraphic assemblages. Each widespread morphostratigraphic unit records a different phase and direction of ice flow. Phases 1, 2, and 3 predate several later phases of ice flow during deglaciation.

During phase 1, Keewatin Ice flowed northwestward across the entire island with a nearly straight flowline and apparently was warm based everywhere except on parts of the northern plateau. It left a field of megaflutes and a drumlin field on the western part of the island. The megaflutes, conspicuous on satellite imagery but not on airphotos, are about 20 km long; the drumlins appear superimposed on the megaflutes in the same direction.

During phase 2, Keewatin Ice remained cold based over the northern plateau and became cold based over the western part of the island, thus preserving the landforms created there during phase 1. Over the rest of the island, the ice had a markedly curved flowline, which swept from 350° to 300° downflow. The large Crooked Lake drumlin field which records this phase of flow grades downice into the equally large Ommanney Bay ribbed moraine field. The change from longitudinal to transverse bedforms along phase 2 flowlines indicates a change in flow dynamics, possibly from extending to compressive flow. The contact between landforms of phases 2 and 1 parallels phase 2 flowlines for a distance of 130 km and is represented by a single, continuous, streamlined ridge of till along much of its length. This ridge formed along the zone of shear between cold- and warm-based ice and is referred to as a lateral shear moraine. The change in basal ice temperature between phases 1 and 2 may have been caused by thinning of the ice sheet or by decreasing air temperature at the ice sheet surface, either of which would have resulted in downward migration of the 0°C isotherm from the glacier sole into the bed. The westward curvature of phase 2 flowlines may reflect increased sensitivity to subglacial topography after thinning or rotation of flow toward the cold-based, non-sliding ice on the west. Thus, the changes in flowline configuration and in basal thermal regime between phases 1 and 2 either may have a common cause or the one may have triggered the other. The change appears to have been sudden, for no intermediate flows disturbed the phase 1 terrain.

L'unique affleurement de till plus ancien indique une glaciation due au passage des glaces laurentidiennes dirigées vers le nord, sans doute pendant la phase isotopique 6 de l'Illinoien. Les dépôts non glaciaires connus qui reposent sous le till sont attribués au Sangamonien, période durant laquelle l'île émergente avait un climat semblable au climat actuel. L'englacement wisconsinien est indiqué par des sédiments sous-jacents au till, des sédiments glaciaires proximaux et des sédiments glaciomarins qui ont été datés, par la méthode des séries de l'uranium, de la transition entre les phases isotopiques 5 et 4, soit 80 ka.

La glaciation wisconsinienne est représentée par une seule nappe de till. Les faciès morphologiques du till forment trois assemblages morphostratigraphiques qui se recoupent entre eux. Chaque unité morphostratigraphique étendue témoigne d'une phase et d'une direction d'écoulement glaciaire différentes. Les phases 1, 2 et 3 sont antérieures à plusieurs phases tardives de l'écoulement des glaces survenu au cours de la déglaciation.

Durant la phase 1, les glaces du Keewatin se sont écoulées vers le nord-ouest en traversant tout l'île selon un trajet d'écoulement presque linéaire, et apparemment avaient une base chaude partout sauf sur des portions du plateau septentrional. Elles ont formé dans la portion occidentale de l'île un champ de mégacannelures et un champ de drumlins. Les mégacannelures sont visibles sur l'imagerie satellitaire mais ne le sont pas sur les photographies aériennes, elles ont environ 20 km de long; les drumlins sont apparemment surimposés aux mégacannelures suivant la même direction.

Durant la phase 2, les glaces du Keewatin ont continué à former un glacier à base froide sur le plateau septentrional et ont constitué un glacier de ce type dans la partie occidentale de l'île, conservant ainsi les formes topographiques apparues durant la phase 1. Dans le reste de l'île, les glaces avaient une trajet d'écoulement nettement courbe, qui passait de 350° à 300° en aval. Le vaste champ de drumlins de Crooked Lake qui témoigne de cette phase d'écoulement passe graduellement en aval des glaces au champ de moraines côtelées tout aussi vaste. Le passage d'une configuration longitudinale à une configuration transversale du lit glaciaire selon les lignes d'écoulement caractérisant la phase 2, indique une variation de la dynamique de l'écoulement, peut-être due à l'apparition d'un écoulement compressif. Le contact entre les formes de relief typiques des phases 1 et 2 est parallèle aux lignes d'écoulement typiques de la phase 2 sur une distance de 130 km et est représenté par une seule crête profilée et continue de till, sur une grande partie de sa longueur. Cette crête s'est formée le long de la zone de cisaillement entre les glaces à base froide et les glaces à base chaude, et est considérée comme une moraine de cisaillement latérale. Les variations de la température basale des glaces entre les phases 1 et 2 ont peut-être pour origine l'amincissement de l'inlandsis ou la réduction de la température atmosphérique à la surface de l'inlandsis, phénomènes qui l'un ou l'autre ont sans doute causé une migration descendante de l'isotherme de 0° C, de la semelle du glacier jusque dans le lit du glacier. La courbure vers l'ouest des lignes d'écoulement de la phase 2 reflète peut-être une sensibilité accrue à la topographie subglaciaire après l'amincissement des glaces ou la rotation de l'écoulement glaciaire en direction des glaces à base froide, stationnaires, situées à l'ouest. Ainsi, les variations de configuration des lignes d'écoulement et les variations du régime thermique de la phase 1 à la phase 2 ont une cause commune, à moins que les unes aient généré les autres. Il semble que ces variations aient été soudaines, car aucune coulée intermédiaire n'a perturbé le terrain de la phase 1.

During phase 3, the expansion eastward of cold-based ice, not only preserved the phase 2 drumlin and ribbed moraine fields but continued to preserve the phase 1 terrains. Ice flow switched to an eastward direction and remoulded the till sheet over eastern and northern Prince of Wales Island. Drumlins and flutings formed mostly in low areas of convergent flow. Ribbed moraine formed in the contact zone between warm- and cold-based ice at the head of a drumlin field, possibly because of infolding of debris caused by alternate basal sticking and sliding.

The change from phase 2 to 3 is thought to have been sudden because no intervening flows disturbed the phase 2 terrains. Between phases 2 and 3, the position of the island relative to major ice divides changed markedly; during phases 1 and 2, the island lay beneath flowlines extending from a divide far to the south, likely over Keewatin; during phase 3, it lay beneath flowlines extending from a divide over adjacent M'Clintock Channel to the west. A low rate of basal flow in a broad zone adjacent to a divide thus succeeded faster flow from a more distant ice divide. The lower basal flow rate over Prince of Wales Island during phase 3 probably produced less strain heating in basal ice and led to expansion of the zone of cold-based ice, thus halting basal sliding.

Later shifts in the boundary between cold- and warm-based ice during various, short-lived flow phases of local deglaciation can be traced by mapping areas of remoulded and nonremoulded till that can be related to various ice marginal positions. The distribution of subglacial meltwater features and proglacial sediments support inferences of basal thermal conditions and indicate that, even where ice was warm based, rates of basal melting were low. Most subglacial meltwater features formed during phase 3 and later. None are associated with the megaflutes and large drumlins of phases 1 and 2.

The island has a complex permafrost history because glaciations juxtaposed warm- and cold-based ice across broad areas and because changing flow dynamics caused boundaries between the two to shift. Permafrost likely ranges in age from Illinoian or older to Holocene. Much of the permafrost on Prince of Wales Lowland probably formed subglacially during the Wisconsinan.

The island lies in the tail of a very large zone of dispersion of debris from the Precambrian Shield to the south and of debris from Peel Sound Formation to the south and east. These dispersions, which exceed 700 km, can be explained by ice flow phases 1 and 2. During phase 3, large volumes of debris were dispersed eastward >120 km from carbonate rocks of Prince of Wales Island

Pendant la phase 3, l'expansion vers l'est des glaces à base froide a non seulement contribué à conserver les champs de drumlins de la phase 2 et les champs de moraines côtelées, mais a aussi continué à conserver les terrains de la phase 1. L'écoulement des glaces a pris une direction est et a remanié la nappe de till dans l'est et dans le nord de l'île du Prince-de-Galles. Des drumlins et des cannelures se sont principalement formés dans les régions basses où l'écoulement est convergent. Des moraines côtelées se sont déposées dans la zone de contact entre les glaces à base chaude et les glaces à base froide, tout à fait en amont du champ de drumlins, peut-être en raison de l'involution des débris due à l'alternance des processus d'adhérence et de glissement à la base des glaces.

Le passage de la phase 2 à la phase 3 a sans doute été soudain, puisque pendant cette période aucun écoulement n'a eu lieu qui ait perturbé les terrains de la phase 2. Entre les phases 2 et 3, la position de l'île par rapport aux grandes lignes de partage glaciaire a fortement varié; pendant les phases 1 et 2, l'île se trouvait au-dessous de lignes d'écoulement ayant pour origine une ligne de partage glaciaire située loin au sud, probablement au-dessus des glaces du Keewatin; pendant la phase 3, elle se trouvait au-dessous de lignes d'écoulement ayant pour origine une ligne de partage glaciaire située dans le détroit de M'Clintock adjacent, à l'ouest. Une faible vitesse d'écoulement basal dans une vaste zone adjacente à une ligne de partage glaciaire a donc succédé à un écoulement plus rapide issu d'une ligne de partage plus distante. La plus faible vitesse d'écoulement dans l'île du Prince-de-Galles pendant la phase 3 a probablement réduit le réchauffement causé par les déformations dans la glace basale et a permis l'expansion de la zone de glaces à base froide, donc mis fin au glissement basal.

Il est possible de déceler des variations ultérieures de la limite entre les glaces à base froide et les glaces à base chaude pendant diverses phases d'écoulement de courte durée accompagnant la déglaciation locale, en cartographiant des secteurs de till remanié et de till non remanié qui peuvent être corrélés avec diverses positions de la marge glaciaire. La distribution des structures créées par les eaux de fonte sous-glaciaires et les sédiments proglaciaires semble confirmer les hypothèses relatives aux conditions thermiques basales et indique que, même lorsque les glaces avaient une base chaude, les vitesses de fonte étaient faibles au niveau basal. La plupart des structures créées par les eaux de fonte sous-glaciaires sont apparues pendant la phase 3 et ultérieurement. Aucune de ces structures n'est associée aux mégacannelures et grands drumlins des phases 1 et 2.

Le pergélisol de l'île a une histoire complexe parce que les glaciations ont juxtaposé les glaces à base chaude et les glaces à base froide sur de vastes étendues et parce que les variations de la dynamique de l'écoulement ont fait fluctuer les limites entre les deux. L'âge du pergélisol en grande partie se situe a partir de l'Illinoian ou plus âgé jusqu'à l'Holocène. Une grande partie du pergélisol des basses-terres du Prince-de-Galles s'est probablement formé dans un milieu subglaciaire au cours du Wisconsinien.

L'île se trouve dans le sillage d'une très vaste zone de dispersion de débris, du Bouclier précambrien vers le sud, et de la formation de Peel Sound vers le sud et vers l'est. Ces traînées de dispersion, qui dépassent 700 km de longueur, peuvent s'expliquer par les phases 1 et 2 d'écoulement glaciaire. Pendant la phase 3, de grands volumes de débris se sont dispersés vers l'est à plus de 120 km, des roches carbonatées de l'île du Prince-de-Galles jusqu'au golfe de as far as Gulf of Boothia. Dispersion was greatest in two plumes that represent ice streams. Debris concentrations decline nearly linearly downice in ice streams and exponentially elsewhere. Most till was derived locally; 69% of samples have >90% of debris derived locally; only 8% have <70% of debris derived locally.

Some parameters of till composition are most useful as indices of transport. Lithic composition of the granule fraction is best whereas other parameters are variously compromised by ambiguous relationships with parent materials. For example, matrix carbonate content undermeasures the proportion derived from carbonate bedrock because the rock has a variable, but typically large, component of fine detrital quartz; it overmeasures the proportion derived from sandstone because the sandstones are dolomitic. Sand and silt contents vary between lithic facies and reflect provenance and transport loosely; but large within-facies variation is not readily explained. Clay content varies significantly but cannot be related to material or process; glacial comminution of a wide range of rocks yielded similar amounts of clay.

Each of the three main phases of Wisconsinan ice flow accomplished substantial debris dispersion. Chronology of the northeastern ice sheet margin suggests that phases 1 and 2 date from the early part of Wisconsin Glaciation, beyond the range of radiocarbon dating, when a thick, grounded outlet glacier extended to the mouth of Lancaster Sound. Phase 3 likely represents a regional ice capture event that resulted from thinning and failure of the Lancaster Sound ice stream and headward propagation of the capture area, ultimately to Prince of Wales Island, resulting in a regional ice configuration such as shown by Dyke and Prest (1987c) for the interval 18-12 ka. Phase 3 flow had been beheaded by 11 ka when the oldest radiocarbon dated moraines were forming on northwestern Prince of Wales Island. Deglaciation of the island was complete shortly after 9.2 ka.

Major ice marginal deposits were laid down as end moraine belts along the northwestern, north-central, and eastern side of the island. The bulkiest moraines, on the order of 100 m thick and 10 km wide, probably consist mainly of relict glacier ice, mantled by till. Others, apparently not ice cored, include large blocks of rock, which likely indicates readvance of a cold-based marginal fringe.

Postglacial clastic sediments consist predominantly of raised beach deposits, along with minor deltaic and alluvial deposits. Net sediment transfer from land to sea during postglacial time represents about 0.8 cm of average denudation of the island, or only 0.8 mm per thousand years. This low rate results more from the low slope gradients that characterize the island than from the numerous

Boothia. La dispersion a atteint son maximum dans deux traînées qui correspondent à des langues de glace. Les concentrations de débris déclinent presque linéairement en aval des glaces dans les langues glaciaires et exponentiellement ailleurs. La plupart des tills avaient une provenance locale; 69 % des échantillons ont plus de 90 % de débris de provenance locale; seuls 8 % ont moins de 70 % de débris de provenance locale.

Quelques paramètres de la composition du till sont surtout utiles comme indices du transport sédimentaire. La composition lithique de la fraction granulaire est le meilleur indice, tandis que d'autres paramètres sont diversement biaisés par des relations ambiguës avec la roche mère. Par exemple, la teneur en carbonates de la matrice donne une mesure inférieure de la proportion de matériaux issus du substratum carbonaté, parce que la roche a une composante variable, mais typiquement importante, de quartz détritique fin; elle donne une mesure excessive de la proportion de matériaux issus des grès, les grès étant dolomitiques. Les teneurs en sable et silt peuvent varier d'un faciès lithique à un autre et reflètent assez peu la provenance et le transport des sédiments; toutefois de grandes variations à l'intérieur des faciès sont difficiles à expliquer. La teneur en argile varie de façon significative, mais ne peut être associée à un matériau ou à un processus quelconques; le broyage glaciaire d'une grande variété de roches a donné des quantités similaires d'argile.

Chacune des trois principales phases de l'écoulement des glaces wisconsiniennes a produit une dispersion substantielle des débris. La chronologie de la marge nord-est de l'inlandsis suggère que les phases 1 et 2 datent de l'époque initiale de la glaciation wisconsinienne, trop ancienne pour être datée par la méthode du radiocarbone, et pendant laquelle un épais glacier émissaire échoué s'étendait jusqu'à l'entrée du détroit de Lancaster. La phase 3 représente probablement un épisode de capture des glaces dû à l'amincissement et à l'interruption de la langue glaciaire du détroit de Lancaster, ainsi qu'à la progression en amont de la zone de capture, laquelle a fini par aboutir à l'île du Prince-de-Galles et par créer une configuration régionale des glaces telle qu'indiquée par Dyke et Prest (1987c) pour l'intervalle 18 à 12 ka. L'écoulement survenu pendant la phase 3 avait été interrompu dès 11 ka, époque à laquelle les plus anciennes moraines datées par la méthode du radiocarbone se formaient dans la partie nord-ouest de l'île du Prince-de-Galles. La déglaciation de l'île s'est achevée peu après 9,2 ka.

D'importants dépôts de marge glaciaire se sont accumulés sous forme de zones morainiques frontales sur les bords du nord-ouest, du centre nord et de l'est de l'île. Les plus grosses moraines, qui atteignaient approximativement 100 m d'épaisseur et 10 km de large, se composent sans doute principalement de glaces résiduelles de glacier, recouvertes d'un manteau de till. D'autres moraines, apparemment sans noyau de glace, comprennent de gros blocs rocheux, qui probablement indiquent une réavancée des glaces de la marge d'un glacier à base froide.

Les sédiments clastiques post-glaciaires se composent surtout de dépôts de plage soulevée, ainsi que de quelques dépôts deltaïques et alluviaux. Le transport net de sédiments des terres vers la mer pendant l'époque post-glaciaire représente environ 0,8 cm de dénudation moyenne de l'île, soit environ 0,8 mm seulement par millier d'années. Ce faible taux est davantage le résultat des faibles inclinaisons qui caractérisent les pentes de l'île que de la présence de sédiments en place, car peu de sédiments lacustres post-glaciaires se sont accumulés.

internal sediment traps, for little postglacial lacustrine sediment has accumulated. However, postglacial fluvial erosion and deposition have been extensive in areas of moderate relief where even small streams have eroded canyons into bedrock and formed fans at canyon mouths. Beaches developed extensively from erosion of till during emergence where the terrain had sufficient slope to allow a critical water depth at the shoreface. Beaches probably average only a metre in thickness and development seems to rely largely on delivery of material to the shore by sea ice push where it can be reworked by even small waves.

Wetlands, most of which form peat, cap most areas of fine marine and lacustrine sediment. Peat accumulates in basins with about 2 m of closure relief or less; deeper basins hold lakes. Although peat accumulates at moderately high rates, shallow relief of basins and susceptibility to erosion limit its thickness. Many peatlands show various stages of degeneration as ice-wedge systems degrade, seemingly triggered by local base level lowering. Numerous palsen occur in wetlands, most commonly at margins of ponds. Organic mounds at dry sites appear to result from animal activity.

Two large, active zones of wind erosion occur along Peel Sound and near M'Clintock Channel. Eroding substrates consist mostly of sandy marine sediments, stripped bare of vegetation but little deflated. Eroding winds come from the NNW, likely in winter.

A number of concerns arise from consideration of the surficial geology and possible future land uses. These range from potential conflicts between location, and hence extraction, of resources and critical winter wildlife habitat to the activity status of a wide range of geomorphological processes and seismicity, many of which are not sufficiently understood.

Future mineral exploration will likely use drift as a prospecting medium. Concentrations of base metals and uranium in till show two types of distribution. Cobalt, nickel, chromium, and iron exhibit variations in background that can be linked to provenance and transport. Copper, lead, zinc, manganese, arsenic, and uranium distributions show no consistent relationships with bedrock source; all display persistent variabilities that remain unexplained. Most samples that contain anomalously high concentrations of trace elements come from the northern plateau of Prince of Wales Island and from Russell Island.

Cependant, l'érosion fluviatile et la sédimentation post-glaciaires ont été importantes dans des régions de relief modéré où même de petits cours d'eau ont creusé des canyons dans la roche en place et formé des cônes alluviaux au débouché de ces canyons. Des plages se sont formées à grande échelle par suite de l'érosion du till durant une période d'émersion, alors que le terrain avait un gradient suffisant pour permettre une profondeur d'eau critique dans la zone infratidale. Les plages n'ont probablement qu'un mètre d'épaisseur et leur développement semble dépendre largement de l'apport de matériaux au rivage par les poussées de glace de mer, là où ces matériaux peuvent être remaniés même par de petites vagues.

Les terres humides, dans la plupart desquelles se forme de la tourbe, coiffent la majorité des secteurs contenant des sédiments marins et lacustres fins. La tourbe s'accumule dans des bassins ayant une fermeture structurale d'environ 2 m; les bassins plus profonds contiennent des lacs. Bien que la tourbe s'accumule à un rythme moyen, le faible relief des bassins et sa susceptibilité à l'érosion limitent son épaisseur. De nombreuses régions de tourbières manifestent divers stades de désagrégation à mesure que se dégradent les réseaux de coins de glace, apparemment sous l'effet d'un abaissement local du niveau de base. Il existe de nombreuses palses dans les terres humides, le plus souvent en marge des étangs. Les tertres organiques observés dans les sites secs sont sans doute le résultat des activités d'animaux fouisseurs.

Deux grandes zones actives d'érosion éolienne apparaissent dans le détroit de Peel et près du détroit de M'Clintock. Les terrains exposés à l'érosion se composent le plus souvent de sédiments marins sableux, qui sont totalement dépourvus de végétation, mais subissent peu de déflation. Les vents qui causent l'érosion viennent du nord-nord-ouest, probablement en hiver.

Un examen de la géologie des formations en surface et des utilisations possibles des terres éveillent plusieurs inquiétudes à propos des conflits qui pourraient survenir entre la situation des ressources et par conséquent leur exploitation, et également à propos d'un habitat hivernal critique pour la faune, à propos de l'activité d'une vaste gamme de processus géomorphologiques et à propos de la sismicité, détails qui en grande partie sont insuffisamment compris.

Il est probable que l'exploration minérale comprendra l'exploration du drift. Les concentrations de métaux communs et d'uranium dans le till montrent deux types de distribution. Le cobalt, le nickel, le chrome et le fer présentent des variations des valeurs de fond qui peuvent être liées à la provenance et au transport des sédiments. Les distributions du cuivre, du plomb, du zinc, du manganèse, de l'arsenic et de l'uranium ne montrent pas de relations cohérentes avec le substratum qui est la source des matériaux sédimentaires; tous ces métaux manifestent une variabilité qui reste inexpliquée. La plupart des échantillons contenant des taux anormalement élevés d'éléments traces viennent du plateau septentrional de l'île du Prince-de-Galles et de l'île Russell.

FIELD WORK AND RESPONSIBILITIES

This report on the Quaternary geology of Prince of Wales Island is the third of a series dealing with the central Arctic (Fig. 1). Field work began in 1975 and culminated in maps and reports for Somerset Island (Dyke, 1983) and Boothia Peninsula and northern Keewatin (Dyke, 1984). This report results from helicopter traversing on Prince of Wales Island during 1 week in 1975 and from ground traversing during summer field seasons in 1984, 1985, and 1986. Preliminary terrain inventory maps and a report were released after the survey of 1975 (Netterville et al., 1976a,b). Field work in 1984 was preceded by interpretation airphotos at a scale of 1:60 000 by the senior author to provide a basis for selecting field camp areas and for planning research.

Twenty-five field camps were deployed by fixed-wing aircraft out of Resolute Bay, Cornwallis Island. Each was occupied by two people for about 10 days. The crews traversed on all-terrain motor tricycles and used interpreted airphotos for navigation and plotting of samples and observations. The terrain of most of the island is highly suited to this form of field work. Traverses were as long as 120 km, and over three field seasons we traversed about 25 000 km by tricycle (Fig. 2).

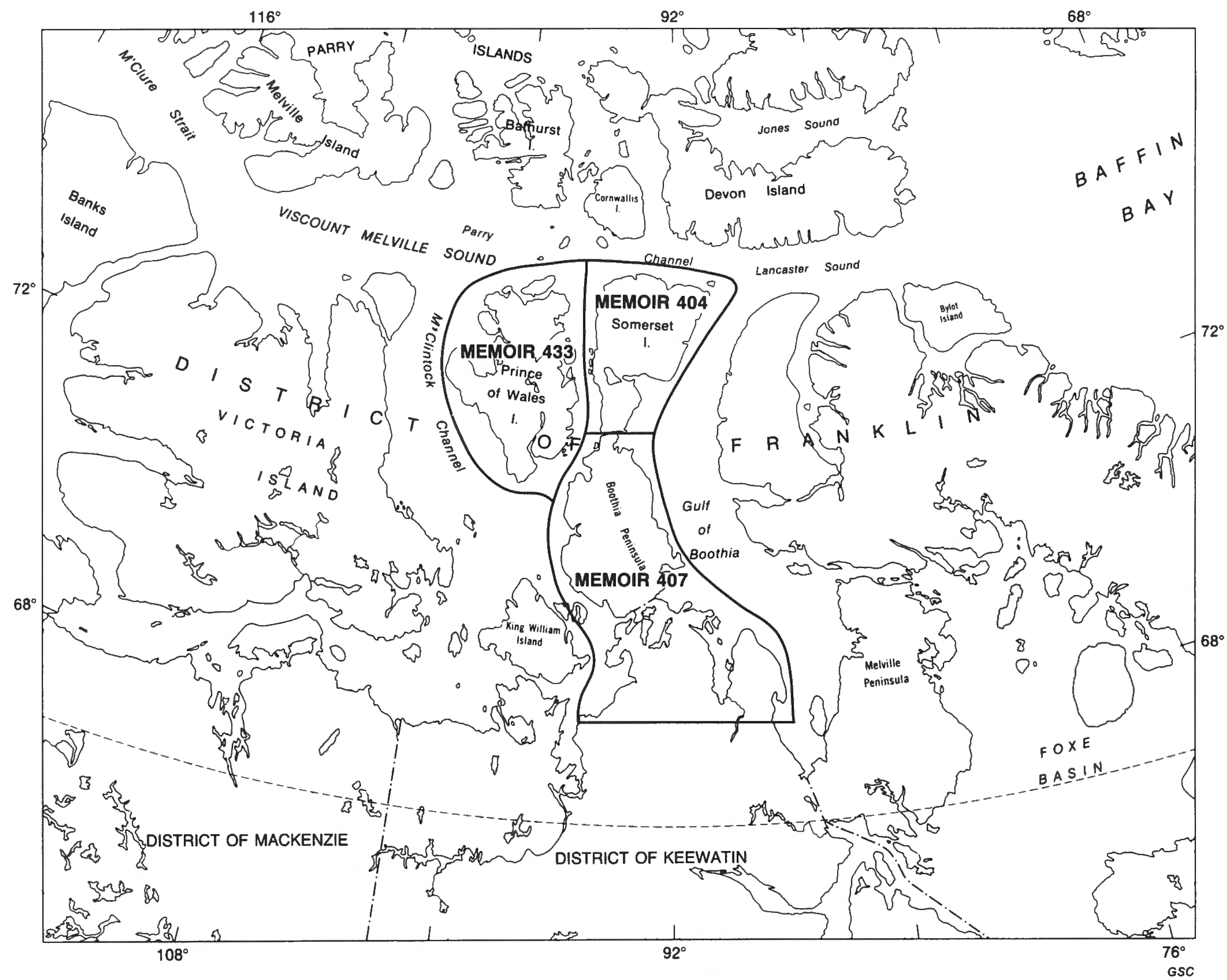

Figure 1. Location of the study area and areas covered by related reports.

Camps were located to address questions that arose during preliminary airphoto interpretation rather than to achieve uniform observation and sampling. Hence, one third of the island remains unstudied in the field. One day of helicopter traversing at the end allowed inspection of widely scattered features and sampling of materials not traversed on the ground.

The field work on Russell Island was led by Green, on southern Prince of Wales and on Pandora islands by Morris, and on western and northern Prince of Wales and on Prescott islands by Dyke. Green (1986) and Morris (1988) presented their results in a masters and a doctoral thesis, respectively, at the University of Alberta, both supervised by England. Both theses included surficial geology maps. The surficial geology maps at a scale of 1:250 000 included here were modified by Dyke during final airphoto interpretation to ensure uniform application of mapping criteria and conformity to a common legend.

PREVIOUS RESEARCH

The first map portrayals of Quaternary features on Prince of Wales Island were on the earliest versions of the Glacial Map of Canada (Prest, 1957; Falconer et al., 1958). These displayed a few northwestward oriented ice flow features on

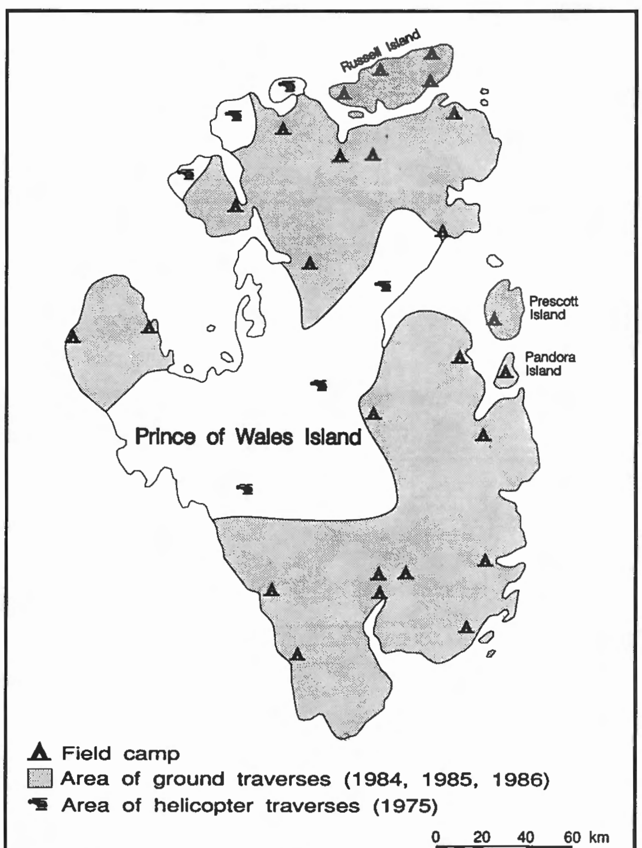

Figure 2. Camp locations and generalized ground traverses.

Prince of Wales Lowland and a few features with other orientations, apparently derived from observations from aircraft by Fortier (1948) and from description of landforms observed on newly acquired airphotos by Jenness (1952).

Jenness clearly considered that Prince of Wales Lowland had been glaciated by continental ice from the south but that the northern plateau remained "untouched by continental ice but possibly subjected to local glaciation." Prest (1957) echoed this interpretation, as did Craig and Fyles (1960). Style and age of glaciation remained unclear, however, for Bird (1959) considered that Prince of Wales and Somerset islands were glaciated but probably by an independent small ice cap. Craig and Fyles (1960), following Jenness' interpretation, placed most of the island within the limit of the Wisconsinan Laurentide Ice Sheet but placed the northeastern part within the "Ellesmere-Baffin Glacier Complex."

The first systematic mapping of Quaternary features of the island was by Craig (1964). He mapped major ice and meltwater flow features and postglacial marine limit during "Operation Prince of Wales" in 1962, a reconnaissance that also examined Somerset Island, Boothia Peninsula, and King William Island. His map was the source of information on the second Glacial Map of Canada (Prest et al., 1968), which displayed northward and eastward flow features on the island. Craig correctly interpreted the relative ages of the two major flow events, the eastward being younger. He showed that the island had been inundated by Laurentide Ice Sheet rather than by ice from local or northerly sources. He abandoned the earlier speculation of Craig and Fyles (1960) that placed the Late Wisconsinan limit of Laurentide glaciation "...between the southern lowlands with fresh glacial landforms and the northern highlands that are reported to bear only indefinite evidence of glaciation." Two radiocarbon dates on marine molluscs from adjacent Somerset Island, along with two more dates on molluscs collected by Bird (1959), one from the Transition Bay area of Prince of Wales Island, provided the first chronological control on deglaciation and were used by Prest (1969) in the first synthesis of ice retreat for North America.

Little is known of the Quaternary geology of the surrounding marine channels. Blake and Lewis (1975) illustrated three types of bottom encountered in Barrow Strait (just south of Lowther Island, Fig. 1) and at the north end of Peel Sound: bedrock, marine clay, and till-like material with an armour of stones.

More complete studies of channels in the south-central Queen Elizabeth Islands (MacLean et al., 1989) indicate that sea bed Quaternary sediments reach 100 m in thickness and typically consist of glacial drift, thought to be till, overlain by glaciomarine sediment and, in places, by postglacial marine mud. Glacial drift is the most widespread and thickest of surficial sediments; glaciomarine and postglacial sediments are localized. Sparse radiocarbon dates indicate that the drift is of Late Wisconsinan age and that deglaciation of eastern Barrow Strait occurred about 10 ka.

RELATED REPORTS FROM CURRENT RESEARCH

Two major aspects of the current research, each with a large radiocarbon data base, are subjects of separate reports. Conclusions are presented summarily in the section on "Quaternary History" but the data are not reviewed.

Much effort was devoted to dating postglacial emergence. Although sea level history is normally important in arctic Quaternary studies, in this study its importance was enhanced by early indications that postglacial crustal recovery was tectonically influenced. Consequently, we dated 130 samples of driftwood, whalebone, and shells to construct 14 emergence curves. These data are treated in detail by Dyke et al. (1991) who also synthesized sea level data from neighbouring islands and the northern mainland.

The frequency distribution of radiocarbon dates on bowhead whale bones and on driftwood from Prince of Wales and neighbouring islands reveals a four-part subdivision of sea ice and climatic conditions during postglacial time as described in another report (Dyke and Morris, 1990).

SCOPE OF THIS REPORT

In the second section we describe pre-Quaternary physiographic evolution of Prince of Wales Island in the context of the evolution of the Arctic Archipelago. Physiographic evolution of the archipelago is unresolved and poorly studied because geomorphologists have focused mostly on the record of glacial and marine events and because geological mapping is only starting in the inter-island channels (MacLean et al., 1989). Five major planation surfaces are here recognized on Prince of Wales Island along with a system of relict fluvial channels, all older than the archipelago. These erosional features are correlated tentatively with sedimentary rocks of Sverdrup Basin to the north. Two hypotheses of origin of the inter-island channels, fluvial and tectonic, are evaluated.

In the third section on surficial materials and landforms we describe surface materials in stratigraphic order, based on the first detailed mapping of the island (Maps 1689A and 1690A, in pocket). The fourth section presents data on till composition and glacial dispersion. These data are used in the next section to interpret the Quaternary history of the region. Changes in basal thermal regime of the ice sheet during Wisconsin Glaciation are linked, perhaps causally, to changes in flow dynamics and to large, sudden shifts in flow direction. These changes have led to contact relationships between cross-cutting morphostratigraphic units that have not been described from elsewhere.

The last two sections deal with applied aspects of the research. The sixth section summarizes information particularly relevant to land use concerns and recommends ways to minimize environmental impacts. The final section emphasizes till provenance in interpreting trace element concentrations in 793 samples. Field and laboratory data on till are tabulated in Appendices 1 and 2.

The rest of this introduction describes the climate, vegetation, soils, and bedrock geology of the island as they pertain to physiography, Quaternary geology, and environmental concerns.

CLIMATE AND SEA ICE

The only weather data from the island are those collected during summers by field parties such as ours. Parties have reported weather data sporadically to Polar Continental Shelf Project, Energy, Mines, and Resources Canada, where they are archived.

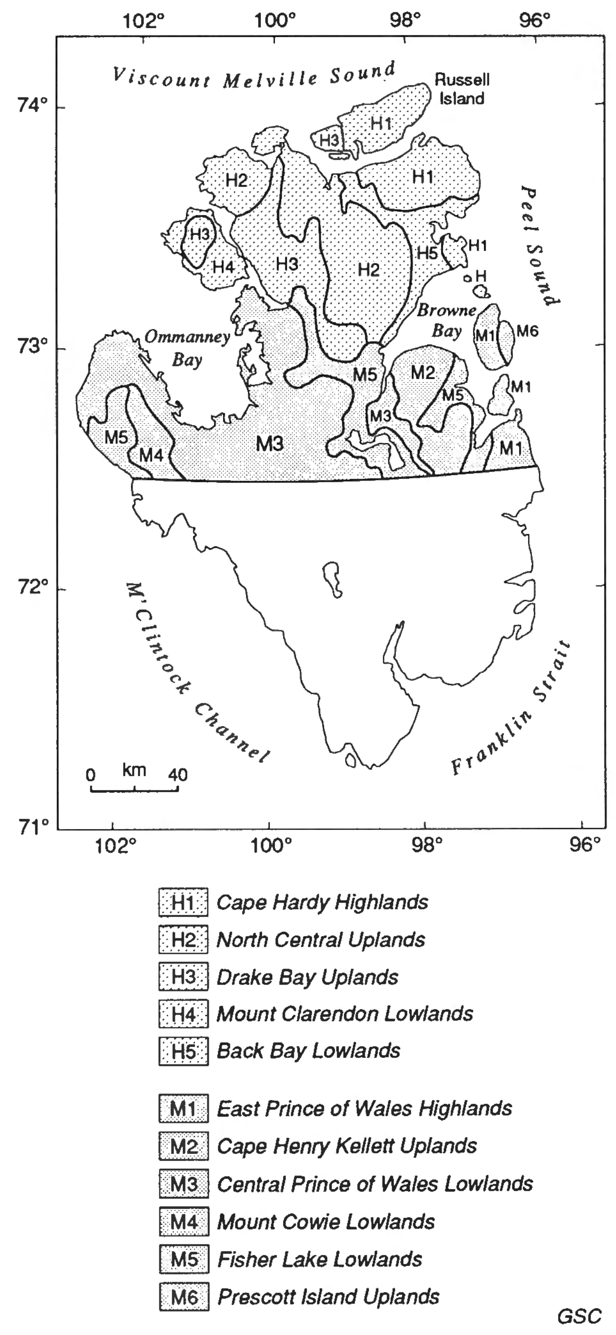

Figure 3. Ecological districts of Prince of Wales Island, after Woo and Zoltai, 1977.

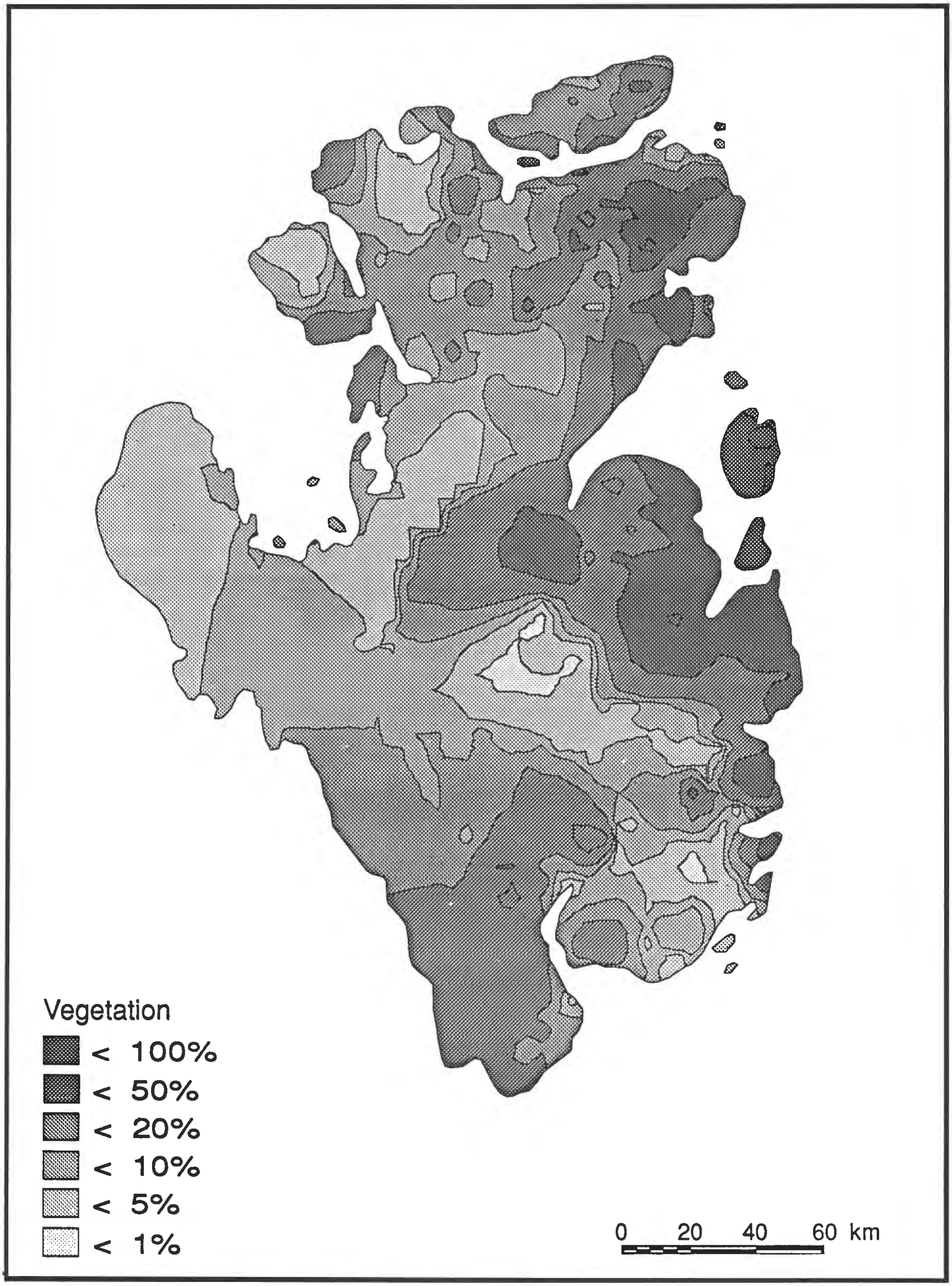

Figure 4A. Vegetation cover percentage on till, Prince of Wales Island.

Geological field work can be done effectively only in July and August of most years because nearly complete snow cover lasts till the end of June and freezeup and autumn snowfall start in late August. During our field work, weather was rarely pleasant. Temperatures rarely exceeded 5°C and mostly hovered between 3° and 0°C. High winds were the norm, more than half the summer precipitation fell as snow (usually snow pellets), and fog was a major obstacle to navigation, particularly on the northwest part of the island and on Russell Island.

Sea-ice conditions in adjacent channels are among the most severe in the Arctic. Ice drifts southward, enters the cul-de-sacs of M'Clintock Channel and Peel Sound – Franklin Strait, and piles against Victoria and King William islands and the

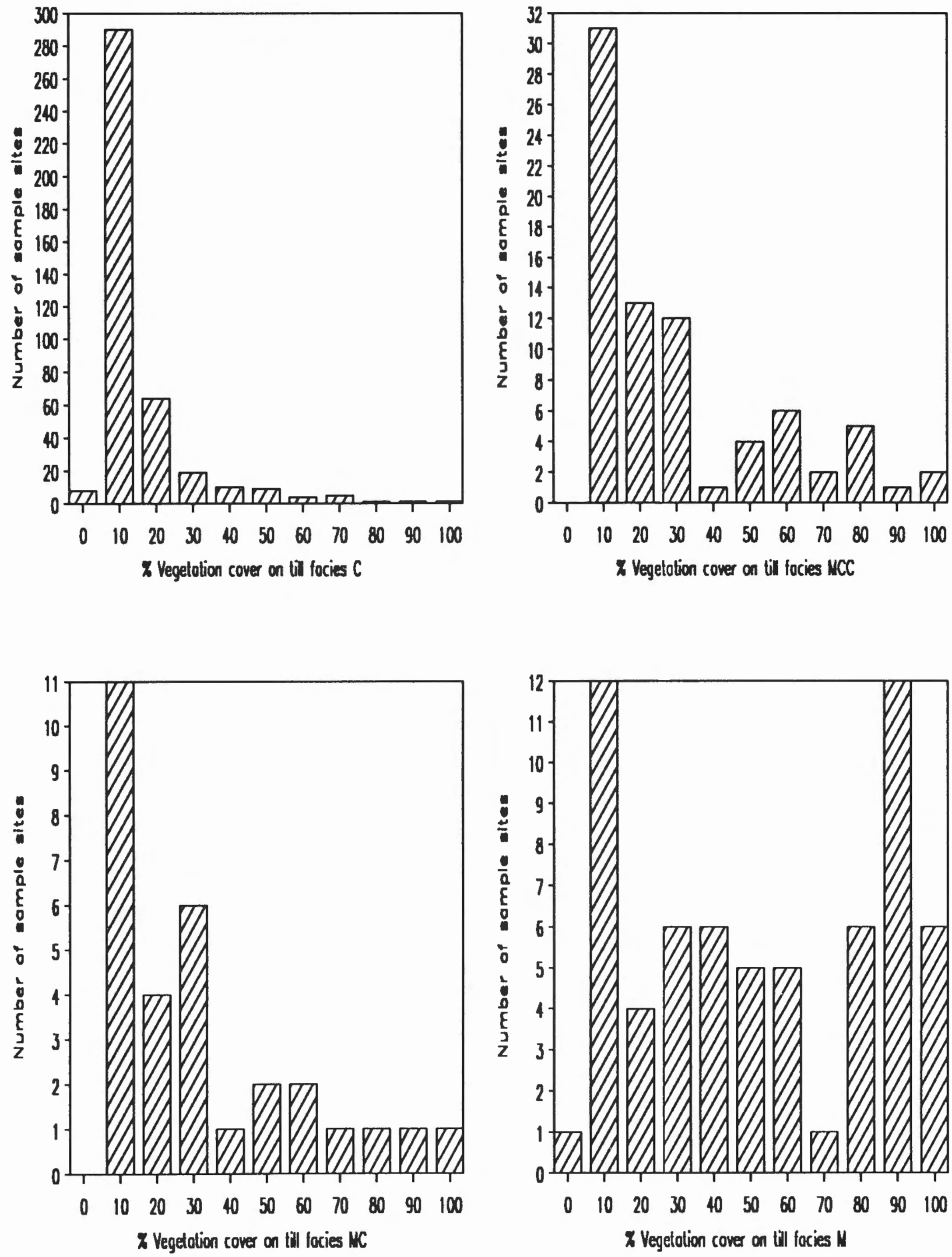

Figure 4B. Histograms of vegetation cover percentage on lithic facies of till.

mainland. Because the ice can only melt in situ, the channels rarely open under the current climate. This ice cover acts as a fundamental biological barrier, separating western from eastern arctic marine mammal populations, especially whales and walruses (Harington, 1966; Dyke and Morris, 1990). It also accounts for the failure of the nineteenth century Franklin expedition to penetrate the Northwest Passage and for the fact that Prince of Wales Island was among the last to be explored. As described by Dyke and Morris (1990), this sea ice barrier has not always been as extensive or persistent as it is today.

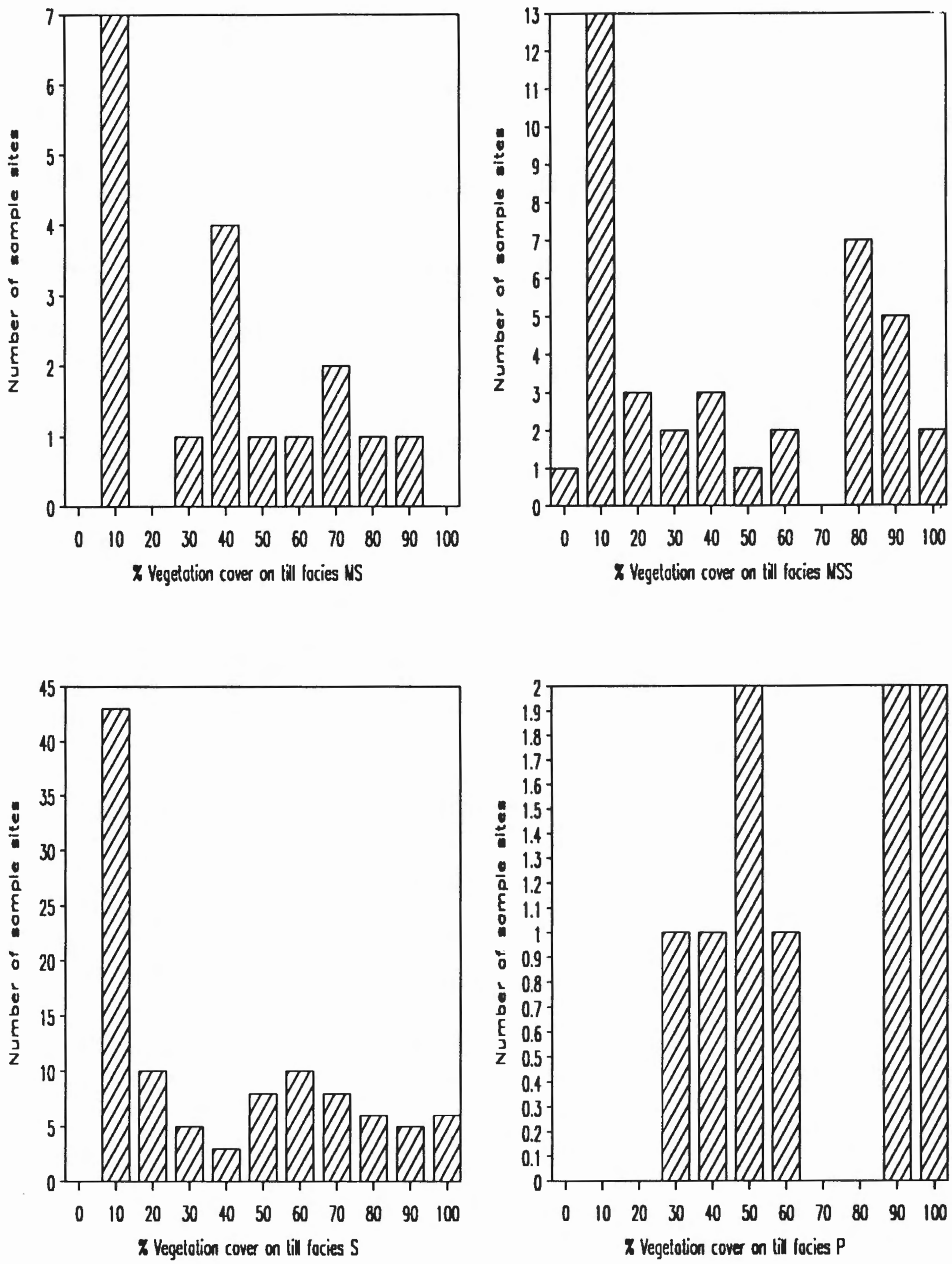

Figure 4B (cont.)

VEGETATION AND SOILS

Woo and Zoltai (1977) made the only extensive surveys of vegetation and soils of Prince of Wales Island. They divided the island into two ecological regions and each region into districts. The northern third of the island lies in the High Arctic, the rest in the Mid-Arctic region (Fig. 3). All soils are within the cryosolic order because permafrost lies within 1 m of the surface. Regosolic Turbic Cryosols occur on 50-80% of High Arctic terrains. This soil subgroup characterizes areas of polar desert vegetation, which dominates districts H1, H2, H3, and H4. Polar deserts here have 1-10% vegetation covers on calcareous till and are comprised of *Papaver-Draba* communities, typically with *Papaver lapponicum* ssp., *Draba* ssp., *Cerastium* ssp., and *Saxifraga oppositifolia*. Brunisolic Turbic Cryosols occur on 10-40% of High Arctic terrains and characterize areas where dwarf shrubs provide about 30% cover. They are most common on sandy and gravelly marine deposits of district H5 and are comprised of *Saxifraga-Draba*, *Saxifraga-Papaver*, *Saxifraga-Dryas*, *Saxifraga-Salix*, and *Salix-Dryas* communities. Gleysolic Turbic Cryosols occur on 10-60% of High Arctic terrains and characterize poorly drained areas with nearly complete covers of mosses, grasses, and sedges. They exceed 20% cover only in the poorly drained Back Bay Lowland of district H5.

The same soil subgroups occur in the Mid-Arctic region. Regosols occupy 0-60% of Mid-Arctic terrains and occur in polar desert and dwarf shrub communities that provide 5-15% ground covers. Regosols occupy 40% of districts M4 and M6 and 60% of M3. Brunisols occupy 20-70% of Mid-Arctic terrains in dwarf shrub communities that cover 30-60% of the ground. They are dominant soils of districts M1, M2, and M5 and are co-dominant in M4 and M6. Mid-Arctic dwarf shrub communities have a wider range of community types than those in the High Arctic and include *Salix-Alopacurus*, *Saxifraga-Cetraria*, *Salix-Dicranum*, and *Saxifraga-Polyblastia* communities. Gleysols occupy 20-40% of Mid-Arctic terrains and occur mostly under sedge meadows that provide nearly continuous vegetation covers on fine marine sediment in district M5.

We routinely estimated the vegetation cover percentage at till sample sites. As till covers about 70% of the island, these data are a useful extension of information provided by Woo and Zoltai. Vegetation cover ranges from nil on parts of the extremely calcareous till that characterizes most of the

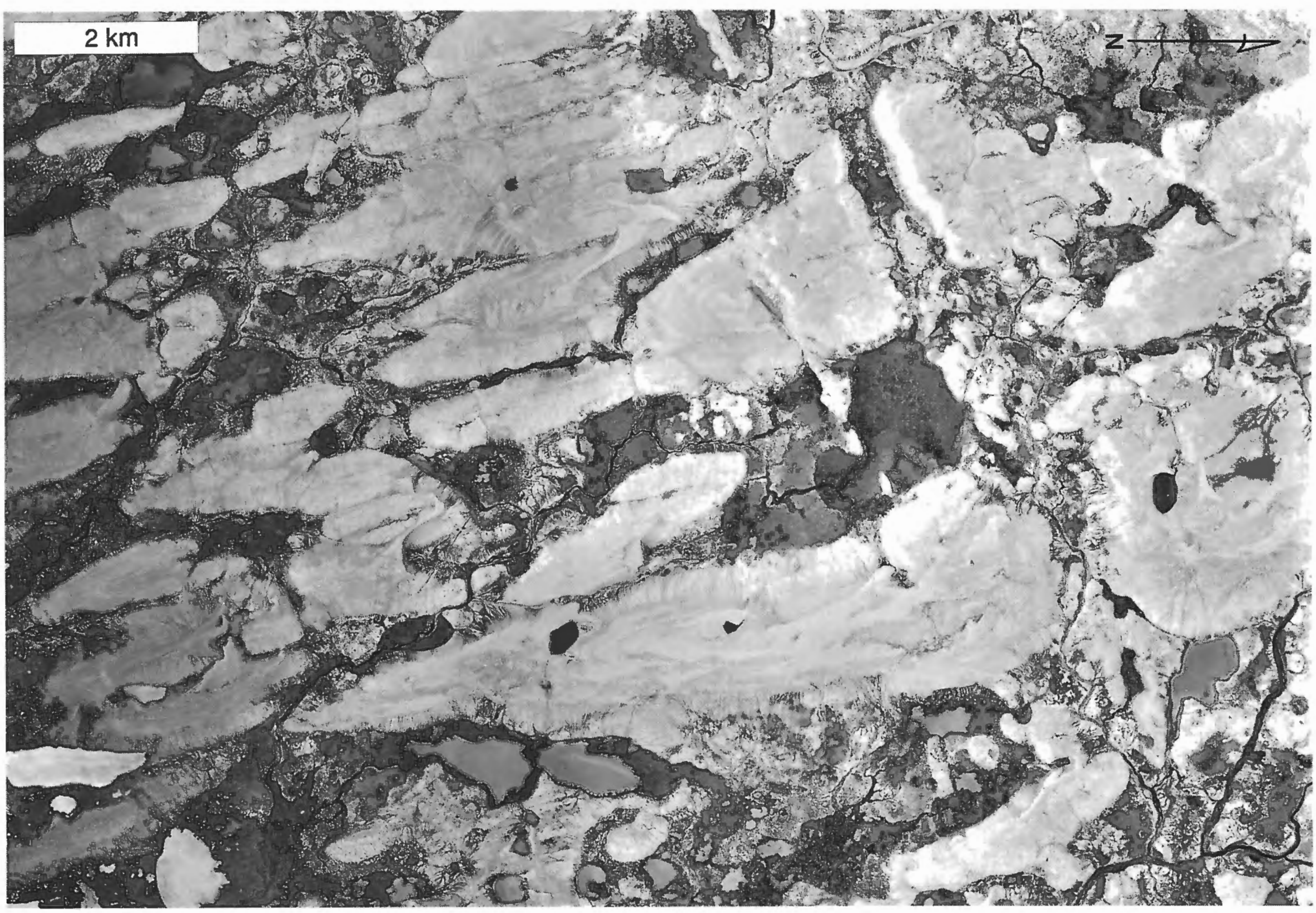

Figure 5. Contrasting vegetation covers on till and beach gravel, light toned and poorly vegetated, and on fine marine sediment, dark toned and well vegetated. NAPL A16174-161

island to as high as 100% where the till includes more acidic debris (Fig. 4A). These contrasting vegetation covers on different lithic facies of till (Fig. 4B; facies defined in Table 2 and discussed in section on *Till composition and glacial dispersion*) greatly aid airphoto interpretation and account for the spectacular appearance of the Transition Bay dispersal plume (Dyke and Morris, 1988).

Vegetation cover contrasts also aid identification of other materials on airphotos. Most fine marine deposits occupy poorly drained basins and are covered by peat-forming wet meadows; on airphotos, they contrast starkly with adjoining poorly vegetated till (Fig. 5). Even calcareous till has more plant cover than dry, gravelly, marine deposits that have been derived from it, which provides a further useful contrast. Numerous field observations confirm these relationships between material and vegetation cover. The relationship breaks down in areas of intensive wind erosion where all materials are stripped bare and mapping is more difficult.

BEDROCK GEOLOGY

The bedrock geology of Prince of Wales Island (Fig. 6A) was first mapped and described systematically during Operation Prince of Wales by Blackadar and Christie (1963) and Blackadar (1967), though its outlines were known earlier (Fortier et al.,1963). Revision mapping was provided by Christie et al. (1966), and more detailed sedimentologic and stratigraphic studies were reported by Miall (1970a,b), Mortensen (1985), and Mortensen and Jones (1986). Like other central Arctic areas, the bedrock geology here is largely a product of tectonic movement of Boothia Arch (Fig. 6B). Movements of the arch resulted in clastic sedimentation along its flanks while carbonates accumulated on more distal shelves.

The aspect of the geology that is most important to study of Quaternary sediments is the distribution of bedrock lithologies (Fig. 6A). This distribution, along with ice flow direction and rate, largely controls the composition of glacial deposits.

Precambrian metasediments and intrusive rocks outcrop in a north-south trending belt along the east coasts of southern Prince of Wales, Pandora, and Prescott islands. These rocks comprise mainly granitic gneiss, which is intensively folded and includes narrow bands of marble. They are flanked on Prescott Island by a small area of late Precambrian red quartzose sandstone of the Aston Formation.

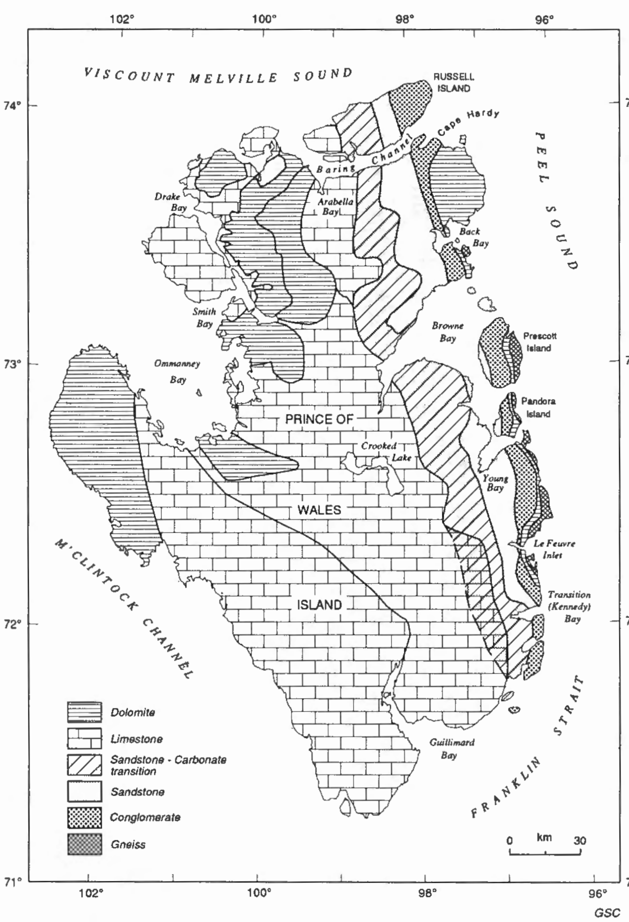

Figure 6A. Bedrock geology of Prince of Wales Island compiled from Christie et al., 1966.

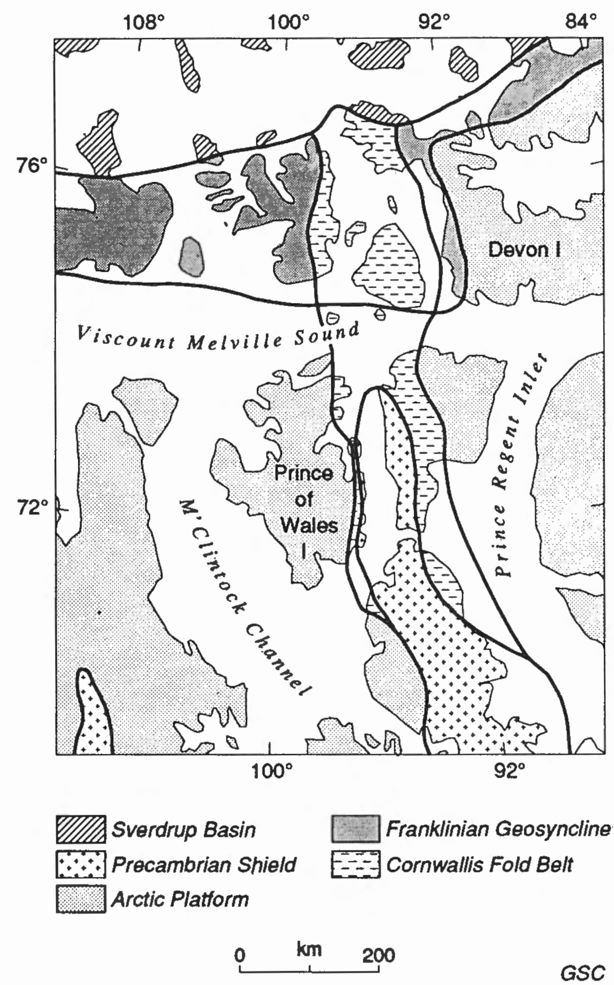

Figure 6B. Tectonic units of central Canadian Arctic.

Precambrian rocks are flanked by a band 1 km wide of steeply dipping or overturned carbonate rocks of Ordovician and Silurian age comprising the Allen Bay, Cornwallis, and Read Bay formations of Christie et al. (1966). These carbonates are less tilted north of the Precambrian rocks and cover an extensive area north of Back Bay. They are overlain to the west by clastic rocks of the Silurian-Devonian Peel Sound Formation but are exposed broadly again on the western part of the island where they are nearly flat lying.

Peel Sound Formation grades westward from conglomerate, through a conglomerate-sandstone facies, to sandstone and siltstone with carbonate interbeds, to muddy carbonates with limy mudstone beds, to more pure carbonate rocks. Miall (1970b) showed the clastic content of the carbonate rocks to be highly variable. Most rocks he examined contain silt-size quartz and have insoluble residues as high as 45%. This variable, but typically large, clastic content of carbonate rocks seriously limits the usefulness of the carbonate content of till as an index of debris source and transport (see *Till composition and glacial dispersion*).

The Paleozoic sedimentary facies have distinctive colours and other properties that facilitate Quaternary studies. Near its eastern contact with pre-Devonian carbonates, Peel Sound conglomerate contains clasts of dolomite, and some beds are grey. However, most of it has a deep red sand matrix and clasts of shield rocks. Peel Sound sandstone also is deep red. The westward transition from Peel Sound sandstone to grey carbonates occurs along a 10-km belt, wherein clastic red beds are a major component. The eastward contact between red Peel Sound rocks and older grey carbonates is more abrupt. These colour and compositional contrasts aid in assessing dispersal of debris by ice sheets. A further aid is the distinctive, well rounded clasts of various lithologies found in Peel Sound conglomerate.

The structural geology of the island is fairly simple, but interpretation is evolving. The eastern fringe has been affected by the Boothia Uplift, which was active during several major pulses starting in the late Proterozoic and extending into the Tertiary, but particularly during the Late Silurian to Early Devonian (Kerr and Christie, 1965). The uplift involves a 1000-km long basement block bounded on the west (on Prince of Wales Island) by steeply to moderately east-dipping reverse faults and on the east (e.g., on Somerset Island) by normal and reverse faults. Erosion of uplifted area exposed Proterozoic basement by stripping Cornwallis Fold Belt rocks during the Devonian.

The fold belt is exceptionally narrow on Prince of Wales Island in comparison to on Somerset Island (Fig. 6B), which indicates that the uplift had an east-west asymmetry. The uplift long was regarded as a simple basement horst that produced faults and drape folds in cover strata (Kerr and Christie, 1965; Kerr, 1977). Based on the asymmetry of clastic wedges (Peel Sound Formation) adjacent the uplift, Miall (1983) suggested that it is a deep-seated, east-dipping thrust block. Okulitch et al. (1986) further proposed that the uplift involved up to 30 km of west-directed thrusting of basement as an imbricate mass mantled by faulted and drape-folded cover. This proposal was based in part on gravity data (Berkhout, 1973) that suggest the presence of low-density sediments below basement rocks in Peel Sound.

Tertiary faulting of the uplift produced grabens on Somerset Island and Boothia Peninsula. "Some older faults of the uplift may have been reactivated at this time. Peel Sound may be a fault controlled topographic depression of Tertiary age" (Okulitch et al., 1986). The uplift is a zone of moderately high seismicity (Basham et al., 1977; Hasegawa, 1988).

PRE-QUATERNARY PHYSIOGRAPHIC EVOLUTION

INTRODUCTION

The large physiographic elements of Arctic Canada form a mosaic of erosion surfaces, expressed as upland plateaus and lowlands on the islands, separated by a maze of marine channels that are comparable in width to the islands themselves. The erosion surfaces predate formation of the inter-island channels. The channels were formed in Late Tertiary time, after deposition of Beaufort Formation sediments along the margin of the Arctic Ocean from a contiguous hinterland to the east and south. Hence, the geographic character of the northern part of the continent has evolved more recently than that of the Canadian Shield; landscapes of the archipelago are comparable in age to those of the cordillera.

The nature of this physiographic evolution of the archipelago, however, remains unsettled. In this section we review two prevalent hypotheses regarding the origin of the inter-island channels. We then define the major pre-Quaternary, rock-cut physiographic units of Prince of Wales Island and propose a tentative correlation with the stratigraphic record of Sverdrup Basin to the north.

ISLANDS AND CHANNELS

Currently there are two schools of thought regarding the physiographic origin of the Arctic Archipelago. One holds that the inter-island channels formed by fluvial erosion during the Tertiary (e.g., Fortier and Morley, 1956; Pelletier, 1966; Trettin, in press), the other, that they resulted from Tertiary tectonism (e.g., Kerr, 1980). The fluvial hypothesis of Fortier and Morley arose from their contention that the inter-island channels resemble a network of dendritic rivers draining an Arctic and an Atlantic watershed (Fig. 7A). Bird (1967) also derived an interpretation of the drainage evolution of arctic Canada that appears to have been based on the assumption that the inter-island channels are of fluvial origin (Fig. 7B). The tectonic hypothesis of Kerr (Fig. 7C) arose in part from a coincidence of faults with channel margins, notably the north side of Lancaster Sound. But Kerr's model is based mostly on the interpretation that long, straight to gently curving, parallel, coastline cliffs are fault-line scarps. Hence, both hypotheses are essentially geomorphological.

The two hypotheses are not incompatible in so far as a subaerial valley of tectonic origin would capture drainage and fluvial modification would ensue. But they have widely divergent implications regarding regional geological structure, late Tertiary sediment distribution, sea level fluctuations, crustal subsidence, and geomorphological evolution, and their implicit predictions differ.

Whatever their origin, the channels are younger than Beaufort Formation fluvial deposits of the western Arctic. Beaufort Formation is of Miocene and Pliocene age (Tozer and Thorsteinsson, 1964) and occurs mainly between Banks and Meighen islands. Its distribution is interrupted by channels that extend to the continental shelf from the interior of the archipelago. One of these, M'Clintock Channel – Viscount Melville Sound – M'Clure Strait, passes by western Prince of Wales Island.

Fluvial hypothesis

The fluvial hypothesis is favoured by many geologists (Thorsteinsson and Mayr, 1987; Ricketts, 1987; Trettin, in press). Furthermore, two geomorphological analyses often are quoted to support it (Pelletier, 1966; Bornhold et al., 1976). The hypothesis is not, however, without problems and observations that initially appear supportive are not necessarily so. Even the central argument, that the inter-island channels resemble a dendritic river network, is dubious. A set of lines forming a dendritic network can be drawn through the channels. But other patterns of subparallel lines passing roughly north-south and east-west would outline most of the channels without evoking a fluvial pattern analogy.

The hypothesis has obvious problems in terms of both morphology and scale. The inter-island channels are commonly >100 km wide and 500 m deep and have nearly constant widths and depths from end to end. Furthermore, Parry Channel joins two ocean basins, extending from Baffin Bay to Arctic Ocean. There is no analogous valley of known fluvial origin elsewhere in the world. The feature that most closely resembles it is that occupied by the Red Sea, which is clearly tectonic.

If the inter-island channels represent the valleys of rivers that carried and deposited the Beaufort sediments or if they are fluvial features entirely of post-Beaufort age, large changes of sea level must have occurred since Beaufort time (Fig. 8). The Beaufort Formation is interpreted as a coastal plain deposit (Tozer and Thorsteinsson, 1964). During its deposition, relative sea level was probably 100 m or so higher than it is today; the sediments occur some hundreds of metres above sea level on Banks Island. The channel floors in the central Arctic at that time must have been hundreds of metres higher still to provide the gradients necessary to transport the sediments. The floor of M'Clure Strait now extends >500 m below sea level. If the channel of which it is a part is mainly of fluvial origin, there must have been a post-Beaufort interval during which sea level was >500 m lower than present; this interval must have been long enough for fluvial erosion to lower the floor of the strait about 700 m.

Presumably during this interval as well, there must have been much erosion of channel reaches farther upstream, but the channels must have had gradient enough to ensure net erosion all along their lengths. This requires high elevation in what is now the central archipelago. If this hypothesis of fluvial erosion of the inter-island channels is correct, a post-Beaufort deltaic accumulation roughly equal to channel volume must have formed at the mouth of each channel. As no voluminous post-Beaufort deposits are known, the fluvial hypothesis can not be taken as proven.

Hence, the fluvial hypothesis contains a series of implicit predictions of: locations of large sediment bodies of post-Beaufort age; relative sea level oscillations of hundreds of metres since Beaufort time; and hundreds of metres of crustal subsidence of the central archipelago since erosion of the channels. These predictions indicate appropriate tests but no test has been attempted.

Bird's (1967) hypothesized drainage evolution is multi-staged (Fig. 7B). The final stage is nearly identical to the Fortier and Morley hypothesis. However, to arrive at a fluvial explanation for Parry Channel and the several other channels that join it at right angles from both north and south, he hypothesized an initial stage of north-flowing, parallel rivers. There followed a stage when a large river flowed westward along the entire length of Parry Channel. During a still later stage the eastern half of Parry Channel was captured by an east-flowing stream entering a newly formed Baffin Bay (Fig. 7B). Although conceivable, it is difficult to think of why the westward drainage of Bird's second stage would not have been captured by the already established northward draining valleys. To avoid this situation, one has to invoke a 1000-km long drainage divide nearly coincident with the north side of Parry Channel, the new river valley (Fig. 7B).

Glacial modification

Adherents of the fluvial hypothesis call on glacial deepening and widening of channels to account for their grossly oversized forms; straight, cliffed sides; and nearly constant widths. The problem with this explanation is that there is no independent evidence of glacial erosion of that magnitude. Such erosion would necessarily have resulted in deposition of comparable magnitude beyond the channels yet no Quaternary deposits of such enormous bulk have been found. Evidence of glacial erosion of small, that is "normal," scale within the channels does not support any particular hypothesis of channel origin. The appropriate test of the glacial hypothesis lies in locating the required deposits.

Channel morphology has been invoked as evidence of glacial erosion (Pelletier, 1966) but this argument is circular and based on form analogy that is not constrained by scale. Pelletier's argument that the channels are glacially modified fluvial valleys rests on the contention that they have U-shaped transverse profiles, that they have medial ridges, that end moraines occur on the continental shelf in front of them, and that some tributary valleys have cirque-shaped heads, now submerged. The argument suffers from gigantism but is constantly used to support the hypothesis that the channels are glacially modified fluvial valleys. Hence, it is worthy of scrutiny.

The U-shaped valley illustrated by Pelletier is the bed of Prince Gustaf Adolph Sea, which is 160 km wide and 400 m deep on the figured profile. The U-shaped appearance relies on diagrammatic vertical exaggeration. Normal U-shaped glacial valleys that are on the order of 400-2000 m deep, such as the fiords and valleys of eastern Baffin Island, are only a few kilometres wide.

The medial ridge illustrated by Pelletier is about 250 km long and its southern, emergent part is Lougheed Island. This ridge is orders of magnitude larger than any similar landform known to be of glacial origin.

Similarly, the postulated end moraines on the continental shelf are comparable in size to adjacent islands. Although the glacial hypothesis calls for enormous glacial deposits in this position, it is unlikely that any single glacial event formed moraines so large, for the largest moraines elsewhere in the world are many orders of magnitude smaller. If it did, the channels, by implication, formed largely during that one event and all should have giant terminal deposits.

The six drowned "cirques" adjacent the northwestern part of the archipelago have floors that are as much as 425 m below sea level and sidewalls as much as 30 km apart. One near Brock Island is larger than the island! Features identified as drowned cirques in the southeastern part are just as large; the one off Coburg Island is about twice the area of the island. If these features are cirques, they formed, presumably rapidly, during a Quaternary low stand of sea level for which there is no other evidence and no obvious cause. No cirques anywhere else approach these sizes. Cirques occur profusely in eastern Arctic

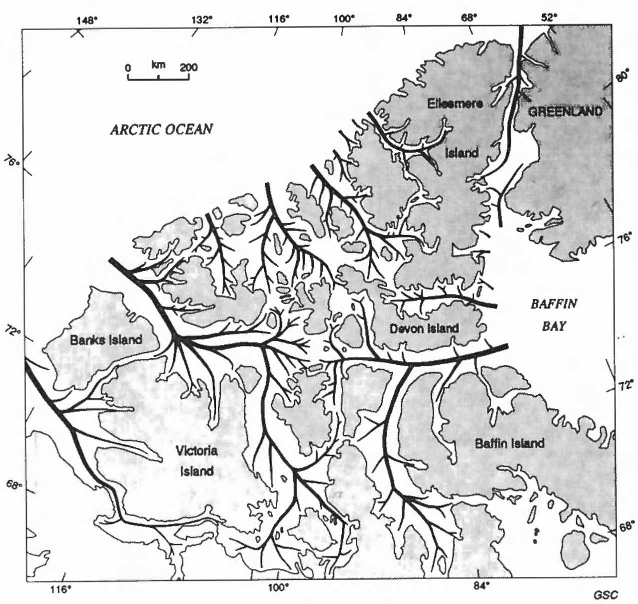

Figure 7A. Tertiary drainage system hypothesized by Fortier and Morley, 1956.

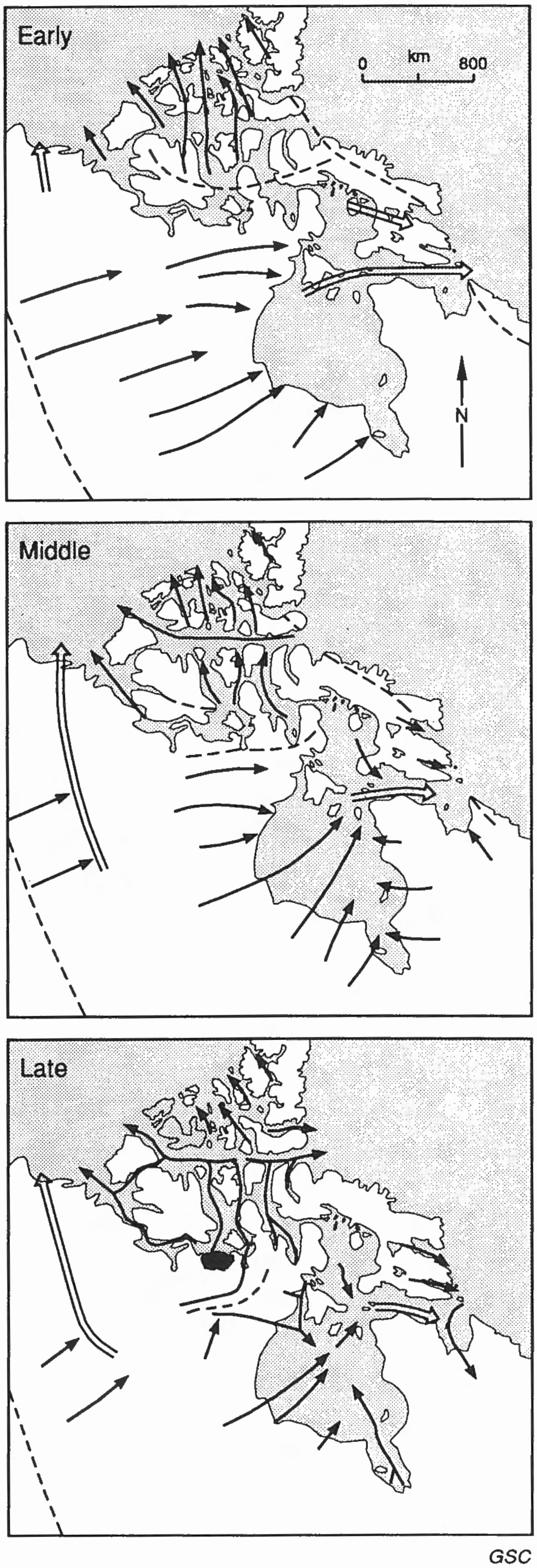

Figure 7B. Tertiary drainage evolution hypothesized by Bird, 1967: (1) early, (2) middle, and (3) late stages in the development of drainage in northern Canada.

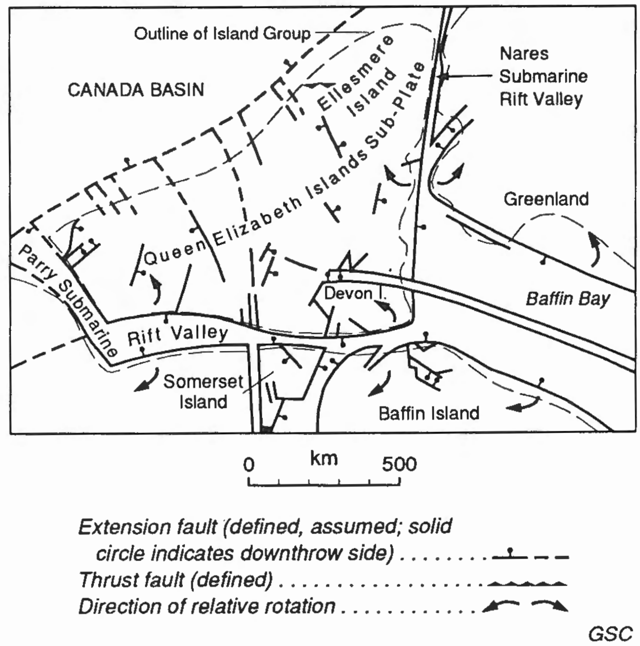

Figure 7C. Final phase of the Eurekian Deformation in Miocene or Pliocene time, the last stage in the tectonic evolution of Arctic Canada as hypothesized by Kerr, 1980.

mountains and are minuscule in comparison, yet have been occupied by glaciers, and hence evolving, throughout most of the Quaternary.

Another geomorphological study is sometimes quoted in support of the fluvial hypothesis and bears on the question of glacial modification. Bornhold et al. (1976) used detailed bathymetric surveys of the central segment of Parry Channel (Barrow Strait and vicinity) to reconstruct intricately preserved, integrated, fossil stream networks arranged into five watersheds. These drowned fluvial valleys are similar in form to canyons on Somerset Island that Dyke (1983) considered to be older than the inter-island channels. Bornhold et al. concluded that the presence of relict stream networks on the channel floors supported the Fortier and Morley hypothesis. But they can be explained just as well by a tectonic hypothesis of channel origin. More important, they indicate that the channels have suffered little lowering of their floors by Quaternary glacial erosion. At least locally, this negates glacial erosion as an explanation of the grossly oversized nature of the channels.

The fluvial hypothesis has become almost inextricably interwoven with other hypotheses regarding extent and style of Quaternary glaciation (Pelletier, 1966; England, 1987). Thus, it has had a fundamental influence on development of concepts of the nature of regional Quaternary glaciations (Blake, 1970; Sugden, 1977), which, unfortunately, has involved some circular reasoning; in some models the channels, themselves, are the primary or only evidence, not only of ice extent but of type of ice flow.

Tectonic hypothesis

Kerr's tectonic hypothesis (Fig. 7C) is similar to an earlier interpretation by Bird (1967), although Bird arrived at this congruent interpretation from a different basis. He observed the remarkable accordance of surface elevations on several islands and peninsulas of the central and eastern Arctic. This accordant surface cuts across such diverse rocks as Precambrian gneisses of Boothia Arch, steeply dipping carbonates of Cornwallis Fold Belt, and flat-lying carbonates of Lancaster Basin. Bird named this the Barrow Surface and concluded that it formed on a contiguous landmass. He postulated that the inter-island channels formed by later rifting of this landmass to produce large intersecting grabens. Unfortunately, he did not integrate this idea into his hypothesis of drainage evolution already discussed.

The tectonic hypothesis neither predicts any regional changes of relative sea level nor requires voluminous deltaic sediments of post-Beaufort age at the channel mouths. Nor does it require vast glacial modification of the inter-island channels. It does predict that faults with large vertical offsets are located near, and parallel to, channel margins. As yet field support for this hypothesis is not strong because few such faults have been mapped. Its main strength lies in the problems inherent in the alternative hypothesis.

PRINCE OF WALES ISLAND

Like the marine channels that surround it, the major physiographic elements of Prince of Wales Island formed before the Quaternary. The major elements are erosional planation surfaces at various levels and large channel-like forms. Each planation surface cuts across more than one type and age of bedrock. Hence, they are neither depositional nor structural surfaces.

The highest land occurs along the eastern side of the island where broad, flat summits reach elevations of about 400 m (Fig. 9). The highest areas comprise nine remnants of what once was likely a continuous plateau surface. These remnants are separated by bays and marine channels such as Baring Channel, Browne Bay, and Young Bay. The highest summits on the plateau remnants decrease gradually in elevation southward from 410 m south of Cape Hardy to 200 m northeast of Coningham Bay. The regularity of this decline (Fig. 9) suggests tilting since formation of the plateau. Bird (1967) included several of these plateau remnants in his Barrow Surface, which is more widely preserved on Somerset Island and Boothia Peninsula to the east. There, however, the surface is nearly level at about 400 m. The difference in elevation and gradient of Barrow Surface on either side of Peel Sound implies a difference in tectonic history.

The high eastern plateau remnants of Barrow Surface are separated from Prince of Wales Lowland by lower plateaus. The lower plateaus display three levels of summit accordance (Fig. 9). North of Browne and Ommanney bays, summits on the plateau are between 195 and 230 m. On southeastern Prince of Wales Island, summits on the lower plateaus are mostly at 165 m. Three smaller plateau blocks with summits at just over 100 m occur along the east side of Ommanney Bay, and a fourth plateau at that level occurs west of the head of Browne Bay. The lower plateaus, therefore, appear to step down in elevation from north to south and from east to west. This arrangement is more suggestive of different ages of fluvial planation than of tectonic tilting or offset of a single erosion surface.

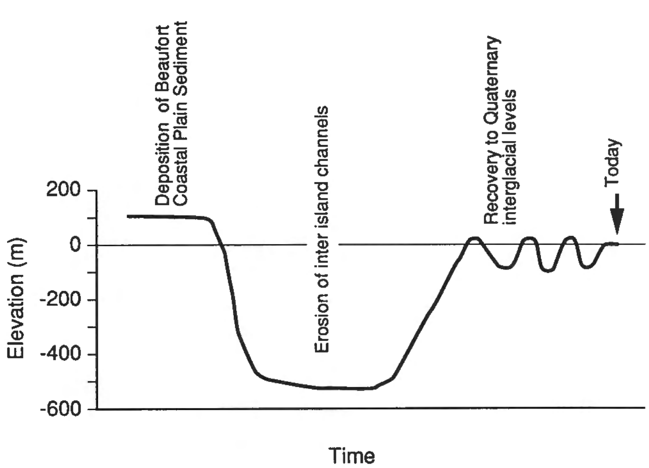

Figure 8. Changes of relative sea level implied by the fluvial channel hypothesis.

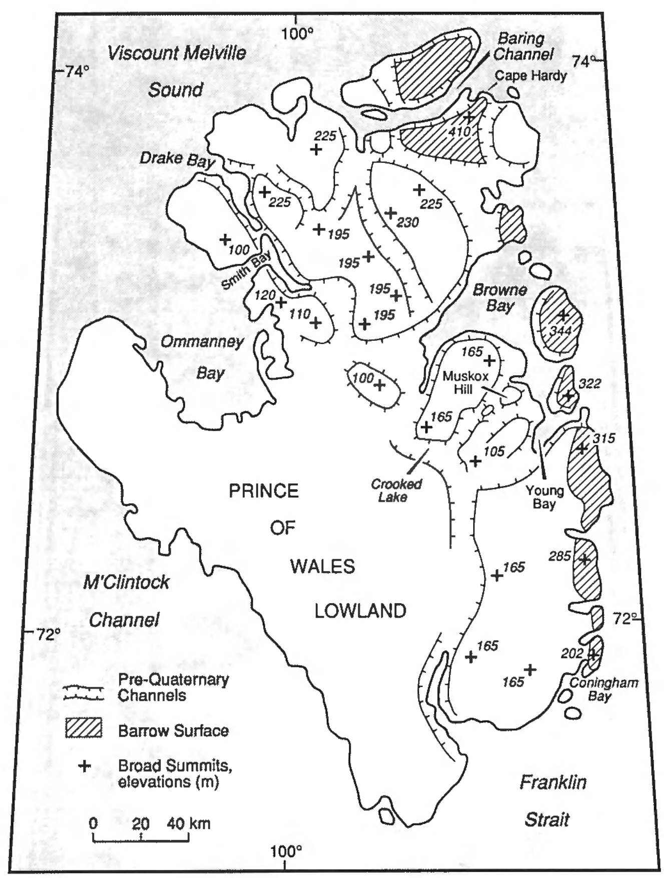

Figure 9. Pre-Quaternary physiographic elements of Prince of Wales Island.

The three elevational elements of the lower plateau system are separated by a system of large channels. The channel sides, where not degraded by later erosion, are long, parallel, sweeping, bedrock escarpments that are among the most prominent landforms in the interior. Escarpments inland from Young Bay and Muskox Hill (Fig. 9 and 10) are 2030 m high and are separated by broad, flat, valley floors that are 7-13 km wide. Isolated, scarp-bounded, ovoid hills, which are plateau remnants, rise from the middle of one channel. The largest channel-side escarpment crosses the island from Browne Bay to Drake Bay (Fig. 10) and is as much as 120 m high. Parallel, sinuous escarpments to the south, along with this one, outline a channel-like form 20 km wide.

These channels are likely ancient fluvial forms. Their sinuous shapes include large meander-like segments, such as at Crooked Lake and the entire stretch between Smith Bay and Browne Bay (Fig. 10). Ovoid to circular plateau

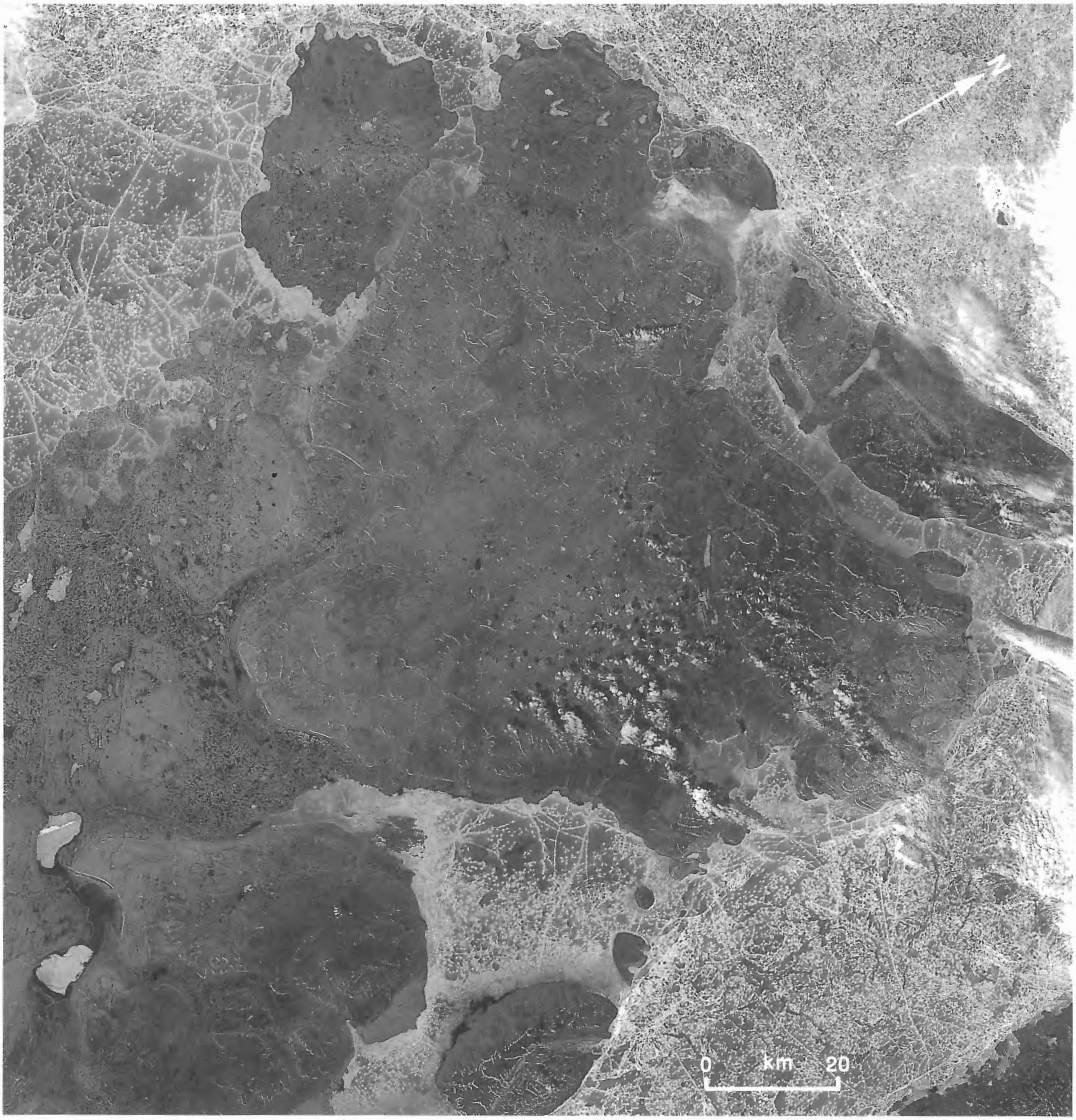

Figure 10. Large pre-Quaternary fluvial channels of Prince of Wales Island as they appear on a satellite image at a scale of 1:1 000 000. See Figure 9 for place names and interpretation.

remnants, such as Muskox Hill, that rise from flat valley floors are difficult to account for other than by fluvial erosion. Tectonic origin is unlikely because none of these escarpments have been mapped as faults, which presumably was considered during bedrock mapping (Christie et al., 1966). On the contrary, many escarpments cut sharply across major bedrock contacts and indicate no lithologic control. The notable exception is the channel that trends southward from Cape Hardy (Fig. 9). Its western margin is the prominent escarpment that marks the eastward limit of Peel Sound conglomerate. East of there is the largest area of carbonate rocks of Allen Bay and Cornwallis formations on the eastern side of the island. Peel Sound conglomerate has been stripped from that area; the river that removed it may be that which made the channel. Hence, the coincidence of this channel with a major lithological contact represents the spatial limit of erosion rather than structural or lithological control of relief.

Prince of Wales Lowland is another large pre-Quaternary physiographic element. It occupies central and western parts of the island and the floors of the largest channels that transect the lower plateaus. Hence, the lowland appears to be coeval with the youngest generation of fluvial channels. It is almost entirely drift covered so the elevation and morphology of its rock floor are unknown. Subtracting the relief of glacial features, the rock surface of much of the lowland is probably about 50 m asl. It slopes gently into M'Clintock Channel, Franklin Strait, and Viscount Melville Sound. As such, it is an emergent shoulder of a larger lowland system as shown by Bostock (1970). This interpretation neither precludes the existence of lower, younger, erosional surfaces in the marine channels, nor does it necessarily indicate an erosional origin of these channels. The sags in the lowland, such as that occupied by Ommanney Bay, may be structurally controlled for Ommanney Bay sits on a broad, shallow syncline (Christie et al., 1966). M'Clintock Channel may be of similar origin.

In summary, the large, rock-cut, physiographic elements of Prince of Wales Island reveal a multi-staged, geomorphological evolution that predates marine inundation of surrounding channels. In sequence, the major events were: planation of Barrow Surface, uplift and tilting of Barrow Surface, planation of the 230 m plateau surface, uplift, planation of the 165 m plateau surface, uplift, planation of the 100 m plateau surface, uplift, and erosion of Prince of Wales Lowland. The uplifts led to incision of the large fluvial channel systems that transect the plateaus and separate their different elevational elements.

The oldest physiographic element, Barrow Surface, is post-Devonian because it cuts across Peel Sound Formation. Each planation yielded a lot of sediment but we have no straightforward way of correlating erosional events with the depositional record, even though the latter is well known and well dated. We can not tell from the forms of the ancient fluvial channels on Prince of Wales Island whether the rivers flowed generally southward or northward. However, no post-Devonian rocks occur between Prince of Wales Island and the Shield, whereas rocks of that age are widespread in the islands to the north and less so to the west. Presumably, therefore, the ancient rivers of Prince of Wales Island flowed away from the Shield.

The pre-Quaternary fluvial channels of Prince of Wales Island represent wide, low-gradient reaches of rivers that must have been comparable in size to the largest rivers of North America today. The sediments they carried likely were dominated by suspended load and fine bed load materials. If these rivers extended to the present continental limits, hundreds of kilometres to the west, they could not have deposited the Beaufort Formation gravels, the youngest pre-Quaternary sediments that are widespread there. Because there are no appropriate Beaufort-age or younger sediments that can be correlated with these channels, the channels more likely correlate with older sediments that were deposited into basins nearer by. The youngest pre-Beaufort sediments in the Arctic Islands are Late Cretaceous to Early Tertiary Eureka Sound Group sandstones. Possibly the youngest generation of channels on Prince of Wales Island correlates with these deposits. Small remnants of Eureka Sound sandstone occur in grabens on Somerset Island and on northern Boothia Peninsula and some basins in Parry Channel contain Tertiary sediments that are possibly correlative. Eureka Sound Group was widespread throughout the Arctic Islands prior to erosion brought on by the last major uplift, the Cretaceous to Tertiary Eurekian Deformation (Kerr, 1980).

If the youngest generation of ancient fluvial channels on Prince of Wales Island and erosion of Prince of Wales Lowland correlate with Eureka Sound Group, the youngest sediments of Sverdrup Basin, older planation events likely correlate with older Sverdrup Basin sediments. These sediments range in age from Mississippian to Cretaceous. The upper Paleozoic fill consists mainly of carbonate rocks, evaporites, and clastic rocks, whereas the lower Mesozoic fill is almost entirely clastic (Balkwill et al., 1983). The source of clastic sediment in the central and western Sverdrup Basin must have been upland areas of the craton to the south. The change in nature of sedimentation in the early Mesozoic possibly signifies an increase in intensity of erosion in source areas, and that in turn presumably signifies uplift of source areas. This uplift may have been the one that raised Barrow Surface. Sverdrup Basin is thought to have maintained a nearly constant extent between Mississippian and early Cretaceous time (Balkwill et al., 1983). The general configuration of the coastline at that time implies northward drainage across Prince of Wales Island, Parry Channel, and Bathurst Island into the basin.

COMPARISON WITH SOMERSET ISLAND

Since the early attempt of Bird (1967) to analyze the pre-Quaternary physiographic elements of the southern Arctic Islands, little progress has been made in mapping and describing these elements at a regional scale. This limits the extent to which comparisons can be usefully made from island to island. Dyke's (1983) comments on the pre-Quaternary physiography of Somerset Island form the basis of the comparison that follows.

Somerset Island is underlain by the same suite of bedrock formations as underlie Prince of Wales Island. Yet the physiography of the two islands is strikingly different. Whereas Prince of Wales Island has a series of erosional surfaces stepping down from Barrow Surface to Prince of Wales Lowland, Barrow Surface is preserved over almost all of Somerset Island. Apparently planation events of long duration that grossly modified the surface of Prince of Wales Island did not much affect Somerset Island. Barrow Surface of Somerset Island, like the erosion surfaces of Prince of Wales Island, is incised by pre-Quaternary fluvial channels. But the Somerset Island channels are canyons. They are about 1 km wide and 100 m deep with entrenched meanders of a few kilometres wavelength, whereas the Prince of Wales Island channels are 10-20 km wide, mostly a few tens of metres deep, with meanders of tens of kilometres wavelength. As mentioned, the Prince of Wales Island channels resemble lower reaches of very large rivers. The Somerset Island channels resemble middle and upper reaches of much smaller rivers.

Clearly, these two adjacent islands experienced different erosion histories between the end of the Devonian and the Tertiary. Further recognition of such differences in the region ultimately will contribute to fuller paleogeographic reconstruction of pre-Quaternary times. As an example, provided the correlations of erosional and depositional events postulated above are generally correct, we conclude that more of the clastic sediment in Sverdrup Basin came from the area west of Boothia Arch than from the Arch itself or from the area just east of it.

SURFICIAL MATERIALS AND LANDFORMS

INTRODUCTION

Maps 1689A and 1690A show the distribution of the major ages and genetic categories of surficial materials. Pre-Quaternary surficial materials, consisting of competent bedrock of Precambrian igneous and metamorphic and Paleozoic sedimentary lithologies, exhibit different weathering, edaphic, and geotechnical characteristics that are important in land use considerations. The attribute most important to this study, however, is the morphology of the rock surface because it resulted from Quaternary glacial and periglacial processes and so allows us to assess the extent of Quaternary erosion. The map legend divides Quaternary materials according to whether they were formed or deposited before, during, or after the last (Wisconsin) glaciation.

The discussion below generally follows the order of units in the legend. We also discuss materials exposed in sections below Wisconsinan till, but with no mappable surface exposure. Thin postglacial eolian and organic sediments are discussed but not mapped so as not to obscure the distribution of underlying materials.

ROCK: QUATERNARY MODIFICATION (units Ra and Rb)

Rock outcrop collectively accounts for about 15% of material at the surface. Bedrock is well exposed only along the high eastern side of the island. In the interior rock outcrops mainly in escarpments of the pre-Quaternary fluvial channels and in small, postglacial stream cuts. Small, generally frost-shattered, outcrops are scattered throughout areas of till veneer. Rock terrains bear abundant signs of glacial erosion, indicated most typically by rock-basin lakes on the order of 1 km across and 10 m deep.

Depth of glacial erosion of bedrock in areas of thick drift such as Prince of Wales Lowland is difficult to assess. Likely, however, the largest lakes there (e.g., Crooked and Fisher lakes) occupy glacially excavated rock basins. Surrounding slope angles indicate that these lakes are no more than a few tens of metres deep. Preservation of pre-Quaternary fluvial channels, discussed already, indicates that net Quaternary erosion of the island has not exceeded a few metres on average. Most glacial drift on the island is locally derived and average drift thickness, on the order of 10 m, may not seriously undermeasure net Quaternary glacial erosion.

RESIDUUM AND COLLUVIUM (unit C)

Rock and weathered rock (residuum) are distinguished from each other by extent of weathering and morphology. Residuum is restricted to one high area on central northern Prince of Wales Island where silty rubble of entirely local origin overlies carbonate rock on summits and gentle hillslopes. The bedrock is obscured entirely by its weathering products and by colluvium derived from it. The smoothly graded slopes show no signs of glacial modification.

This area closely resembles areas of residuum and related colluvium that occupy much of central Somerset Island. Dyke (1983) interpreted these as areas that had been covered by cold-based ice during Quaternary glaciations. The same explanation is invoked for the Prince of Wales Island residuum because large areas at similar or higher elevations downice of the residuum bear obvious signs of glaciation. Hence, one small part of the island escaped any obvious modification by glacial erosion during the Quaternary.

The residuum is traversed by two streams that are unique among streams on the island. They are underlain by wide, braided alluvium, whereas other streams are mostly erosional and are interrupted by lake basins.

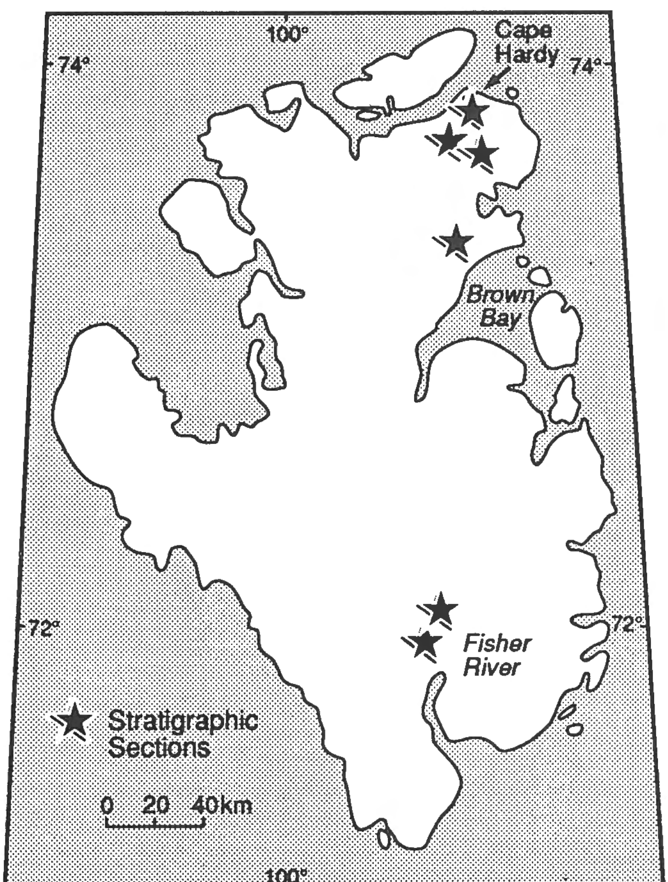

Figure 11. Locations of sections exposing sediments below Wisconsinan till on Prince of Wales Island.

QUATERNARY SEDIMENTS BELOW TILL (not mapped)

Sediments underlying Wisconsinan till are exposed at few sites and exposures are small. Stream-cut exposures are described here from Fisher River, near the north shore of Browne Bay, and near Cape Hardy (Fig. 11).

Two 6-10 m sections along the west bank of Fisher River expose glacial and fluvial sediments below till. The lowest unit, exposed in only one section, is a diamicton with striated, angular to subangular clasts supported by compact mud matrix. Its clasts have a NW-SE fabric, and Morris (1988) interpreted it as till. Several metres of overlying gravel consists mostly of boulders at the base and fines upward to sand. Imbrication of clasts in this unit indicates southward water flow as in Fisher River. The sand is capped by till that extends to the surface (Fig. 12) and has an E-W fabric. The surface till at the other section along Fisher River is underlain by planar bedded sands.

The fluvial sands in both sections contain abundant but small fragments of redeposited marine shells. A high-pressure radiocarbon date, a uranium-series date, and

Figure 12A. Fisher River stratigraphic section; person is excavating in gravel below till. GSC 1991-406

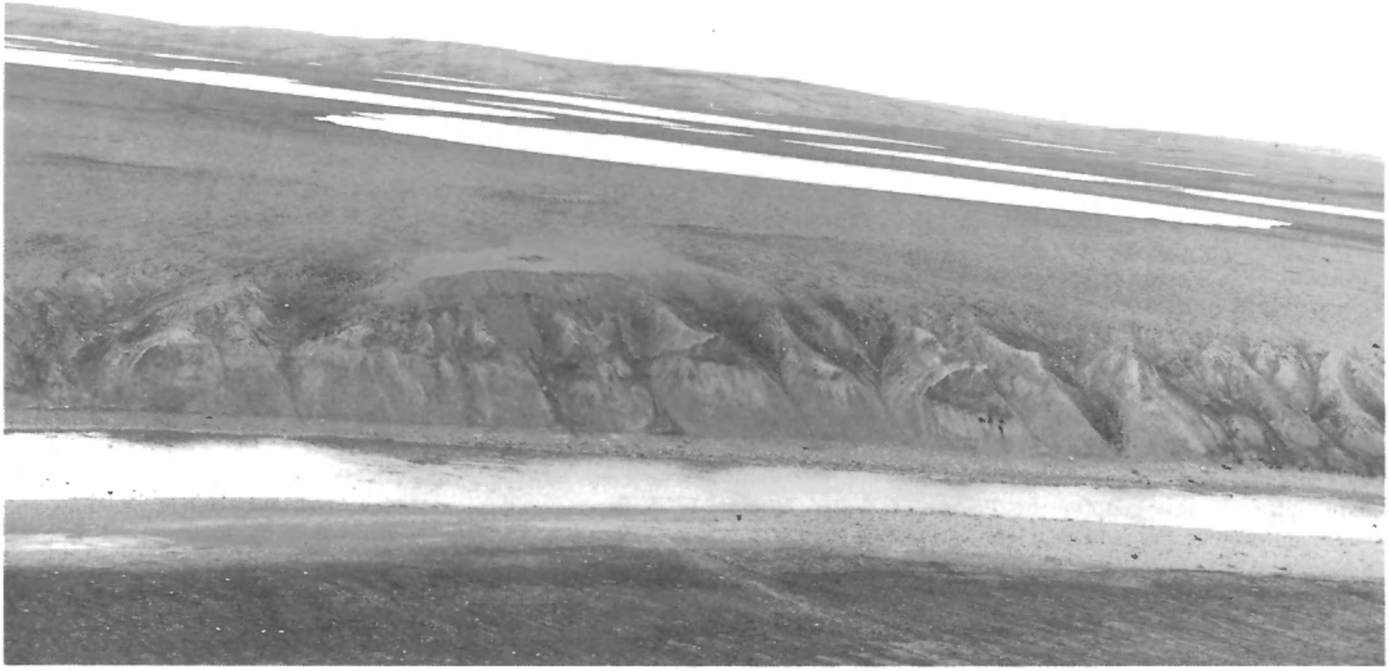

Figure 12B. Distant view of Fisher River stratigraphic section showing gravel overlain by till with the contact at middle level; locally, left of centre, beach gravel overlies the till. GSC 1991-407

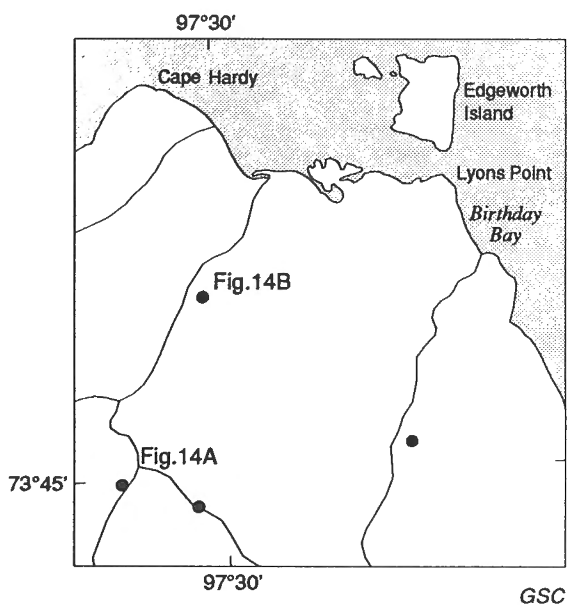

Figure 13. Location of sections exposing sediments below the Wisconsinan till in the Cape Hardy area; sections illustrated in Figures 14A and 14B are located.

amino acid ratios were determined for a sample of *Hiatella arctica* from one section (Table 1). At face value, the uranium-series date, 34 000 years, indicates a Middle Wisconsinan age for the fluvial sediments. The radiocarbon age of >49 000 BP (GSC-4470), however, indicates that the uranium-series date should be regarded as a minimum age estimate and hence that the sediments may be older than Middle Wisconsinan. The amino acid ratios (Table 1) are similar to ratios in erratic shells in surface till on Prince of Wales and Somerset islands. These ratios were considered to represent a Sangamonian age by Dyke and Matthews (1987). Higher amino acid ratios of redeposited *Hiatella arctica* shells from the subtill sand of the other Fisher River section (Table 1) indicate a greater age. Either two ages of fluvial sediment underlie the upper till along Fisher River or, more likely, two ages of shells have been redeposited into one fluvial unit.

A stream cut north of outer Browne Bay (Fig. 11) exposes 2 m of grey sand and gravel below red till, which is overlain by glaciomarine and marine sediment. The sand and gravel have imbricated clasts and crossbeds that indicate eastward flow toward Browne Bay, as in the present stream. Fragments of redeposited marine shells from the sand have amino acid ratios comparable to those from the Fisher River samples (Table 1), which suggests the presence of at least two ages of shells.

Subtill sediments are exposed in several stream cuts near Cape Hardy (Fig. 13). One cut exposes 3.5 m of pink gravelly sand below a 65-cm-thick red to reddish brown stony till (Fig. 14A). The sand is capped by a black, humus-rich horizon that has irregular upper and lower boundaries and varies from 5 to 17 cm in thickness. The humic horizon is discontinuous; single pieces can be traced for only 1-2 m, and stringers of it protrude into overlying till. This horizon, interpreted as a buried soil, is better developed than postglacial soils normally seen on sand. It contains a pollen assemblage similar to that in a nearby postglacial peat except that its assemblage includes exotic pine pollen, which is not

Table 1. Radiocarbon and uranium-series dates and amino acid ratios on *Hiatella arctica* shells of pre-Late Wisconsinan age, Prince of Wales Island.

Sample and location	Amino acid ratio		Radiocarbon age	Uranium-series age	Comment
	Free	Total			
84-DCA-8S Fisher River	0.40 0.39 0.41	0.106 0.126 0.117		>200 000 (UQT-444)	from gravel below till
	(AAL-4305)				
84-DCA-26S Fisher River	0.16 0.20 0.20	0.044 0.148 0.042	>49 000 (GSC-4470-HP)	35 000 (UQT-445)	from gravel below till
	(AAL-4306)				
84-DCA-805B Arabella Bay	0.24 0.27 0.24	0.076 0.056 0.063			from till above marine limit
	(AAL-4304)				
84-DCA-856 Browne Bay	0.24 0.25 0.37	0.050 0.048 0.097			from gravel below till
	(AAL-4302)				
84-DCA-896 Browne Bay	0.17 0.17 0.24	0.048 0.050 0.053			from glacio-lacustrine sediment
	(AAL-4203)				
85-DCA-14S Muskox Hill			>33 000 (S-2712)		from gravel above m. l.
85-DCA-92S Muskox Hill			>33 000 (S-2713)		from gravel above m. l.
85-DCA-303 Cape Hardy	0.23 0.23 0.25	0.076 0.058 0.061			from sand below till
	(AAL-4617)				
85-DCA-315 Cape Hardy	0.20 0.18 0.12	0.053 0.052 0.035		80 000 (UQT-446)	from marine sediment below till
	(AAL-4618)				
85-DCA-328 Cape Hardy	0.48 0.48 0.54	0.113 0.127 0.126			from marine sediment below till
	(AAL-4623)				
85-DCA-381 Cape Hardy area	0.18 0.25 0.19	0.040 0.084 0.082			from glacio-lacustrine sediment
	(AAL-4624)				
85-DCA-383 Cape Hardy	0.14 0.14 0.14	0.046 0.045 0.050			from glacio-lacustrine sediment
	(AAL-4625)				
86-DCA-415 Cape Richard Collinson			39 400 ± 1900 (GSC-4322)		from marine sediment in moraine

present in the postglacial deposit (Hooper, 1986). Sand below the buried soil is folded and locally assumes a near-vertical dip. Where steeply dipping, the sand is loose, even below the permafrost table, and contains linear cavities that parallel bedding. Such deformation of sand is seen commonly beside ice wedges and the loose sand with cavities likely represents an underconsolidated ice-wedge cast. The buried soil extends across the deformed sand and hence postdates it. Redeposited shell fragments of *Hiatella arctica* from the sand have amino acid ratios (Table 1) that fall within the Sangamonian group 2 of Dyke and Matthews (1987).

Glaciomarine sediment is exposed below till farther down the same stream (Fig. 14B). Red till nearly 1 m thick overlies stony mud with abundant paired valves of *Hiatella arctica*. The till is overlain by a similar fossiliferous stony mud, succeeded upward by marine mud, fluvial gravel, fluvial sand with organic detritus, and stony colluvium. Shells from the stony mud below till yielded a uranium-series age of 80 ka and have amino acid ratios (Table 1) that correspond to group 2 of Dyke and Matthews (1987). Hence, this sediment likely records proximal glaciomarine sedimentation during englaciation at the close of Sangamon Interglaciation. Shells from the stony mud above till have amino acid ratios typical of the Holocene and a radiocarbon age of 9280 ± 90 BP (GSC-4250).

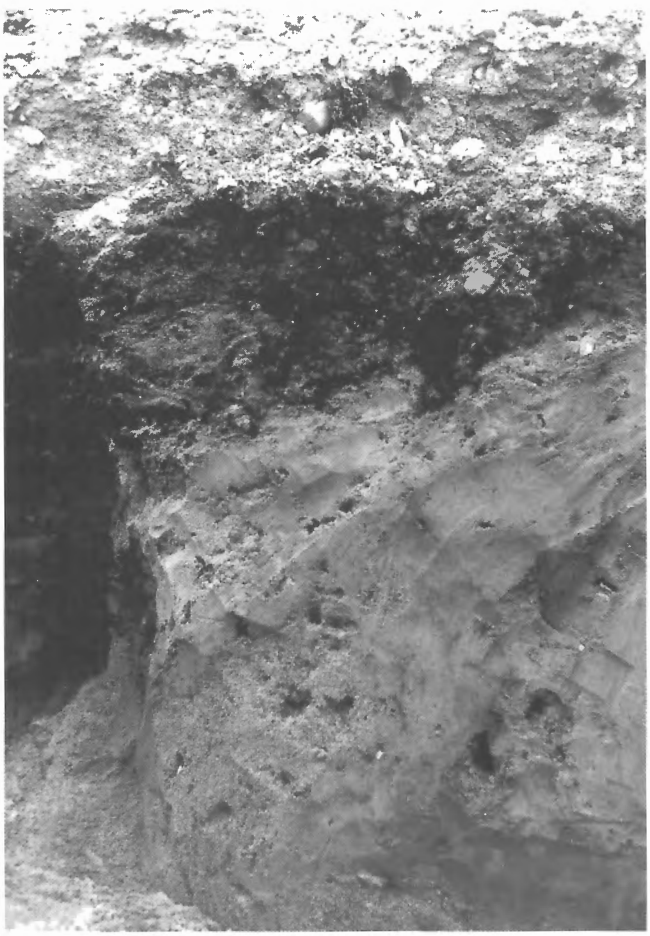

Figure 14A. Folded sand capped by a paleosol and overlain by till near Cape Hardy (see Fig. 13); cavity on left-hand side is an excavated, underconsolidated, ice-wedge cast. GSC 1991-408

TILL AND TILL LANDFORMS

Till is the predominant Quaternary material. It outcrops without significant interruption over about 70% of the island and occurs at shallow depth beneath marine deposits over another 10%. On maps 1689A and 1690A till is divided according to morphology into veneers, megafluted till plains, drumlin fields, ribbed moraine fields, till blankets and streamlined till plains, and end moraines.

Cross-cutting morphostratigraphic units reveal that major till landform assemblages were established during three main ice flow phases, referred to as phases 1, 2, and 3 from oldest

Figure 14B. Stony glaciomarine sediment, the layer behind the tape measure, underlying till. Shells from this unit have a uranium-series age of 80 ka and amino acid ratios indicative of Sangamonian age. GSC 1991-409 to youngest, respectively. These phases occurred before deglaciation and were followed by other short-lived, shifting ice flows related to ice-marginal retreat. Except for till veneers, which have not been stratigraphically subdivided, till units are discussed here in stratigraphic order. Compositional variation of till is discussed in *Till composition and glacial dispersion* and trace element geochemistry in *Economic geology*.

Till veneer (unit Tv)

Till is mapped as a veneer where it is less than about 2 m thick, not thick enough to mask the small-scale roughness of underlying bedrock. Areas of till veneer occur mainly along the high eastern plateau in contact with bedrock. Farther inland they occupy summits. Till thickness and elevation are negatively correlated, as is common, perhaps because higher

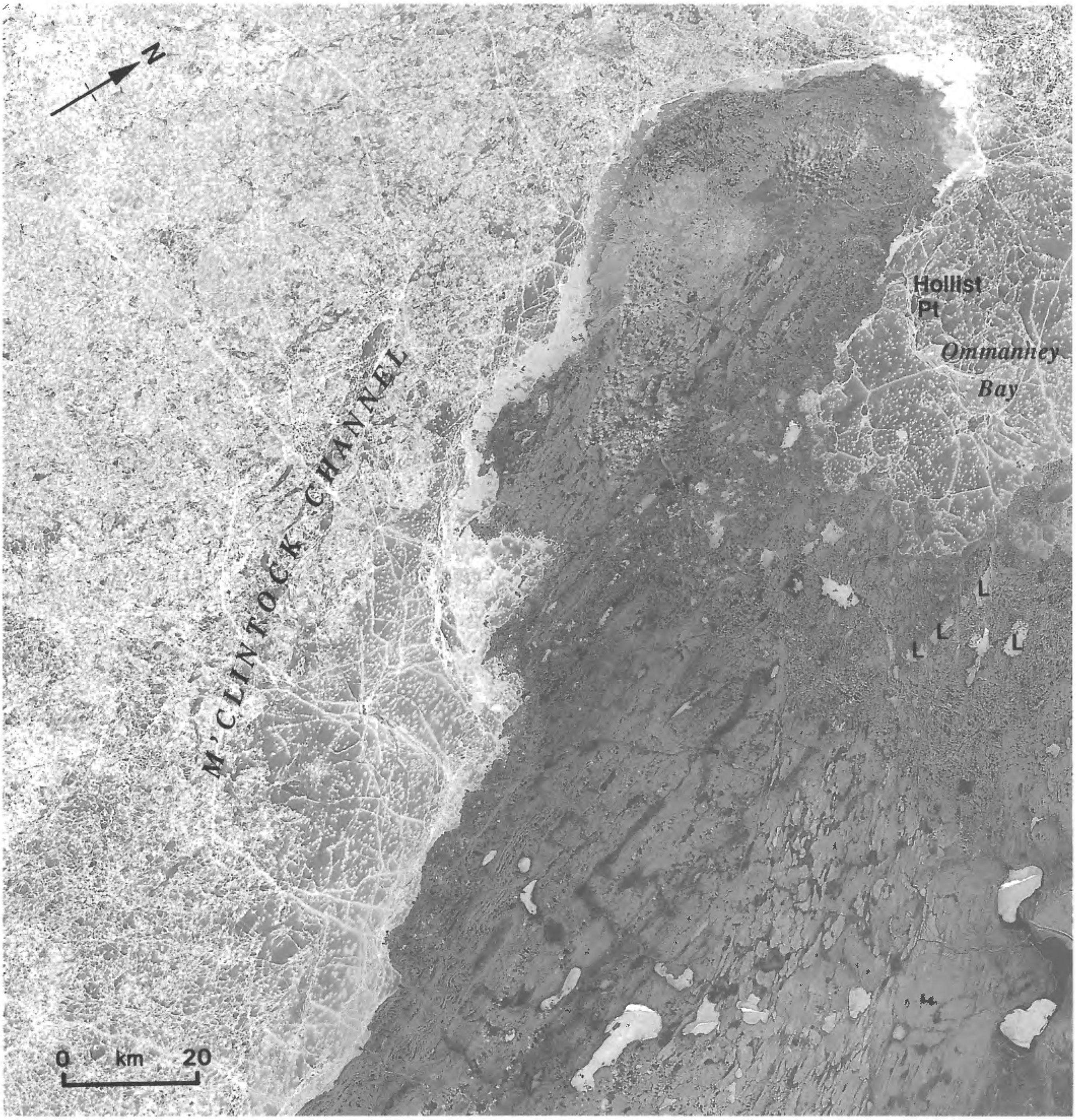

Figure 15. Satellite image at a scale of 1:1 000 000 of western Prince of Wales Island showing megaflutes of Arrowsmith Plains crosscut in the east by the Crooked Lake drumlin field. "L" denotes lakes aligned along phase 1 flowlines.

parts of the glacier bed extended into cleaner ice and hence debris accumulated slowly, or perhaps because higher areas experienced net erosion.

Till veneer is rarely streamlined. Flutings, striae on underlying rock, and adjacent ice-moulded rock indicate that most till veneer was laid down during the latest ice flow phases. But in places, such as north of Guillimard Bay and north of Crooked Lake, flutings and ice-moulded rock indicate deposition during phase 2.

Arrowsmith till plain with megaflutes (unit T^1p)

The large, nearly featureless Arrowsmith Plains in western Prince of Wales Island is underlain mostly by till. The plain, stretching from the southern tip 170 km along M'Clintock Channel and about 40 km inland, occupies about one-third of Prince of Wales Lowland and extends offshore.

The plain is crossed from the south-southeast by broad, shallow valleys, some occupied by lakes and partly filled by glaciomarine sediment. Intervening rises are 1-3 km wide but only about 10 m high. On satellite images at a scale of 1:1 000 000, they appear as distinct glacial flutings (Fig. 15). Individual flutes are as much as 20 km long. They are too large and of too little relief to recognize on airphotos at a scale of 1:60 000 and are not shown on the enclosed maps. Ice flow features that are portrayed on the maps within unit T^1p are smaller, superimposed forms that show on the airphotos parallel to the megaflutes.

At the north end of the megafluted plain, south of Ommanney Bay, ribbed moraine is superimposed on the megaflutes, but the trend of the flutes is discernible through the ribbed moraine field on the satellite image (Fig. 15). Farther north, along the west side of Ommanney Bay, megafluted till has been partly remoulded into smaller, streamlined forms with a different orientation (Map 1690A). Again, the older forms are not discernible on the airphotos but show up clearly on the satellite image. The peninsula south of Hollist Point is an example of a partly remoulded megaflute (Fig. 15). The older form is seen clearly on the image, but the more subtle reworking by younger ice flow is not.

The eastern side of the megafluted till plain is crosscut by the Crooked Lake drumlin field (unit T^2d). Near the north end of the drumlin field, the older megaflutes are partly preserved and the smaller drumlins are superimposed. The megaflutes are recognizable on the satellite image because bordering lows are partly filled by marine sediment, which supports more vegetation than adjacent till. They are not readily discernible on the airphotos. The farther northward extension of the older flowline is picked out by an alignment of four large lakes in the central part of the Ommanney Bay ribbed moraine field (unit $T^{12}r$).

Mount Cowie drumlin field (unit T^1d)

A drumlin field 35 km long and 20 km wide occupies the centre of the peninsula west of Ommanney Bay. It is here named for a prominent hill at its south end, Mount Cowie. Drumlins are as much as 4.5 km long and 30 m high. Megaflutes about 20 km long continue through this area from Arrowsmith Plains (Fig. 15). The drumlins, the most conspicuous landforms on the airphotos and as viewed on the ground, are superimposed forms in the same orientation. A few drumlins are asymmetric and their tails trail north-northwest, giving the sense of phase 1 ice flow.

Crooked Lake drumlin field (unit T^2d)

The Crooked Lake drumlin field, 115 km long and 45 km wide, occupies most of eastern Prince of Wales Lowland. The larger drumlins are 5 km long, 1.5 km wide, and 30 m high. Drumlin form is best developed in the central and western parts of the field, where features are ovoid to teardrop-shaped in plan (Fig. 16) or, exceptionally, barchan-shaped (Fig. 17). Along the eastern side, features grade to long, narrow flutings (Fig. 15).

The Crooked Lake drumlins resemble the Mount Cowie drumlins in size and form but appear to be first order bedforms, rather than ornaments on larger forms with the same alignment, as are the Mount Cowie drumlins. As mentioned, the Crooked Lake drumlins overlie older megaflutes with different orientation at the north end of the field. Preservation of the older bedforms indicates that the Crooked Lake drumlins are depositional rather than erosional forms.

All asymmetric forms in the Crooked Lake drumlin field indicate generally northward ice flow. At the south end, drumlins are oriented north, but farther down flow orientation swings gradually counterclockwise, until at the north end, it is northwest. The regular change in orientation indicates that the drumlins formed under a part of the ice sheet with a strongly curved flowline.

As mentioned, the Crooked Lake drumlin field crosscuts the megaflutes of Arrowsmith Plains to the west. At the south end, the Crooked Lake drumlins diverge from the megaflutes by about 20°, whereas at the north end they converge at about 30°. No trace of this flow pattern is found on Arrowsmith Plains.

The Crooked Lake drumlin field grades northward into the Ommanney Bay ribbed moraine field. The contact between the two landform assemblages is digitate and difficult to discern (gradational). The few occurrences of streamlined till within the ribbed moraine field represent direct extensions of flowlines from the drumlin field.

The eastern side of the Crooked Lake drumlin field coincides roughly with the margin of Prince of Wales Lowland. However, this limit is more likely due to remoulding of till east of the lowland during younger ice flow phases (see below) than to the extent of ice during phase 2. The eastern margin displays a crosscutting relationship with younger till and outliers of Crooked Lake drumlins form islands surrounded by younger till east of Guillimard Bay and Fisher Lake (Map 1690A). Because these outliers extend close to Franklin Strait, ice flow during phase 2 likely extended across all of southern Prince of Wales Island. South of the drumlin field, west of Guillimard Bay, the till was remoulded by younger flow, but phase 2 flow accounts for the alignment of many long, narrow lakes there.

Lateral shear moraine

The western margin of the Crooked Lake drumlin field is remarkably abrupt. Its northern part is defined by a narrow, streamlined, smoothly curved ridge of till 68 km long, mostly <1 km wide, and lying parallel to the drumlins themselves. On airphotos, swells along this ridge appear as long, narrow drumlins without distinct ends; the continuity of the ridge is not apparent until viewed at the smaller scale of the satellite image (Fig. 15). Along its southern part, the western margin of the drumlin field is similarly well defined by a closely spaced, heel-to-toe alignment of narrow drumlins (Map 1690A). With little more attenuation, these drumlins would have coalesced to complete a ridge along the entire western boundary of the drumlin field. The elevation of this sharp western boundary changes by only 30 m along its 115 km length. Because it stretches across the centre of the flat Prince of Wales Lowland, its location must have been determined by some factor other than topography.

Dyke and Morris (1988) considered possible modes of formation of the western boundary ridge and concluded that it is a lateral shear moraine. Shearing is thought to have occurred along an abrupt boundary between cold-based ice over Arrowsmith Plains and streaming, warm-based ice over the Crooked Lake drumlin field. This interpretation can account for the presence and streamlined aspect of the ridge along the northern part of the contact, the heel-to-toe alignment of drumlins along the southern part, and the parallelism of the contact and the drumlins. Interpretation of the boundary ridge as a lateral moraine outlining a surge is not satisfactory because that would imply that Arrowsmith Plains were ice-free at that time. During phase 3, ice originated from there, as discussed later, so the plains were not likely ice-free during phase 2.

Hence, between phases 1 and 2, flow dynamics changed, apparently abruptly. During phase 1, ice flowed across Prince of Wales Lowland with a perfectly straight flowline and left a uniform field of very large bedforms (megaflutes) from end

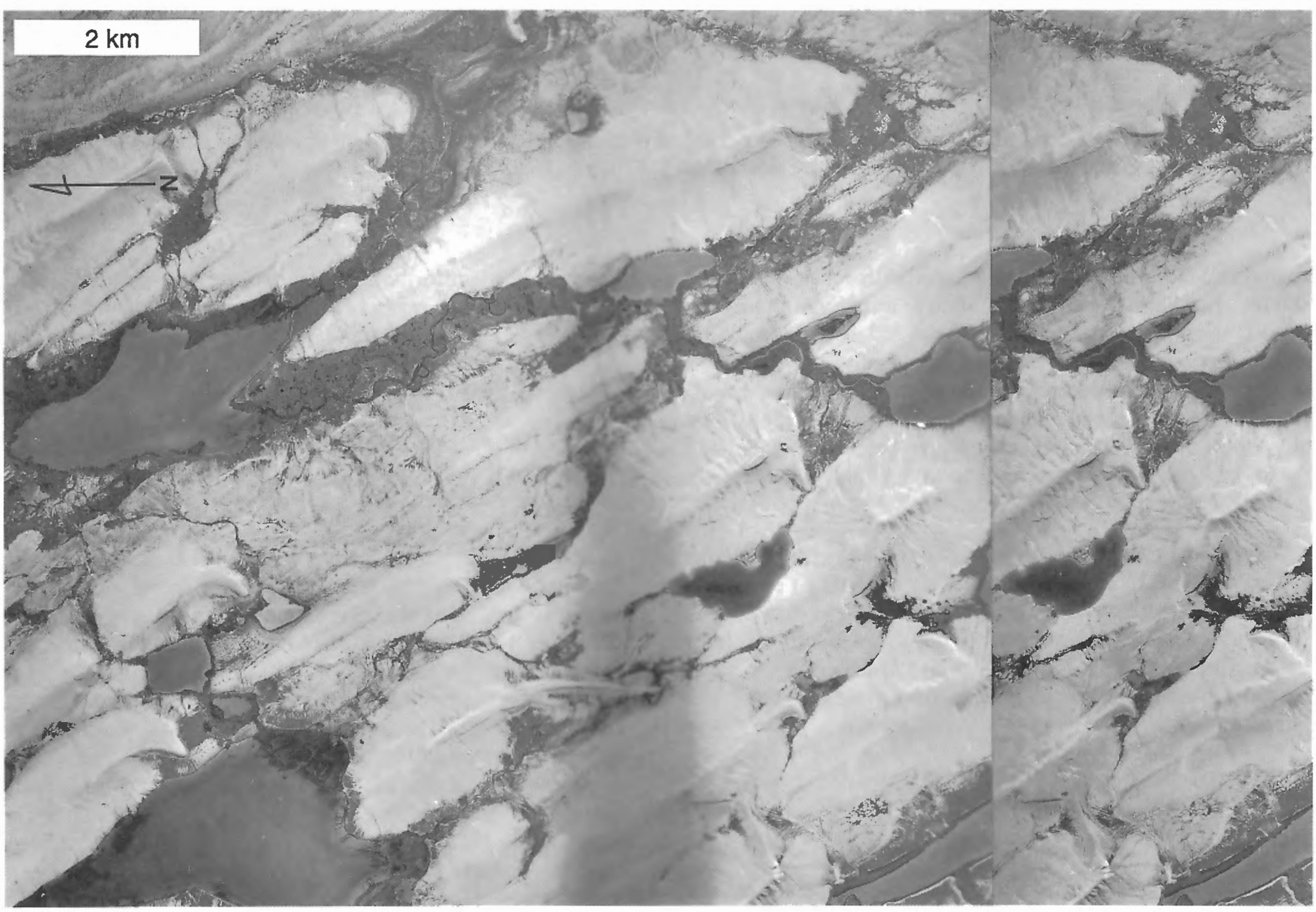

Figure 16. Part of the Crooked Lake drumlin field. NAPL A16174-36 and 37

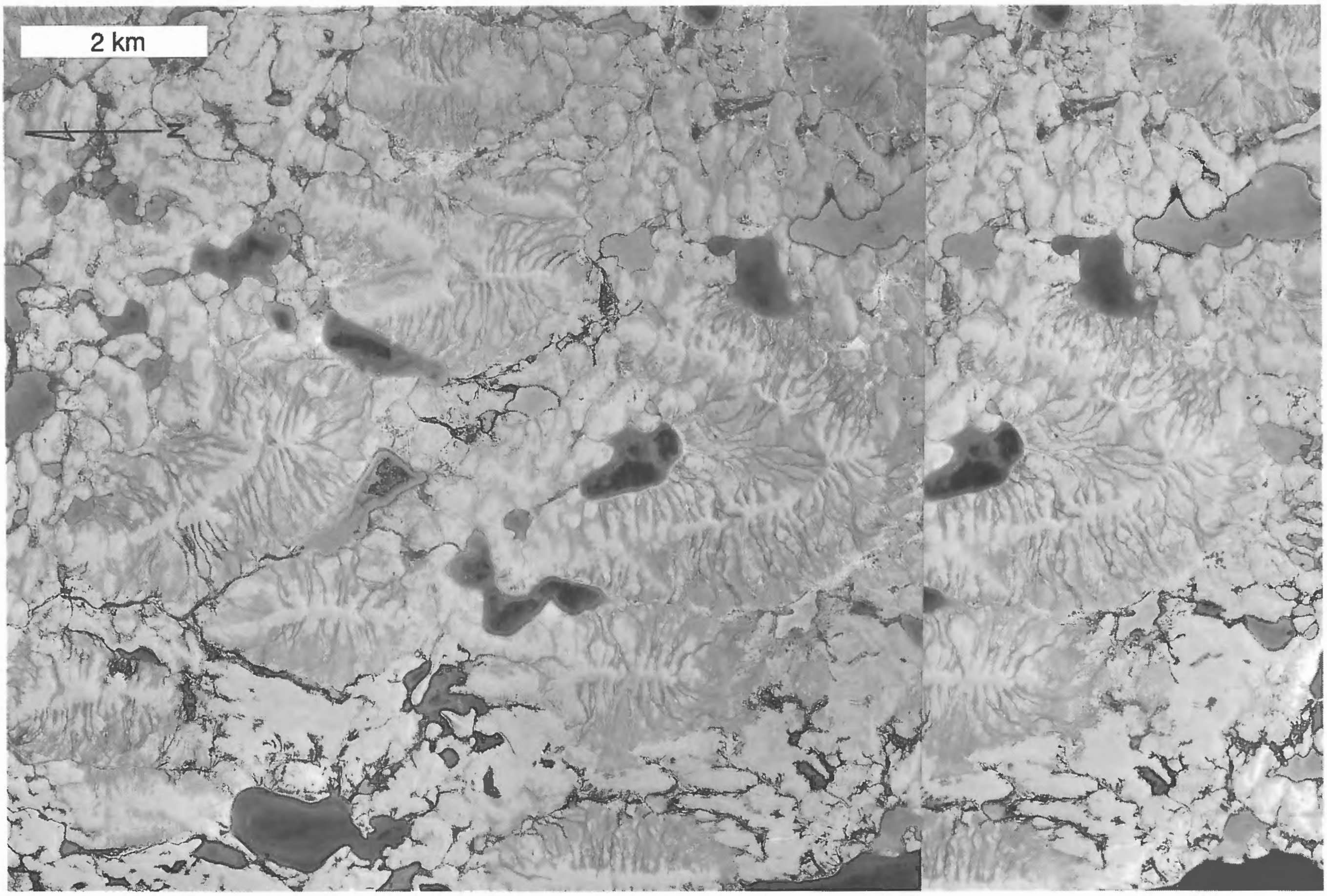

Figure 17. Barchan-shaped drumlins in the Crooked Lake drumlin field. Also note small east-oriented drumlinoid forms, part of head of Transition Bay drumlin field. NAPL A16153-125 and 126

to end and likely from side to side; the bedforms indicate that the ice was warm-based and flowing at a regionally uniform rate. During phase 2, ice flowed across the lowland with a markedly curved flowline and made smaller bedforms (drumlins) on the eastern side. Ice on the western side must have been cold-based because the older landscape there survived unaltered. The boundary between cold- and warm-based ice was abrupt and curvilinear and was probably a vertical zone of shear in the ice.

Nothing in the Quaternary geology of Prince of Wales Island as presently known indicates a cause of this change in ice sheet dynamics. A similarly abrupt and larger shift in flow direction and basal thermal boundaries occurred later between phases 2 and 3. In *Quaternary history*, we speculate on possible trigger mechanisms originating beyond the island.

Ommanney Bay ribbed moraine field (unit $T1^2r$)

The Ommanney Bay ribbed moraine field wraps around the head of Ommanney Bay. It has a width of 90 km and maximum length (along flowline) of 50 km. Its most conspicuous landforms are short, sinuous, subparallel ridges, 2-5 m high, that resemble the classic ribbed moraine of Keewatin. The ridges trend northeast, at a right angle to drumlins of the Crooked Lake field. Where not ridged, the till is hummocky and disorganized.

The ribbed moraine field seems to have formed roughly contemporaneously with the Crooked Lake drumlin field or during an interval between formation of that drumlin field and formation of the megaflutes of Arrowsmith Plains. Its contact with the drumlin field is gradational, flutings within the ribbed moraine field trend the same as the drumlins, and the ribs extend at right angles to the drumlins. However, the ribbed moraine field is much wider than the drumlin field (Map 1690A). Hence, its formation predates formation of the drumlins, at least in part, because the flowlines that formed the drumlins would have extended across only part of the ribbed field. The lateral shear moraine at the side of the drumlin field protrudes into the ribbed field, which also possibly indicates that the drumlin field is slightly younger than the ribbed field. West of the lateral shear moraine, the ribbed moraine is superimposed on the megaflutes of Arrowsmith Plains. Hence, it is younger than the megaflutes.

The trend of the ribs indicates that the field was formed by ice flowing generally northward. Because the ribbed field seems somewhat younger than the megaflutes and somewhat older than the drumlin field, it may have formed in response to the change in basal ice conditions between phases 1 and 2.

Till blanket and streamlined till plain (unit T^3b)

Eastern, northern, and parts of western Prince of Wales Island are underlain by 2-5 m thick till. The till forms a blanket on broad interfluves and fields of drumlinoid ridges and flutings, mostly <5 m high, in lower areas. The streamlined forms result from a sequence of shifting ice flows, the oldest of which was eastward.

Eastward flow is recorded most obviously on southeastern Prince of Wales Island. Two fields of closely spaced, small drumlins and flutings occupy broad, shallow troughs leading to Le Feuvre Inlet and Transition Bay (Map 1690A; Fig. 18A). Flow diverged slightly over higher ground between the Transition Bay and Le Feuvre Inlet drumlin fields. The Transition Bay drumlin field (Fig. 18B) exhibits

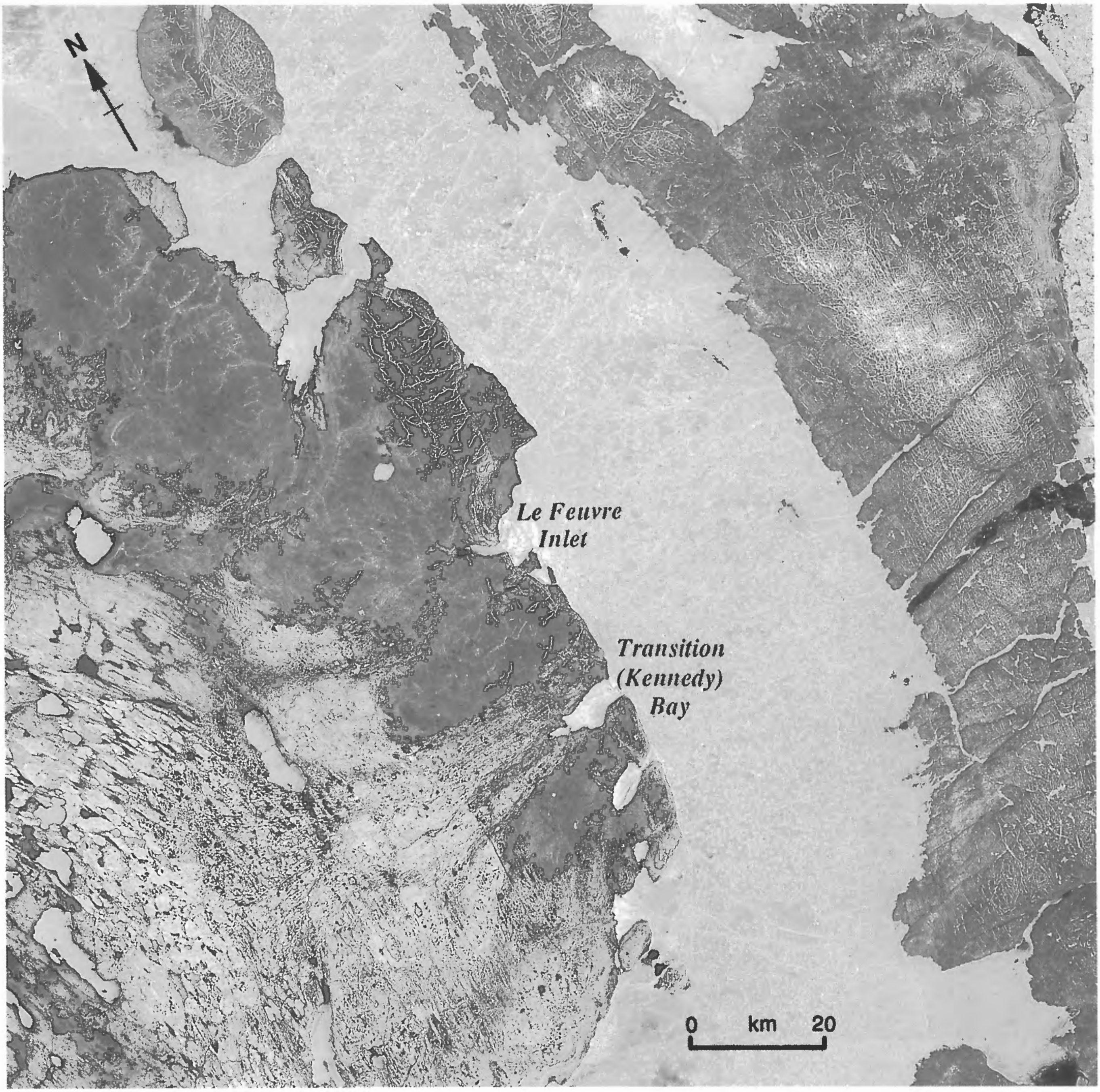

Figure 18A. Satellite image at a scale of 1:1 000 000 showing the Transition Bay drumlin field and dispersal plume in relation to older bedforms.

a strong flow convergence at its head. The head of the Le Feuvre Inlet drumlin field shows a flow curvature that indicates the same ice source.

The eastward flow is clearly younger than the northward flow recorded by the Crooked Lake drumlin field. Streamlined forms at the head of the Transition Bay drumlin field are superimposed on the larger Crooked Lake drumlins; in places the younger drumlins form tails extending eastward nearly at right angles from the older drumlins that served as obstacles to flow (Fig. 19).

The head of the Transition Bay drumlin field forms a large, ragged re-entrant into the Crooked Lake drumlin field, which resulted from erosion of the older drumlins during formation of the younger. East of Fisher Lake (Map 1690A), all traces of the Crooked Lake drumlin field have been destroyed within the limits of the Transition Bay drumlin field. But south and north of the younger drumlin field, a few remnants of the older field have survived. Modification of the older Crooked Lake drumlins decreases westward from Fisher Lake, as does the size of the Transition Bay drumlins, until Transition Bay forms are only weakly developed and are restricted to lows among the older drumlins. This morphological zonation implies that ice was more erosive within the Transition Bay drumlin field than on either side and that ice in the source area, west of the head of the drumlin field, was cold-based and protective.

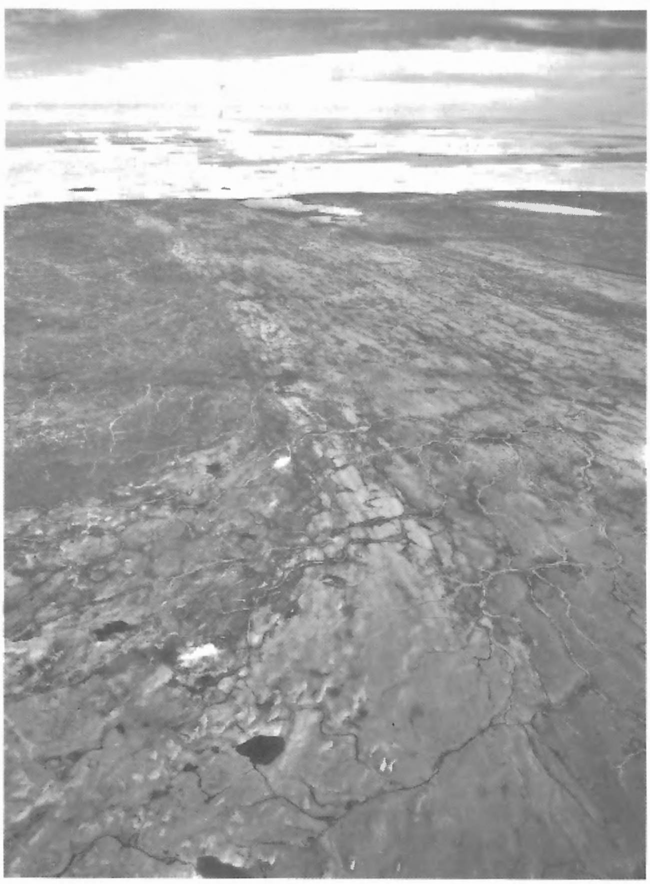

Figure 18B. Eastward oblique view down the Transition Bay dispersal plume entering Peel Sound in the background. The plume is the broad swath of streamlined, light-toned till on the right-hand side of the image. NAPL T436R-19

The Le Feuvre Inlet drumlin field is not as well developed as the Transition Bay field. Streamlined forms are smaller, less densely arranged, and exhibit no clear internal zonation of forms. This development and the fact that the drumlin field does not form an erosive headward re-entrant into the Crooked Lake terrain indicates a lesser discharge of ice through it than through the Transition Bay field.

Morphological evidence of a general eastward flow of ice north of the Le Feuvre Inlet drumlin field includes flutings on till veneer (unit Tv) southeast of Young Bay, large ice-moulded forms on gneiss on Pandora and Prescott islands, and early eastward striations (cut by younger striations) on eastern Russell Island. These features occur on the highest ground on the eastern side of the area, higher than any terrain to the west. Hence, they must have formed when the entire island was ice covered. They likely correlate with the Transition Bay and Le Feuvre Inlet drumlin fields, though they could be slightly older if the lowland drumlin fields continued to be occupied by ice after exposure of the higher terrain during deglaciation. Nevertheless, evidence of a pervasive, due-eastward flow is found from the south to the north end of the map area. It undoubtedly dates from the same general interval, phase 3, and occurred after the flows that generated the Arrowsmith megafluted till plain, the Mount Cowie drumlin field, the Ommanney Bay ribbed moraine field, and the Crooked Lake drumlin field to the west.

Other fields of small drumlinoid forms with northeast orientation on till unit T^3b occupy valleys leading to Young Bay and inner Browne Bay and a plateau surface of intermediate elevation southeast of inner Browne Bay. These fields indicate topographic deflection of flow from the general eastward course and can be assigned reasonably to deglacial flow phases after phase 3.

Similarly, various flow patterns inscribed on till unit T^3b on northern Prince of Wales Island, on the peninsula west of Ommanney Bay, and on southernmost Prince of Wales Island are assigned to later flow phases because of their relationships to end moraines or other ice marginal features. These features are discussed in terms of their relation to end moraine systems (see *End moraines*). They include: a long train of drumlinoid forms crossing the northern plateau, converging northwestward upon Arabella Bay, and indicating a flow source over Browne Bay; lightly inscribed, cross-cutting flutings on a lowland south of Reliance Bay; and northward and westward oriented forms west of Ommanney Bay.

Also during deglaciation light, parallel, northeast oriented scratches were made on the till of Arrowsmith Plains, the Crooked Lake drumlin field, and the Ommanney Bay ribbed moraine field. These subtle features show well on airphotos (Fig. 20) but would pass unnoticed on the ground. In size they resemble iceberg scours, but they are perfectly parallel over a large area and align with streamlined till forms tens of kilometres farther downice. Five small drumlinoid forms, a

Figure 19. Crooked Lake drumlins trending from right to upper left crosscut by Transition Bay drumlins trending from right to lower left. GSC 1991-410

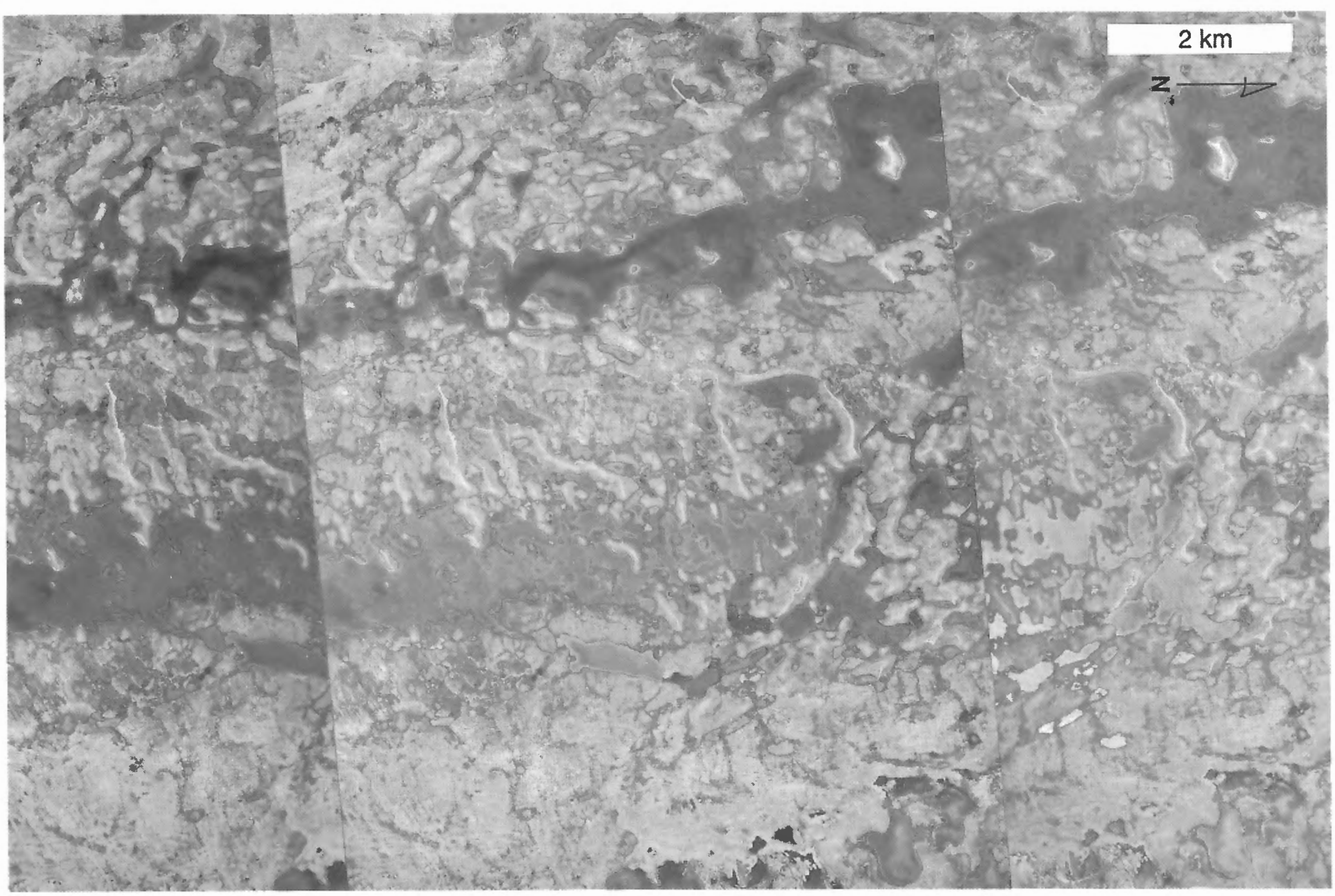

Figure 20. Late, east-northeast ice flow scratches on till surface of Arrowsmith Plains, best developed on lower part of left-hand pair. NAPL A16200-5, 6, and 7

large subglacial meltwater channel, and an esker set into the western part of the Ommanney Bay ribbed moraine field also indicate this ice flow direction. This evidence suggests that the scratches were made at the base of the ice, likely by slight basal slippage.

Fisher Lake ribbed moraine field and related deposits (unit T^3r)

Ribbed moraine formed during phase 3 in five areas between inner Browne Bay and the south tip of the island. All but one of these deposits is of minor extent.

The Fisher Lake ribbed moraines form a discontinuous field about 10 km wide that arcs west and south from Fisher Lake. Thus, it partly circumscribes the head of the Transition Bay drumlin field. Ribs are transverse to the trend of Transition Bay drumlins, and headward extensions of the drumlin field separate components of the ribbed field. These ribbed moraines contact the Transition Bay drumlin field on the east and the Crooked Lake drumlin field on the west. Therefore, they formed at the boundary between cold- and warm-based ice. Their flowline relationship with the Transition Bay drumlin field is the opposite of that between the Crooked Lake drumlin field and the Ommanney Bay ribbed moraine field, which passes downice from drumlins to ribs.

Other small occurrences of ribbed moraine are related to deglacial ice flows into inner Browne Bay, Young Bay, and Franklin Strait.

End moraines (unit T^3m)

End moraines comprised of, or mantled by, till form three belts, each containing several morainal ridges and less organized morainal topography. The largest belt, extending 230 km across the northwestern part of the area, is one of the most continuous morainal systems in that part of the Archipelago invaded by the Keewatin Sector of Laurentide Ice Sheet. Another belt stretches about 80 km across the north-central part of the island. End moraines occur more sporadically inland of Peel Sound, between Young and Guillimard bays. End morainal accumulations comprised of glaciofluvial and glaciomarine sediments are discussed in later sections.

Features indicative of ice cores

The moraine systems are comprised mostly of till at the surface, but two widespread features indicate that buried glacier ice forms their bulk. These features are kettles and large frost-fissure polygons.

Large parts of the moraine systems are disrupted by kettles, many appearing to have lowered their floors right through the deposits. Among the morphological facies of till, kettles are restricted to the end moraines, though they also occur in the ice contact facies of glaciomarine deposits.

In continuous permafrost, kettles have a particular significance. Buried glacier ice will not melt if protected by a debris mantle slightly thicker than the active layer. Similarly, lowering of kettle floors will cease when enough debris melts out to insulate the ice from summer heat. The large, deep kettles, therefore, must represent parts of the moraines that consisted of ice with little debris. Morainal ridges between kettles may consist largely of ice with a till cover only slightly exceeding the postglacial maximum thaw depth.

The bulkier end moraines are ubiquitously patterned by frost-fissure polygons, presumably ice-wedge polygons. The polygons are generally rectilinear and large, mostly 50-100 m across, and are conspicuous on airphotos but less striking on the ground. Their occurrence so faithfully coincides with the end morainal facies of till that they are in themselves a useful prompt. Such polygons do not occur on other morphological facies of till on the island, even though end morainal till is not texturally or compositionally distinct. Hence, we need to explain their unique occurrence on end moraines.

Polygon size is inversely proportional to the coefficient of thermal expansion of material in which they form, specifically material just below the permafrost table (P.A. Egginton, personal communication, 1990). The coefficient of thermal expansion of fine till is higher than that of sand and gravel, so polygons should be smaller on till than on sand or gravel. Because polygons on sand and gravel here are 10-50 m across, the 50-100 m polygons on the end moraines are oversized. That is, there is a mismatch between polygon size and properties of the material. We infer that polygon size on the moraines is not controlled by the properties of the surface till but by the properties of different material at shallow depth, just below the active layer. We believe this material to be ice, because ice has a much lower coefficient of thermal expansion than does clay till. Hence, we can account for the large polygons; other features, such as kettles, also imply an ice core.

Northwestern end moraine belt

The northwestern moraine belt is divided into four segments by Ommanney Bay, Drake Bay, and Baring Channel. Moraines continue into the water and may form significant seabed features. Each segment consists of several morainal ridges that formed as ice retreated haltingly. Although the segments are all generally correlative, the number and bulk of moraines diminish northeastward, which possibly indicates that moraine systems in the southwest formed over a longer time. Ice flow and meltwater features on adjoining till (unit T^3b) reveal changes in ice flow during the moraine-forming interval.

Rawlinson Hills End Moraine System

This system spans the peninsula between M'Clintock Channel and Ommanney Bay forming Rawlinson Hills, the most prominent relief on Prince of Wales Lowland (Map 1690A). The range of hills is more than 50 km long, as much as 13 km wide, and consists of 13 or so nested morainal ridges, some running nearly the width of the peninsula. The larger ridges rise 40-60 m, exceptionally 80 m, and are about 1 km wide. Moraine slopes are moderately steep, some attaining angle of repose, and crests are broad and undulating. Ridges trend persistently northeast in the eastern part of the system. In the western part, ridges close to Viscount Melville Sound show the same trend, but ridges farther east trend north.

Curvature of the moraines and ice contact escarpments indicate that they formed when ice stood along their southeast sides. Minor flutings on till east of Cape Richard Collinson record a westward flow that likely accompanied the change in moraine trend there. Flow to the moraines on the east side is recorded by minor flutings on till (unit T^3b) along the west side of Ommanney Bay. These flutings approach the moraine obliquely, presumably because of drawdown into the bay. The Mount Cowie drumlin field, which records flowlines nearly normal to the moraines and which, at first glance, appears to record the moraine-forming flow, dates from an older ice flow phase, as already discussed.

The highest parts of the moraine system rise to about 140 m elevation, only a few metres above postglacial marine limit. Hence, the moraines were deposited on the sea floor. The south end of the system is comprised entirely of glaciomarine sediment (see *Ice contact glaciomarine sediments*).

The ridges and overall morainal topography are disrupted by steep-sided kettles up to 5 km across that appear to penetrate to, or near, the base (Fig. 21). About one-third of the system has collapsed by kettling. Some kettles are filled partly by glaciomarine sediment, which indicates that melting occurred quickly, shortly after deposition and before emergence.

Mount Clarendon End Moraine System

This northeast trending system stretches across the peninsula between Ommanney and Drake bays (Map 1689A). It is 25 km long and 10 km wide and forms the most prominent range of hills on the north side of Ommanney Bay. It includes Mount Clarendon, which rises to about 130 m elevation from a till plain at about 30 m. The system contains 12 or so nested

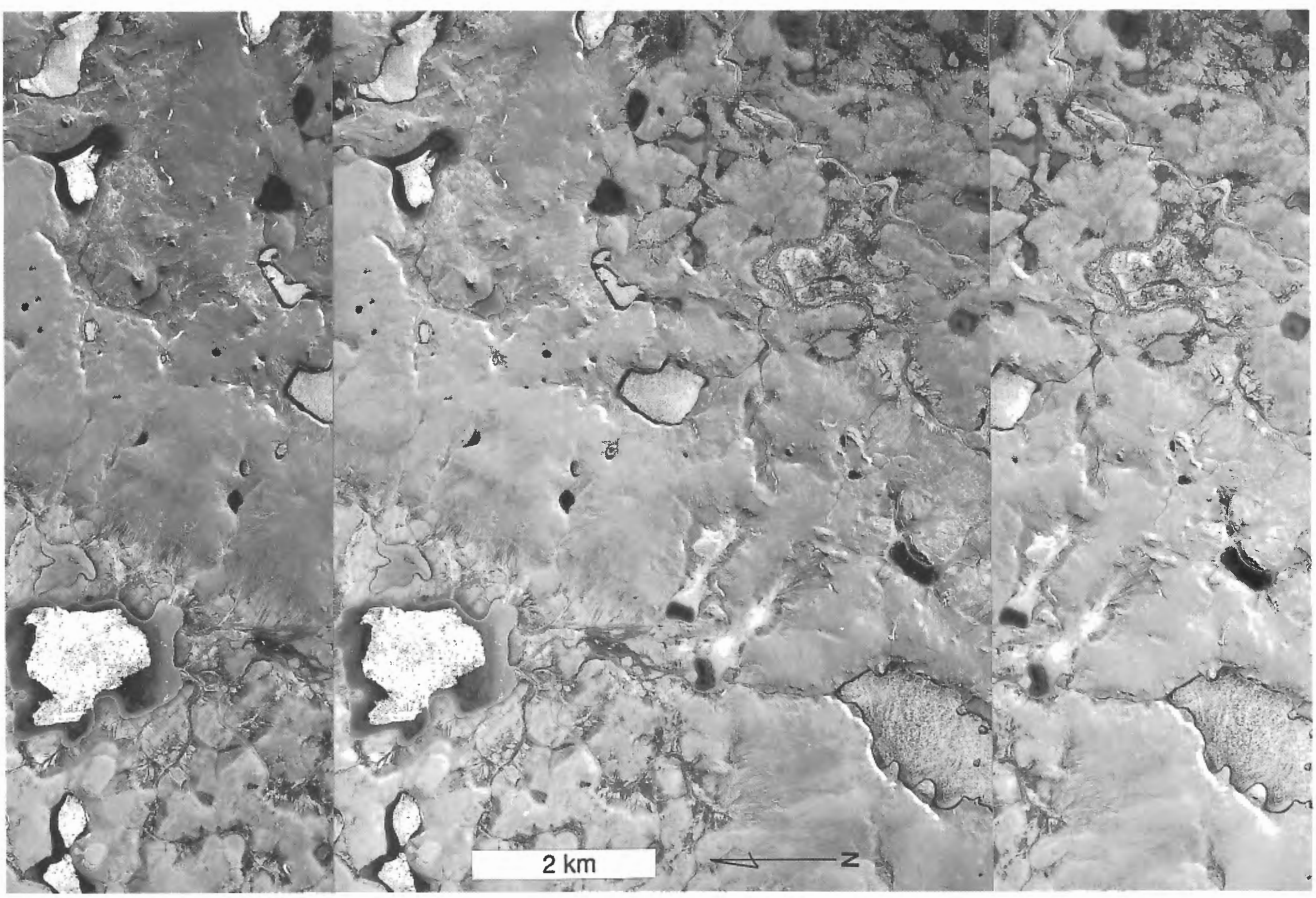

Figure 21. Part of Rawlinson Hills End Moraine System showing broad morainal ridges disrupted by kettles. NAPL A16197-44, 45, and 46

ridges, and small outlier ridges occur to both east and west. The ridges have broad, undulating crests and steep flanks, many at angle of repose (Fig. 22).

In the western and northern parts of the system, ridges parallel the axis of the morainal belt, but at the south end prominent ridges trend southeast. The northwest side slopes gently down to the adjacent till plain, whereas the east and south sides drop off steeply at ice contact escarpments. Hence, the system formed as ice retreated first eastward, then southward.

Flutings and other ice-flow indicators on till (unit T^3b) adjacent to the moraines indicate shifting flows that bracketed and accompanied their deposition (Map 1689A). Flutings adjacent the northwest flank trend northeast and presumably date from a phase of generally northward flow before formation of the moraines. Flutings adjacent the southwest flank near Harrison Point likely record westward flow just before formation of the moraines. Meltwater channels and eskers east of the moraines confirm final northward flow and southward retreat there.

Steep-sided, flat-floored kettles up to 5 km wide disrupt about 50% of the morainal system. Kettles are largest and most closely spaced on the proximal side (Fig. 22). As in Rawlinson Hills, many kettles are filled partly by glaciomarine sediment, which shows that the ice melted before emergence.

Donnett Hill End Moraine System

The Donnett Hill End Moraine System extends with minor breaks for 50 km northeast from Drake Bay to Baring Channel and is up to 20 km wide. The system climbs from low ground at Drake Bay to the plateau surface at about 200 m. Most of it lies inland of postglacial marine limit, and hence, was deposited along a subaerial ice margin. The system has six or seven nested morainal ridges, one of which traverses more than half its length. Ridges trend mostly along the axis of the morainal belt, but, near Baring Channel, they bend and follow the coastline northwestward, descending to sea level at Emily Bay. Here an outlet glacier flowing along the channel from Arabella Bay formed the moraines.

The ridges are tens of metres high, about 1 km wide, and slope moderately (Fig. 23). They are not as bulky as the ridges of Rawlinson Hills or Mount Clarendon systems. This difference may reflect either differences between subaerial

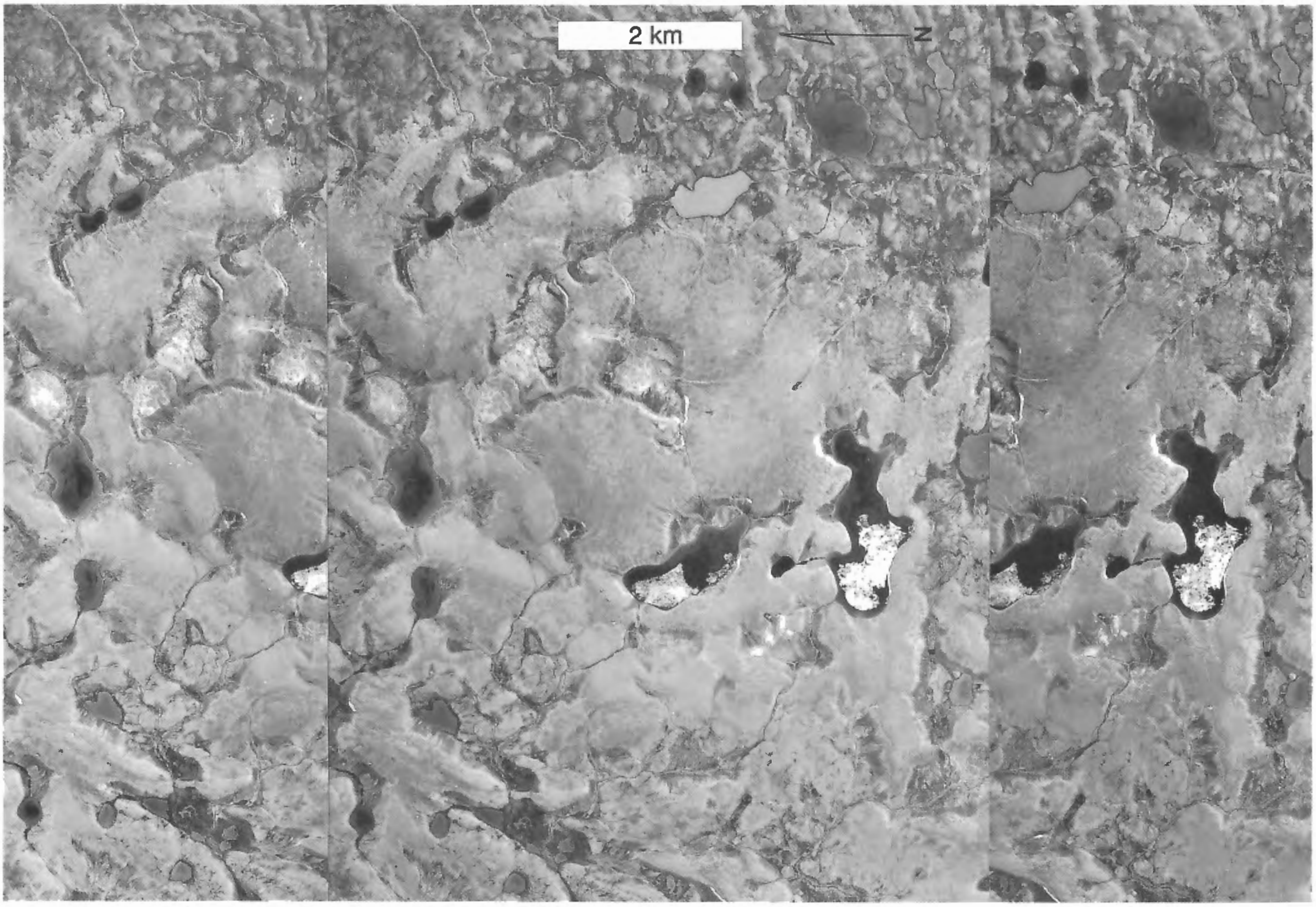

Figure 22. Part of Mount Clarendon End Moraine System showing broad morainal ridges disrupted by kettles. NAPL A16197-86, 87, and 88

and submarine moraine-forming processes or simply a lesser delivery of debris to higher parts of the ice margin than to lower parts or both.

Kettles pock about 20% of the morainal system. Below marine limit, kettles are deep and steep-sided. Above marine limit, they are shallower and have more gently sloping sides; consequently, disruption of moraines above marine limit is minor. The difference in kettling above and below marine limit indicates that ice blocks below marine limit melted before emergence (some kettles contain glaciomarine sediment) and that the submarine active layer was deeper than the subaerial active layer.

Meltwater and ice flow features indicate changing flows as ice retreated to and across the morainal system. West of the moraines, on the lowland between Reliance and Drake bays, are two sets of small till flutings (Map 1689A, Fig. 24); one is superimposed lightly on the other in places. The earlier flow arced northward, then northwestward, whereas the later arced westward, then southwestward across the same area. Both sets of flutings indicate flowlines that were curved sharply on a flat bed. From this we infer drawdown into calving bays, likely small transient features, located first near the mouth of Reliance Bay, then near the mouth of Drake Bay. The younger flow features extend eastward and upslope to the distal flanks of the Donnett Hill End Moraine System, where small drumlins are oriented normal to moraine trend. Hence, northwestward flow was established just before formation of the oldest ridges in the moraine system. Northwestward flow to the moraines is indicated also by eskers in, and upice of, the system and by subglacial and proglacial meltwater channels (Map 1689A). Other meltwater channels and small drumlin fields east of the moraines record a further shift of flow to the northeast into Arabella Bay after ice cleared from the west end of Baring Channel.

Russell Island End Moraine System

The Russell Island End Moraine System spans the 45-km length of that island. It comprises the thickest till on Russell Island but is less continuous, less bulky, and narrower than other parts of the northwestern morainal belt. It broadens along a central lowland and forms a field of minor morainal ridges and hummocky till with a few metres of relief. The more prominent ridges are at the east end, which was laid down above marine limit and has only small kettles (Fig. 25). The western part was laid down mostly below marine limit

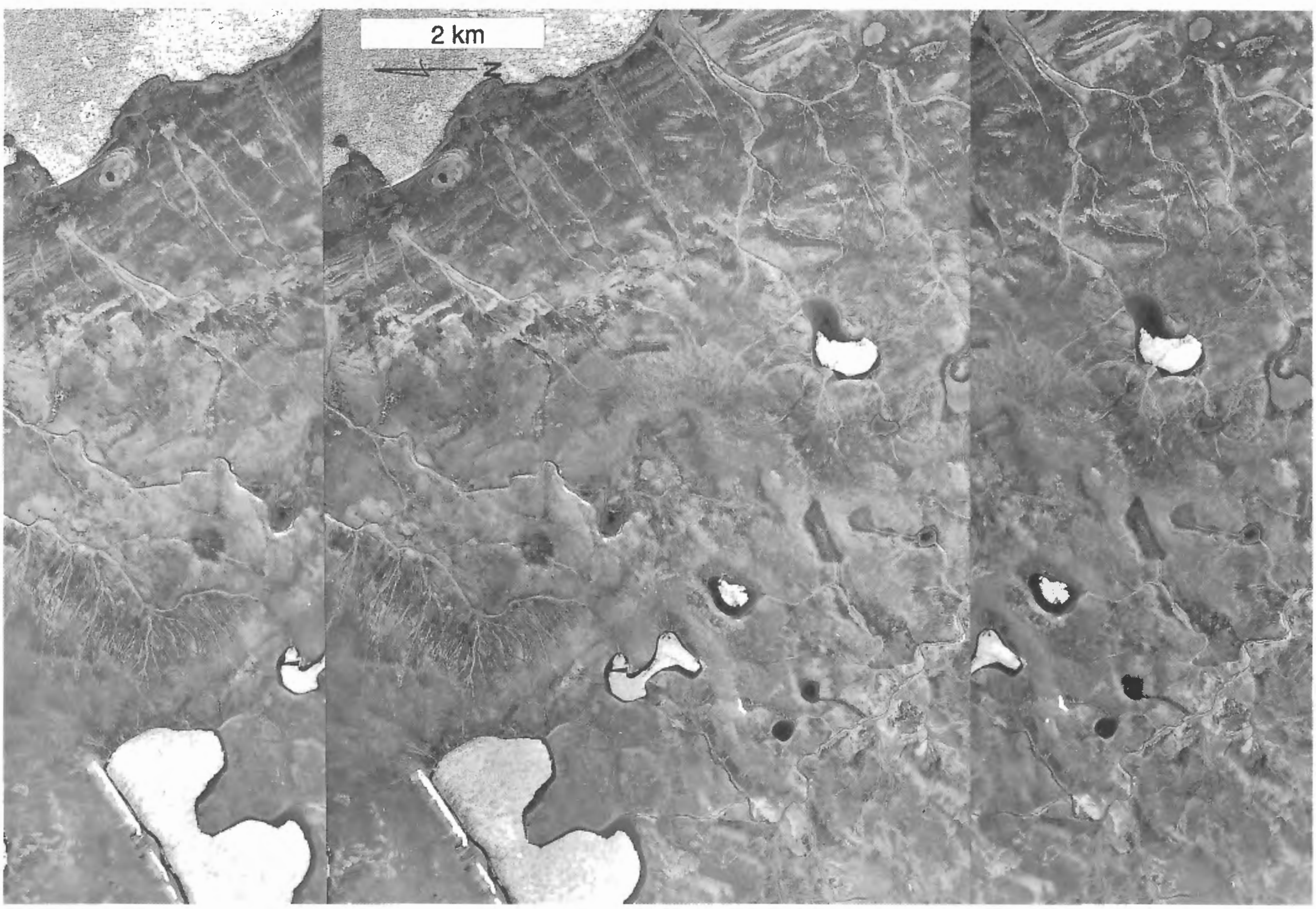

Figure 23. Part of Donnett Hill End Moraine System showing kettled ridges south of Baring Channel. NAPL A16189-4, 5, and 6

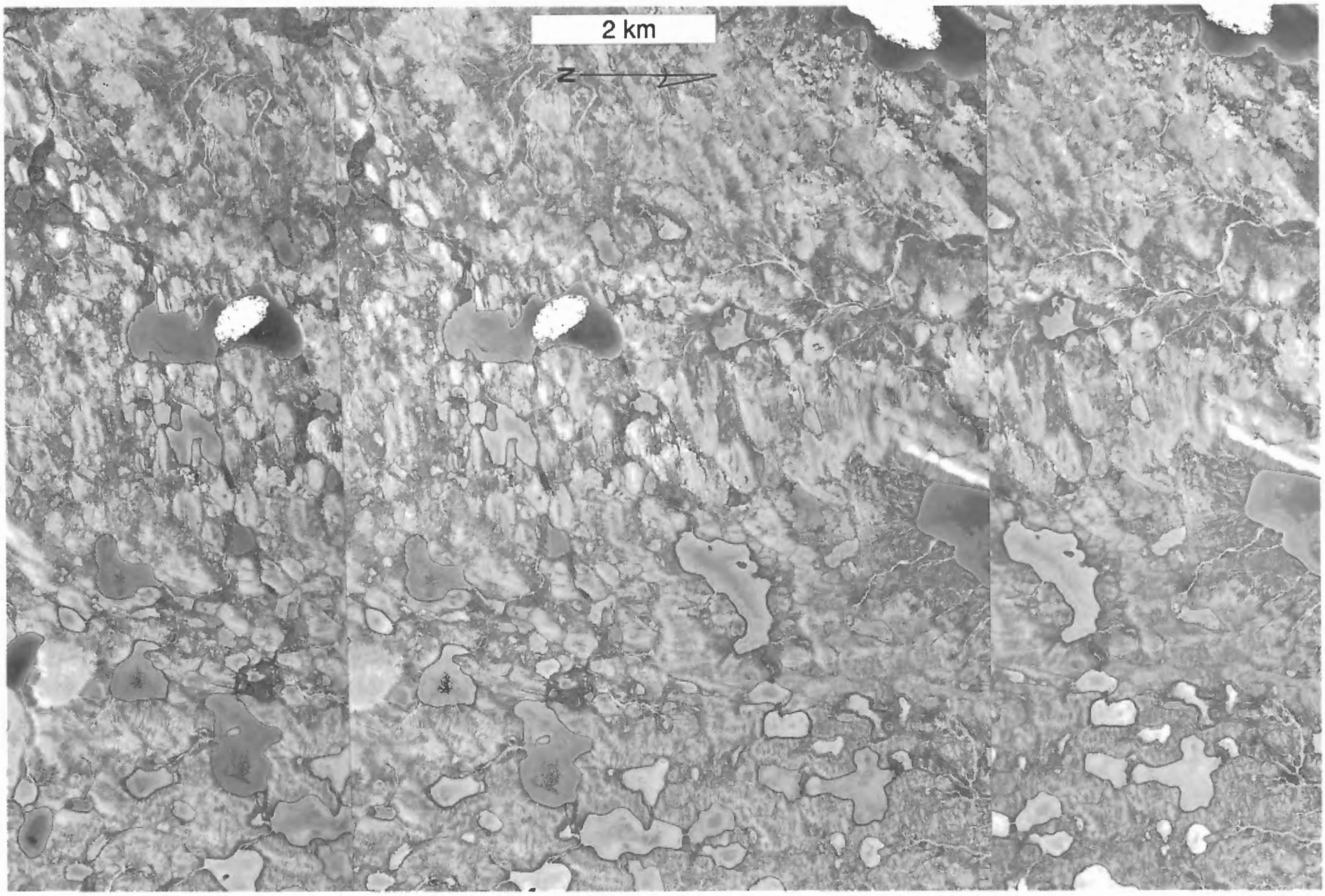

Figure 24. Two sets of lightly inscribed flutings on lowland till plain west of Donnett Hill End Moraine System. NAPL A16189-104, 105, and 106

and ridges there are lower and kettles more common. Moraines parallel the north coast, except at the west end where they parallel Baring Channel and form lateral ridges that correlate with those near Donnett Hill on the other side of the channel.

Ice flowing to the moraines from the southeast strongly moulded bedrock at the east end of the island (Fig. 26A). Tails on the downice side of hard cobbles in conglomerate allow a certain interpretation of sense of flow (Fig. 26B).

North-central end moraine belt

A belt of moraines crosses Prince of Wales Island from Smith Bay to Baring Channel, mostly above marine limit. The moraines are of two sorts but are not divided on the geological map.

Moraines in the valley leading to Smith Bay and in the northern half of the belt share characteristics with those of the northwestern belt, already described. Some smaller occurrences lack distinct ridges, but stand in relief above surrounding till, are typically kettled, and have the large, rectangular polygons that characterize larger moraines.

Moraines in the southern part of the belt differ in important aspects from other moraines on the island and likely formed differently. The largest set comprises eight nested ridges midway between Smith and Browne bays. Ridges are 10-20 m high and a few hundred metres wide, with slopes approaching angle of repose. In places crests are narrow and jagged; the high-standing, jagged parts consist of blocks of rock many metres across, which gives the appearance that the moraines are composed largely of ice-thrust bedrock slabs or megaclasts. Till elsewhere on the moraines is commonly very stony.

In a morainal area north of Beams Brook headwaters, steeply dipping slabs of rock with intervening diamicton give rise to parallel ridges. Bedrock here is horizontally disposed, so we infer that the rock slabs, which dip against final ice flow, are imbricate ice-thrust masses.

A prominent moraine 15 km northeast of Smith Bay appears similar on airphotos to those just described (Fig. 27). Large blocks or slabs of resistant material (rock) are discernible, mainly on the crest and resting on till. However, their appearance may be due to backwasting of the slopes, which would exhume blocks along the crest.

These steep, narrow moraines with megaclasts lack both the kettles and large polygons that characterize most other moraines in the area. We infer, therefore, that they are not extensively ice cored, though small bodies of buried glacier ice may occur.

The morphological and compositional differences between these and the other moraines imply that they formed by different processes. Incorporation of large rock masses suggests a cold-based margin that was thrusting frozen-on rock and till to form the narrow ridges. This interpretation is preferred over shearing and stacking of debris within the ice because that would lead to formation of ice-cored moraines. Till behind these moraines is not streamlined, possibly because of the postulated cold-based condition. Similarly, the only terrain on the island that shows no sign of glacial erosion, hence must have been covered by cold-based ice (unit C, described in *Residuum and colluvium*), lies just behind the largest set of these moraines.

Eastern end moraine belt

The eastern end moraine belt is the smallest of the three. Its largest component is located just south of the head of Young Bay, but smaller, generally single, moraines that date from the same interval of deglaciation occur northward to inner Browne Bay and southward to Guillemard Bay (Map 1690A).

The moraines south of Young Bay consists of eight closely spaced ridges near the base of the slope from the plateau to the east. The ridges have broad, hummocky crests and only moderate slopes. They lack kettles and large ice-wedge polygons, but numerous flow-slide scars on their flanks and on adjacent hummocky and lightly fluted till may signify buried glacier ice locally. A small set of ridges 5 km to the southwest appear on the airphoto to be superimposed by lightly inscribed southeast-oriented flutings, which possibly indicates a readvance. Moraine curvature, topographic position, and orientations of streamlined till forms and meltwater channels indicate that these moraines were formed by ice along their west sides.

A moraine northeast of the mouth of Guillimard Bay is concave to the north-northwest. Till (unit T^3b) behind it has southeast-oriented streamlined forms over a broad area, which are correlated with the moraine. The moraine and flow pattern indicate that southern and western Prince of Wales Island remained ice covered until deglaciation of Franklin Strait.

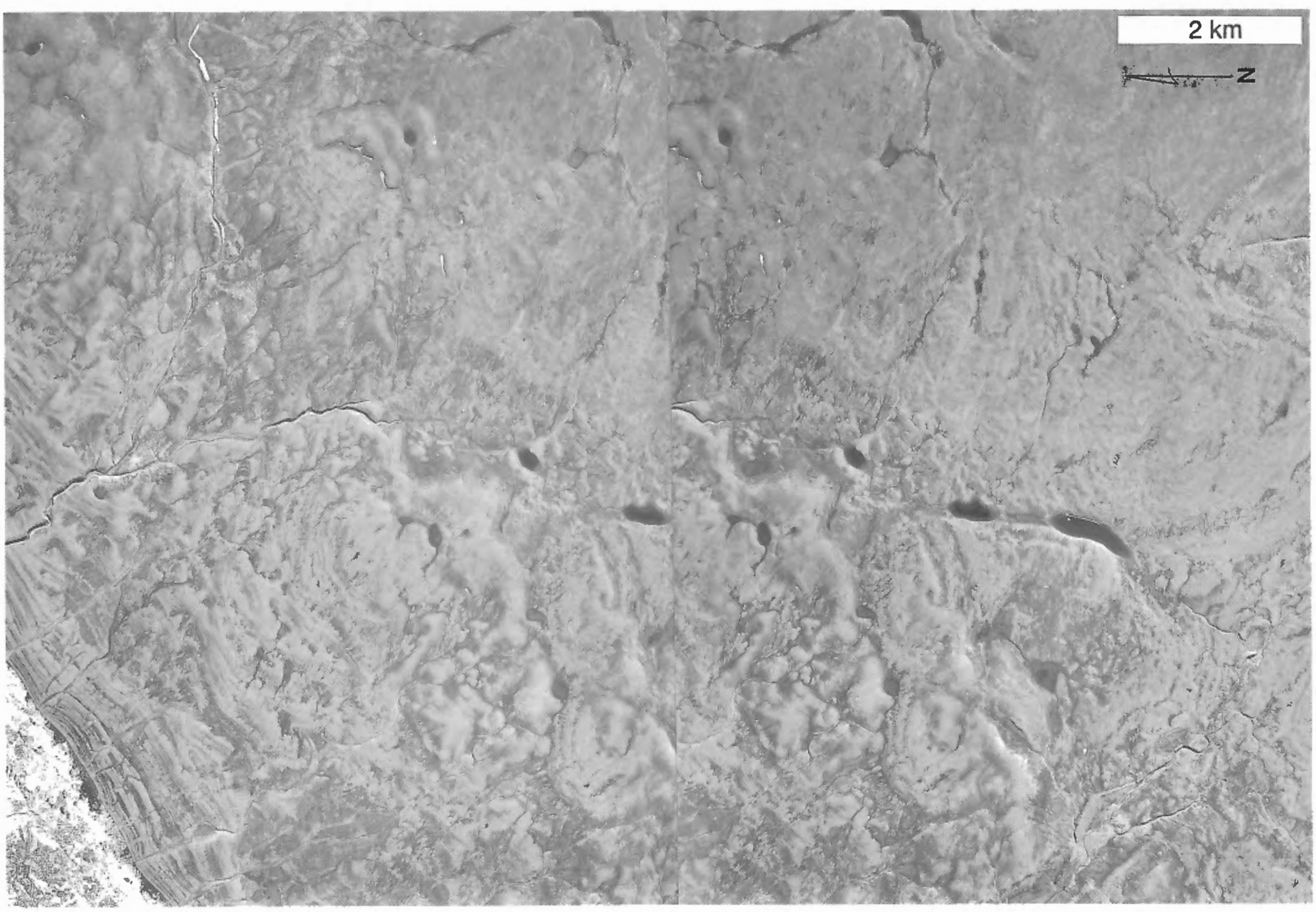

Figure 25. End morainal ridges with small kettles on eastern Russell Island. NAPL A16153-69 and 70

Figure 26A. Ice moulded bedrock on eastern Russell Island. NAPL A16188-33, 34, and 35

Figure 26B. Miniature crag-and-tail in conglomerate on eastern Russell Island. Crag is formed by a large quartzite cobble with tail in lee to right. Lens cap gives scale. GSC 1991-411

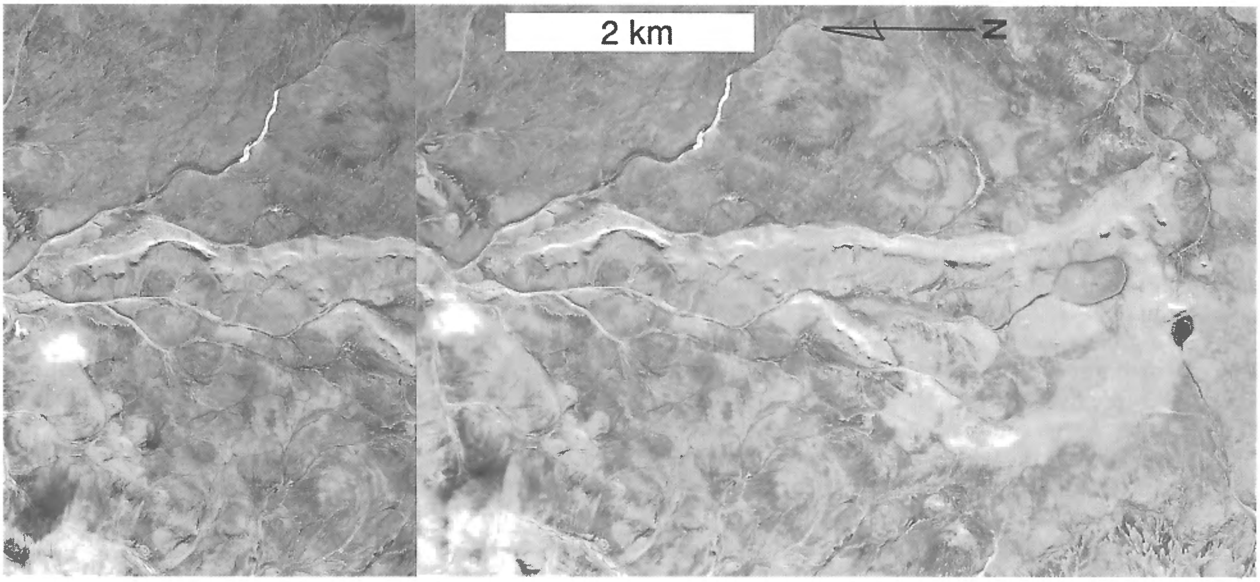

Figure 27. Prominent end morainal ridges northeast of Smith Bay with megaclasts forming jagged and steep-sided areas along crests. NAPL A16174-106 and 107

GLACIOFLUVIAL SEDIMENTS AND LANDFORMS

Glaciofluvial sediments are a minor part of the Quaternary assemblage, covering <1% of the terrain. Occurrences are small and scattered, generally <10 m thick, and composed mostly of gravel. Hence, materials that form the largest and most easily exploited granular resources in many parts of Canada are scarce here.

On maps 1689A and 1690A, glaciofluvial sediments are divided into two groups: deposits laid down in contact with ice and deposits laid down beyond ice. Each is subdivided into two morphological facies. Erosional glaciofluvial landforms are much more widespread than these deposits and are useful in interpreting ice flow directions and basal ice conditions. They are discussed below, along with associated deposits, according to the environment in which they formed, subglacial or ice marginal.

Ice contact stratified drift (units Gh and Gr)

Ice contact stratified drift comprises eskers and kames scattered throughout the area. The eskers and subglacial meltwater channels formed mostly, but not exclusively, during final phases of deglaciation in wet-based areas just behind the ice margin. Kames and lateral meltwater channels formed along the margin.

Eskers and subglacial meltwater channels

Eskers here are small, simple forms. The largest is 18 km long, the highest part of it forming Mount Cowie, where it rises 10 m or so above Arrowsmith Plains; the name is more a tribute to the monotonous relief of western Prince of Wales Island than to the size of the esker. Other eskers are typically 2-10 km long, about 5 m high, and about 10 m wide; all are simple, single ridges and many connect with subglacial meltwater channels of comparable width and depth.

Most eskers formed during ice flow phase 3 or later, for most are superimposed on till unit T^3b. This association supports the inference that this till formed under warm-based ice. But even here meltwater features are small and discontinuous; evidently, the ice sheet lacked a large internal or basal network of meltwater streams, which perhaps indicates low rates of basal melting. The only "swarm" of eskers is on the peninsula south of Drake Bay, where a dozen short, parallel eskers and connecting subglacial meltwater channels formed during northward flow just after ice pulled back from the Mount Clarendon End Moraine System. These and other eskers on unit T^3b formed in the ice marginal zone as indicated by their relationship to ice marginal features and by alignment along deglacial flowlines.

Some esker-like features on the older till units may have formed during phase 3 as well. If they are eskers, at least two of them would have formed well behind the ice margin. Either they could indicate small, isolated corridors of warm-based ice that extended for a while headward into the cold-based ice zone within which the older tills and their landforms were preserved during phase 3; or they could have formed englacially and lowered by meltout onto the older till. A small, segmented feature oriented east on unit T^1p, east of Harvey Point, crosses the megaflutes of Arrowsmith Plains and hence postdates them. It aligns with drumlins in the axis of the Transition Bay drumlin field and small tributaries join it from the southwest, which suggests that it was formed by eastward flowing water. Similarly, the Mount Cowie esker crosses the megaflutes of Arrowsmith Plains. It continues across part of the Ommanney Bay ribbed moraine field at a right angle to the flowline of ice that formed the ribbed moraine. It curves slightly to align with a subglacial meltwater channel incised in the ribbed moraine, where the ribbed moraine has been remoulded partly into northeast trending flutings. Hence, though the esker lacks a clearly directional morphology, it likely indicates eastward meltwater flow after phase 2.

If the direction of flow of these two eskers is properly interpreted, they must have formed before deglaciation of Ommanney Bay and likely before formation of the Rawlinson Hills End Moraine System. Ommanney Bay and Rawlinson Hills were among the areas to be deglaciated earliest. Once deglaciated, the source of eastward flowing ice during phase 3 had been removed. Therefore, the eskers date from phase 3 rather than from a subsequent deglacial flow phase. Thus, they predate northward oriented flutings that record deglacial flow into Ommanney Bay a few kilometres north of the Mount Cowie esker, and their preservation during this later flow indicates that they were overlain by cold-based ice.

Other small esker-like features on Arrowsmith Plains trend north-northeast near Thackeray Point. These features either may have survived from phase 1 or may record local, temporary, wet-based ice streaming into the Transition Bay drumlin field.

No eskers occur in the Crooked Lake drumlin field of phase 2, but four occupy the distal Ommanney Bay ribbed moraine field, thought to have formed at the same time. These eskers form a parallel set and trend along the flowline of ice that formed the ribbed moraine. Hence, they could date from phase 2, though they could just as well date from later deglacial flow into Ommanney Bay after phase 3.

As mentioned, subglacial meltwater channels that connect with eskers are comparable in size to the eskers, as though the eskers represent storage of material eroded from the channels. However, larger channels either lack associated eskers or have small eskers set in them or at their mouths. One large channel crosses Russell Island along the deglacial ice flowline. Another occurs just behind and parallel to the Rawlinson Hills End Moraine System; it likely resulted from drawdown flow into Ommanney Bay as recorded by flutings on till unit T^3b nearby. Two large, rock-cut channels southwest of Arabella Bay display a 90° change in meltwater flow (Fig. 28). The older channel formed by northwest flow toward the Donnett Hill End Moraine System, whereas the younger formed by northeast flow after the sea calved a bay in the ice front behind the moraine system. A sandur at the mouth of this channel grades to marine limit.

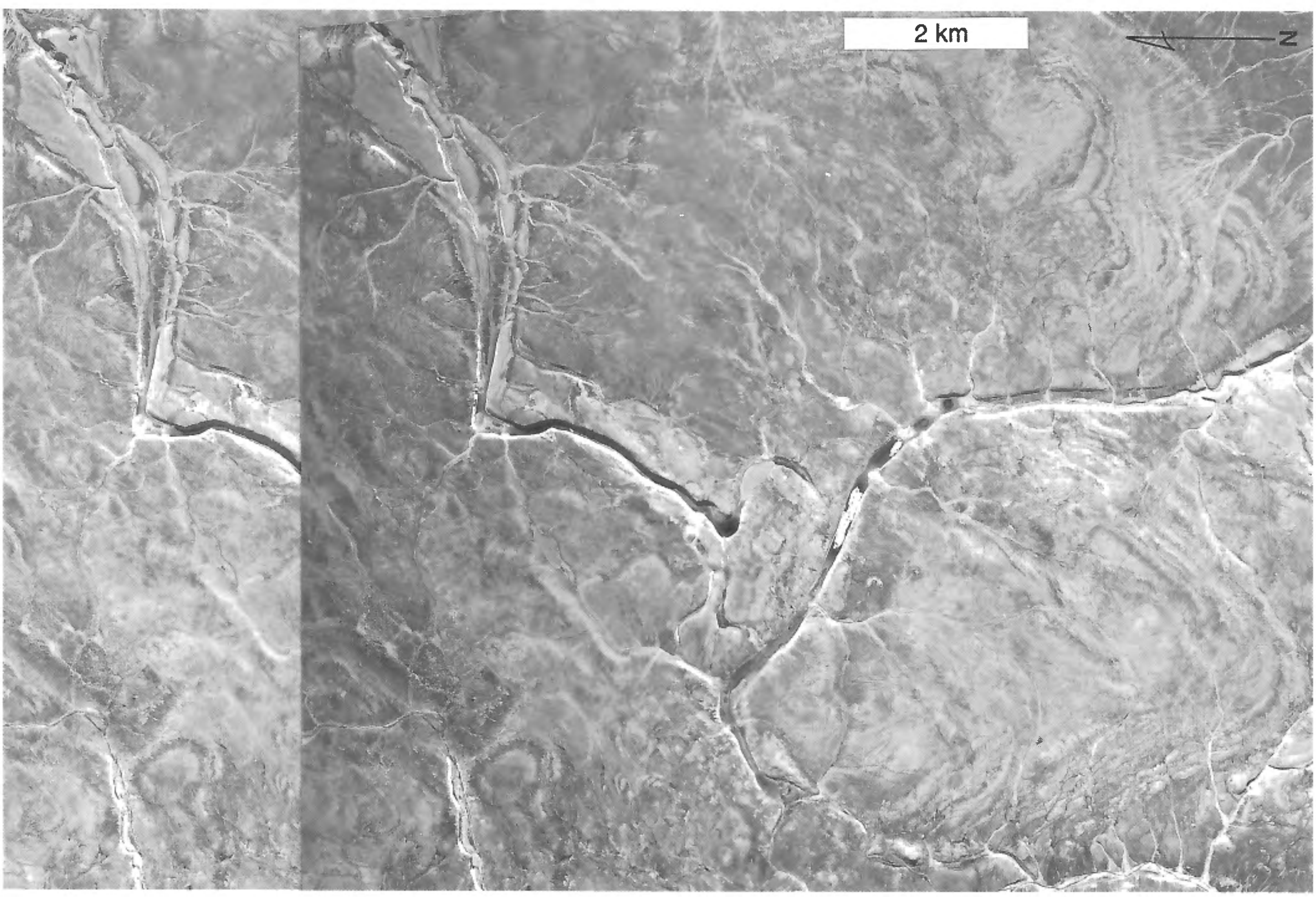

Figure 28. Subglacial meltwater channels on the plateau southwest of Arabella Bay. NAPL A16174-8 and 9

Till adjacent to subglacial meltwater channels for tens to hundreds of metres is distinctly modified. The upper part commonly is exceedingly stony or is stone armoured (Fig. 29). The stone armour forms a rill pattern in places, with rills uniting toward the channels. Subglacial meltwater seems to have flowed in sheets that either became channelled at the centre or later became channelled. The till must already have been deposited to be thus modified, so we infer that it was deposited by lodgment. Still, some larger channels are filled partly by till (to too large an extent to be accounted for by postglacial solifluction) so in places till deposition continued after channel cutting.

The depth of modification by subglacial meltwater sheetflow seems to have been only a few tens of centimetres, less than the active layer thickness. Till from low in the active layer rises in numerous decimetre-scale diapirs through the armour of clasts to form sorted circles of high relief. Identical features occur where till rises through thin beach gravels.

Most subglacial meltwater channels, like eskers, are in till unit T^3b and formed during deglaciation, as already illustrated for specific features. Again this relationship indicates warm-based ice in the area of unit T^3b, though the size and number of channels seem to indicate a low rate of basal melting. No meltwater channels or other meltwater features are associated with glacial bedforms of phases 1 and 2, so meltwater activity was not important in forming the megaflutes of Arrowsmith Plains or the drumlins of the Mount Cowie or Crooked Lake drumlin fields (cf. Shaw and Sharpe, 1987).

Kames and ice marginal meltwater channels

Kames, like eskers, are scattered, isolated bodies. The larger kames are parts of end moraine systems, though nowhere do they dominate. They are most common in the north-central end moraine belt, possibly because most of it formed along a terrestrial ice margin. One diffuse morainal belt consists mostly of kames. It extends north-south just east of Prince of Wales Lowland. The kames occupy summits that extend above marine limit. Adjacent ice marginal and proglacial meltwater channels indicate that the kame moraine belt formed along westward retreating ice. Other kames farther west on south-central Prince of Wales Lowland may record continuation of westward retreat.

Lateral meltwater channels differ from other meltwater channels and from postglacial channels in topographic position; they nearly follow contours of hillsides, decreasing in elevation down glacier. They formed where meltwater coursed along valley ice lobes. Meltwater was prevented from dispersing submarginally either because the margin was frozen to its bed or because of outward subglacial water pressure. Because subglacial meltwater features do not occur on the same slopes, lateral channels here likely indicate a cold-based ice margin. Lateral channels are also abundant on

Figure 29. Stone armour resulting from meltwater erosion of till adjacent to large subglacial meltwater channel shown in Figure 28. GSC 1991-412

Somerset and Baffin islands where they formed during retreat of cold-based ice caps, but they do not occur in Keewatin where the marginal zone appears to have been warm-based during retreat (Dyke and Dredge, 1989).

In that they are subaerial features, they are restricted to terrain that was not submerged at time of ice retreat. On southern Prince of Wales Island, they occur in the kame moraine belt just described and in abundance on hillslopes of the eastern plateau. They are even more common on the northern plateaus.

These channels are incised mostly in till; rarely they extend into rock. Some are no more than ribbons of stone armour on till, barely recessed (Fig. 30). They are more conspicuous on airphotos than on the ground because their continuity is disrupted and margins distorted by solifluction. Most are well formed channels, 1-2 m deep. In several south trending valleys on the northern plateau, they occur more profusely on western than on eastern valley sides, which perhaps reflects greater ice ablation during afternoons. Some western valley sides are so riddled with lateral channels that ridges between them are no wider than channel floors (Fig. 31). Local patterns of ice retreat there are recorded in great detail.

Proglacial outwash (units Gp and Gf)

Proglacial outwash was deposited as sandurs and fans, which, being subaerial deposits, are restricted to areas above marine limit. The largest deposits cover only a few square kilometres. Many, because they grade to marine limit or to glacial lake shorelines enable us to define these former water plains. The largest deposits are at the mouths of meltwater channels (e.g., Fig. 28) and represent deposition of the coarser material ripped out to form the channels. Nowhere, however, was sedimentation sufficient to produce glaciomarine deltas such as are common in areas of Laurentide glaciation farther south. Where lateral meltwater channels are closely spaced, fans formed at marine limit at their mouths and coalesced laterally as the ice receded to produce bands of gravel along hillsides (Fig. 31). Here again, most material in these deposits is likely material stripped from the channels; little came directly from ice.

GLACIOLACUSTRINE SEDIMENTS AND LANDFORMS (unit L)

A dozen or so glacial lakes formed where the ice front retreated downslope on the northern plateau. All indicate generally southward retreat, and hence, accord with other ice margin indicators. Extensive lacustrine sediment veneer rings the residuum- and colluvium-mantled summit between Smith and Browne bays. The configuration indicates that the summit appeared first through the ice as a nunatak, then formed a re-entrant in the ice margin, open to the north.

Figure 30. Small lateral meltwater "channel" expressed as a stone lag on till. GSC 1991-413

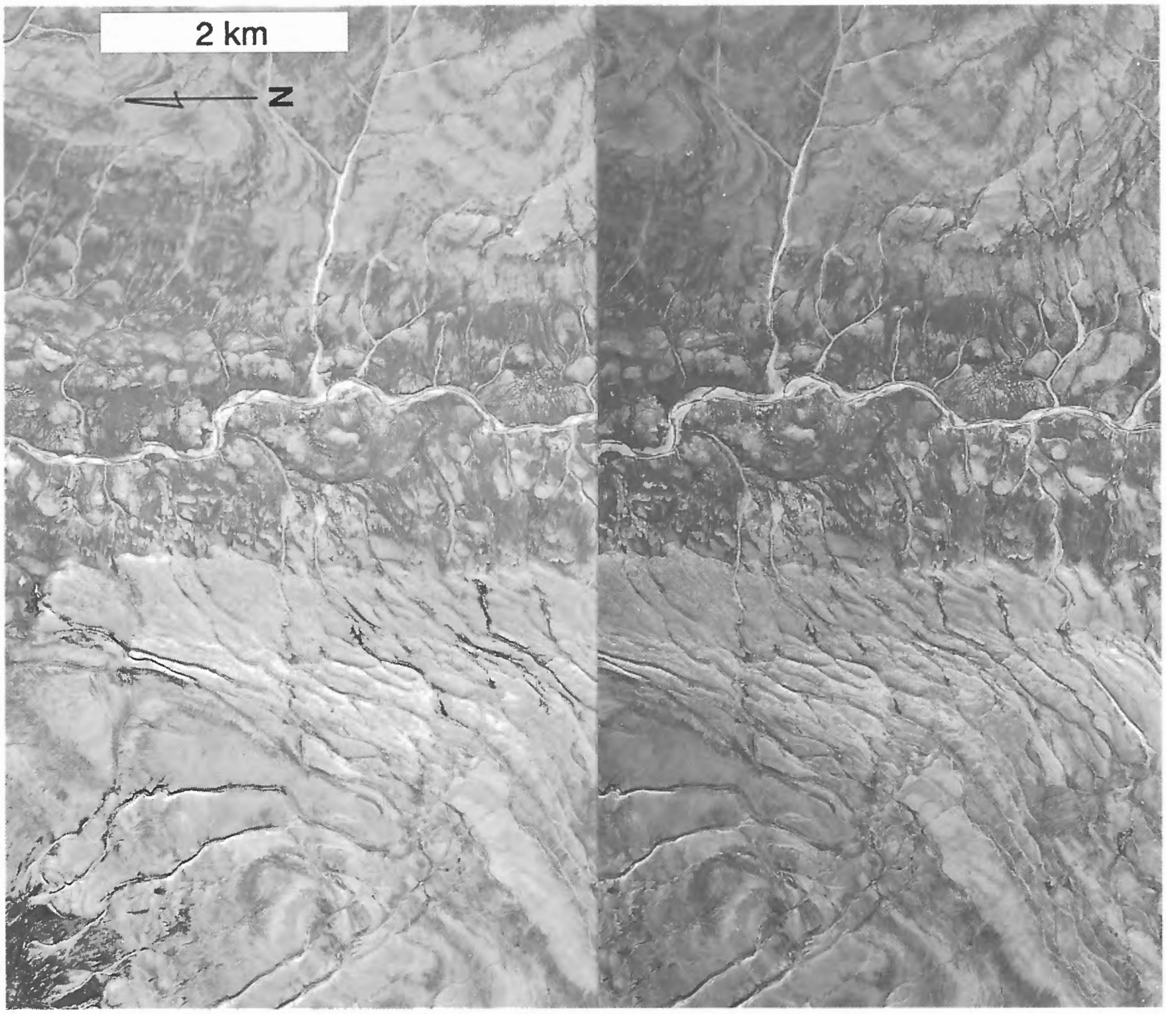

Figure 31. Nested lateral meltwater channels with coalescent fans at their mouths graded to marine limit marked by the contact between light-toned fan gravels and dark-toned marine silts. NAPL A16174-13 and 14

Glacial lakes are identified from fine waterlaid sediment in basins above marine limit and exceptionally from shoreline features. The fine deposits are sufficiently water retentive that they are well vegetated. The sediment is mostly stony, sandy silt about 1 m thick. Larger deposits fill basins enough to form plains.

A coarser deposit, mostly sand, nearly filled a glacial lake between Baring Channel and Back Bay. It is flanked by myriad lateral channels and much of the material may have come from the channelled slopes. A moraine at the south end marks the ice margin that held up the lake in its final phase. The outlet leads northwest from the deposit, which lies at 135 m asl, 40 m above marine limit. Sparse marine shell fragments from the lacustrine sand have amino acid ratios indicating Sangamonian age (Table 1). Such shells also occur in till and in at least two other glaciolacustrine deposits and have been redeposited from the ice sheet.

The occurrence of marine shells in lacustrine deposits confuses distinction of marine and lacustrine deposits. Lacustrine deposits occur sporadically at all elevations down to marine limit, as expected. A useful distinguishing criterion is the lower elevational limit of subaerial glaciofluvial features or deposits in the vicinity of waterlaid deposits. If lateral or proglacial channels or outwash occur lower than fine, waterlaid sediment, that sediment must be lacustrine.

An elevational sequence of landforms and deposits on southeast-facing slopes northwest of inner Browne Bay illustrates this point (Map 1689A). Glaciofluvial fans with apexes at 120 m end at a former water plain at 110 m, below which lies fine, waterlaid sediment that extends a few metres lower. Just east of there, two proglacial meltwater channels lead to a sandur that ends at more waterlaid sediment at 95 m. Nearby, lateral channels descend to a sharp washing limit at 95 m. The higher waterlaid sediment is glaciolacustrine; the lower sediment is marine.

GLACIOMARINE SEDIMENTS AND LANDFORMS

Glaciomarine sediments are locally dominant materials. Being fine grained and water retentive, they are lushly vegetated and largely covered by peat. Much of the plant biomass of the area occurs on them so they provide vital wildlife habitats. They cover about 10% of the area, the largest deposit covering about 800 km^2, and are up to 30 m thick. They are mostly silt with clay and fine sand, laid down in water tens of metres deep. Dropstones, including boulders, are common in these sediments, which in places are so stony as to resemble till. They are variably fossiliferous, barren over large areas and intervals, and prolifically shell-bearing in others.

On Maps 1689A and 1690A these deposits are divided into ice contact and proglacial facies, each to be discussed separately. Iceberg scours are widespread glaciomarine landforms not at all restricted to areas of glaciomarine sediment.

Ice contact glaciomarine sediments (unit Mm)

Occurrences of this facies are restricted to one part of the island. Numerous conical kames about 10 m wide sit on the till ridges of Rawlinson Hills End Moraine System. They resemble moulin kames, normally composed of glaciofluvial sediment, but were deposited in the sea and are composed of stratified silt, clay, and fine sand with dropstones and gravelly surface lags. The forms may result from deposition in narrow recesses in the ice front. Other minor bodies form ice contact terraces, built of similar material, also resting on the till ridges. The steep slopes of these minor deposits are being modified by gulleying and liquefaction.

The southern third of Rawlinson Hills End Moraine System is entirely ice contact glaciomarine sediment (Fig. 32). It forms a 5-10 km wide belt of hummocky terrain with local relief of about 10 m. Several high end morainal ridges occur in the belt. Large kettles in the southwestern part indicate that it accumulated among blocks of ice, perhaps grounded icebergs.

The morainal ridges are hummocky and pitted in places and simple, sharp-crested, forms elsewhere. They rise well above surrounding hummocky sediment. Typically they are 20-30 m high, but near the south end sedimentation progressed to sea level and made about 90 m of relief. Here the moraine includes an ice contact gravel delta, the only part that is mostly coarse material. A ridge farther north consists of glaciomarine sediment at one end but till at the other, with a sharp transition. The compositionally different segments have different morphologies (Fig. 32).

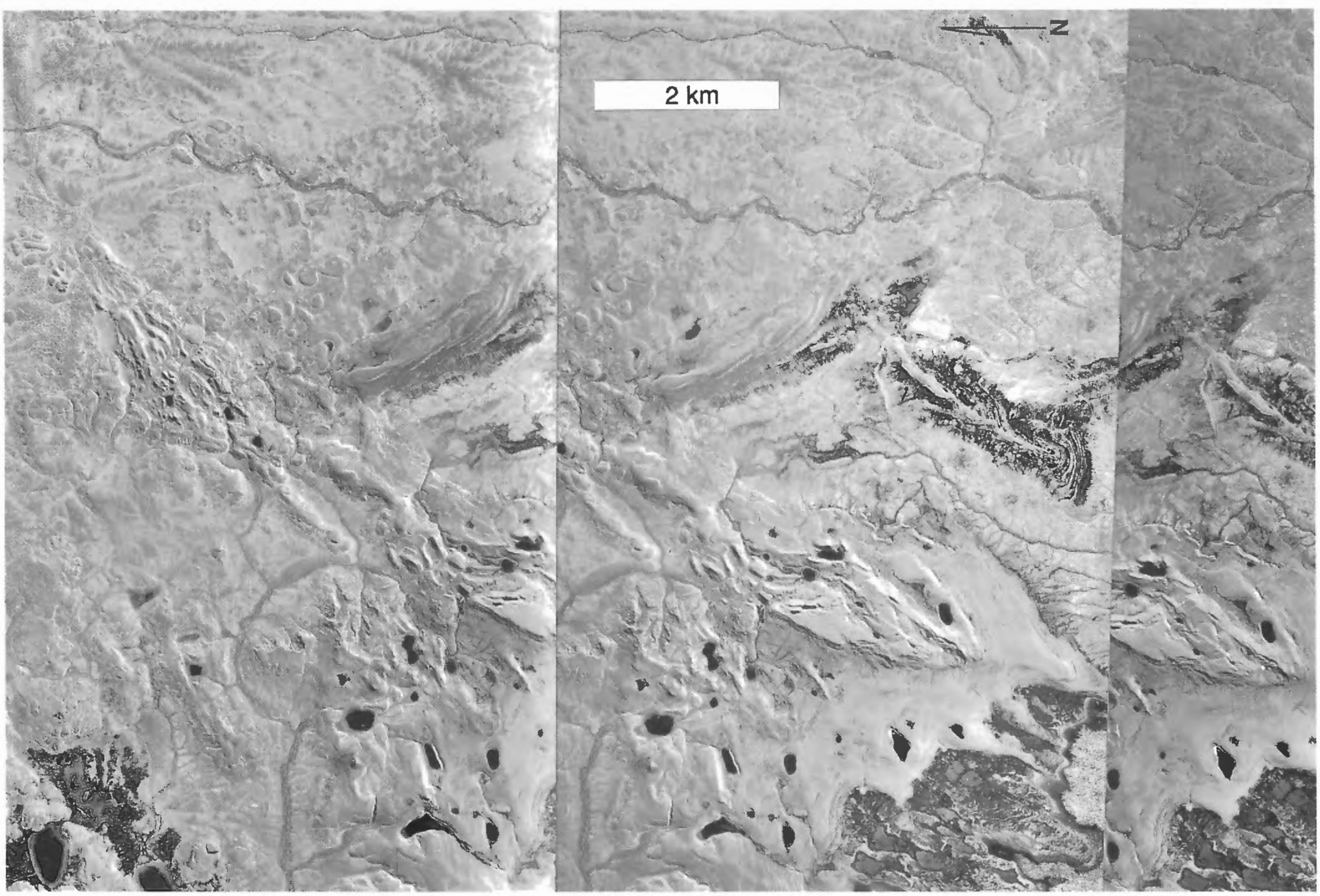

Figure 32. Ice contact glaciomarine sediment comprising part of Rawlinson Hills End Moraine System. NAPL 16197-70, 71, and 72

The overall ice contact deposit is mainly silt and fine sand that, in the ridges, includes rhythmic beds up to 1 m thick. These beds seem horizontal on the proximal flank of a moraine (Fig. 33). Fluvial erosion accounts for much of the relief on the moraine slopes and exposes thick, persistent, horizontal beds (Fig. 34). The surface bears a variable sprinkling of dropstones. Where stones abound, the surface resembles that of till; other areas are stone-free.

Figure 33. Thick, horizontally bedded sediment exposed in a morainal ridge composed of glaciomarine sediment. Trikes on top of ridge provide scale. GSC 1991-414

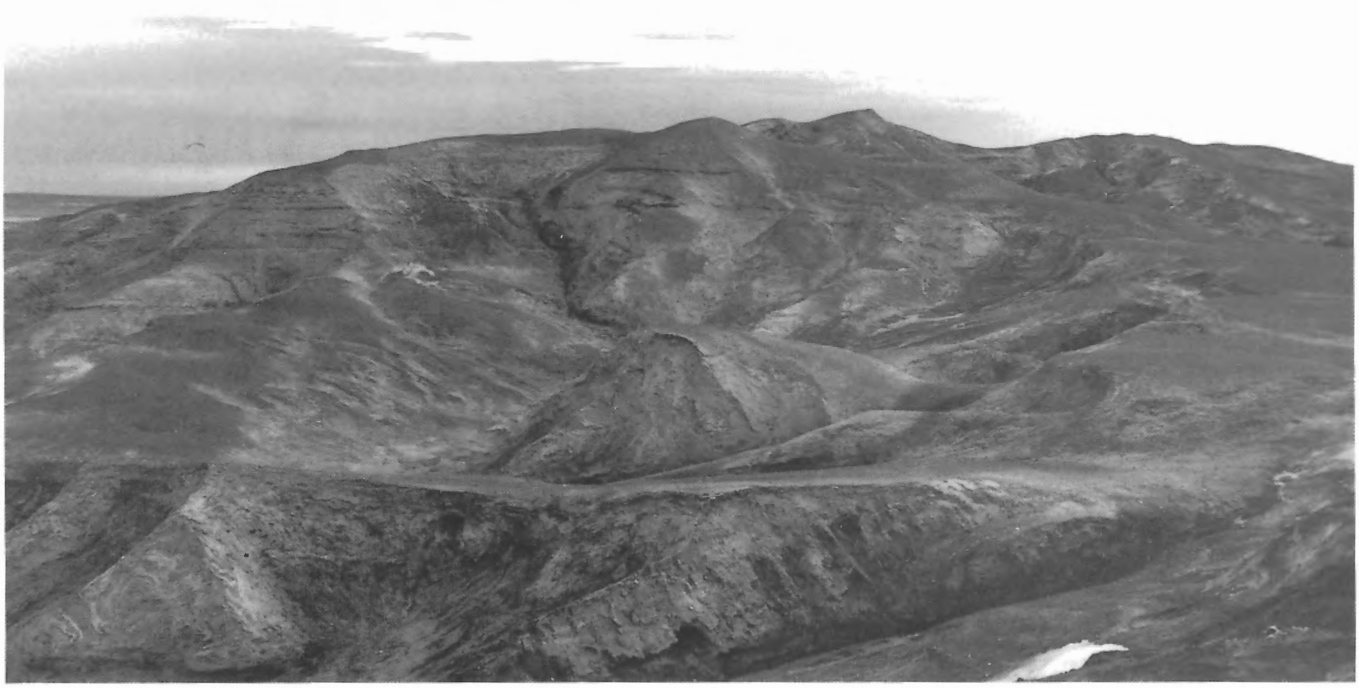

Figure 34. Fluvial erosional relief on part of the Rawlinson Hills End Moraine System where composed of fine glaciomarine sediment. GSC 1991-415

Deepwater proglacial marine silts (units Mb and Mv)

Most glaciomarine sediments settled in proglacial basins far enough from ice that they lack ice contact features. Deposits are more-or-less evenly split between those <2 m thick that form veneers over till (unit Mv) and those 2-30 m thick that blanket the morphology of till underneath or form plains (unit Mb).

These deposits occupy most broad, shallow basins of Prince of Wales Lowland and valleys in the north and east. They fringe, hence extend beneath, many lakes. Most bodies probably are <5 m thick, but this depth is hard to assess because few are dissected.

The thickest, most extensive deposit is east of Rawlinson Hills End Moraine System. It probably settled in a basin made between the retreating ice front to the southeast and end moraines to the northwest. Thus, it represents a continuation of sedimentation that formed the southern part of the moraine system. The ice margin apparently released much sediment over 40 km. Why it did so here yet not along most of the margin is not obvious, but perhaps signifies slower recession here.

Much of the centre of this deposit has badland topography with up to 30 m of relief caused by thermokarst (Fig. 35A) and associated stream erosion (Fig. 35B). Massive ground ice in walls of thermokarst depressions (Fig. 35C) and extent of erosion suggest that much of the apparent sediment thickness results from ground ice inclusions. This ice is likely segregation ice derived from saline pore water since emergence rather than buried glacier ice, because it is impossible to accumulate thick glaciomarine sediment over large areas of glacier ice. Most fine marine deposits here, at least those now eroding, contain saline ground ice; their surfaces commonly show salt efflorescence.

As ice retreated in the sea across the island, it released little sediment into water. Currents moved what was released into lows. Evenly spread, the sediment would be only centimetres thick. Such low net glaciomarine sedimentation, in an area where thick and extensive till indicates a debris-rich ice sheet, can be interpreted variously. Perhaps most glacial debris was lodged as till before retreat, hence the retreating ice front was relatively clean; or perhaps the main mechanism of retreat was calving with bergs ablating little locally.

Most proglacial marine silt likely was laid down within a few kilometres of the ice because sediment supply was greatest during retreat. Indeed, some sediments extend to marine limit; others are focused in front of meltwater channels or sandurs. The deposit at Donnett Hill, for example, reaches marine limit just beyond a ridge of the Donnett Hill End Moraine System. Similarly, a thick deposit in front of a sandur graded to marine limit southwest of Arabella Bay was laid down along with the sandur. Extensive marine silts in the valleys south of Arabella Bay extend in many places to marine limit where they contact outwash at the mouths of meltwater channels (e.g., Fig. 31). Radiocarbon dates on shells and whale bones from these proglacial sediments help define the chronology of deglaciation and sea level change outlined in *Quaternary history*.

Iceberg scours

Iceberg scours are common, widespread lineaments on till and glaciomarine sediment on Prince of Wales Lowland. Typical lineaments are 1 km long, 1 m wide, and <1 m deep;

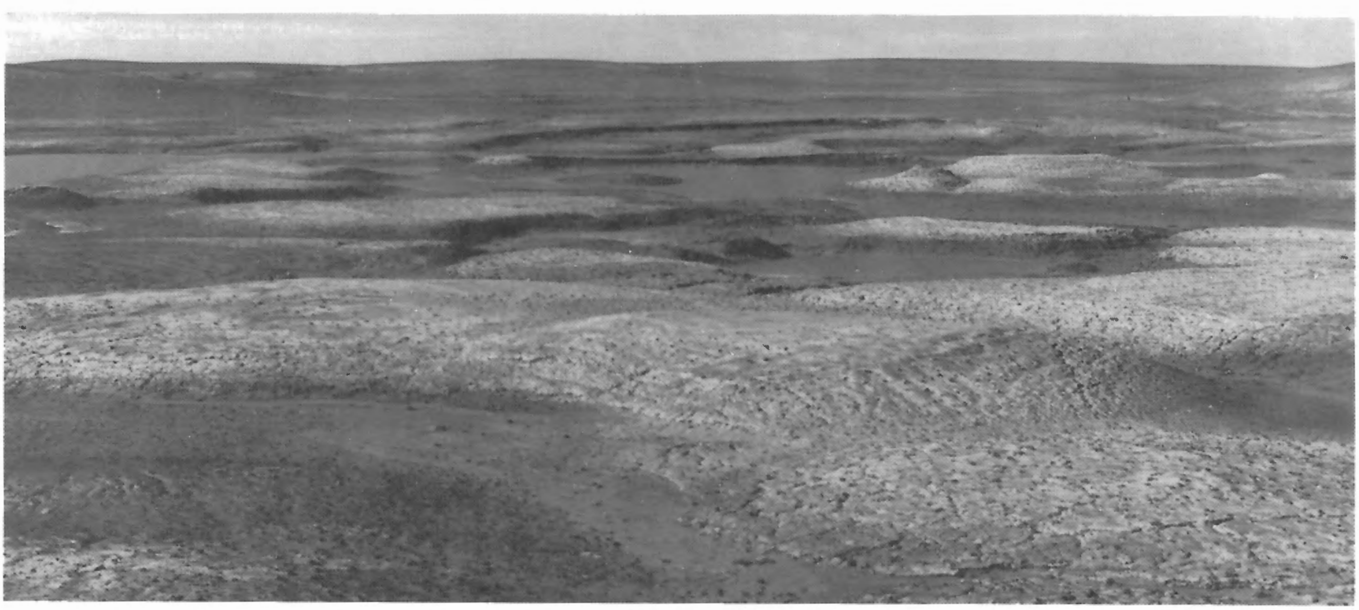

Figure 35A. Thermokarst ponds on deepwater proglacial marine silt blanket southeast of Rawlinson Hills. GSC 1991-416 the largest are about 3 km long. Most are straight but some curve. They stand out clearly on airphotos but pass almost unnoticed on the ground where they are easily mistaken for frost fissures. Periglacial features disrupt and distort them, and mass movement since emergence likely has lessened their depth.

Scours occur densely in fields and sparsely elsewhere. They are much more common where relief is minimal, such as Arrowsmith Plains, than in rougher terrain at the same elevation, such as Crooked Lake drumlin field. Apparently seabed roughness constrained berg movement.

Figure 35B. Thermokarst-triggered stream erosion on proglacial marine silts southeast of Rawlinson Hills. GSC 1991-417

Figure 35C. Massive ground ice exposed in sidewall of a thermokarst pond in glaciomarine sediment. GSC 1991-418

Scours between fields have random trends; within fields they generally trend parallel to final glacier flow, as though meltwater drove the bergs. Thus, the scour field at the head of Ommanney Bay has northward oriented features and the field at the head of Browne Bay has northeastward oriented features. A northward trending field occurs on the lowland south of Back Bay. The relationship between scour trend and deglacial ice flow direction, hence ice margin orientation, indicates that iceberg scours here date from deglaciation.

Most bergs left the mark of a single keel, but scours on a plain of glaciomarine sediment south of Crooked Lake are uniquely different. Here a multi-keel scour about 1 km wide has many parallel keel marks 2-3 km long (Fig. 36); the largest keel mark is about 100 m wide. Some marks change slightly in width, and hence spacing, thinning in the presumed direction of movement (toward the viewer, Fig. 36), likely because of keel wear. Relief across these marks is tiny – decimetres at most.

The keel marks are unvegetated and light toned; areas between are well vegetated (Fig. 36). Materials appear to be the same in both areas, slightly stony clay-silt. Yet something prevented plants from growing on the keel marks throughout the 8000 years since emergence. The keels probably compacted the sediment under them. But if this accounts for the lack of plant growth, the surprising implication is that 8000 years of freezing and thawing has not loosened the sediment. Thus, the vegetation difference is unexplained.

We take these unique features to be ice island scours. Ice islands are large, tabular icebergs; some form today by calving from the floating ice shelves of Ellesmere Island. However, we are not aware of any scours produced by a modern ice island. Nor are we aware of other scours like those described above. The multi-keel scours could indicate that an ice shelf formed during final ice wastage south and west of Crooked Lake. This would explain the lack of deglacial modification of older landscapes there.

Figure 36. Ice island scour with multiple keel marks on glaciomarine sediment south of Crooked Lake. GSC-204788-F

MARINE SEDIMENTS AND LANDFORMS

Marine sediments of postglacial age lack any glacial affinity and were laid down during shoreline regression from marine limit. Marine limit is as high as 188 m in the northwest, near Donnett Hill, but is at about 100 m over most of the island. Postglacial marine sediments lie mostly below 100 m, where they commonly dominate. Deltaic and beach facies are distinguished on the maps. Beach sediments are by far the more widespread.

Deltaic sediments (unit Mt)

Raised deltaic sediments comprise upward coarsening sequences of clay, silt, sand, and gravel up to 20 m thick forming dissected terraces. Areally they are minor materials, accounting for <1%. Locally they form the largest resources of granular materials. Gravel topset beds are mostly <1 m thick; sand forms the bulk of most deposits. Most are shell-bearing and many have thin beds of fine plant detritus.

The largest deposits, each about 5 km^2, occur at the heads of Le Feuvre Inlet and of Transition, Back, and Arabella bays. Five smaller deposits of about 1 km^2 each occur along Baring Channel on Prince of Wales Island and another on Russell Island. Generously allowing an average thickness of 10 m, yields 250 million m^3 of postglacial deltaic sediment. This represents an average net denudation of the island (33 338 km^2) of 0.8 cm, or 0.8 mm/1000 years. Although denudation rates were higher than that in the nine drainage basins that produced deltas, most basins shed no mappable material into the sea.

The small deltas illustrate how little sediment moved from land to sea during postglacial time. This lack of movement has resulted partly from derangement of the drainage system, with its numerous terrestrial sediment traps, and mainly from the low gradients of most slopes. Current estuarine deltaic sedimentation proceeds mostly in front of the streams that built the raised deltas, much of the sediment being derived from erosion of the raised features.

Beach sediments (unit Mr)

Raised beaches occur extensively on westward sloping bevels of Arrowsmith Plains in the southwest, between Guillimard and Willis bays in the southeast, between Young and Back bays in the northeast, and along northern Russell Island. They developed on terrain with enough slope to exceed a critical water depth at the shoreface. Nearly level expanses of Arrowsmith Plains have clast-thick armours of stones developed by wave erosion of till, but proper beaches did not form.

Raised beaches are of two main compositions: gravel and sand. Not divided on Maps 1689A and 1690A, they can be crudely separated by referring to the bedrock geology; beaches over Peel Sound sandstone are mostly sand, whereas beaches over other rocks are mostly gravel. Thus, mainly sand beaches occur along Peel Sound; mainly gravel beaches elsewhere.

Most raised beaches overlie till and hence developed by erosion of till. Sand beaches are thickest, with several metres of foreset bedded sand, incised by gulleys in places. Thickening of many gravel beaches stopped once the till was armoured by more than 0.5 m of gravel because little wave energy was (and is) available. But thicker gravels accumulated in places, likely with the aid of sea ice.

Sea ice pushing of material landward to the shoreline happens along with beach formation and alters beach ridges landward of the one being formed. Though momentarily destructive, disrupting beach form and scouring through the deposit, it dumps loose, wet debris on the beach from the shoreface and leaves it in steep hummocks and ridges that are easily reworked by small waves such as develop in shore leads. The thicker gravel beaches likely would not have formed without this aid, for beach gravel moves little along shore by wave action to otherwise thicken beyond the armouring stage. Dyke et al. (1991) described incorporation of shells into beaches after being carried ashore with sediment on sea ice. The waves are so gentle that even their delicate periostraca and ligaments survive. Though well preserved, these shells are centuries to millennia older than the enclosing beach.

Where the backshore slopes very gently and streams bring sediment to the shore, such as along the north shore of outer Browne Bay, raised beaches do not rest directly on till, but on intertidal to shallow subtidal deposits 1 m or so thick. These are flat-bedded sand and mud with organic-rich beds and pure black beds of plant detritus. The sand and mud beds are either brightly oxidized to red and orange or reduced to grey and olive green. Their many colours, fossils, and position beneath beaches make them distinct.

Where beach gravel is thinner than the depth of summer thaw, about 1 m, till diapirs have intruded (Fig. 37). This action mixes till with the gravel and, along with crumbling of clasts by frost, yields a material so changed that its genesis would be doubted if it were not for the strandlines that are still conspicuous. Such alteration tells whether the beach is thick or thin.

FLUVIAL SEDIMENTS AND LANDFORMS (unit A)

Fluvial sediments make up <1% of surficial materials. They are mostly gravel with sand beds, occurring as fans (unit Af), alluvial terraces (unit At), or active braided channels (unit Ap). Fans, especially small and steep ones, are of coarsest material. Braided alluvial plains and fans set into glaciomarine sediment south of Rawlinson Hills are mostly sand.

Beds of most streams on the island are cut in till, and hence are gravel-armoured and likely now immobile. Even larger rivers, such as Fisher and Dolphin rivers, have only short alluvial reaches, mostly <5 km long.

Large, thick alluvial fans debouch from canyons cut in bedrock. Canyon cutting responds to postglacial relative sea level fall. Because sea level is still falling, canyon cutting and fan building continue, and fan profiles keep changing. Hence, some deposits combine active fans incised a few

Figure 37. Till diapirs rising through thin beach gravel. Individual cells are about 0.5 m diameter. GSC 1991-419

metres into relict ones. Most canyons are hundreds of metres wide and tens of metres deep. Fans at their mouths apparently contain most of the eroded material. Thus, the fans consist mostly of fluvial gravel and lack the debris flows common in alpine fans.

Most scarp-crossing streams have largely graded their courses, each with its pair of canyon and fan. Large fans occur along the high escarpment between Browne and Smith bays. The largest impinges on Scarp Brook and dams a lake. Several other escarpments, such as along the west sides of Prescott and Pandora islands, around Mount Mathias, and between Cape Hardy and Back Bay, are picked out by smaller fans.

In summary, fluvial erosion and deposition have varied with relief. Small streams with steep gradients but with bankfull flow for only the weeks of snowmelt have eroded into limestone, dolomite, and sandstone at a rate that kept pace with base level lowering. Where relief is low, little erosion and deposition have occurred. A deranged drainage with lakes limits sediment throughput, but little sediment has accumulated even in lakes. Lacustrine deltas are rare and small. The largest, in Fisher Lake, fills little of the basin. Hence, low relief is the main limitation on fluvial activity.

ORGANIC SEDIMENTS AND LANDFORMS (not mapped)

Most wetlands, and hence peatlands, overlie fine, marine and lacustrine sediments. Furthermore, except in areas of wind erosion (see *Eolian sediments and landforms*), these sediments are much better vegetated than adjoining terrain. Basinal deposits are saturated through the summer and have thin peat covers. All are patterned by ice-wedge polygons, mostly low centred. Fine deposits on slopes commonly dry out and vegetation is disrupted by mud hummocks. Only small pockets of peat have built up, but organic soils are developed better than elsewhere, though disrupted by frost churning.

Peaty mounds of several kinds are common in wetlands. One kind occurs in degrading peatlands; other kinds occur in and by shallow water, apparently as a result of the growth of peat and ground ice. Yet another kind occurs at drier sites where mammals and birds fertilize the soil.

Peatlands with degraded ice-wedge polygons

Many former wetlands of a hectare or so have dried out because sill erosion has arrested peat accumulation. These have distinctive morphologies: steep-sided, flat-floored troughs about 1-3 m wide and 1-2 m deep separate roughly rectangular peat blocks about 10 m across. Trough floors generally occur at the base of the peat. The tops of most peat blocks are dry, barren, and eroded by wind, although some are colonized by plants that normally grow on drier sites.

The rectilinear troughs result from melting of ice wedges, which is obvious where this process is starting (Fig. 38). At this stage, the troughs and peat blocks resemble high-centre ice-wedge polygons. Woo and Zoltai (1977, p. 52) referred to them as such, but high-centre polygons normally result from ice-wedge growth rather than degradation. Hence, we refer to these as peatlands with degraded ice-wedge polygons.

Incision of the troughs improves drainage of the active layer, which dries and erodes the peat. Once the troughs penetrate through the peat, sides of peat blocks retreat by mass wastage and by fluvial erosion during snowmelt. Burrowing by small animals and rooting and wallowing by muskoxen further erode them. Eventually blocks diminish to mounds or disappear, by which stage the polygonal pattern is erased.

Figure 38. Peatland south of Reliance Bay in initial stage of degradation. GSC 1991-420

New peat accumulates in the over-widened troughs. Regrowth of peat over remnant older peat could lead to complex peat stratigraphy. In places, overturned blocks of older peat will be grown over and the collective deposit will include intervals near the base with stratigraphic age reversals.

Paired radiocarbon dates from bases and tops of peat indicate accumulation rates of about 1 m/1000 years (Ovenden, 1988). Such rates would have led to deposits up to 10 m thick at sites where peat accumulated throughout postglacial time. Observations, however, indicate that maximum peat thicknesses are only 1-2 m.

The morphology of degraded peatlands and limited peat thicknesses suggest that peat development here is self-arresting. Peat accumulates in depressions on fine grained sediments. These depressions have only 1-2 m of closure relief; lakes occupy deeper basins. As peat thickens, ice wedges develop and grow upward, their tops staying within 10-30 cm of the surface. When the peat exceeds the elevation of the basin sill, runoff across it begins to erode it. Once sill erosion starts, ice wedges in the peat start to erode and provide more runoff. Further runoff is channelled increasingly along ice-wedge troughs.

If the hypothesis of self-arresting peatland development is correct, inferring paleoclimate on the basis of intervals of peat formation based on sampling of radiocarbon ages of peat exposed in degraded peatlands is unsound (cf. Ovenden, 1988, p. 2). The sections exposed in these peatlands are easily sampled and are an important source of material for paleoecological analyses. One drawback, however, is that it is impossible to tell in the field when peat development stopped or how much of the peat was eroded. Radiocarbon dates show that the tops range from a few centuries to 7000 years old (Ovenden, 1988).

Palsa-like mounds in wetlands

Many aggradational or deformational organic mounds occur in the peatlands and other wetlands. Some occur alone, but most occur in clusters. The mounds are 0.3-1.5 m high and 3-15 m wide. They occupy three types of sites: in shallow ponds (Fig. 39A), at pond margins (Fig. 39B), and drier sites (Fig. 39C).

Peaty mounds that rise from ponds are nearly circular (Fig. 39A) and seem to be limited to water <1 m deep. None seem to rise much above water so their relief compares with that of related forms. The pond bottoms are comprised of mineral sediment, so the mounds are isolated bodies rather than raised parts of subaquatic peat.

Pond-margin mounds (Fig. 39B) are the most common. They generally lengthen alongshore and coalesce to form peaty shore rims for tens of metres. Adjacent pond floors consist of mineral sediment. Surfaces of the peat mounds are commonly cracked, especially in the direction of elongation. The active layer, 20-30 cm thick, consists of pure peat, as does the upper frozen parts. A pit dug in one feature revealed a core of massive ice.

Figure 39A. Palsen in a shallow pond. GSC 1991-421

The morphologies of many pond-margin mounds indicate that they are eroding on upslope sides and accreting at the water. Eroding sides are concave and cracked into blocks, some of which have fallen away. Accreting sides are convex and flanked by peat benches that extend into the pond at water level. Accretion is not continuous for pillows of peat rest offshore and indicate occasional erosion of peaty shorelines by lake ice.

Peaty mounds at drier sites of peat accumulation (Fig. 39C) are similar in size to those at pond margins. Many occur at junctions of ice-wedge troughs. Hence, they may result from enhanced heaving of the shoulders of ice-wedge troughs that occur at junctions combined with peat accumulation in small pools that occupy them. Segregation ice likely forms in peat aggrading in the troughs, so ice in the overall structure may be of both segregation and intrusive (wedge) origin.

These various mounds resemble palsen. The National Research Council Permafrost Subcommittee (1988) defines a palsa as a peaty mound possessing a core of alternating layers of segregated ice and peat or mineral soil. Without detailed subsurface examination, the peaty mounds on Prince of Wales Island cannot thus be shown to be palsen, though this is the most likely origin of features associated with ponds. Those at drier sites that are associated with ice wedges are not palsen, as defined above, because wedges are intrusive rather than segregated ice.

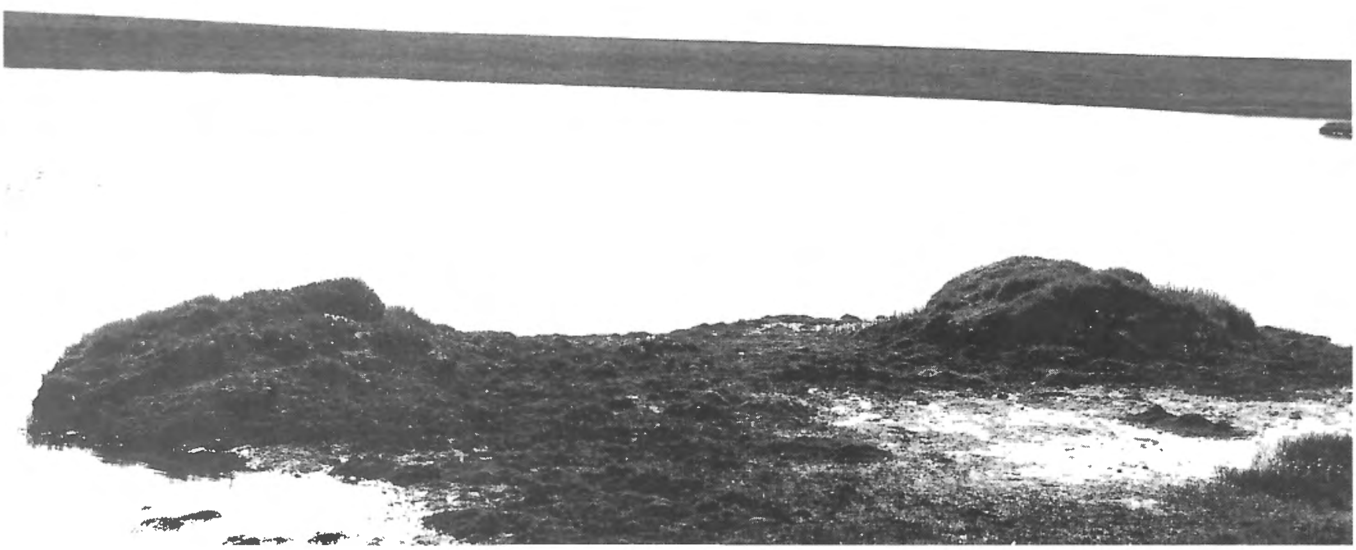

Figure 39B. Palsen at pond margin. Each mound is about 0.5 m high. GSC 1991-422

Figure 39C. A palsa at a drier site of peat accumulation. GSC 1991-423

Washburn (1983) proposed a more general definition for palsen to include both aggradational and degradational forms, including those resulting from degradation of peatlands through melting of ice wedges. By his definition all mounds described above are palsen. For geotechnical purposes, aggradational and degradational mounds have different significance because different processes occur in their vicinity.

Organic mounds resulting from animal activity

Organic mounds resulting from animal activity (Fig. 40) occur at dryland sites, typically hilltops. The substrate is normally till, presumably because it holds enough water for peat to accumulate once started by another influence. The mounds occur alone, which along with topographic position distinguishes them from other kinds of peaty mounds. They are as large as the palsen already described; the feature in Figure 40 is 1.5 x 6 x 9 m and has been reduced by wind erosion. Mounds of this size are common.

Organics accumulate because of animal activity rather than drainage impedance. The mounds are invariably the sites of lemming burrows, fox dens or hunting stations, owl hunting stations, or a combination of these. Animal remains litter them and bone and manure stimulate dense plant growth and organic soil accumulation. The plants trap wind blown silt, which contributes further to accumulation.

From a land use view, these mounds are important for two reasons: 1) Ice segregation and heaving that are occurring in the other mounds are not occurring in them. 2) The size of the mounds indicates that animals use them over many centuries and so they are ecologically important.

EOLIAN SEDIMENTS AND LANDFORMS

Eolian sediment and landforms in the central Arctic are so restricted that they normally are not mapped. Although no mappable eolian deposits occur on Prince of Wales Island, spectacular areas of wind erosion occur along Peel Sound (Fig. 10) and west of Ommanney Bay (Fig. 15). These have well-drained, sandy substrates where material is available for saltation and destruction of vegetation.

The eroded areas along Peel Sound are aligned from Back Bay to Young Bay. Parts of Prince of Wales, Prescott, and Pandora islands are affected. Thus, a large, partly submerged trough funnels the erosive winds. Sand tails trail southward from obstacles. Similarly, sand creates dark streaks on sea ice on the south sides of eroded areas (Fig. 41A). These indicate transport during winter when the ice is not moving. Peak eolian activity occurs in winter elsewhere in the Arctic (McKenna-Neuman and Gilbert, 1986) but not only then (Hodgson, 1982).

Figure 40. Organic mound associated with animal activity. GSC 1991-424

On Prince of Wales Island, erosion is restricted mostly to sandy raised beaches. But on Prescott Island and on Mount Mathias, erosion extends above marine limit and affects sandstone bedrock and sandy till as well. On Mount Mathias a gravel deflation lag covers till.

Nowhere is the surface deeply scalloped; deflation is either not obvious or produces <1 m of relief. Preservation of small sandy, raised beaches also indicates little deflation (Fig. 41B). Limited deflation, yet nearly complete stripping of vegetation, and the sand streaks on sea ice, suggest erosion during winter when frozen ground limits deflation but not removal of plant cover. Winter snow grains at -50°C are as hard as quartz (Dietrich, 1977) and may be important agents of abrasion. But the limitation of wind erosion to sandy substrates shows that blowing snow alone is not enough to keep large areas denuded.

The seaward halves of two forelands between Browne and Young bays, each about 35 km^2, are stripped of vegetation (Fig. 41A,B). The limits of erosion are jagged in places, particularly upwind, but mostly are straight and abrupt. They do not mark a change in elevation or in material. The straight segments follow small raised beach ridges in places. Yet microtopography does not control their location where they approach the coast at a large angle. Perhaps a beach ridge momentarily confines the side of a saltating sand (or snow) stream long enough to ensure the same trajectory downwind.

The straight erosional limits jog abruptly in places. Each jog coincides with a stream, where the limit retreats. Figure 41B shows an offset of about 720 m at a large channel; Figure 41A shows offsets of about 250 m and 100 m at successively smaller channels. Hence, the channels lessen the erosive capability of the wind passing over them in proportional to their sizes, but capability drops to zero only at the edge.

The channels would affect windstorms carrying a sand load in two ways: 1) they would induce turbulence and diminish the load capacity of the airstream; and 2) in summer some sand would get wet and drop from the airstream. Winter windstorms would be affected when the channels are not full of snow.

Because the side of an eroding airstream is at threshold condition, turbulence narrows the erosive path; turbulence nearer the centre lowers erosive capability, but not to zero. Retreat of the limit should then be proportional to the size of the feature inducing turbulence, here a stream channel.

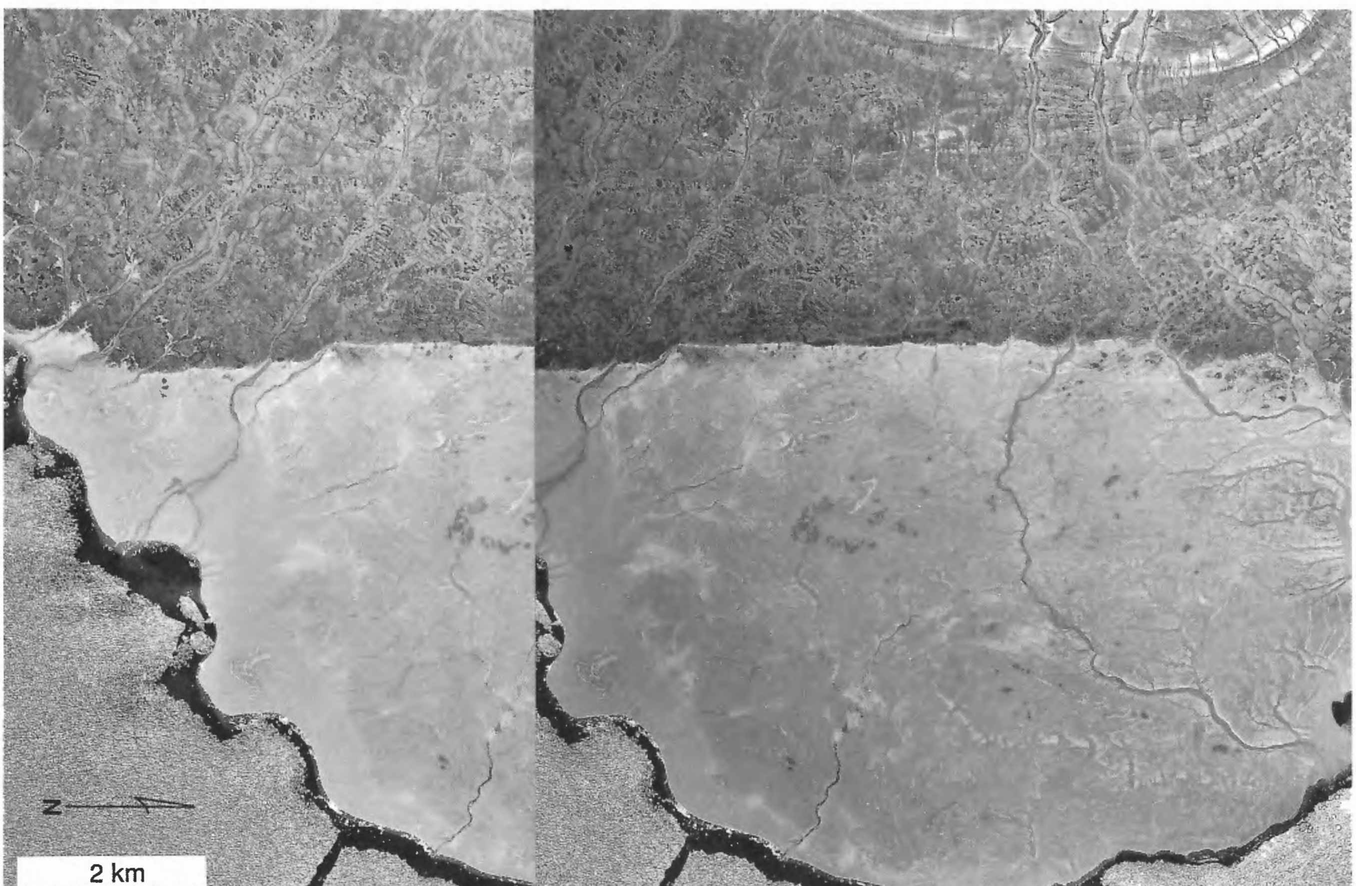

Figure 41A. The more southerly of two large wind eroded (light toned) forelands along Peel Sound. These areas also show well on the satellite image of Figure 10. NAPL A16196-195 and 196

Wind erodes the peninsula west of Ommanney Bay from its centre to M'Clintock Channel, affecting about 600 km^2 that show well on satellite imagery (Fig. 15). Erosion affects mainly the ice-contact glaciomarine sediment of Rawlinson Hills End Moraine System (unit Mm) and proglacial marine silt and fine sand (unit Mb) on either side of it but also extends onto till. As along Peel Sound, deflation is minimal but stripping of vegetation nearly complete. Flutes show in one place that eroding winds come from the NNW, as along Peel Sound. The eroded area has diverse relief and its limit is difficult to see, especially on till, which is normally poorly vegetated.

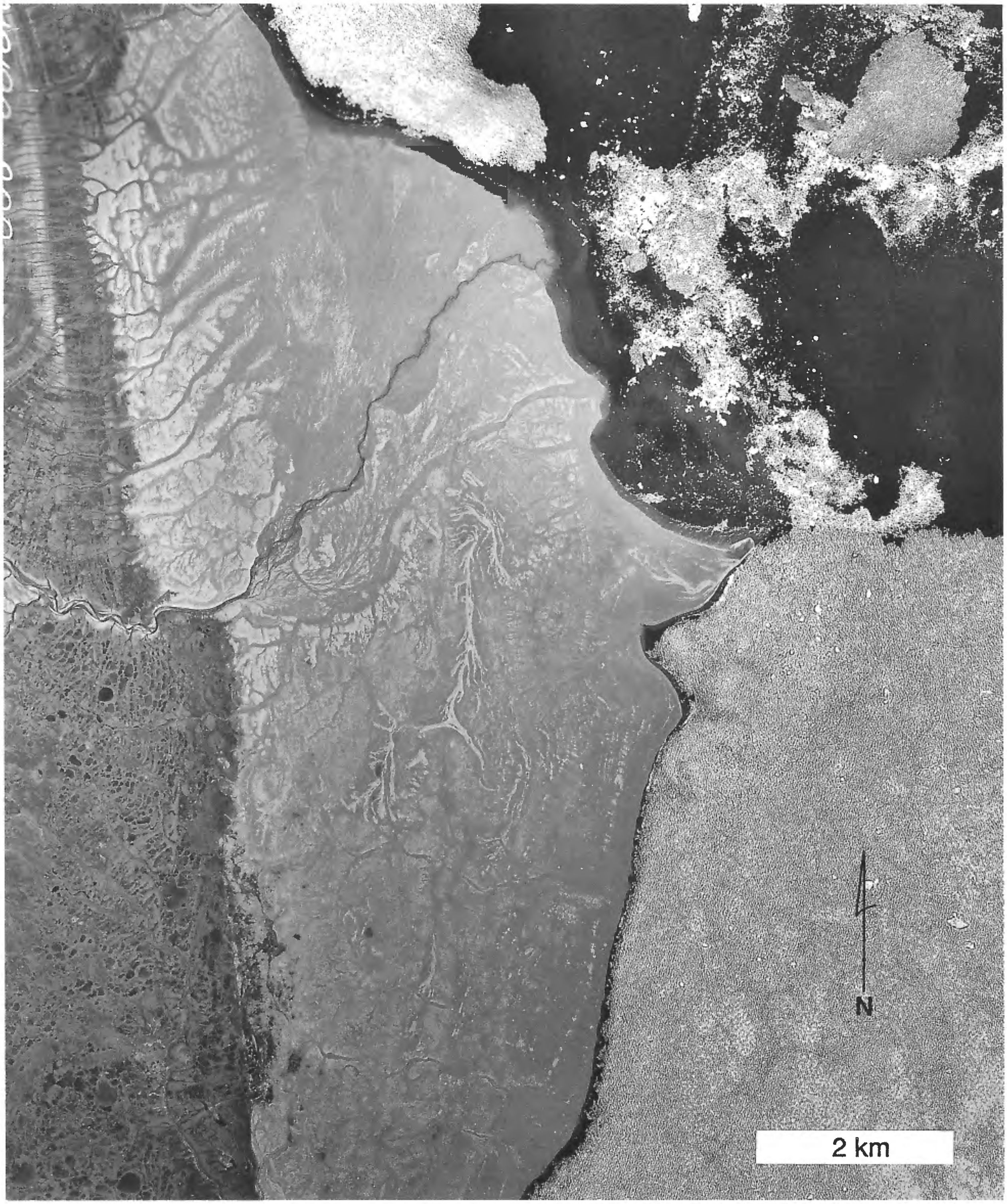

Figure 41B. The more northerly of two large wind eroded (light toned) forelands along Peel Sound (cf. Fig. 10). NAPL A16196-200

TILL COMPOSITION AND GLACIAL DISPERSION

INTRODUCTION

The textural and lithic character of till is determined by the properties of source materials, modulated by processes of glacial entrainment, transport, and deposition, each operating at different times and rates and for different durations. The ultimate source is bedrock under and upice of the till, the properties of which have been observed or inferred. Till composition, therefore, is used to infer glacial events and processes and to assess inferences regarding the nature of bedrock obscured by drift. Some parameters are more useful for this assessment than others.

Till composition was recorded at nearly 800 field sites. These records include clast lithology and abundance, stoniness, and boulder cover. Till was sampled to determine petrology of granules; sand, silt, and clay content of the matrix; calcite, dolomite, and total carbonate content of the matrix; and trace element content of the clay fraction. These and other data are tabulated in Appendices 1 and 2.

This section summarizes the distribution of erratics noted in the field and in the granule fraction of samples and defines lithic facies of till from the granule petrology. Statistical data are stratified to describe each facies. Maps of erratics and till facies and compositional gradients indicate direction, extent, and amount of glacial dispersion.

DISTRIBUTION OF LARGE ERRATICS

Erratics of shield rock, carbonates, sandstone, and conglomerate were recorded at sample sites. These erratics are of cobble and boulder size. Some almost spherical clasts of carbonate rock, sandstone, and gneiss in till were recycled from Peel Sound conglomerate and are recorded as conglomerate erratics, regardless of specific lithology.

Shield erratics of cobble and boulder size are widespread (Fig. 42A), though nowhere abundant beyond the shield. In sedimentary rock terrains, these erratics normally comprise <1% of till clasts. But the boulders are conspicuous because they are darker than other clasts and contribute nutrients to vegetation on abutting, generally barren till. Gneiss boulders are typically the largest clasts in carbonate-rich till because most carbonate debris has been crushed smaller.

Shield erratics occur from end to end of the area but are either less abundant or absent on eastern part of the northern plateau (Fig. 42A). This may reflect divergent ice flow over the plateau during intervals of generally northward flow. The widespread dispersion of shield erratics can be explained by ice flow phases 1 and 2 but some, or even much, of it may have occurred earlier.

Erratics of Peel Sound conglomerate occur mostly close to outcrop or subcrop (Fig. 42B). Short-distance dispersion occurred in several directions. Longer dispersion is recorded by distinct, spherical sandstone clasts spread across Prince of Wales Lowland as far northwest as Smith Bay. They occur there in low abundance and have a sharp lateral limit coinciding with the escarpment descending from the northern plateau. This limit reflects topographic control of ice flowlines during at least part of the phases of northward flow.

Red erratics of sandstone to mudstone (Fig. 42C) are widespread over carbonate rock. In places they were locally derived from minor clastic intervals in the carbonate rock. However, most of those on the lowland probably resulted from northwestward flow of phases 1 and 2. Their absence on the western third of the lowland indicates that ice carrying debris from Peel Sound Formation never flowed across there. Those west of clastic rock on the northern plateau also may have resulted largely from flow phases 1 and 2, but southeast of Arabella Bay more erratics were deposited during an early deglacial flow phase. Common sandstone erratics on carbonates north of Back Bay resulted from eastward dispersion during phase 3.

Carbonate erratics extend widely over noncarbonate rock (Fig. 42D). This further attests to the extent of eastward flow during phase 3. The erratics occur in areas where phase 3 flow is only weakly recorded geomorphologically, as on the eastern highlands between Browne and Transition bays, and in areas where phase 3 flow features were erased by later flows, as on Russell Island and on northeastern Prince of Wales Island.

LITHIC FACIES

The till is divided into ten lithic facies (Table 2). Three nearly pure facies have >90% of granules derived from carbonate, sandstone, or shield rocks; seven mixed facies are variably dominated by a single clast type. Of the 779 classified samples, 538 or 69% have >90% of granules derived from one rock type; only 8% have <70% derived from one rock type. Given the length of glaciations, the many that have occurred, the varied directions of flow during the last (see *Surficial materials and landforms*), each presumably capable of mixing debris, and the polycyclic nature of till, continental glaciers here have been rather ineffective agents of transport.

Distribution

The nearly pure lithic facies correspond closely to known and inferred distribution of bedrock source materials (Fig. 43).

Lithic facies C occupies most areas underlain by carbonate rock. It also occupies much of the belt of bedrock grading from sandstone to carbonate (Fig. 43A). Nearly pure carbonate till in the transition belt probably indicates eastward transport during phase 3. Facies S occupies much of the area underlain by conglomerate, sandstone, and the sandstone – carbonate transition belt (Fig. 43B). Facies P overlies both Precambrian granite and gneiss and Peel Sound conglomerate where it contains abundant shield clasts (Fig. 43C).

Distributions of facies of mixed granule lithology are more informative and can be explained by the geomorphically recorded ice flow events (see *Surficial materials and landforms*). Three pairs of facies represent compositional gradients between the nearly pure facies. Facies MCC and MC, with up to 20% and 30%, respectively, of granules derived from noncarbonate rock, mostly sandstone, are common in several areas where they represent transport of clastic rock debris into carbonate rock areas (Fig. 43D). Occurrences west of the clastic rock contact on southern Prince of Wales Island could represent an as yet unrecognized westward ice flow. But they more likely represent transport of debris during phases 1 and 2 from Peel Sound clastic sediments in Franklin Strait. Because ice flowed nearly parallel to the bedrock contacts then, transport distances can not be determined. The samples northwest of Guillimard Bay, however, record transport of much debris, 10-30% of the granule fraction, >75 km, the minimum distance to the contact. Other samples of these facies overlie dolomites north of Back Bay and record eastward dispersion from Peel Sound Formation during phase 3. Occurrences southeast of Arabella Bay likely resulted from the northwestward flow recorded by a field of drumlins that formed during an early phase of deglaciation (Map 1690A). These samples indicate minimum transport of 10 km. Occurrences in the belt of interbedded sandstone and carbonate rocks on southern Prince of Wales Island are concentrated inland of Transition Bay and of Le Feuvre Inlet. Although some carbonate debris could have been derived locally, the overall distribution indicates introduction of debris from the west during phase 3.

Facies MSS and MS, sandstone-dominated till with 10-20% and 20-30% nonsandstone granules, respectively, are widespread in the sandstone-carbonate transition belt and over sandstone and conglomerate (Fig. 43E). In the transition belt, they could have been derived locally or could have resulted from mixing as carbonate debris came from the west during phase 3. Occurrences over sandstone on Russell Island, on northeastern Prince of Wales Island, on Prescott and Pandora islands, and near Le Feuvre Inlet resulted from eastward transport during phase 3, although some carbonate debris was derived locally from carbonate clasts in conglomerate.

Facies MPP and MP, dominated by Precambrian shield clasts but with 10-20% and 20-30% sedimentary rock clasts, respectively, are restricted to eastern parts of the area (Fig. 43F). The occurrence on the shield rock of Prescott Island represents minor transport of sedimentary rock debris eastward during phase 3, whereas the occurrence on sandstone south of Young Bay likely resulted from northwestward transport during phases 1 and 2.

Facies M, which has the greatest mixture of lithologies with <70% of granules of any one type, is widespread in eastern areas and in general reflects eastward transport across rock contacts during phase 3 (Fig. 43G).

The distributions of lithic facies on their own tell little about former ice flow patterns and even invite erroneous interpretations. However, they can be properly interpreted given morphological evidence of various ice flow events.

Table 2. Definition of lithic facies of Prince of Wales Island till samples

Lithic facies	Percent carbonate granules	Percent sandstone granules	Percent Precambrian granules	Number of samples
C	90-100			422
MCC	80-89			79
MC	70-79			30
S		90-100		107
MSS		80-89		41
MS		70-79		18
P			90-100	9
MPP			80-89	5
MP			70-79	2
M	0-69	0-69	0-69	66
Total				779

Bulk composition of matrix by facies

The bulk composition of the till matrix varies between lithic facies. Variations within a nearly pure facies likely reflect mainly variations within its source rock. Hence, within-pure-facies variation constrains the confidence with which a compositional parameter can be used as an index of glacial transport. Because ice that achieved the greatest mixing of debris (Fig. 42) flowed from carbonate rock to sandstone and conglomerate, bulk composition should change from facies C through MCC, MC, M, MS, MSS, to S and should reflect the control of parent material and of stepwise mixing regardless of transport distance.

Carbonate content

The carbonate content of the matrix of facies C, the granule fraction of which is derived almost entirely from carbonate rock, ranges from 3 to 100%, with a mean of 57% and standard deviation of 17% (Fig. 44A). Some samples at the lower end may be misclassified till derived from grey siltstone or mudstone, not easily distinguished visually in the granule size from carbonate. But clearly glacial comminution of carbonate rock has yielded much matrix, typically 25-60%,

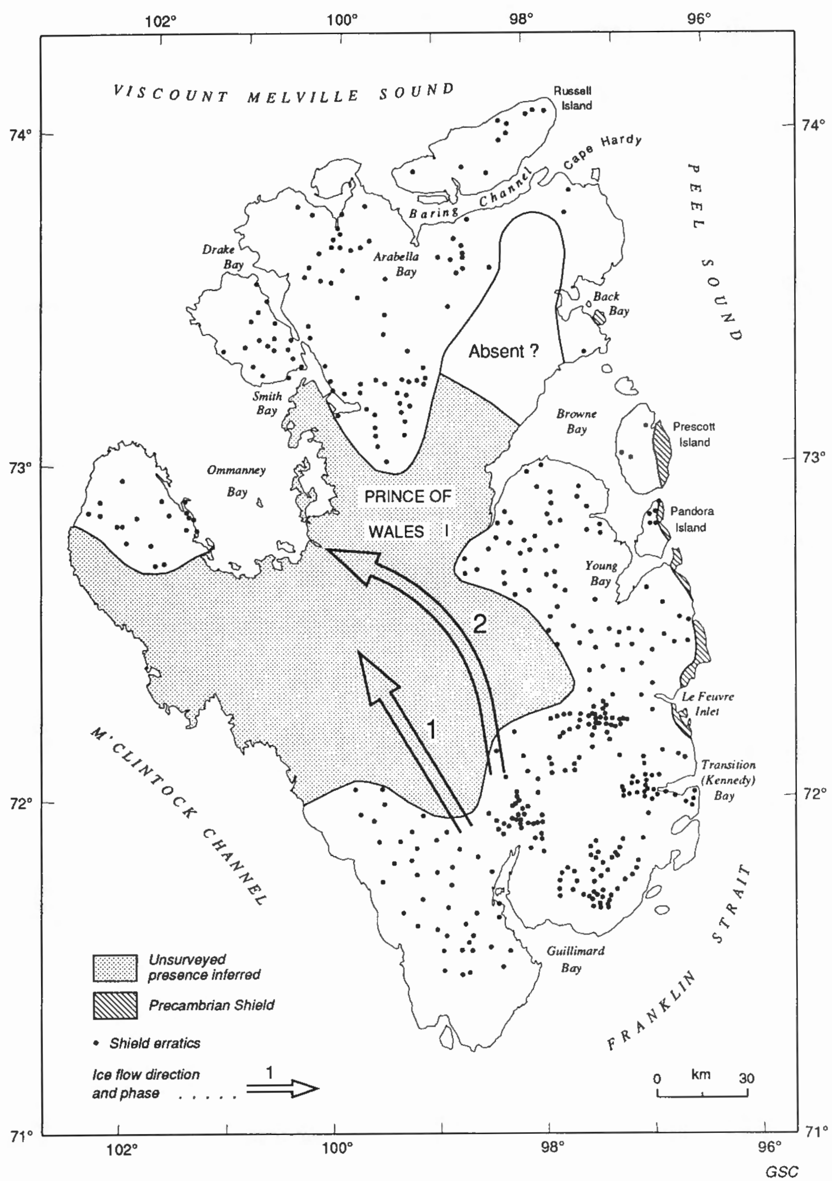

Figure 42A. Distribution of shield erratics observed in the field.

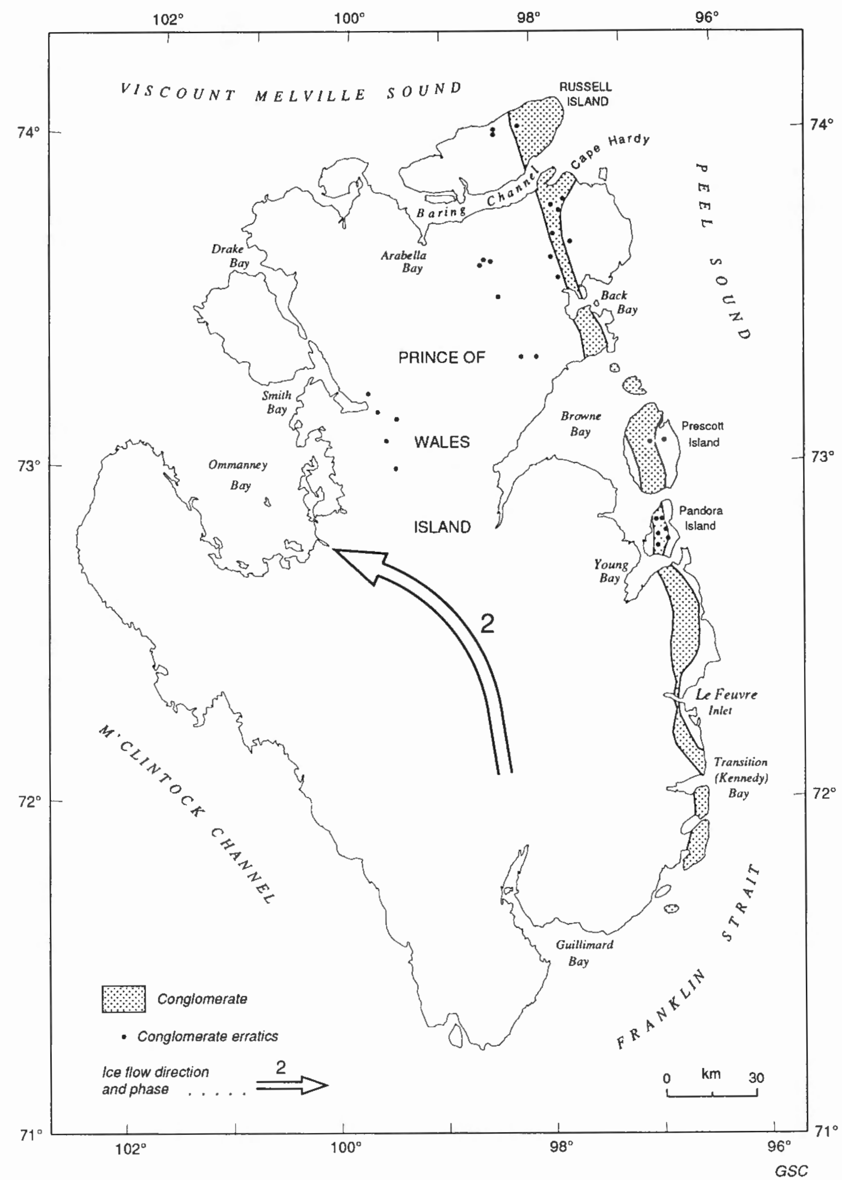

Figure 42B. Distribution of Peel Sound Formation conglomerate erratics observed in the field.

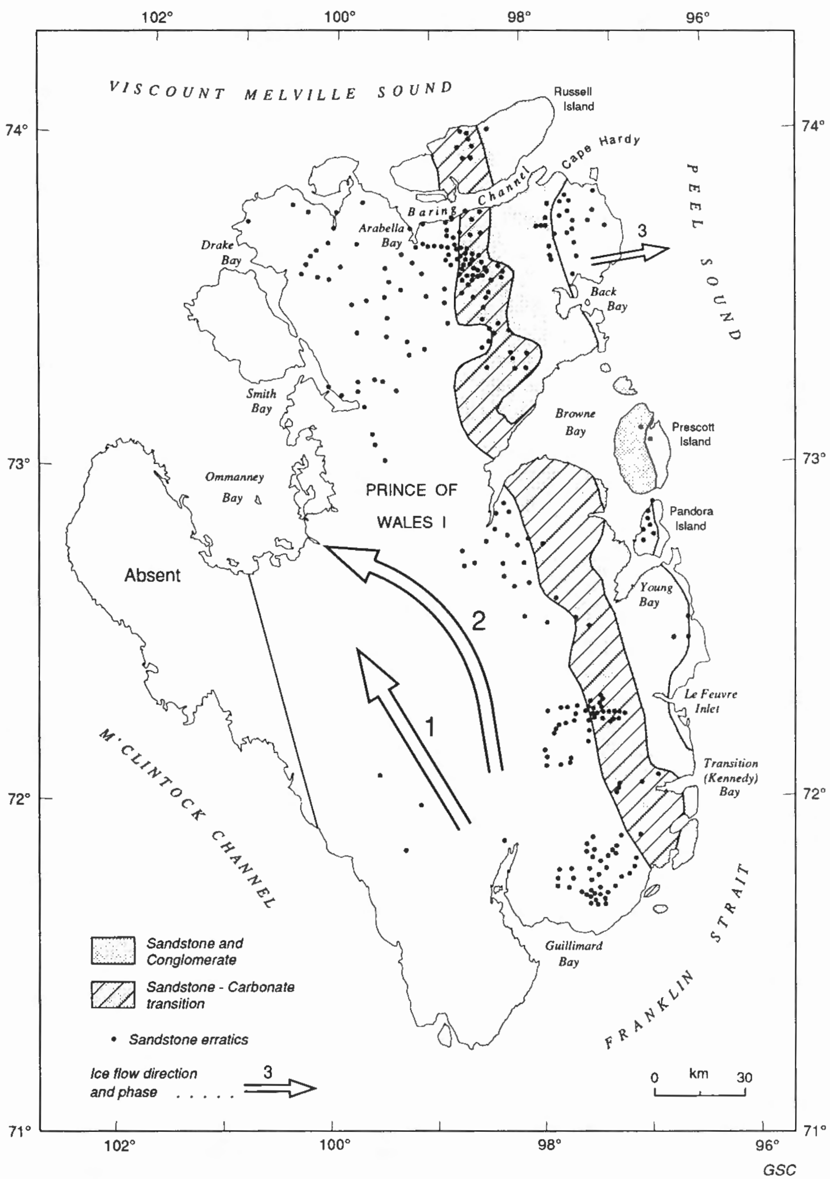

Figure 42C. Distribution of Peel Sound Formation sandstone erratics observed in the field.

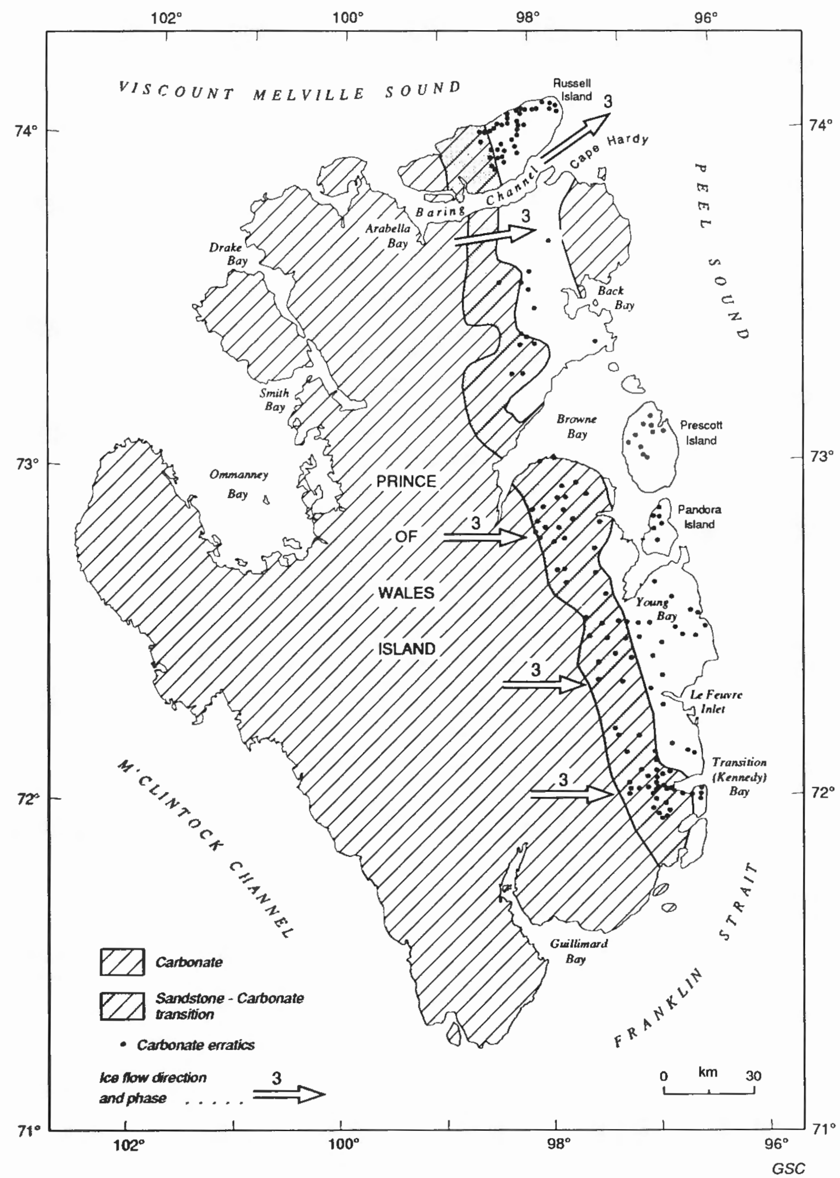

Figure 42D. Distribution of carbonate erratics observed in the field.

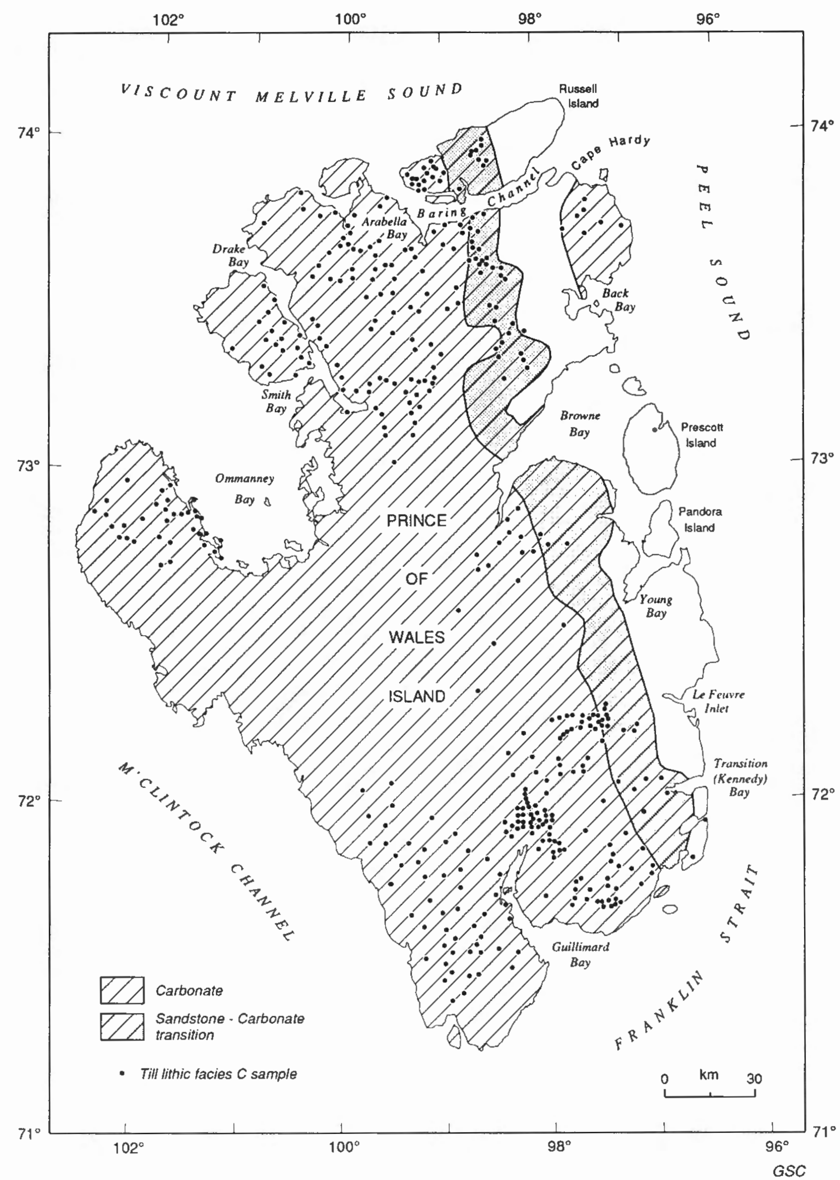

Figure 43A. Distribution of till lithic facies C.

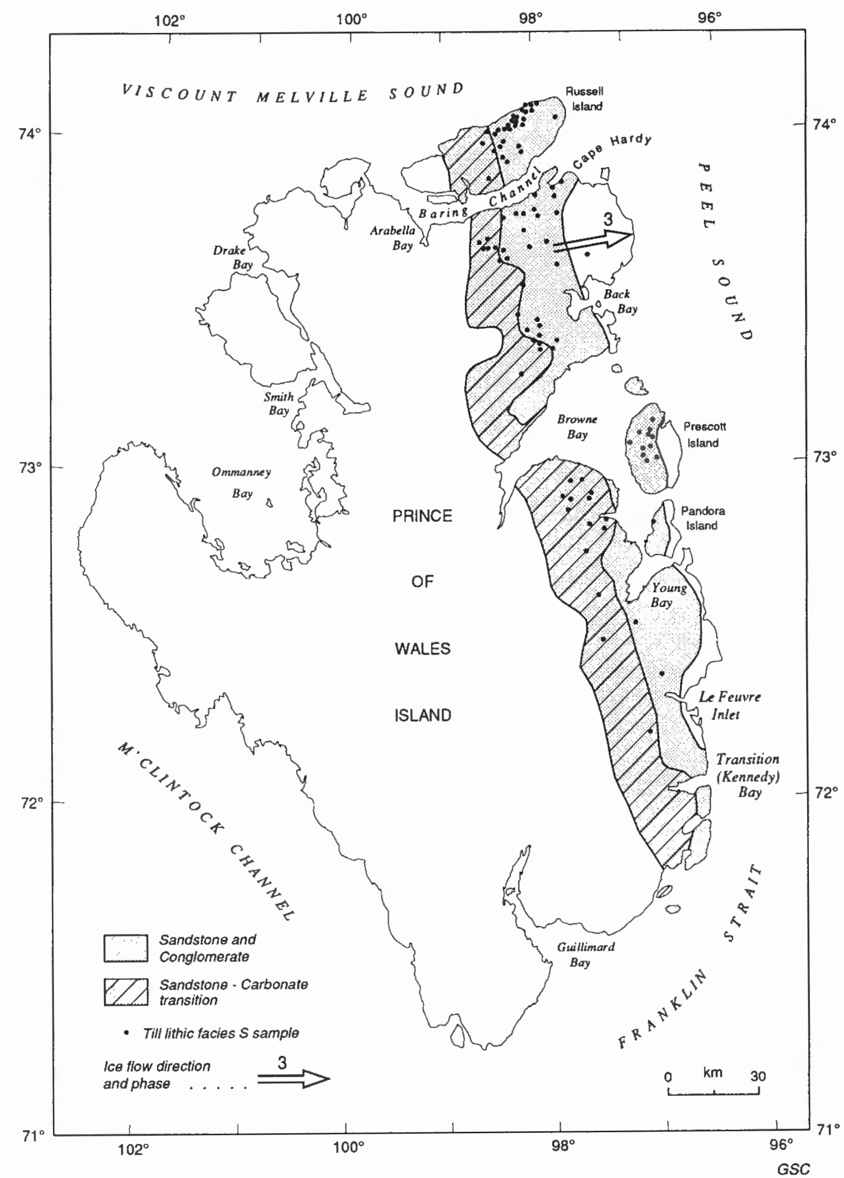

Figure 43B. Distribution of till lithic facies S.

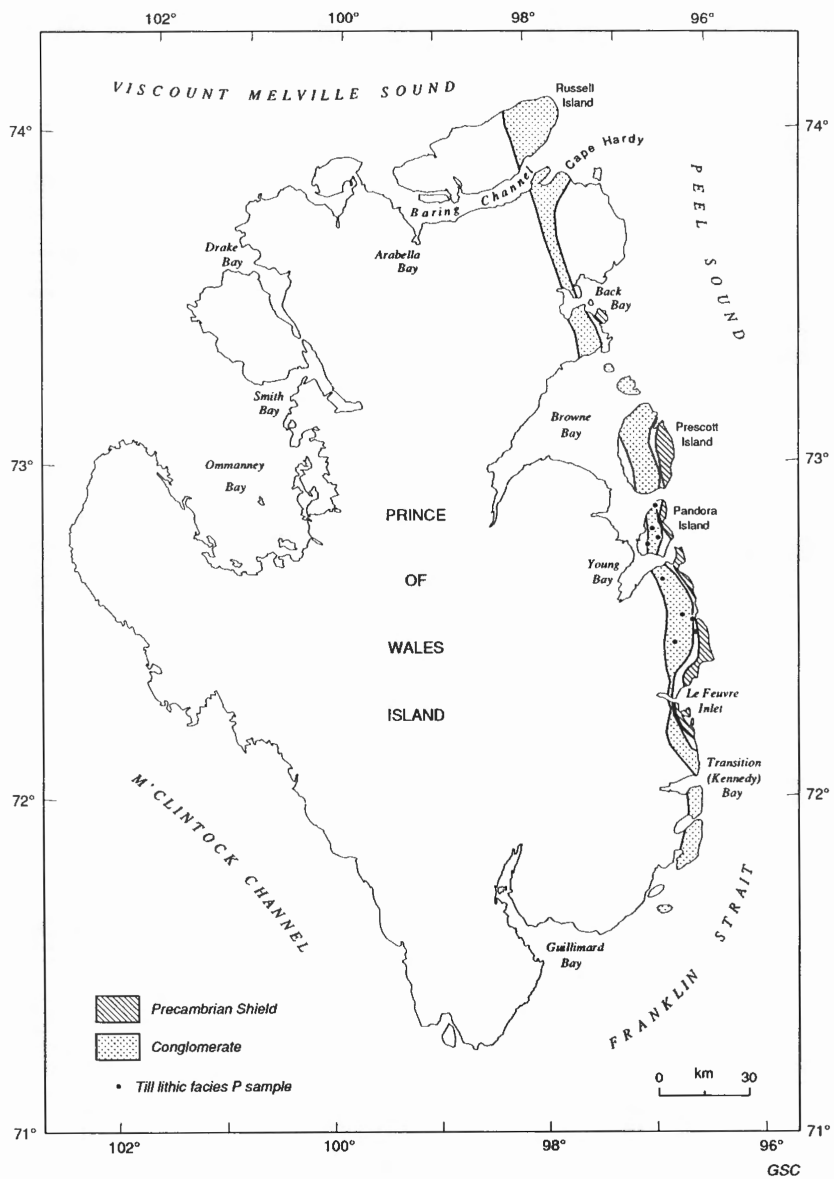

Figure 43C. Distribution of till lithic facies P.

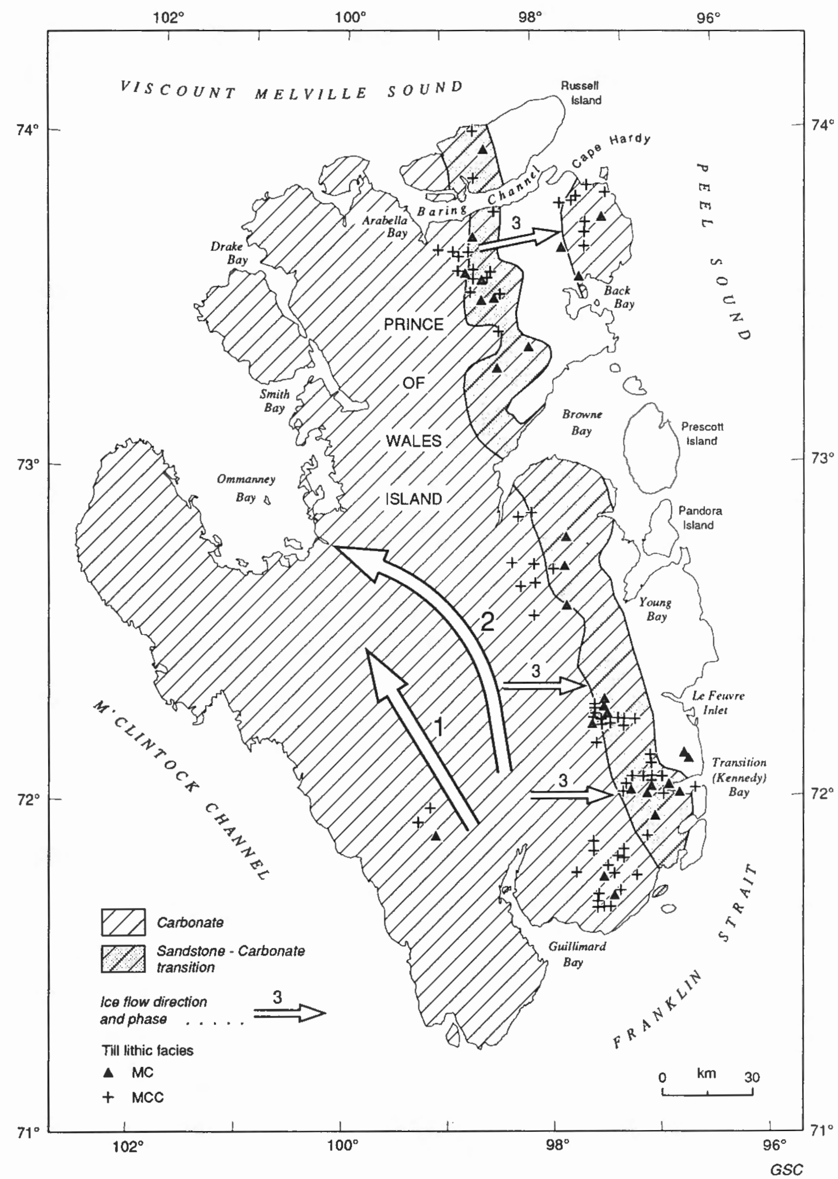

Figure 43D. Distribution of till lithic facies MCC and MC.

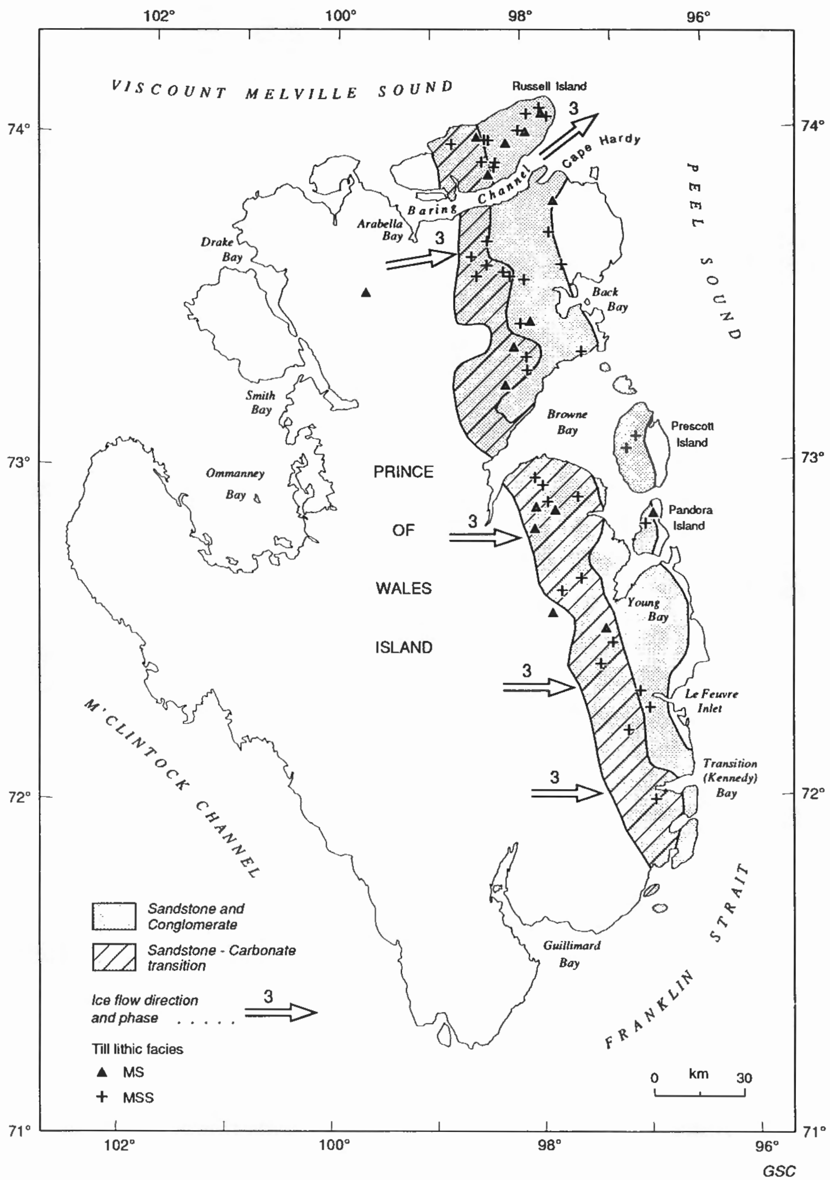

Figure 43E. Distribution of till lithic facies MSS and MS.

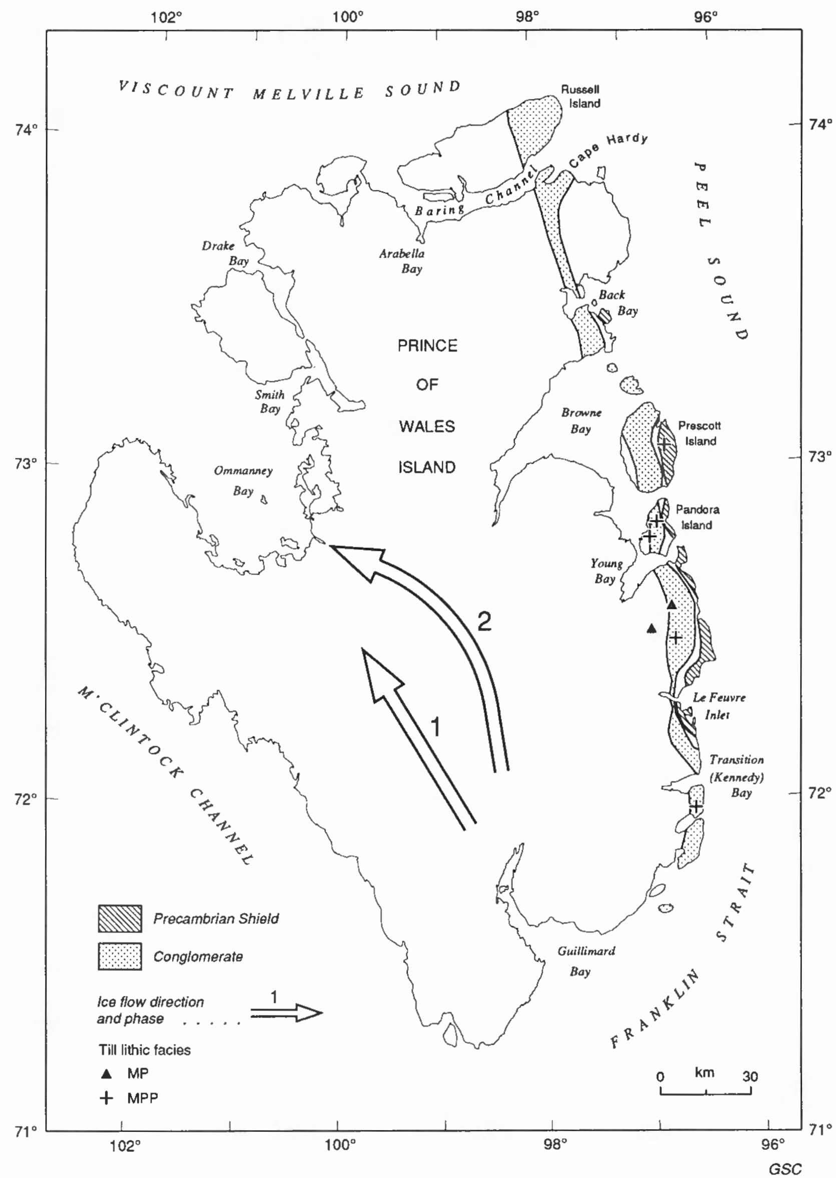

Figure 43F. Distribution of till lithic facies MPP and MP.

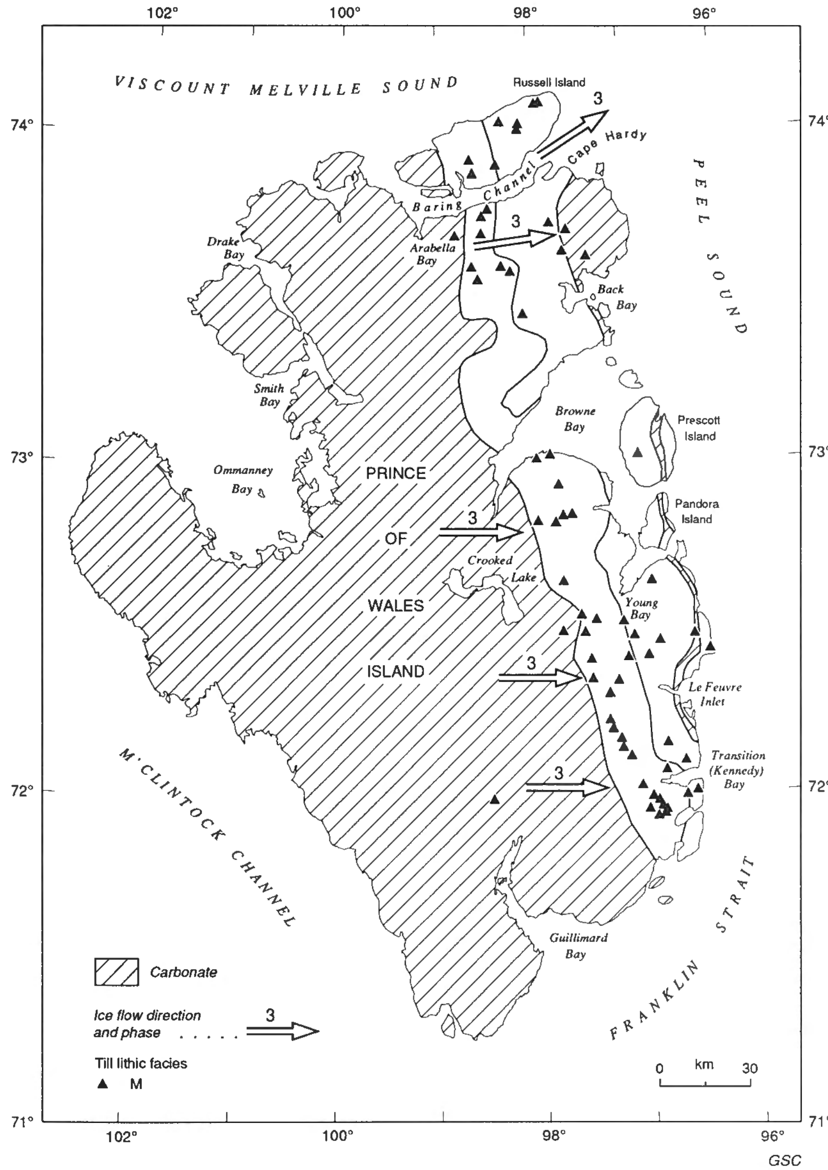

Figure 43G. Distribution of till lithic facies M.

that is not soluble in hydrochloric acid. Miall's (1970b) measurements of concentrations of fine detrital quartz in the carbonate rocks explain this. Thus, the matrix carbonate content of "carbonate facies" till seriously but variably undermeasures the proportion derived from carbonate rock; the carbonate clast proportion of the granule fraction is a much closer measure (Fig. 44B). Unfortunately, the lack of directly comparable measurements for different size fractions hampers assessments of the influence of rock properties on glacial comminution.

The carbonate content comprises both calcite and dolomite. The calcite-to-dolomite ratio frequency distribution for all samples (Fig. 45) indicates that many more samples of till were derived from dolomite than from limestone. Also, maximum and mean dolomite contents persistently exceed maximum and mean calcite contents in all lithic facies (Fig. 44C,D). Yet many samples came from or downice of areas mapped as limestone. This may indicate a need to reassess mapping of bedrock lithology beneath drift on southern Prince of Wales Island, as discussed further below (see *Matrix texture and carbonate content*).

The proportion of the matrix of sandstone-rich till (facies MSS and S) that is carbonate (Fig. 44A), predominantly dolomite (cf. Fig. 44C,D), greatly exceeds the proportion of the granule fraction that are carbonate clasts. This finding could indicate that more fine than coarse glacial debris was transported from carbonate rock onto sandstone or that the sandstone is dolomitic. The latter is a satisfactory explanation, for the bedrock grades from sandstone to limy sandstone to sandy limestone to limestone and dolomite. Hence, the matrix carbonate content of sandstone facies till (S and MSS) exaggerates apparent glacial transport of debris from carbonate rock to sandstone. Along with the insoluble component of the matrix of carbonate derived till, this reduces the precision of matrix carbonate content or either of its components as an index of glacial erosion and transport and confirms clast lithology as a far better index.

Sand, silt, clay content

The sand, silt, and clay content of the till matrix varies as expected between lithic facies (Fig. 46). Along the progression from pure carbonate to pure sandstone or granitic facies, the mean sand content increases systematically from 39 to 65% (Fig. 46A), whereas the mean silt content declines from 43 to 19% (Fig. 46B) and the mean clay content declines from 19 to 14% (Fig. 46C). Despite systematic shift of means, the range of grain sizes in any given facies widely overlaps the ranges in all other facies. This overlap presumably expresses either a heterogeneous texture of source rocks or influences of other factors (e.g., distance of transport, debris concentration in the ice sheet, and postdepositional modification by marine or slope processes) on till grain size characteristics.

The shift in mean clay content between facies is small, perhaps too small to be meaningful. The ice has comminuted a wide range of rock types and produced nearly equal amounts of clay from crushing and abrading each. Hence, clay content of till here can not be expected to provide a clear indication of glacial transport or process. The silt and sand contents can be expected to be more useful and are examined below.

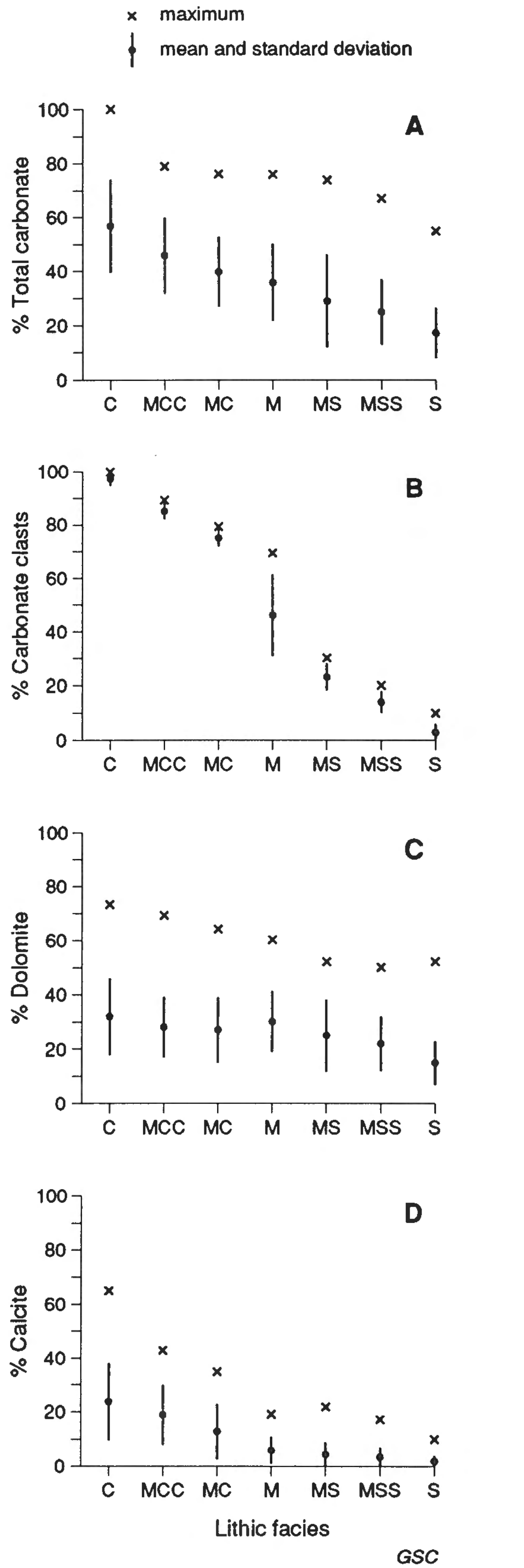

Figure 44. Statistical summary of A, total carbonate; C, dolomite; and D, calcite contents of the matrix of various lithic till facies compared to B, the carbonate clast proportion of the granule fraction of the same facies.

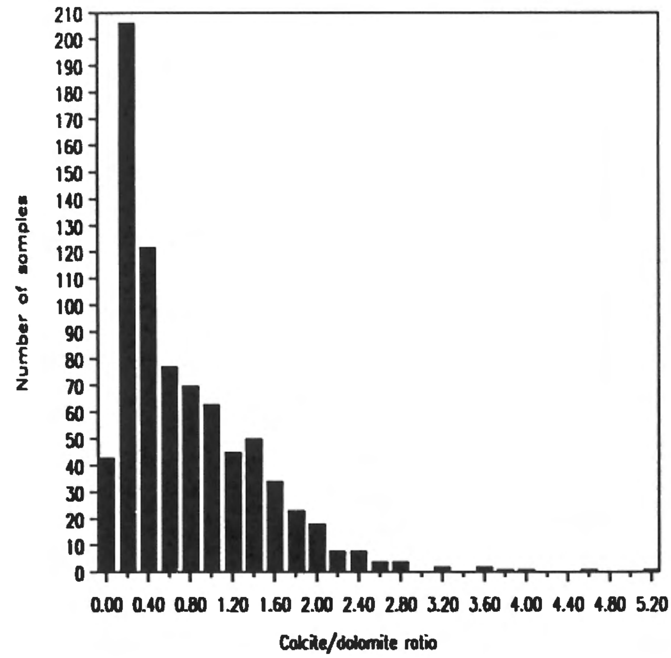

Figure 45. Histogram of calcite-to-dolomite ratios for all till samples.

COMPOSITIONAL GRADIENTS

Granule lithology

The relative proportions of carbonate, clastic (sandstone and conglomerate), and shield clasts of granule size (2-5.6 mm) were determined from 793 till samples. This technique has an advantage over field observation of presence and lithology of erratics, as presented in Figure 42, in that it quantifies abundance. Its disadvantage is that sparse erratics may not occur in kilogram-scale samples.

Shield erratics (Fig. 47A) comprise 0-100% of granules in till. High concentrations (30-100%) occur only over shield rock and conglomerate rich in shield clasts. Over most of the island, the shield component comprises <10% of granules and it appears to be absent on parts of the northern plateau, especially the eastern part. Thus, till on most of Prince of Wales Island has a low and nearly even background of shield-derived material. This distribution suggests that the area lies in the distal tail of a dispersion zone that is larger than the island (Clark, 1987). The distribution can be explained by ice flow phases 1 and 2 although it may be the net result of several glaciations. It agrees reasonably with the distribution of larger shield erratics (Fig. 42A) but exaggerates the area of absence.

Sandstone and conglomerate erratics (Fig. 47B) comprise 0-100% of till granules. Concentrations in the 20-100% range form a distinct band that nearly coincides with the subcrop of clastic rock. Over most of the island, clastic rock clasts comprise less than 10% of the granules. They are absent on the western peninsulas, as are boulder-size sandstone erratics

(Fig. 42C). A local high concentration on the western part of the northern plateau results from erosion of minor redbeds in the carbonate rocks.

Thus, much of the island lies in the tail of a zone of clastic rock dispersion, its distal edge or side defined by the 0% contour. This dispersion can be explained by transport from Peel Sound Formation beneath Franklin Strait during phase 1 and by transport from that formation on the eastern side of the island during the arcuate flow of phase 2. The size of the dispersion implies that these two flow phases lasted much longer than deglacial flows, which lasted for a century or so.

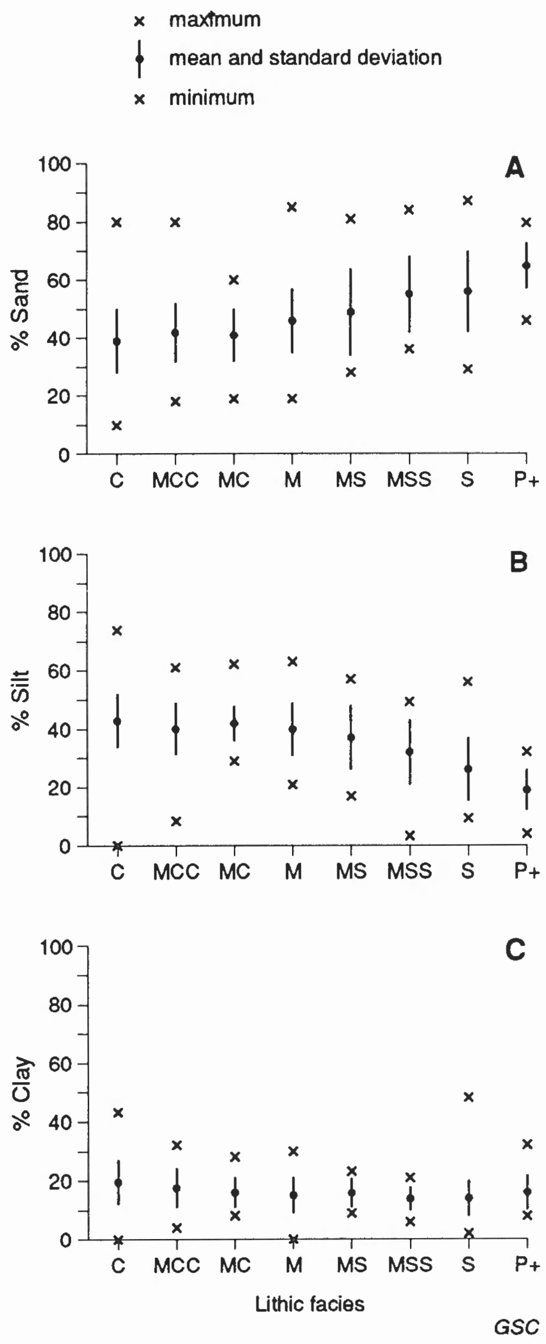

Figure 46. Statistical summary of **A**, sand; **B**, silt; and **C**, clay contents of the matrix of various lithic facies of till.

Other aspects of the distribution of granule-size clastic erratics (Fig. 47B) can be explained by eastward flow of phase 3. Till over carbonate rock south of Cape Hardy has abundant clastic erratics (>20%) dispersed from Peel Sound Formation to the west. Two areas of clastic rock on the southeastern part of the island have suppressed levels of clastic erratics. One corridor of low concentration extends across clastic rock and into Peel Sound at Transition Bay; another noses onto clastic rock west of Le Feuvre Inlet but does not breach it. Clastic clast concentrations there are suppressed relatively by carbonate material from the west.

Carbonate erratics (Fig. 47C) comprise 0-100% of till granules. They make up all granules over much of the western part of the island and most of them over other areas of carbonate rock. Slight depression of carbonate erratic levels results from the diffuse dispersion of clastic and shield erratics into these areas (Fig. 47A,B). Low concentrations occur over noncarbonate rock except at Transition Bay and Le Feuvre Inlet, where plumes of carbonate debris extend eastward across sandstone and conglomerate. These plumes are "Boothia type" dispersal features (Dyke and Prest, 1987; Dyke and Morris, 1988) formed by ice streams; debris is spread much farther downice from source in them than on either side. Elsewhere, concentrations of carbonate erratics drop sharply eastward across noncarbonate rock.

Matrix texture and carbonate content

The discussion of lithic facies above points out the systematic shift in mean grain size, particularly in sand and silt, between facies but also the overlap of textural ranges that may reflect control of factors other than parent material on grain size. The spatial variations in matrix texture (Fig. 48A-C) bears out the relationships between texture and parent material but does little to elucidate the cause of variations that seem attributable to other factors.

Till matrix is coarsest over noncarbonate rocks on the eastern side of the island where it has high sand, low silt, and variable clay content. But influence of substrate is mitigated at and south of Le Feuvre Inlet, particularly at Transition Bay, where finer till is smeared eastward. The plumes of fine till have low sand, high silt, and variable clay content. Thus, as we have surmised, till texture reflects parent material control primarily through inversely related variations in sand and silt, whereas clay remains insensitive to parent material.

Matrix texture varies in a complex manner in the large area of carbonate rock. Silt content is slightly higher, and sand content thus lower, over dolomite than over limestone (Fig. 48A,B). However, this relationship between texture and carbonate rock species does not hold in the clay fraction (Fig. 48C).

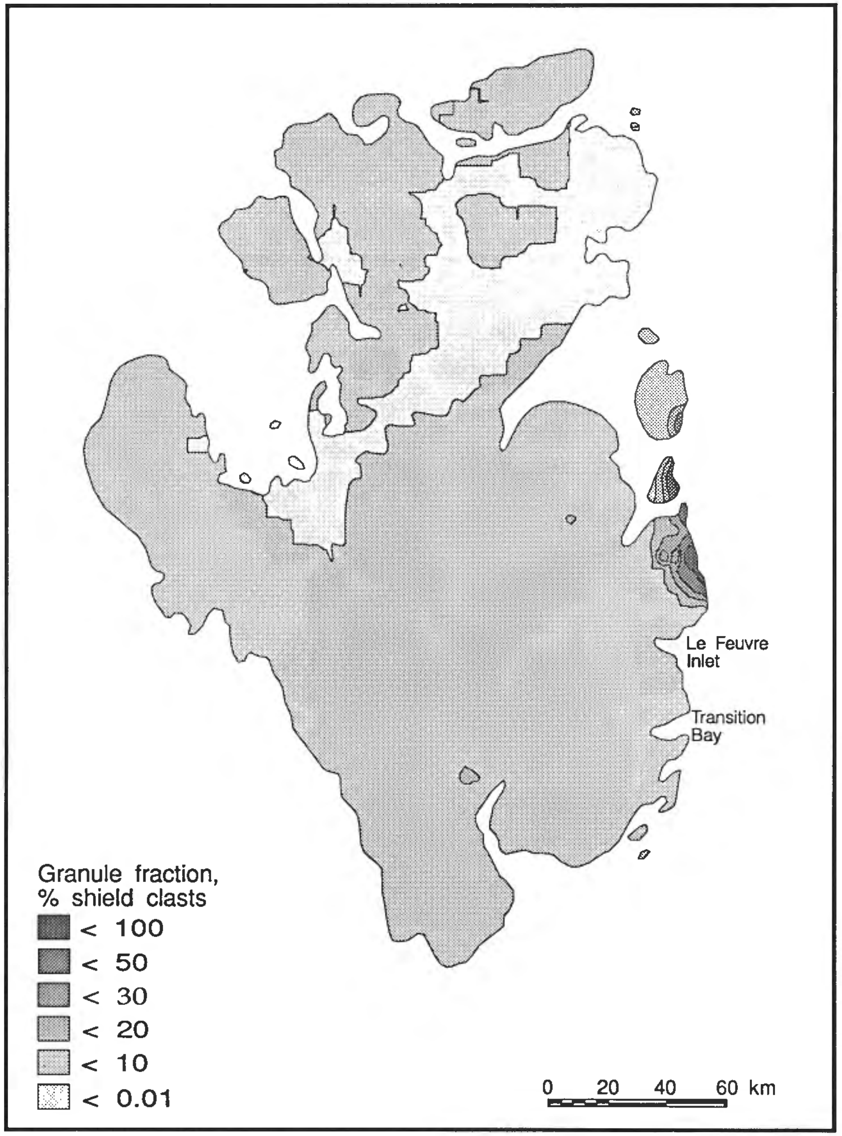

Figure 47A. Concentration of shield clasts in the granule fraction of till samples, Prince of Wales Island.

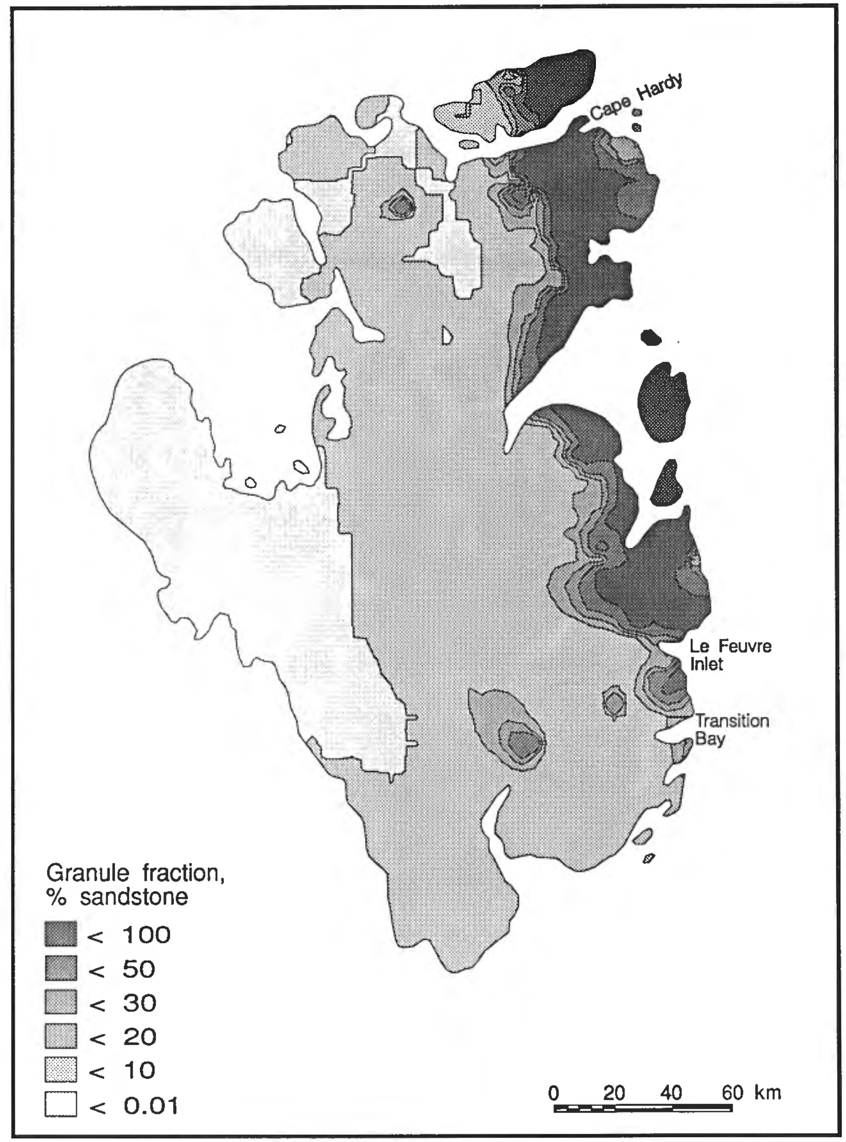

Figure 47B. Concentration of sandstone clasts in the granule fraction of till samples, Prince of Wales Island.

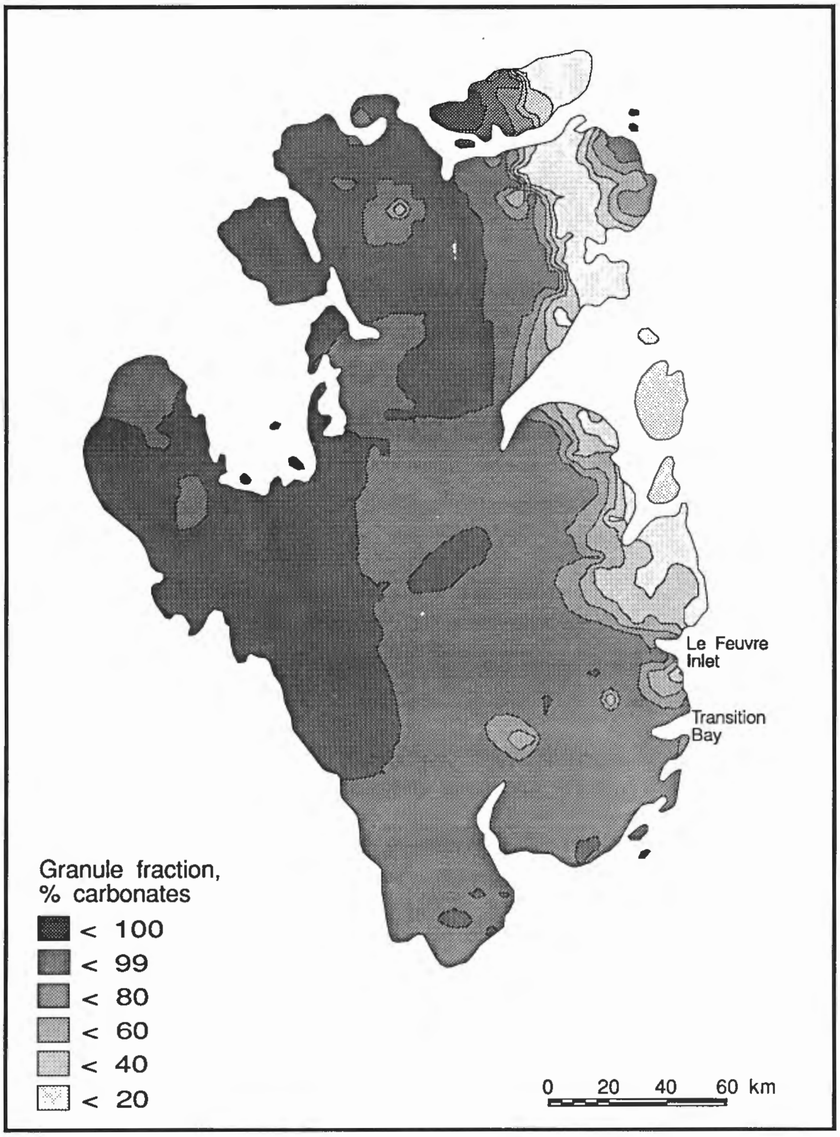

Figure 47C. Concentration of carbonate clasts in the granule fraction of till samples, Prince of Wales Island.

Textural variations also are not readily explained by glacial processes. There appears to be no relationship between morphological facies of till and till texture. Thus, end moraines have essentially the same grain size composition as drumlin fields or till plains. Similarly, tills laid down during the various ice flow phases are indistinguishable texturally (cf. Maps 1689A, 1690A and Fig. 48). In this area, then, till texture varies significantly but is relatively uninformative as regards provenance or formative processes. However, the variations may be important geotechnically.

Variations in carbonate content of the till matrix (Fig. 48D) coarsely reflect provenance and transport during phase 3, among other things. Carbonate content is lowest over noncarbonate rock except near Transition Bay and Le Feuvre Inlet where highly calcareous till plumes cross clastic rocks. For reasons already discussed (see *Lithic facies*), however, matrix carbonate content is not a simple index of till provenance. The plume at Le Feuvre Inlet appears larger than that at Transition Bay, which contradicts other indicators of relative dispersion in the two. The exaggerated width of the Le Feuvre Inlet plume is likely because part of its carbonate derived from calcareous sandstone rather than from limestone to the west.

The calcite and dolomite components of matrix carbonate, taken separately (Fig. 48E,F), should distinguish till derived from limestone and dolomite, respectively. Indeed, dolomite exceeds calcite in till over dolomite rock on western, northwestern, and northeastern parts of the island (Fig. 48F), thus indicating that most till over carbonate rock is locally derived. However, dolomite also well exceeds calcite in till over a large area of southern Prince of Wales Island mapped as dominantly limestone. This high dolomite content could reflect northward dispersion of the bulk of the till there from unmapped dolomite rock south of the island, or it could indicate that bedrock under southwestern Prince of Wales Island is mostly dolomite.

DISPERSAL PATTERNS AND ICE DYNAMICS

Dispersal patterns are complex here because of widely shifting ice flow patterns and spatial variations in basal flow rates. During early phases of the last glaciation, shield erratics and Peel Sound sandstone and conglomerate erratics were dispersed northwestward, possibly augmenting similar dispersion in earlier glaciations. Shield erratics of boulder size are spread from end to end of the area in a uniformly low concentration, <1% of till volume. Debris from Peel Sound Formation dispersed by these early flows is more restricted but locally more abundant. It occurs on eastern Prince of Wales Lowland and the western part of the northern plateau mostly in low concentrations but reaches modest abundance on the southeastern lowland.

The more restricted occurrence of Peel Sound erratics than of shield erratics, despite their larger local source area and greater erodability, indicates that ice flow probably never had a more westward vector than during phase 2. Hence, most shield erratics probably came from Keewatin rather than from the closer Boothia Arch. Transport of shield erratics thus exceeded 700 km. If some were transported from original source during the last glaciation, phases 1 and 2 and preceding buildup phases collectively were longer than subsequent phases.

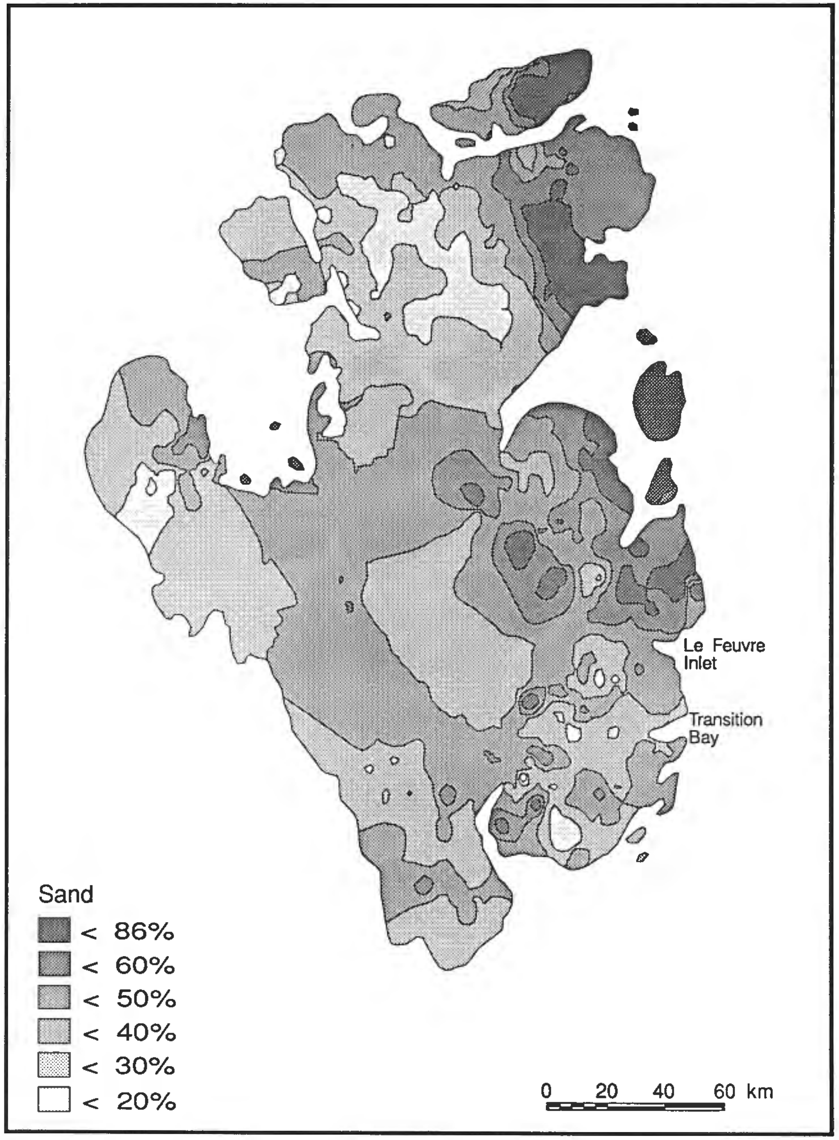

Figure 48A. Sand content of till matrix, Prince of Wales Island.

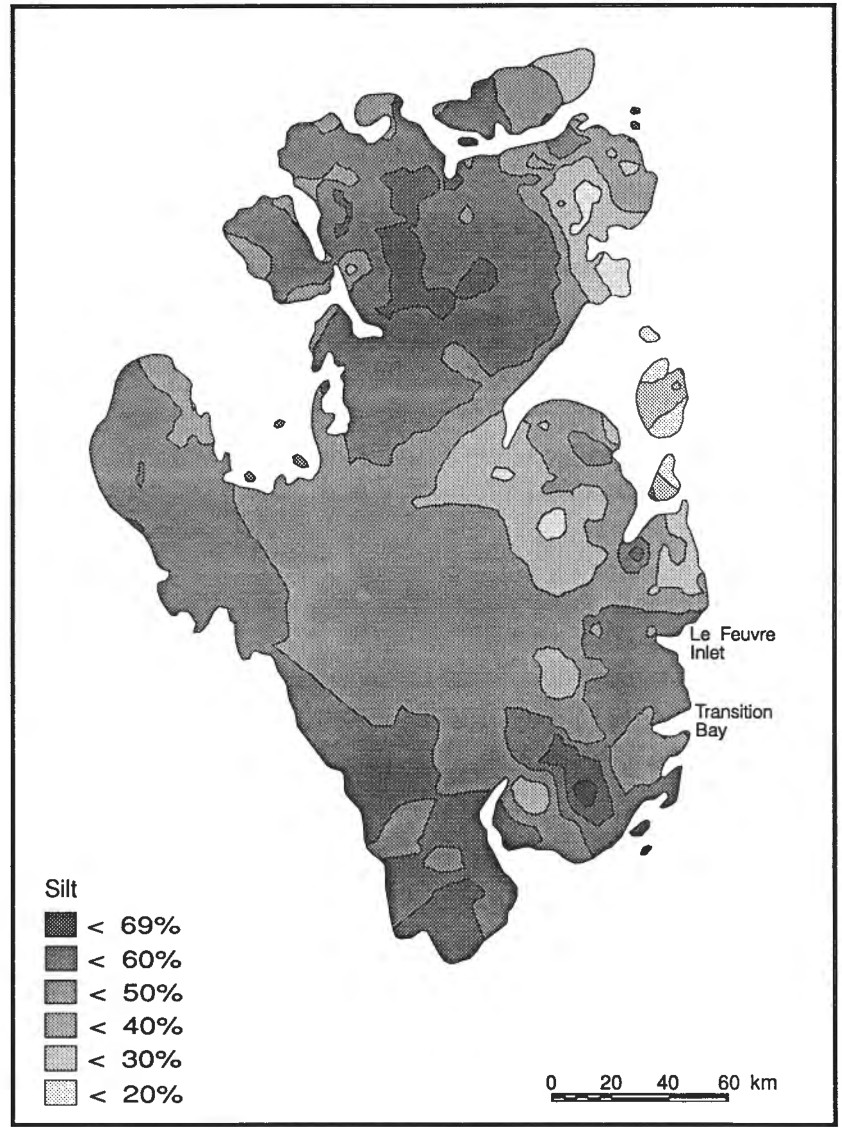

Figure 48B. Silt content of till matrix, Prince of Wales Island.

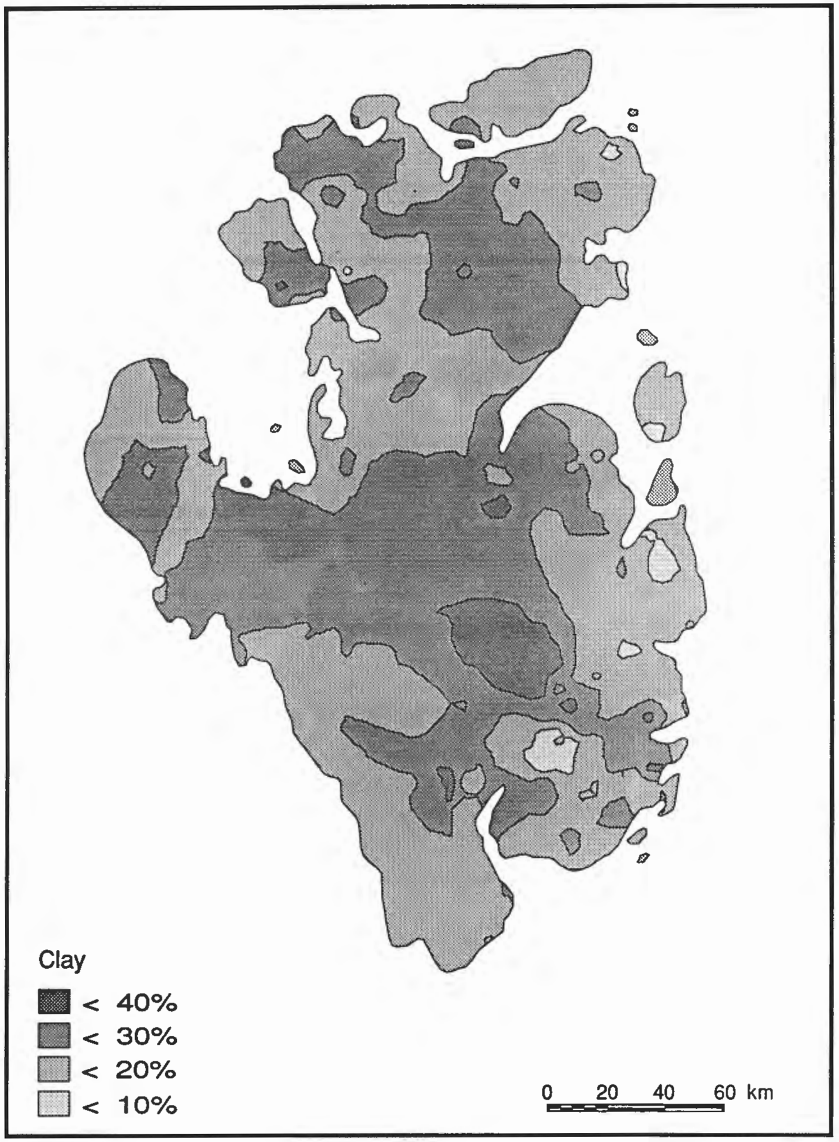

Figure 48C. Clay content of till matrix, Prince of Wales Island.

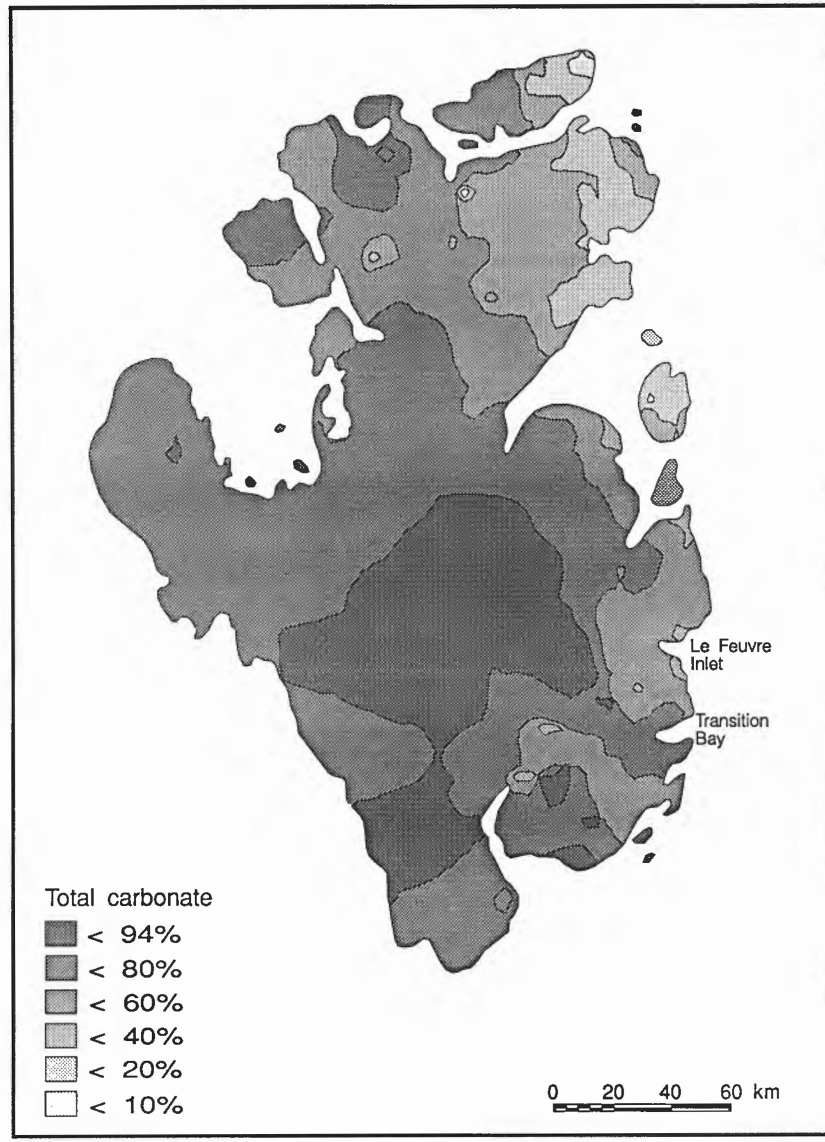

Figure 48D. Carbonate content of till matrix, Prince of Wales Island.

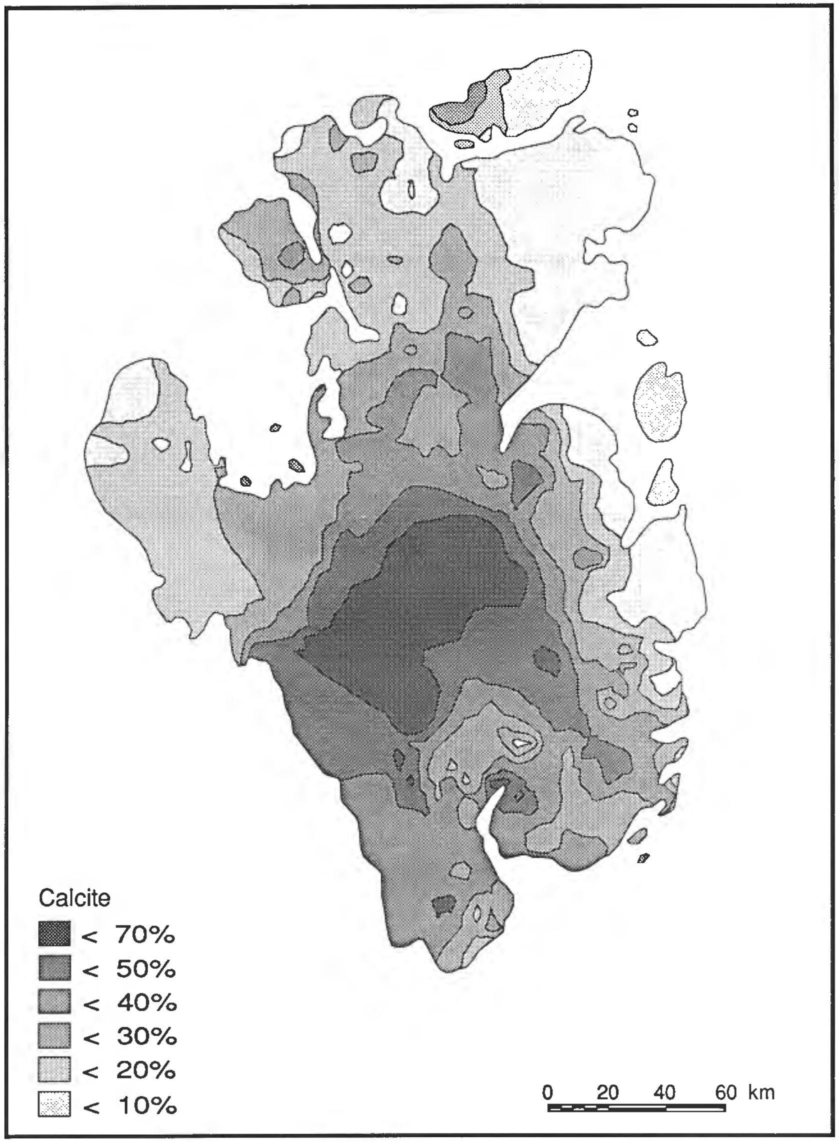

Figure 48E. Calcite content of till matrix, Prince of Wales Island.

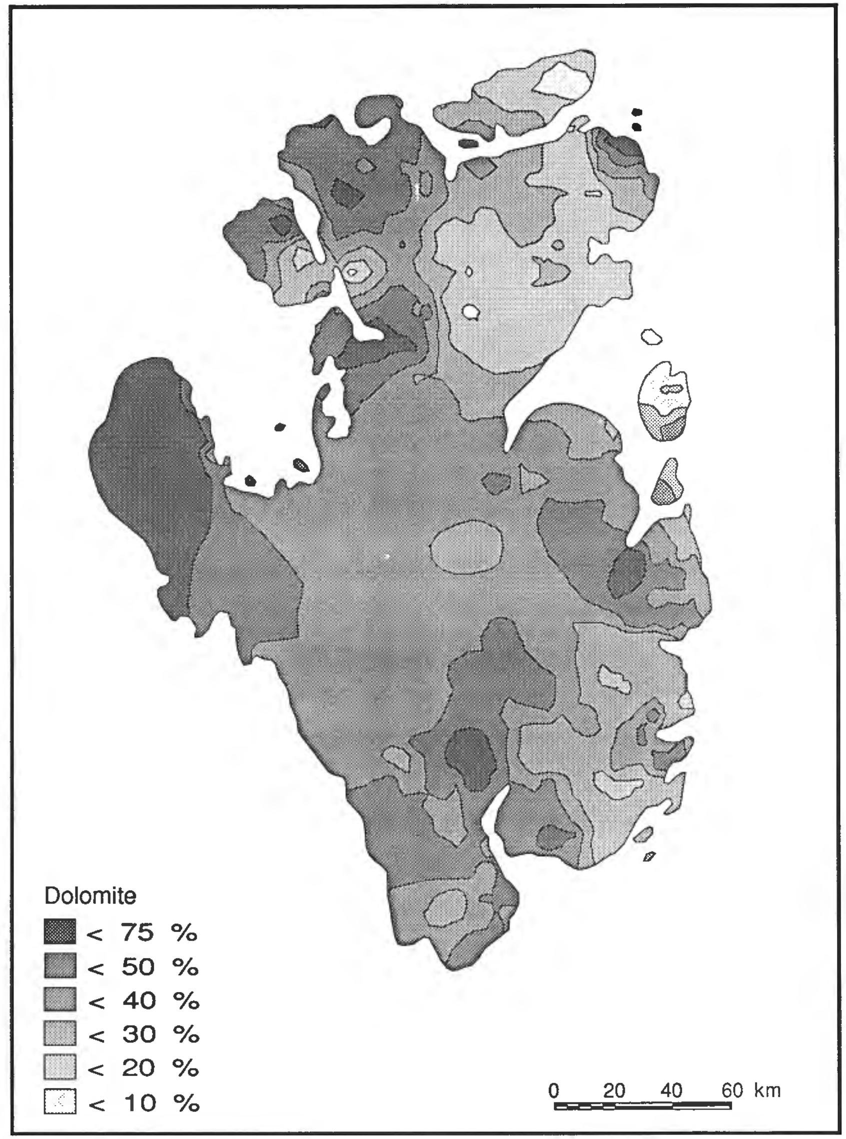

Figure 48F. Dolomite content of till matrix, Prince of Wales Island.

During phase 3 and later, debris was dispersed eastward across north-aligned belts of bedrock, from carbonate rock to sandstone, to conglomerate, to more carbonates, to shield rock and into Peel Sound. Dispersion occurred from the north to the south end of the area but was greatest in two plumes. In the Transition Bay plume, carbonate debris makes up about 70% of granules about 30 km downice of the carbonate rock contact where it enters Peel Sound (Fig. 49, 50); in the weaker Le Feuvre Inlet plume, carbonate debris drops to 10% about 35 km from the contact (Fig. 50). Beyond the dispersal plumes, debris concentrations drop off downice of contacts much more steeply. For example, between the two plumes debris concentrations decline to about 10% within 20 km (Fig. 50); south of Cape Hardy clastic rock granules decline to 10% as little as 3 km downice of the contact (Fig 51). Within the Transition Bay plume debris concentrations decline downice nearly linearly (Fig. 52A); elsewhere they decline exponentially (Fig. 52B). Therefore, the dispersal plumes represent corridors of ice that flowed much faster than ice on either side; i.e., ice streams.

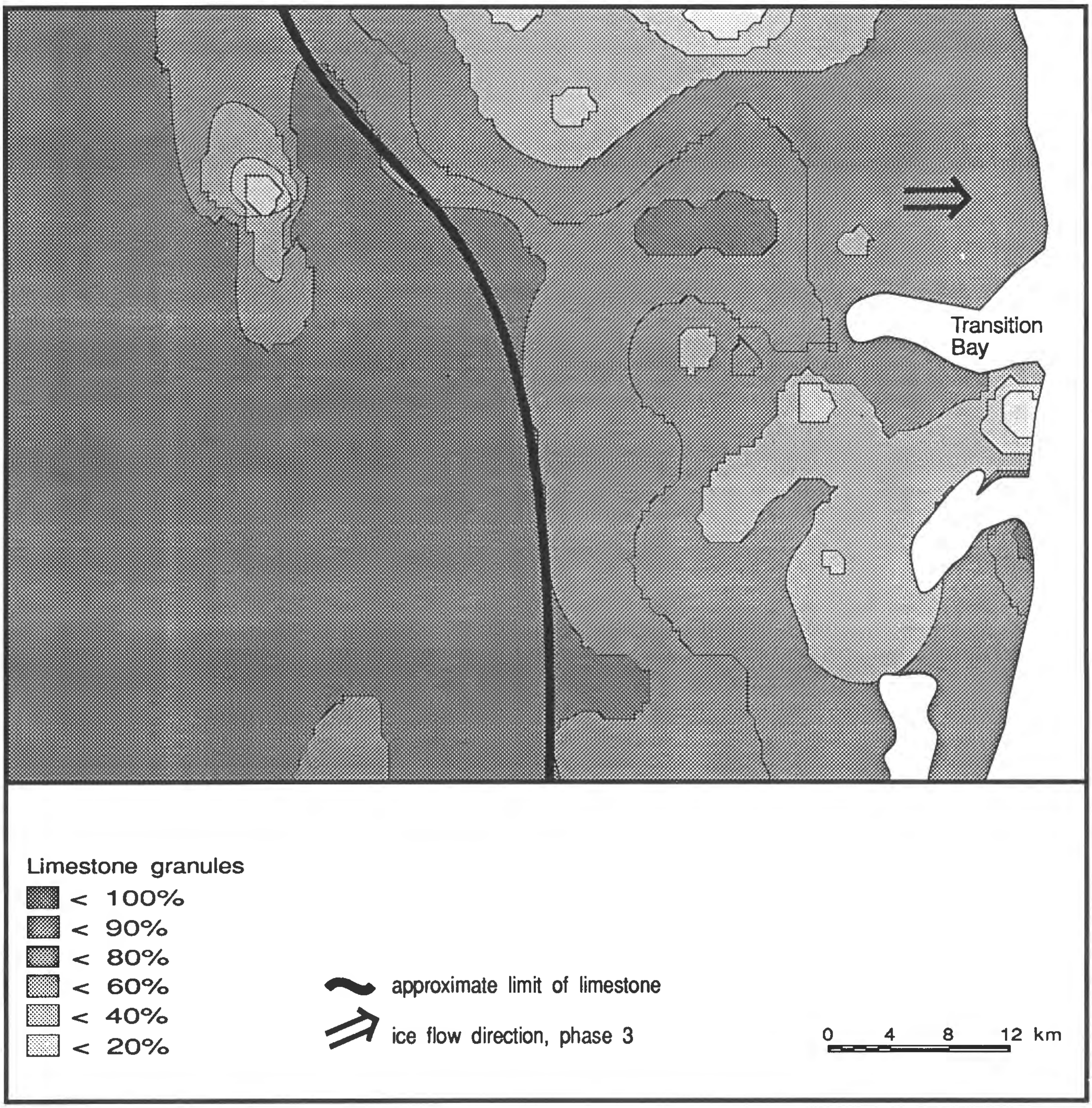

Figure 49. Concentration of carbonate clasts in the granule fraction of till samples from the Transition Bay area, Prince of Wales Island.

The regional extent of ice flow phase 3 and the amount and distance of debris dispersed indicate that it was much longer than any subsequent deglacial flow phase, though not as long as phases 1 and 2 together. Ice flow and till composition data from Somerset Island and Boothia Peninsula (Dyke, 1983; 1984) show that phase 3 flow crossed the area east of Peel Sound and dispersed debris from Prince of Wales Island into Gulf of Boothia (Fig. 50). Carbonate erratic debris concentrations on the eastern part of the shield rocks on Somerset Island are as high as 50% as much as 120 km from nearest source on Prince of Wales Island (Fig. 50). The debris from Prince of Wales Island and from Franklin Strait was dispersed abundantly across the area east of Peel Sound over a zone 150 km wide, i.e., normal to ice flowlines. Dyke (1984) interpreted this zone as the product of an ice stream. In that light, the Transition Bay and Le Feuvre Inlet dispersal plumes are headward components of the previously recognized ice stream.

The exact relationship of the Transition Bay and Le Feuvre Inlet plumes to the wider dispersal train (Fig. 50) is obscured by the lack of data on till composition from the floor of Peel Sound, but tentative conclusions can be drawn. The highest concentrations of erratic debris in the granule fraction of till east of Peel Sound are on northernmost Boothia Peninsula. The 60% and higher contours there outline two plumes, the more northerly of which aligns roughly with the Transition Bay plume. Erratic debris concentrations are as high as 80% at 80 km downice of source (Fig. 50, 52A). Along the flowline extending through Transition Bay, then, debris concentrations drop off very slowly

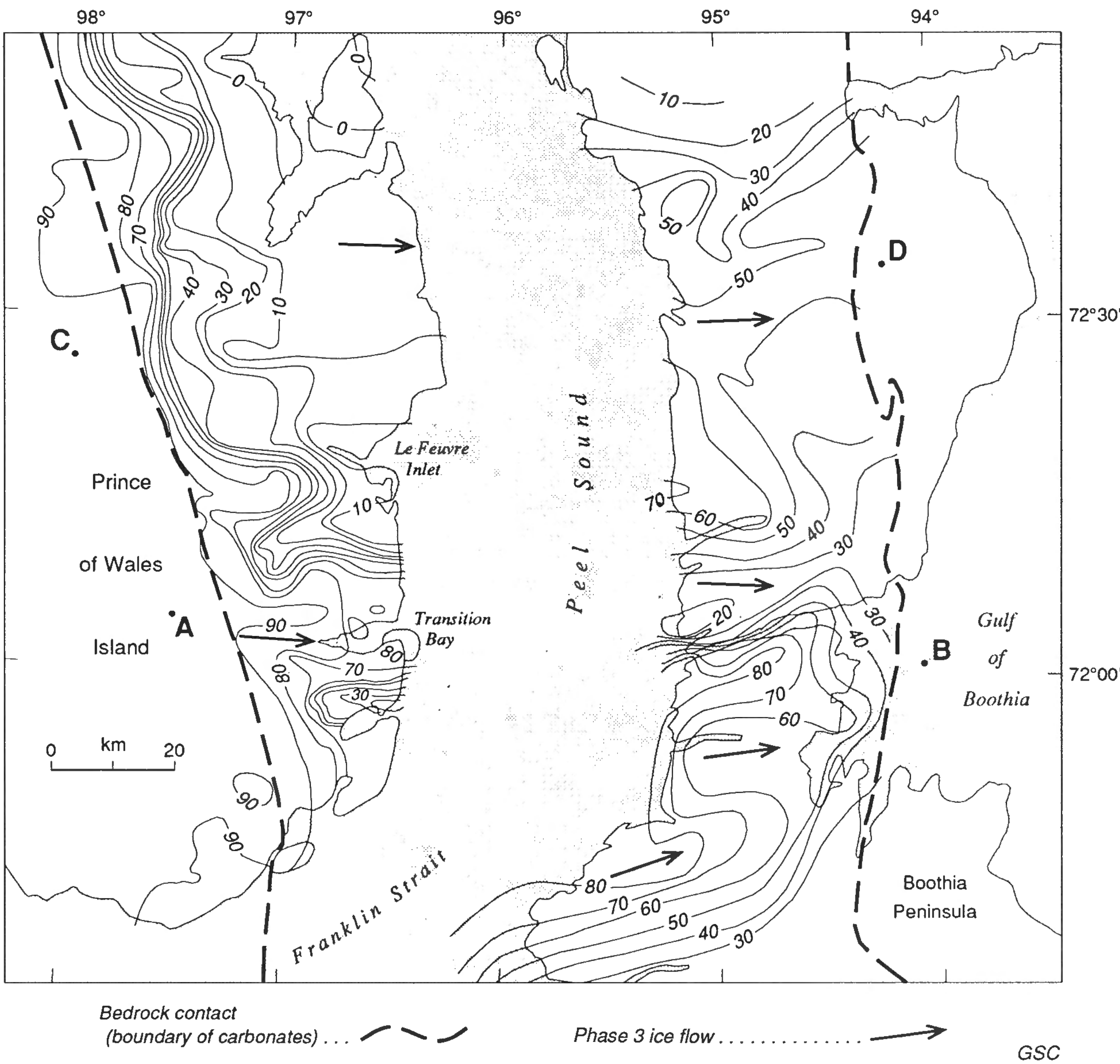

Figure 50. Carbonate erratic concentration in the granule fraction of till on either side of southern Peel Sound (data from the east side sketched from Dyke, 1984).

and nearly linearly for nearly 100 km. The more abrupt drop off at the east end of that profile is not characteristic of the entire zone of dispersion (Fig. 50).

The Le Feuvre Inlet plume does not appear to continue east of Peel Sound. Indeed, erratic concentrations are much higher east of Peel Sound, 40-70% directly downice of Le Feuvre Inlet, than in the distal end of the Le Feuvre Inlet plume, where they have declined to 10%. Its limited nature suggests that the Le Feuvre Inlet plume is younger than the overall zone of eastward dispersion and that it formed largely during deglaciation.

North of Le Feuvre Inlet, carbonate erratic concentrations are generally much lower on the west than on the east side of Peel Sound (Fig. 50, 52B). East of the sound carbonates comprise 30-50% of till granules; west of the sound they comprise <10% over broad areas. This difference can be

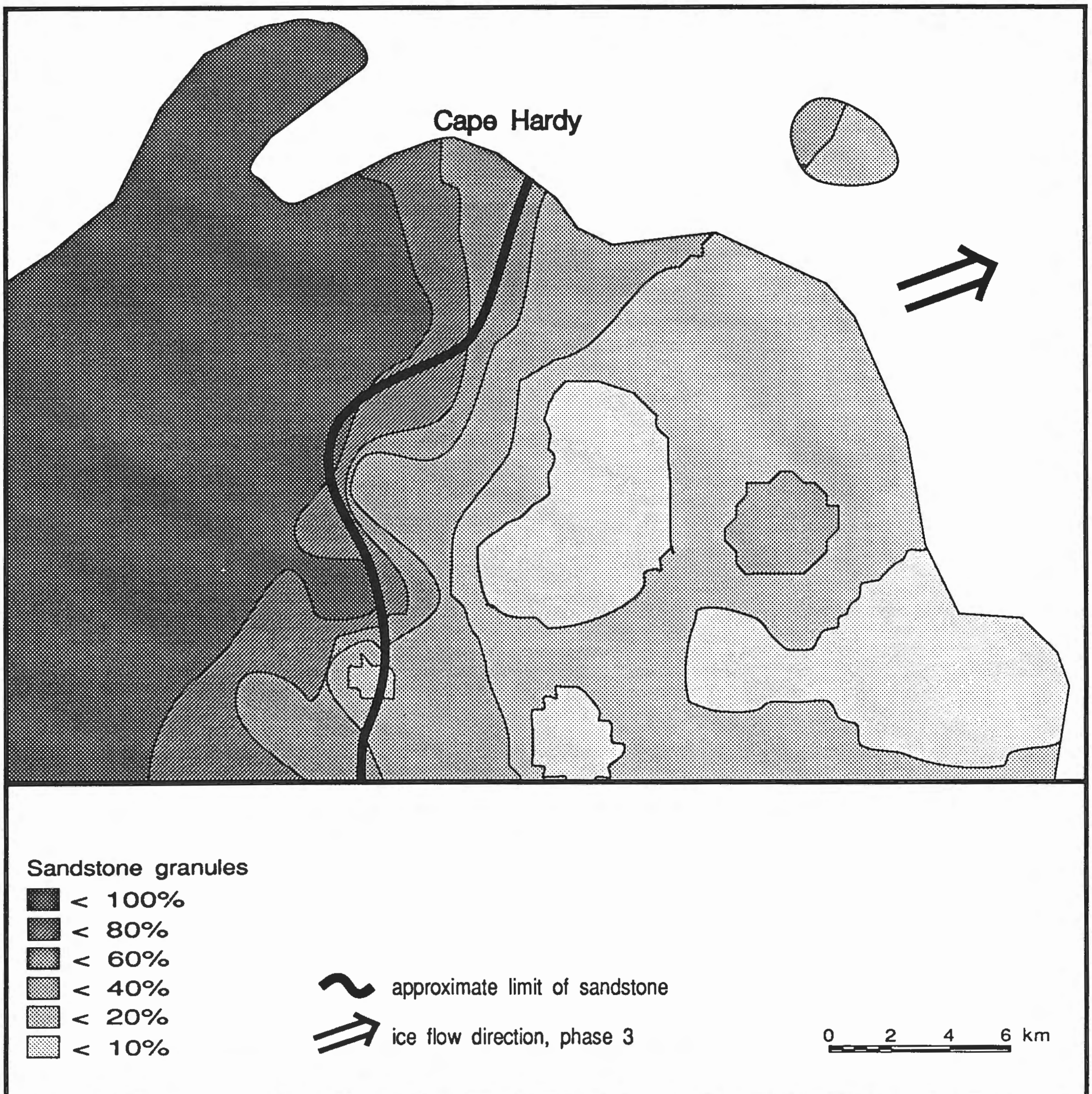

Figure 51. Concentration of sandstone clasts in the granule fraction of till south of Cape Hardy, Prince of Wales Island.

interpreted in various ways, but perhaps the simplest is that much more local debris was incorporated into till north of Le Feuvre Inlet during deglaciation than on adjacent Somerset Island, thus diluting the erratic component. Possibly, though, the carbonate debris on Somerset Island was derived from englacial debris dispersed eastward from Prince of Wales Island during phase 3, having been entrained there during phases 1 and 2. In this way, the phase 3 carbonate debris source may have been within the cold-based ice zone. Much of the carbonate debris on eastern Prince of Wales Island may have been entrained and dispersed later in phase 3 and during deglaciation as the boundary between cold- and warm-based ice retreated. For this explanation to pertain, however, the earlier source of carbonate debris, that which was spread eastward to Somerset Island, must have been largely depleted in the source region, west of Peel Sound (Fig. 52B).

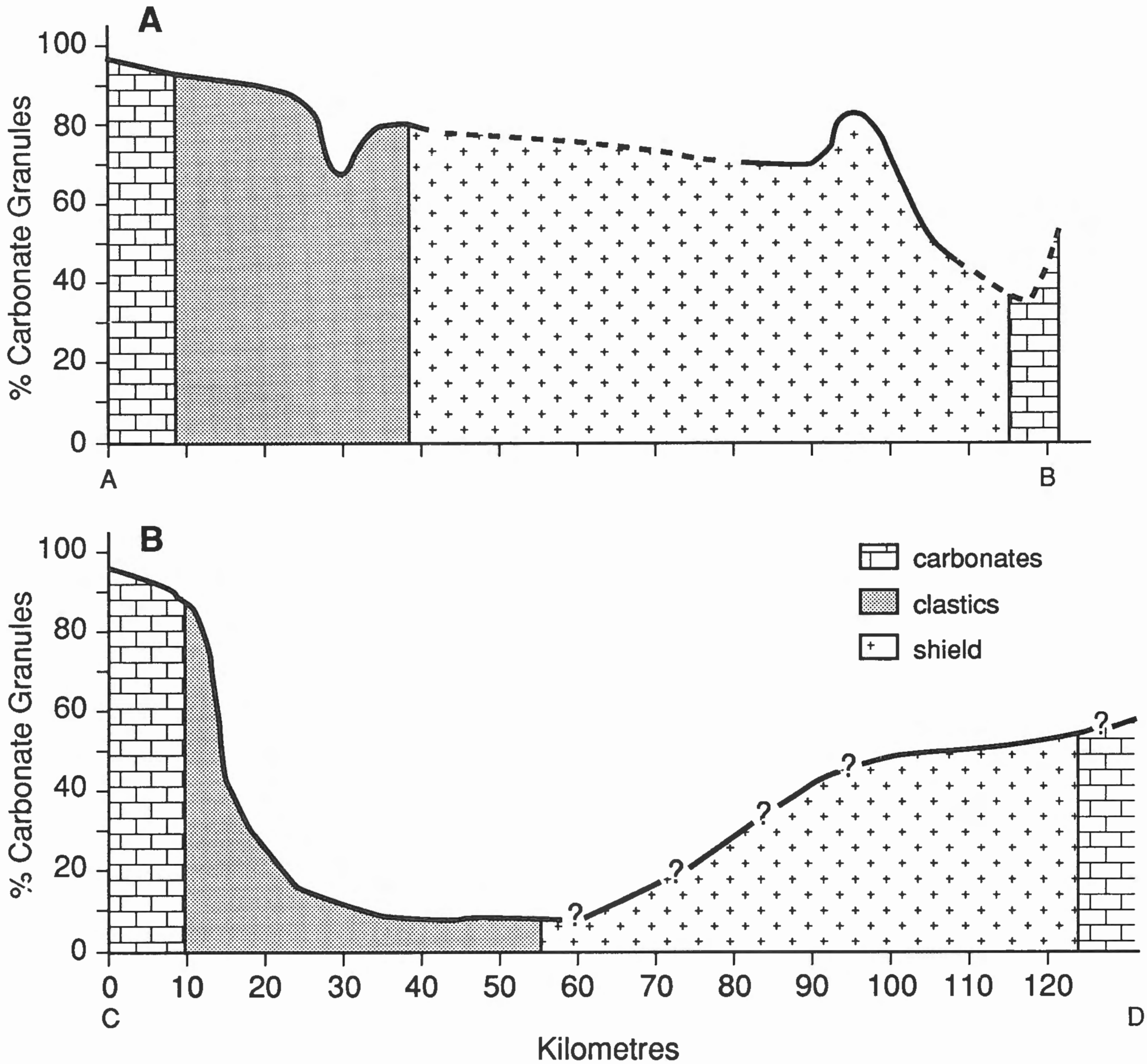

Figure 52. Profiles of carbonate erratic concentrations along ice flowlines: **A**, A-B in Figure 50; **B**, C-D in Figure 50.

QUATERNARY HISTORY

INTRODUCTION

The Quaternary history of Prince of Wales Island is interpreted from three sets of data: 1) the litho- and morphostratigraphy of deposits are portrayed on Maps 1689A and 1690A and described and interpreted in *Surficial materials and landforms*; 2) the compositional variations in till reflect glacial dispersion events described in *Till composition and glacial dispersion*; and 3) age estimates of fossils are provided by amino acid analyses, uranium-series dates, and radiocarbon dates.

The stratigraphy and geomorphology record two glaciations, an interglaciation, and a sequence of postglacial events. They further record three major ice flow phases of the last glaciation and several minor ice flow phases during deglaciation. The fossil ages assign the interglaciation to the Sangamonian Stage and the last glaciation to the Wisconsinan Stage and the early Holocene. They also provide a detailed chronology of deglaciation, of relative sea level change, and of penetration of boreal driftwood and bowhead whales into the central Arctic.

Exceptional and unusual preservation of glacial landscapes from various phases of the last glaciation allows us to infer changes in the basal thermal regime of the ice sheet and, from that, to suggest a history of permafrost.

EVENTS BEFORE WISCONSIN GLACIATION

Evidence of pre-Wisconsinan glaciation is limited to one stratigraphic exposure. The oldest exposed Quaternary sediment, tentatively identified as till, outcrops along Fisher River (Morris, 1988). Clast fabric indicates emplacement by northward flowing Laurentide ice.

Low elevation fluvial gravels outcrop below Wisconsinan till in several sections. These indicate that sea level was similar to present and amino acid ratios of redeposited marine shells indicate a Sangamonian age. At one site near Cape Hardy, subtill fluvial sands are periglacially deformed and capped by a paleosol that includes a well developed humic A-horizon. Its pollen assemblage resembles that in postglacial peat, except it contains exotic pine pollen.

The transition from interglacial to glacial conditions is recorded at a section near Cape Hardy where subtill stony glaciomarine mud contains paired shells of *Hiatella arctica* that yielded a uranium-series age of 80 ka and compatible amino acid ratios. These sediments date from the advance of ice across northern Prince of Wales Island and indicate that relative sea level had risen >30 m above present before the area was ice covered. Thus, >30 m of isostatic depression had occurred in front of the advancing ice, which suggests slow buildup.

WISCONSIN GLACIATION

Wisconsinan time appears to be represented by a single till sheet. Nowhere has more than one till been observed above sediments of apparent Sangamonian age. The till sheet contains several morphostratigraphic units that allow subdivision of the Wisconsin Glaciation into three major ice flow phases.

Ice flow phase 1

The oldest recorded Wisconsinan ice flow occurred when all of Prince of Wales Lowland and likely the entire island was ice covered. Ice flow is recorded by megaflutes on Arrowsmith Plains and by the Mount Cowie drumlin field. Together they sweep from Franklin Strait to Viscount Melville Sound and record nearly straight flowlines with an azimuth of 330° (Fig. 53A). The record of this flow has been eroded elsewhere by later flows.

The bedforms indicate that the ice sheet over the lowland was warm based and sliding, whereas the weathered rock terrain of the northern plateau indicates that it was cold based over that area. Straight flowlines over 225 km indicate little or no topographic control, hence thick ice. The ice margin, therefore, likely lay north of the island, near or beyond what is commonly taken as the Wisconsinan limit of Laurentide ice in this region (Prest et al., 1968). Phase 1, therefore, dates from late in the buildup of the last ice sheet or later. Bedforms indicate flow from the mainland rather than from Queen Elizabeth Islands. During this flow, shield erratics were dispersed northward across the island, though some may have been moved in earlier. The eastern part of the northern plateau bears few, if any, shield erratics, which possibly indicates divergent flow over that area.

Ice flow phase 2

During phase 2, ice flowed across Prince of Wales Lowland with a markedly curved flowline (Fig. 53B). Phase 2 flowlines are recorded by the Crooked Lake drumlin field. At the south end, drumlins are oriented at 355° and at the north end at 300°. Outliers of the drumlin field extend eastward nearly to Peel Sound where they are surrounded by till with later ice flow trends. So at this time the northward flowing ice sheet still spanned the width of the island, at least in the south.

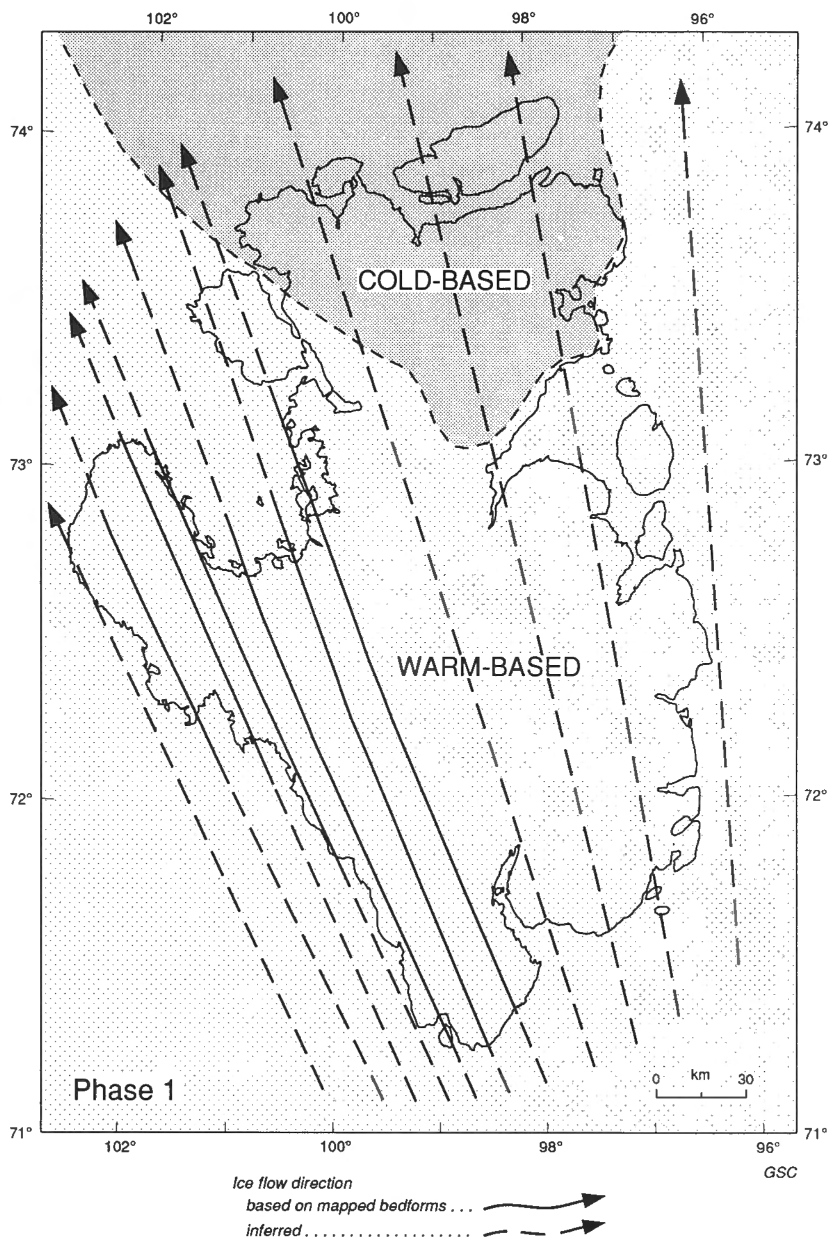

Figure 53A. Ice flow direction and basal thermal conditions during ice flow phase 1, Prince of Wales Island.

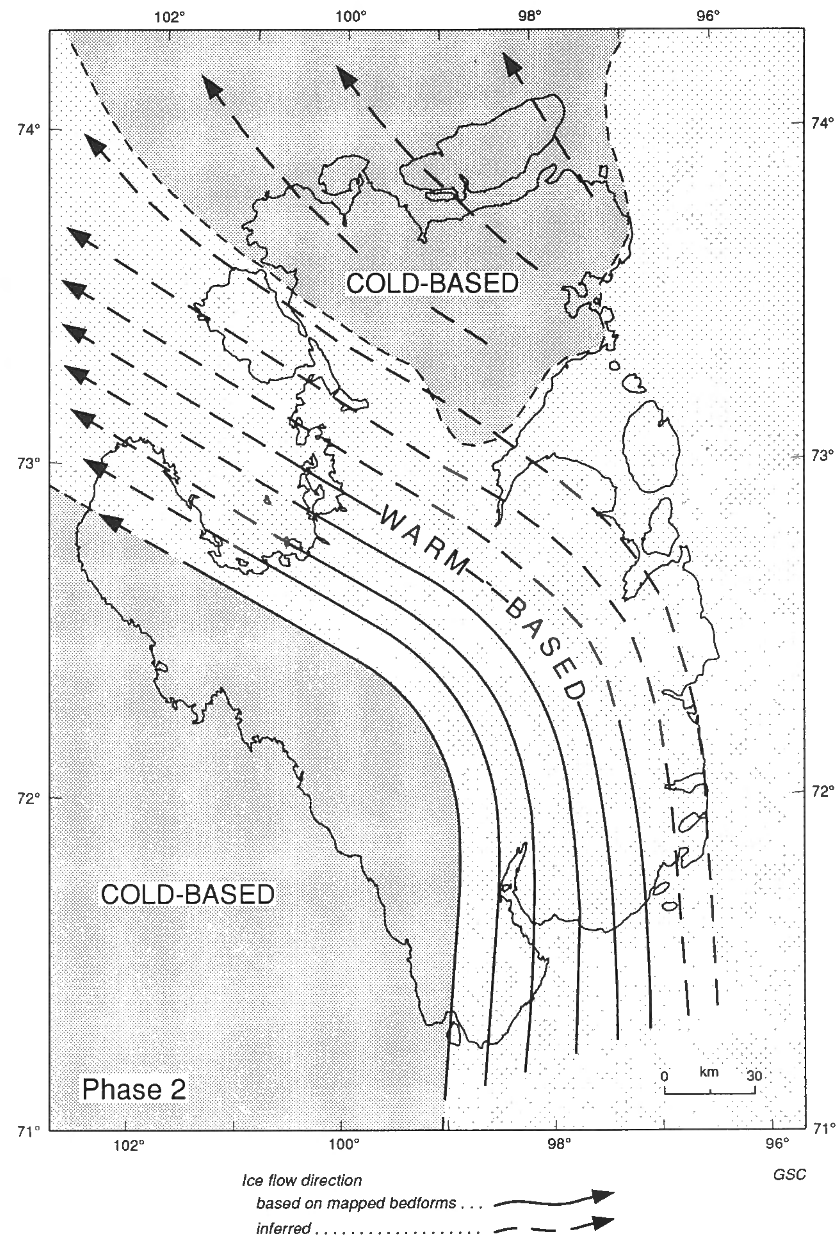

Figure 53B. Ice flow direction and basal thermal conditions during ice flow phase 2, Prince of Wales Island.

The drumlin field grades downice into the Ommanney Bay ribbed moraine field; i.e., bedforms change from streamlined, longitudinal forms to nonstreamlined, transverse forms. This gradation reflects a change in flow dynamics, possibly from a wet, sliding bed to a regelation zone of alternate sticking and sliding. During phase 2, the ice margin was north of the ribbed moraine field and may have been north of the island.

The drumlin field contacts the older Arrowsmith megafluted till plain to the west along a remarkable, nearly continuous, streamlined till ridge interpreted as a lateral shear moraine. Arrowsmith Plains remained ice covered during phase 2 and its lack of alteration indicates that the ice was cold based there. The lateral shear moraine, therefore, marks the boundary between cold- and warm-based ice.

The curve of the Crooked Lake drumlin field and apparently sudden change in ice dynamics from phase 1 to phase 2 require explanation. The curve roughly parallels the eastern margin of the lowland, so it could signify that the ice sheet thinned and that flow was deflected. However, thinning does not explain the change from warm- to cold-based conditions over Arrowsmith Plains that accompanied the change in flow dynamics. A satisfactory explanation would account for both changes.

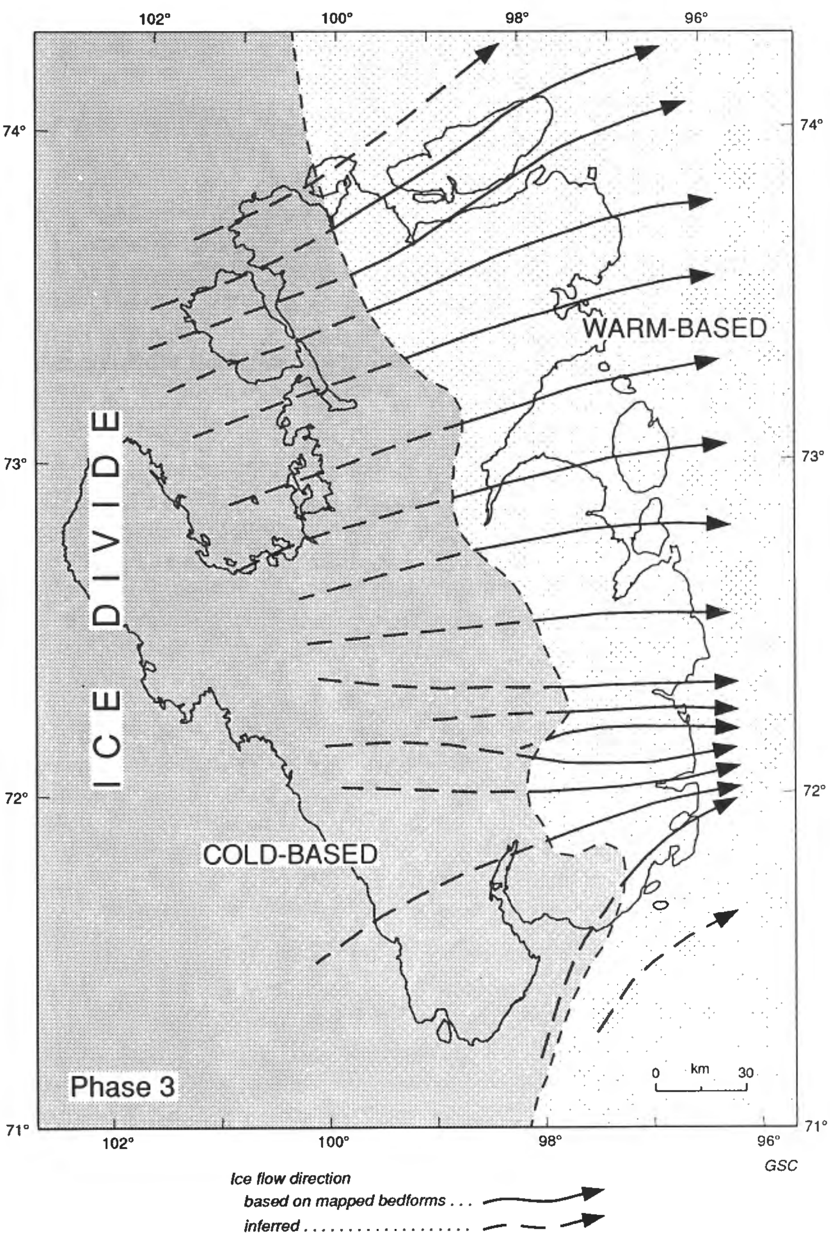

Figure 53C. Ice flow direction and basal thermal conditions during ice flow phase 3, Prince of Wales Island.

The change from warm- to cold-based conditions over Arrowsmith Plains, whatever the cause, would have effected a reduction in ice flow, with basal flow reduced to zero. When the ice froze to its bed, the still-sliding ice farther east may have curved westward because of the drag caused by the cold-based ice. If so, the change in flow pattern between phases 1 and 2 can be explained by the change in basal thermal conditions.

If this juxtaposition of cold- and warm-based ice persisted for long, the faster moving ice would have drawn down the ice surface and captured adjacent flow, thus enlarging its drainage area. How long the condition persisted is not known. But the northwestward dispersion of Peel Sound conglomerate erratics tens of kilometres across Prince of Wales Lowland as far as Smith Bay is best explained by the phase 2 flowline configuration.

The change from warm- to cold-based conditions over Arrowsmith Plains can be variously explained. Either ice thinning at the end of phase 1 could have caused downward migration of englacial and subglacial isotherms; or lowering of mean annual air temperature at the ice surface may have cooled the entire ice mass. These changes should have affected the whole lowland. Conceivably, once part of the ice over the lowland became cold based, more flow was channelled into the remaining warm-based zone and the increase in flow rate, hence in strain heating, maintained warm-based conditions. Alternatively, the ice may have become cold-based over the entire lowland after phase 1 and the phase 2 bedforms represent re-expansion of a warm-based zone.

If the change in ice dynamics between phases 1 and 2 was caused by ice thinning over Prince of Wales Lowland, the ice must have thickened again without bringing on a reversion to phase 1 conditions, or the thinning must have been limited because ice flowed eastward from the lowland during phase 3.

Ice flow phase 3

Between phases 2 and 3, flow switched direction, apparently suddenly, from northward and northwestward to eastward (Fig. 53C). Thus, over central Prince of Wales Lowland, flow direction changed by 150°. Eastward flow is recorded from the south to the north end of the area in several ways: by flutings, ice moulded bedrock, and striae on the highest terrain in the east, superimposed in places by younger ice flow features in different orientations; by the Transition Bay and Le Feuvre Inlet drumlin fields and associated dispersal plumes; by dispersion from Peel Sound red beds across older grey carbonates north of Back Bay; and by dispersion from Devonian grey carbonates eastward across Peel Sound red beds everywhere from Russell Island to Franklin Strait.

This same flow is strongly recorded east of Peel Sound, from northern Somerset Island to central Boothia Peninsula. It carried debris from Prince of Wales Lowland at least to Gulf of Boothia (Dyke, 1984). Hence, phase 3 dates from a time of complete regional ice cover and it created dispersal features that extend more than 150 km.

As mentioned, during phase 3 ice flowed from the Crooked Lake drumlin field and the Arrowsmith megafluted till plain. Because these older landscapes survived unmodified by phase 3 flow, ice over them must have been cold based, or at least not sliding. The boundary between cold- and warm-based ice during phase 3 was about at the contact of till unit T^3b with older till units (Fig. 53C). The Fisher Lake ribbed moraine field occupies the contact zone between warm- and cold-based ice and, like the Ommanney Bay ribbed moraine field of phase 2, is inferred to have formed under transitional, stick and slide, basal ice conditions. Alternate basal sticking and sliding could have resulted from oscillations of the boundary between warm- and cold-based ice or from a patchwork arrangement of small cold- and warm-based areas such that flowlines crossed from one to the other. Either would have caused accelerations and decelerations of flow and attendant infolding and stacking of basal debris.

What caused the sudden rotation of flow between phases 2 and 3? It occurred at a time of near maximal ice thickness when the margin lay well beyond the island. It must have been sudden for no intervening flows are recorded, despite widespread preservation of older terrain. The new eastward flow regime included major ice streams that extended eastward at least to Gulf of Boothia. Furthermore, the zone of cold-based ice on western Prince of Wales Island increased significantly in size, expanding eastward, as the flow switched direction. So again we need to explain both a large, sudden change in flow direction and a coincidental change in basal thermal conditions.

Because flow changed from northward to eastward, the cause was likely an event in the east. The Transition Bay and Le Feuvre Inlet ice streams are features of phase 3; they blend into a wider stream that crossed Somerset Island and entered Gulf of Boothia and may have extended through the gulf and Lancaster Sound as an ice shelf or an ice stream (Dyke and Prest, 1987).

The change from phase 2 to 3 then likely was caused by a change in ice dynamics in Gulf of Boothia, and perhaps even earlier in Lancaster Sound. This change involved a new drawdown flow into these channels that propagated headward to Prince of Wales Island. By effecting a 90° and more shift in flow over Prince of Wales Island, and likely over a broader area, it created a new ice divide over Prince of Wales Lowland or farther west, the M'Clintock Ice Divide (Dyke, 1984; Dyke and Prest, 1987).

Tentative ages of flow phases and origin of phase 3

Exactly when the switches from phases 1 to 2 and 2 to 3 occurred can not be determined directly from the glacial geology of Prince of Wales Island because it remained ice covered during these events. The best that we can do is to draw inferences from the glacial history of the eastern margin of the Laurentide Ice Sheet, particularly the part directly downice of Gulf of Boothia, namely the mouth of Lancaster Sound.

Glacial history of outer Lancaster Sound is documented best on Bylot Island (Klassen, 1989; Klassen and Fisher, 1988). Large lateral moraines along its north coast were laid down by a grounded outlet glacier, the extension of an ice stream flowing out Lancaster Sound. They were formed during Eclipse Glaciation, an event beyond the range of radiocarbon dating. They have been correlated with Early Foxe moraines, which occur all along eastern Baffin Island (Andrews, 1985, 1989). Foxe Glaciation is the eastern Arctic synonym for Wisconsin Glaciation.

The Lancaster Sound outlet glacier and feeding ice stream was one of the largest features of the Early Wisconsinan Laurentide Ice Sheet. Any reasonable ice surface profile extended westward from its terminus would require very thick north-flowing ice in Gulf of Boothia and over adjacent land. Unless ice over Prince of Wales Island was much thicker still, it would not have been drawn into the Lancaster Sound – Gulf of Boothia outlet glacier and may have flowed generally northward, like ice in Gulf of Boothia, much as portrayed in Figure 54 in the reconstruction of Mayewski et al. (1981). Thus, phases 1 and 2 of Prince of Wales Island and the Eclipse Moraines of Bylot Island can be explained by that model, though it was proposed for the Late Wisconsinan.

A younger set of lateral moraines on the north coast of Bylot Island is just above sea level and nearly horizontal. Because Lancaster Sound is very deep, they may have formed at the margin of an ice shelf or of a very low gradient ice stream. Klassen tentatively considered that they date from the Late Wisconsinan and Dyke and Prest (1987) used that and other considerations, such as the elevation of an apparent Late Wisconsinan nunatak on Somerset Island, to infer an ice shelf in Lancaster Sound and Gulf of Boothia at that time.

If the ice in Lancaster Sound and Gulf of Boothia changed from a thick, grounded outlet glacier or ice stream (Fig. 54) to an ice shelf or very low gradient and low level ice stream, drainage of the ice sheet adjacent to Gulf of Boothia would have been captured; flow over Prince of Wales Island would have changed from generally northward to generally eastward. At the same time flow into Gulf of Boothia would have accelerated, leading headward propagation of tributary ice streams. Upice of the ice streams, the newly established ice divide, under which basal ice would be static (Paterson, 1981), would overlie terrain that previously experienced basal flow in a different direction from a more distant ice divide.

The zone of little or no basal flow under the divide of a large ice sheet is about 100 km wide (Paterson, 1981). When a divide shifts into an area that previously experienced basal flow, reduction in basal ice velocity and in strain heating may cause a change in basal thermal condition from warm to cold. This change would occur especially if there were no increase in ice thickness, and none would be expected if the divide shifted because of changes in flow regime.

In summary, we tentatively conclude from consideration of regional Quaternary geology that phases 1 and 2 of Prince of Wales Island date from Early and possibly Middle Wisconsinan and that the configuration of the northern Laurentide Ice Sheet then resembled the model of Mayewski et al. (1981). Phase 3 and the switch from phase 2 are explained as the result of ice stream capture caused by headward propagation of a drawdown of ice over Lancaster Sound and Gulf of Boothia. Because phase 3 began well before onset of local deglaciation (11 ka) when the ice margin lay well beyond the island, and because it operated long enough to disperse large amounts of debris >150 km, it likely dates from a maximal or near maximal phase of the Late Wisconsinan substage.

DEGLACIATION

Deglaciation of Prince of Wales Island is recorded in detail (Fig. 55). End moraines cross its northwestern, north-central, and eastern parts; sidehill meltwater channels define retreat of valley glacier lobes; streamlined till and subglacial meltwater channels record shifts in flow in response to changes in marginal configuration; and radiocarbon dates (Fig. 55; Table 3) provide numeric ages of retreat phases.

Ice marginal features (Fig. 55) are correlated by trend, extrapolation of gradients of lateral channels, pattern of associated ice flow features, and limiting radiocarbon dates. At the same time, local retreat patterns, which can be established solely from the mapped features, check internal consistency of the set of radiocarbon dates.

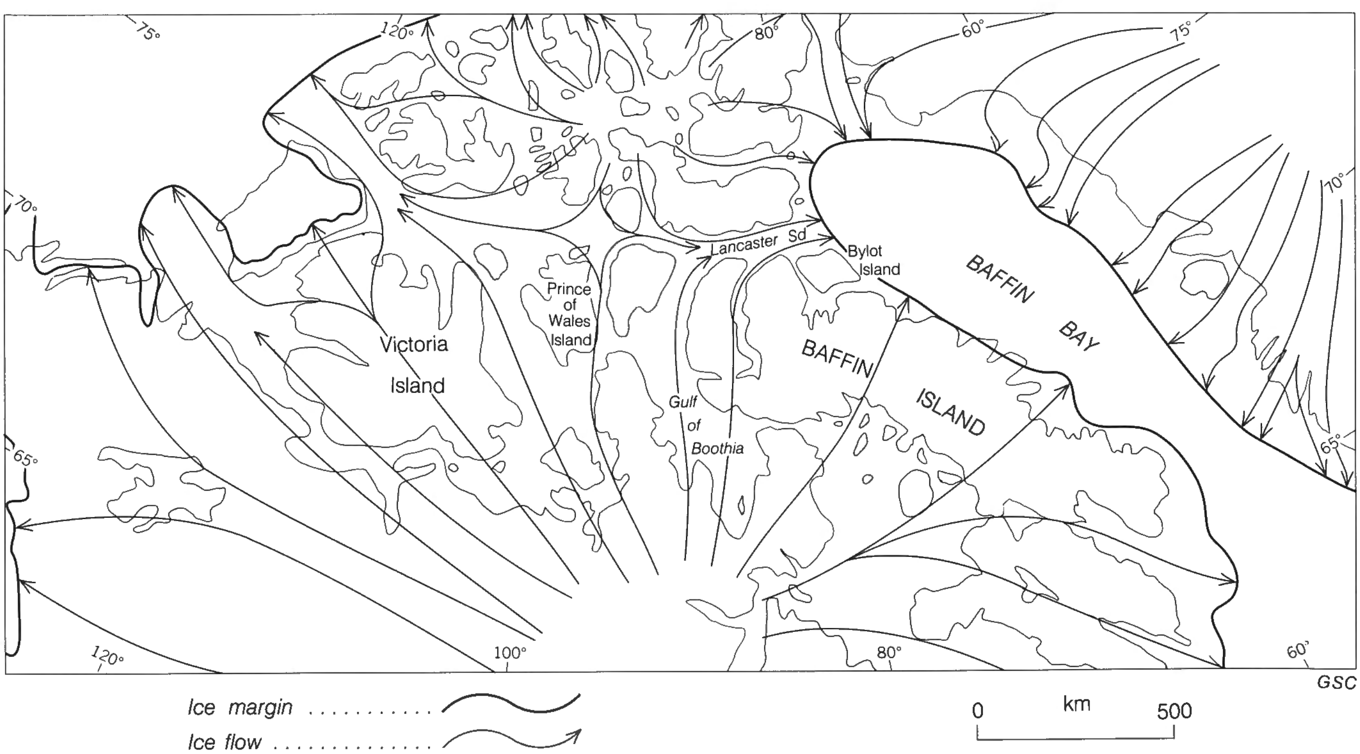

Figure 54. Probable configuration of the regional ice cover during Early Wisconsinan, ice flow phases 1 and 2 on Prince of Wales Island, after Mayewski et al., 1981.

Table 3. Radiocarbon dates pertaining to deglaciation of Prince of Wales Island (see Figure 55)

Lab. number	Date	Material	Elevation	Marine limit
S-2708	11 005 ± 170	shells	133	188
S-2591	10 530 ± 145	bone	54	150±
S-2709	10 435 ± 160	shells	120	133
GSC-4408	10 100 ± 100	shells	104	120
S-2683	10 070 ± 150	shells	70	132
S-2916	10 005 ± 120	bone	62	132
S-2922	10 000 ± 145	bone	66.5	132
GSC-3954	9660 ± 90	shells	70-88	100±
S-2710	9845 ± 150	shells	95	95
S-2706	9375 ± 140	bone	70	95
GSC-4250	9280 ± 90	shells	30	95
GSC-3994	9360 ± 150	shells	84.5	95±
S-2593	9285 ± 135	bone	71	120
S-2590	9605 ± 140	bone	66	132±
GSC-4527	9350 ± 110	shells	96	120
S-2912	9440 ± 135	bone	70	120
S-2918	9505 ± 120	bone	74.5	120
GSC-3697	9470 ± 100	shells	85	95
S-2913	9335 ± 145	bone	57.5	107
GSC-4442	9080 ± 90	shells	107	107
S-2828	9140 ± 130	shells	94	100±
S-2836	9040 ± 130	bone	79.5	100±
GSC-4049	9190 ± 170	shells	97	100±
S-2597	9225 ± 215	bone	99	100±
GSC-3996	8940 ± 130	shells	115.5	115±
L-571B	9200 ± 160	shells	113	115±

Radiocarbon dates pertaining to deglaciation

Where ice retreated in the sea, radiocarbon ages of the oldest marine organisms provide the closest limiting dates on deglaciation. Organisms from sediment that can be related to marine limit, the shore feature formed at the moment of deglaciation, provide direct dates on deglaciation. Twenty-six samples provide direct or closely limiting radiocarbon dates on deglaciation of Prince of Wales Island (Table 3; Fig. 55). Dates of deglaciation progressively decline from the northwestern end moraine belt eastward along Baring Channel, southeastward across Ommanney Bay, and southward along Peel Sound.

Dates from northwestern end moraine belt

The oldest dates come from the northwestern fringe of the island. Seven samples of marine shells and whale bone from the northwestern end moraine belt have yielded radiocarbon ages between 10 and 11 ka. Descriptions of three dated sites in and near the Donnett Hill End Moraine System (Dyke, 1987) are quoted below because they are crucial to the broader interpretation.

"The oldest date on deglaciation currently available from Prince of Wales Island is 11 005 ± 170 BP (S-2708) on shells of *Hiatella arctica* from the surface of glaciomarine stony clays. The clays are situated just beyond a large end moraine of the Donnett Hill End Moraine System and were laid down on the west and northwest flank of Donnett Hill when ice stood at the moraine... The sample came from the surface of sediment remobilized by a recent thermokarst slump at 133 m asl, 55 m below marine limit... In all likelihood, the date pertains to sedimentation of the stony clays and, therefore, to formation of marine limit... because the shells were brought to the surface... by slumping and the surface of the sediment adjacent to the slump is barren of shells...

When ice withdrew from the youngest ridge of the Donnett Hill End Moraine System, the sea entered the valley southwest of Arabella Bay, and a glaciomarine delta was laid down near the retracted ice front at marine limit, recorded by the delta lip at 133 m asl. A large accumulation of stony silts and clays... was laid down in the deeper water prodelta environment. Whole valves of *Hiatella arctica* eroded from prolifically fossiliferous beds at 120 m altitude just in front of the delta lip gave a radiocarbon age of 10 435 ± 160 BP (S-2709), which clearly dates formation of marine limit and deposition of the glaciomarine sediment...

Relatively early deglaciation of the Reliance Bay area is also indicated by a date of 10 530 ± 145 BP (S-2591) on a cranial fragment of a large whale.... This date... shows that whales occupied the area as soon as Viscount Melville Sound became free of glacier ice and allowed their access."

A direct or closely limiting date on the Mount Clarendon End Moraine System is provided by the age of shells (10 100 ± 100 BP; GSC-4408) from the surface of glaciomarine stony mud in a kettle at 104 m asl on the crest of a moraine. Sedimentation occurred when ice was close enough to provide sediment and before relative sea level fell below the kettle rim (about 110 m asl) from marine limit at about 120 m (Dyke et al., 1991).

The age of the Rawlinson Hills End Moraine System is estimated from three limiting dates. A whale skull on a distal ridge of the system dated 10 000 ± 145 BP (S-2922). The skull is about 60 m below marine limit and, thus, may be younger than initial incursion of the sea. Many other whale bones are partly enclosed in glaciomarine silt that comprises one of the younger ridges of the moraine system. The bones appear to be eroding from the silt, hence may date sedimentation. A skull fragment from there dated 10 005 ± 120 BP (S-2916). Shells from the surface of the large glaciomarine silt deposit east of the moraines dated 10 070 ± 150 BP (S-2683). Hence, ice had retreated to or from the youngest ridge of the moraine system by 10 ka.

Dates from Baring Channel area

Age of marine limit and deglaciation at the west end of Baring Channel (11-10.5 ka) is established by dates from the Donnett Hill area already discussed. Deglaciation of the east end of the channel is controlled by one direct and three limiting dates. The direct date, 9845 ± 150 BP (S-2710), is on whole valves and fragments of *Hiatella arctica* and *Mya truncata* from inner foreset beds of a small delta marking marine limit south of Cape Hardy and from beach gravel superimposed on it. Corroborative limiting dates from the same valley are 9375 ± 140 BP (S-2706) on whale bone 25 m below marine limit and 9280 ± 90 (GSC-4250) on *Hiatella arctica* from glaciomarine stony mud 65 m below marine limit. *Mya truncata* valves from horizontally bedded sand and silt with large dropstones on a steep slope just below marine limit farther west, thought to have been deglaciated about the same time, dated 9660 ± 90 BP (GSC-3954).

Dates from Ommanney Bay area

Four limiting dates indicate ice retreat from the outer two-thirds of Ommanney Bay by 9.4 ka. Whale bones resting on the large glaciomarine plain west of the bay dated 9605 ± 140 BP (S-2590). The surface position indicates that sedimentation had ceased by the time the whale died. Two other whales from a valley southeast of Smith Bay dated 9440 ± 135 BP (S-2912) and 9505 ± 120 BP (S-2918); shells from a site near the head of Drake Bay dated 9350 ± 110 BP (GSC-4527). These sites are all a few tens of metres below marine limit (Table 3).

Dates from along Peel Sound coast

Deglaciation of the north end of Peel Sound occurred about 9.8 ka, as already discussed. Progressive southward deglaciation of the sound is recorded by dates from seven other sites, but there is some internal inconsistency in these dates (Table 3), likely caused by sample contamination.

Four dates provide control for correlations displayed on Figure 53. Whale bone from a site behind the youngest ice marginal features dated 9225 ± 215 BP (S-2597). Shells from a site within a few metres of marine limit east of there, hence deglaciated earlier, dated 9190 ± 170 (GSC-4049). Hence, the youngest ice marginal features date about 9.2 ka. Deglaciation of the middle reach of Peel Sound is best controlled by a date of 9470 ± 100 BP (GSC-3697) on articulated shells recently exposed from frozen glaciomarine sediment that extends to marine limit. This date agrees well with the oldest date from adjacent Prescott Island, 9335 ± 145 BP (S-2913) on whale bone.

Paleogeography

The correlated ice marginal features (Fig. 55) are combined with ice flow data (Maps 1689A and 1690A) and sea level data (Dyke et al., 1991) to reconstruct paleogeography for early, middle, and late phases of deglaciation. The retreating ice is divided into cold- and warm-based zones on the premise that streamlined till forms were created by basally sliding ice, whereas areas that were not remoulded by a given flow event experienced no basal flow because the ice was frozen to its bed.

11 ka paleogeography

At 11 ka the ice margin lay along distal ridges of the northwestern end moraine belt. Parts of four peninsulas were deglaciated but lay below sea level (Fig. 56A). The moraines thus formed subaquatically. The large extent and relief of the moraines and their inferred glacier ice cores require that debris accumulated extensively on the ice as much as 100 m above its bed. This accumulation likely reflects climbing flowlines in the marginal ice required to replenish mass loss by ablation during moraine building.

The ice margin at 11 ka had a simple outline reflecting its nearly flat bed. The highest terrain crossed by the margin, between Drake Bay and Baring Channel, created a re-entrant separating two lobes. Flow was drawn into the lobe in Baring Channel from a large area creating an ice stream that entered the channel via valleys that converge at Arabella Bay. Hence, on northern Prince of Wales Island by 11 ka, northwestward flow had replaced phase 3 eastward flow (cf. Figs. 51 and 54). The ice sheet was warm based there and the new flow obliterated the morphological record of earlier flow.

On southeastern Prince of Wales Island, warm-based flow continued as during phase 3. In the ice divide zone, preservation of glacial landscapes formed during phases 1 and 2 indicates continuing cold-based conditions.

10 ka paleogeography

The ice margin retreated little between 11 and 10 ka and continued building large end moraines. The slow retreat could represent a response to climate, or simply topographic anchoring of the margin after an interval of rapid calving across Viscount Melville Sound. At 10 ka the margin stood along the younger ridges of the northwestern end moraine belt in the west and just behind it in the east (Fig. 56B).

The flow pattern and basal thermal zones remained much as at 11 ka. Slight retreat in Ommanney Bay apparently led to a proportional retreat of the boundary between cold- and warm-based ice and formation of lightly inscribed flutings that converge toward the bay. Retreat of the Baring Channel lobe gave rise to more topographically directed flow south of Arabella Bay. Flow pattern and thermal zone boundaries on southeastern Prince of Wales Island remained unchanged.

9.6 ka paleogeography

Retreat quickened after 10 ka, more in the east than in the west. By 9.6 ka the sea had penetrated through Baring Channel and had entered the north end of Peel Sound (Fig. 56C). Possibly the difference in retreat rate was a function of the arrangement of basal thermal zones; the large warm-based zone draining into Baring Channel would have flowed more rapidly than the cold-based ice adjacent Ommanney Bay and would have led to rapid thinning of ice over land and calving at the aquatic ice front.

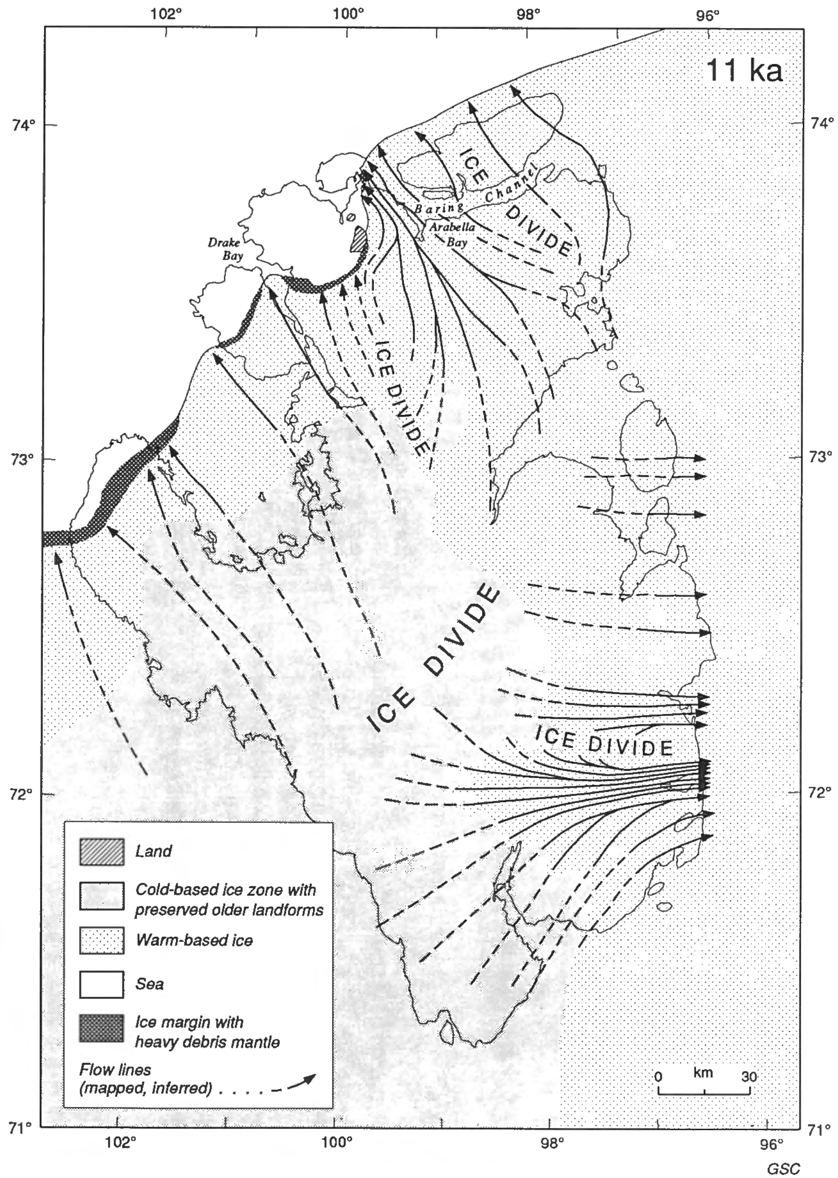

Figure 56. Paleogeography of Prince of Wales Island at **A**, 11 ka; **B**, 10 ka; **C**, 9.6 ka; and **D**, 9.3 ka.

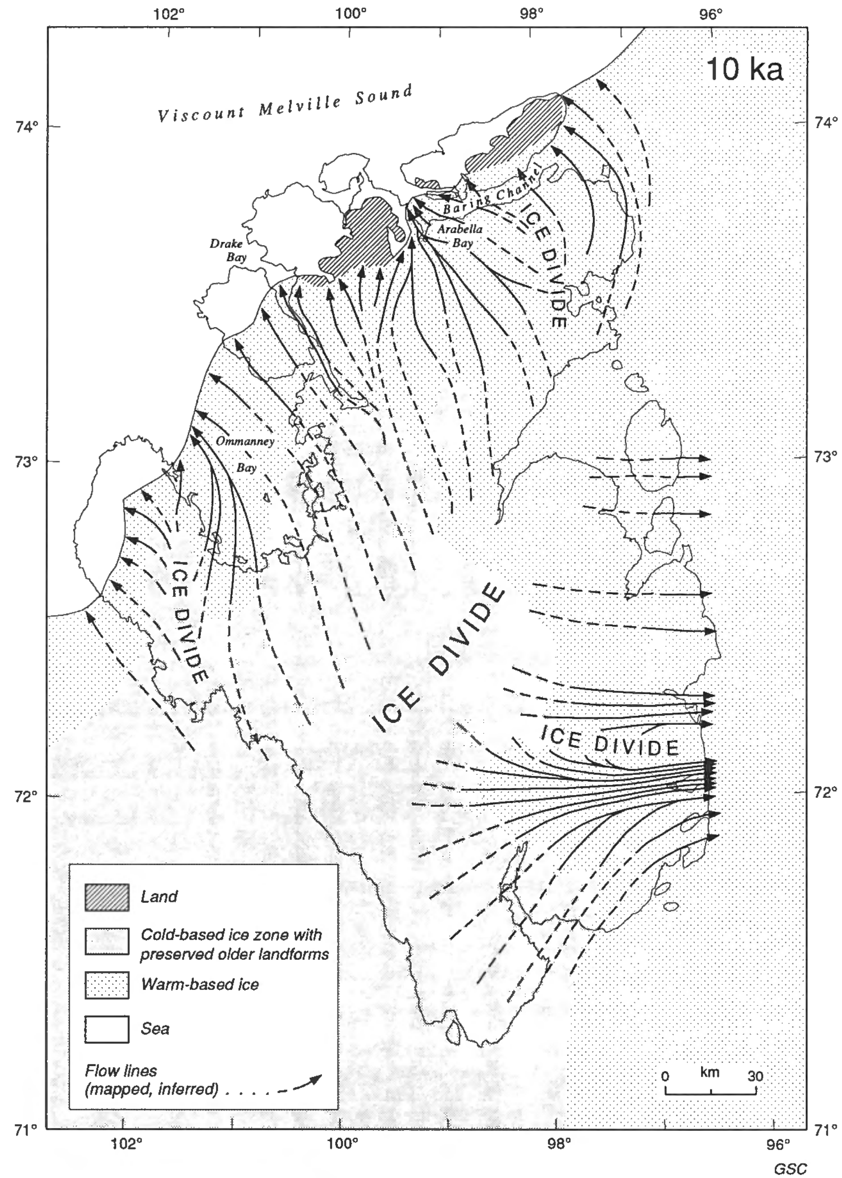

Figure 56B

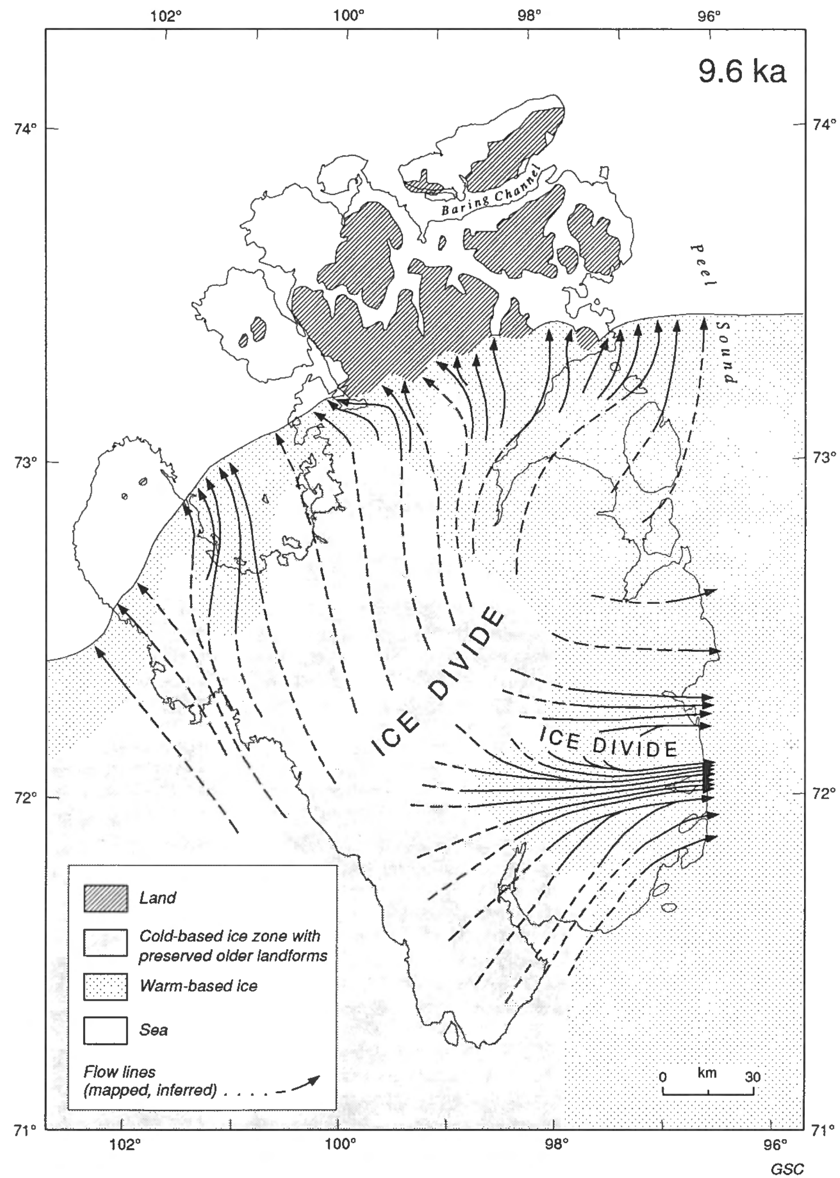

Figure 56C

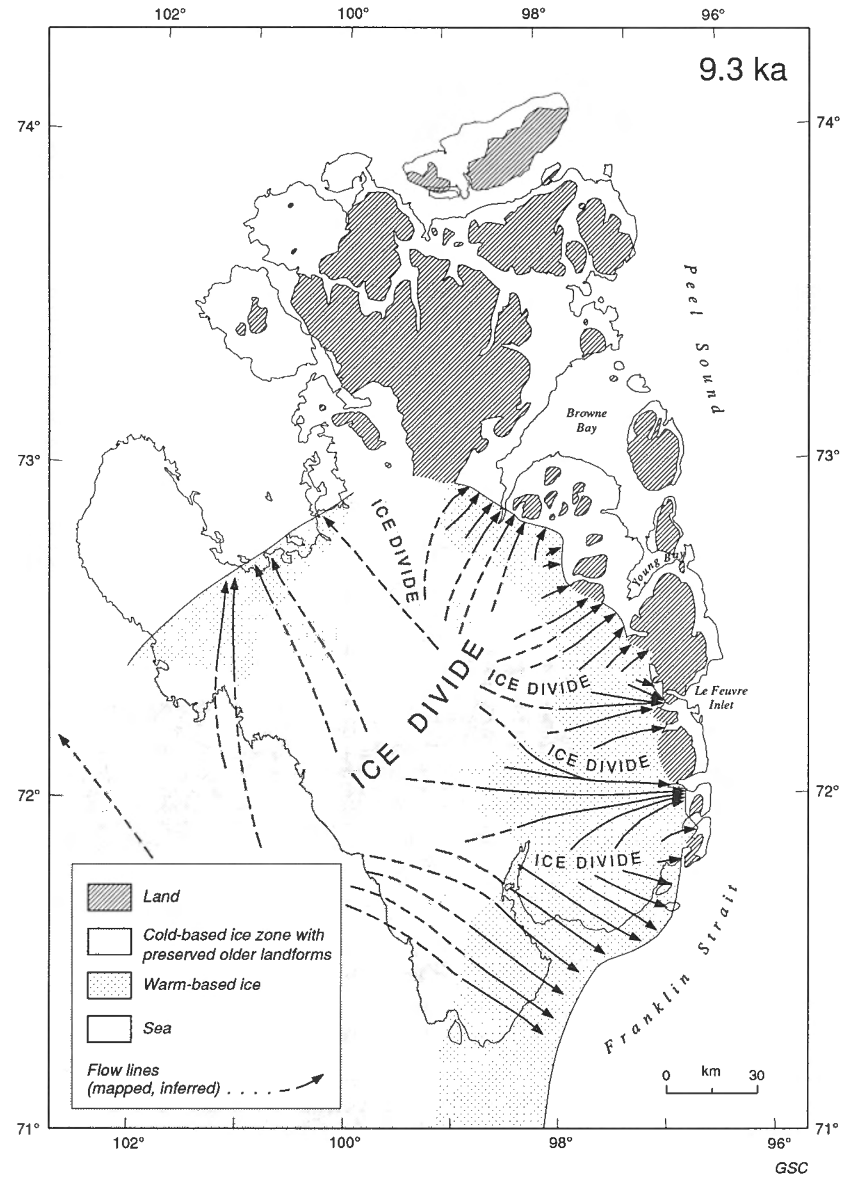

Figure 56D

9.3 ka paleogeography

Rapid retreat continued between 9.6 and 9.3 ka and, as before, was fastest in the east. By 9.3 ka the sea occupied all of Peel Sound and most of the eastern plateau was deglaciated (Fig. 56D). Ice flow changed along the eastern margin where increased topographic channelling created small drumlin and fluting fields leading to Browne and Young bays; flow into Le Feuvre Inlet became more strongly confluent. Southwest of Transition Bay new southeast-oriented flutings formed in response to retreat of the margin into Franklin Strait. The shift of flow was accompanied by retreat of the boundary between warm- and cold-based ice, but the warm-based flow was not long or vigorous enough to erode all older landforms. These youngest ice flow features show that most of Prince of Wales Lowland remained ice covered until the channels to the east were deglaciated.

Retreat after 9.3 ka

End moraines and meltwater channels record continued westward retreat on southern Prince of Wales Island as far as the margin of Prince of Wales Lowland. Two clusters of kames still farther west suggest that westward retreat may have continued across much of the lowland. If so, the retreating ice experienced no basal flow for the older landscapes there were left unmodified. Alternatively, by the time the ice had retreated to the edge of the lowland, it had thinned enough to float and became an ice shelf. This interpretation is preferred because it explains the unique ice island scours with their multiple keel marks in the valley south of Crooked Lake. Ice islands calve from ice shelves.

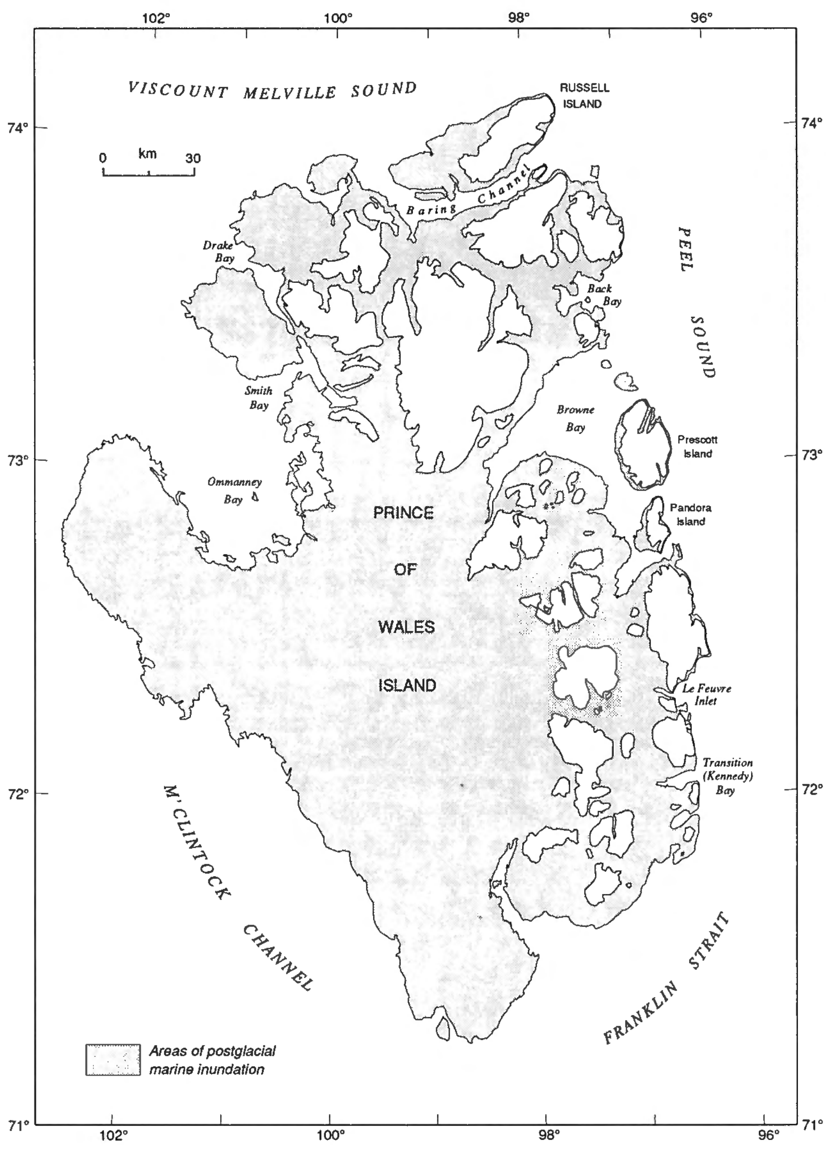

Figure 57. Area of postglacial marine inundation, Prince of Wales Island.

Regional correlations of retreat sequence

The chronology and pattern of ice retreat as summarized are compatible with data from areas to the east (Dyke, 1983; 1984) and are placed in regional context by Dyke and Prest (1987b;c). However, they appear to be incompatible with the chronology of deglaciation of northeastern Victoria and Stefansson islands (Hodgson, 1987). These areas lie 100 km northwest of the northwestern end moraine belt, downice of these moraines as interpreted above. Radiocarbon dates from the moraine belt bracket its age between 11 and 10 ka. However, dates from northeastern Victoria and Stefansson islands indicate that they were finally deglaciated about 9.5 ka, which presents a >1500-year discrepancy in deglaciation of northern M'Clintock Channel.

A possible resolution might arise from reinterpretation of the Rawlinson Hills End Moraine System as either an interlobate system or one formed by ice retreating westward. Although possible, this interpretation is not the most straightforward because: 1) ice clearly retreated eastward from other parts of the northwestern end moraine belt as shown by ice flow and meltwater flow features; 2) there is evidence of late northward ice flow into Ommanney Bay east of Rawlinson Hills; and 3) it would require a different interpretation of the Rawlinson

Hills End Moraine System than of other components of the end moraine belt. Still until this discrepancy is resolved, interpretations should remain flexible.

POSTGLACIAL EMERGENCE AND TECTONICS

Marine limit indicators

Marine limit shorelines have a variety of expressions in the area. They are generally discernible on airphotos, even where weakly developed, because they are not obscured by vegetation. However, because 80% of the land was inundated, including all of Prince of Wales Lowland (Fig. 57), marine limit features occur, with one exception, only in the north and east.

The only marine limit feature on Prince of Wales Lowland is a flat-topped kame delta on the peninsula southwest of Ommanney Bay. This delta, part of the southern Rawlinson Hills End Moraine System, is composed of glaciomarine sediment. Its coarse gravel terrace is the only part of the moraine where sedimentation progressed to sea level.

In higher areas, marine limits are recorded by beaches, upper limits of marine sediments, glaciomarine delta terraces, and washing limits on till. Also lateral meltwater channels commonly end downslope at shoreline features or merge with marine limit shorelines via fan gravels deposited at channel mouths (e.g., Fig. 31). In a few areas where marine limit features are absent, as north of Smith Bay, a consistent lower limit of lateral meltwater channels and a spotty upper limit of marine sediment allow us to estimate marine limit position. Thus, in northern parts of the area, we can trace marine limit directly on airphotos or reasonably interpolate it. We have traced it almost continuously between inner Browne Bay and Allen Lake, a shoreline length of about 120 km, as a washing limit on till, coincident in places with weakly developed beaches and with the upper limit of marine sediment (Map 1689A; Fig. 58).

Marine limit elevations

Elevations of marine limit features were surveyed at 35 sites and interpolated from topographic maps at others (Fig. 59). Marine limit elevation declines to the southeast. The highest is at 188 m at Donnett Hill, the lowest at 95 m along northern and central Peel Sound.

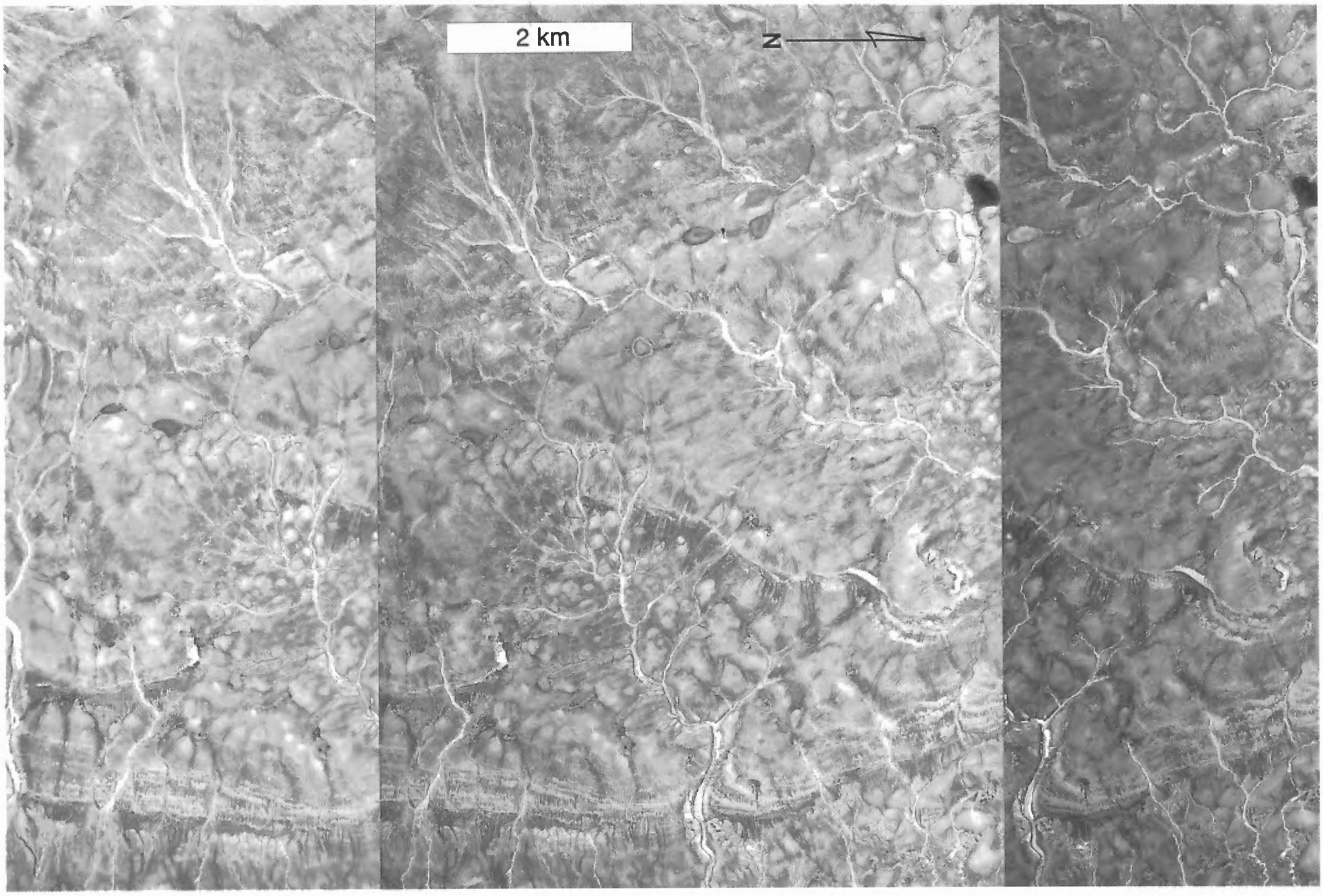

Figure 58. Washing limit on till north of Browne Bay. NAPL A16188-22, 23, and 24

Because marine limit elevation varies largely as a function of the amount of uplift that occurred during local deglaciation, its variability reflects the direction and rate of ice retreat, as superimposed on an earlier pattern of crustal deflection. Thus, slow retreat results in a drop in marine limit upice, whereas rapid retreat results in a rise upice, provided the local direction of ice retreat is toward the area of greater crustal depression (Andrews, 1970).

The configuration of marine limit elevations (Fig. 59) provides a test of the interpretation of retreat patterns based on other data. It is entirely congruous with the described pattern of ice retreat. The 50 m drop across the Donnett Hill End Moraine System, from 188 m at Donnett Hill to 133 m at Arabella Bay, records emergence as ice retreated across the system between 11 and 10.5 ka. Its further decline to about 100 m in valleys south of Arabella Bay records continued emergence with further retreat. The similar decline to 95-100 m farther east along Baring Channel and Allen Lake trough reflects eastward retreat between 10.5 and 9.7 ka. The slight rise southward along Peel Sound from 104 m at Back Bay to 115 m at Transition Bay results from rapid marine incursion along its length between 9.7 and 9.3 ka. Retreat was rapid enough to allow the marine limit to maintain a positive gradient that reflects the pre-existing pattern of crustal deflection (Morner, 1974). The decline inland of southern Peel Sound from 115 to 100 m reflects emergence during the century or so of westward retreat there. The 15 m difference, if not due in part to crustal deflection, suggests that the westward retreat lasted about two centuries rather than one as shown on Figure 53.

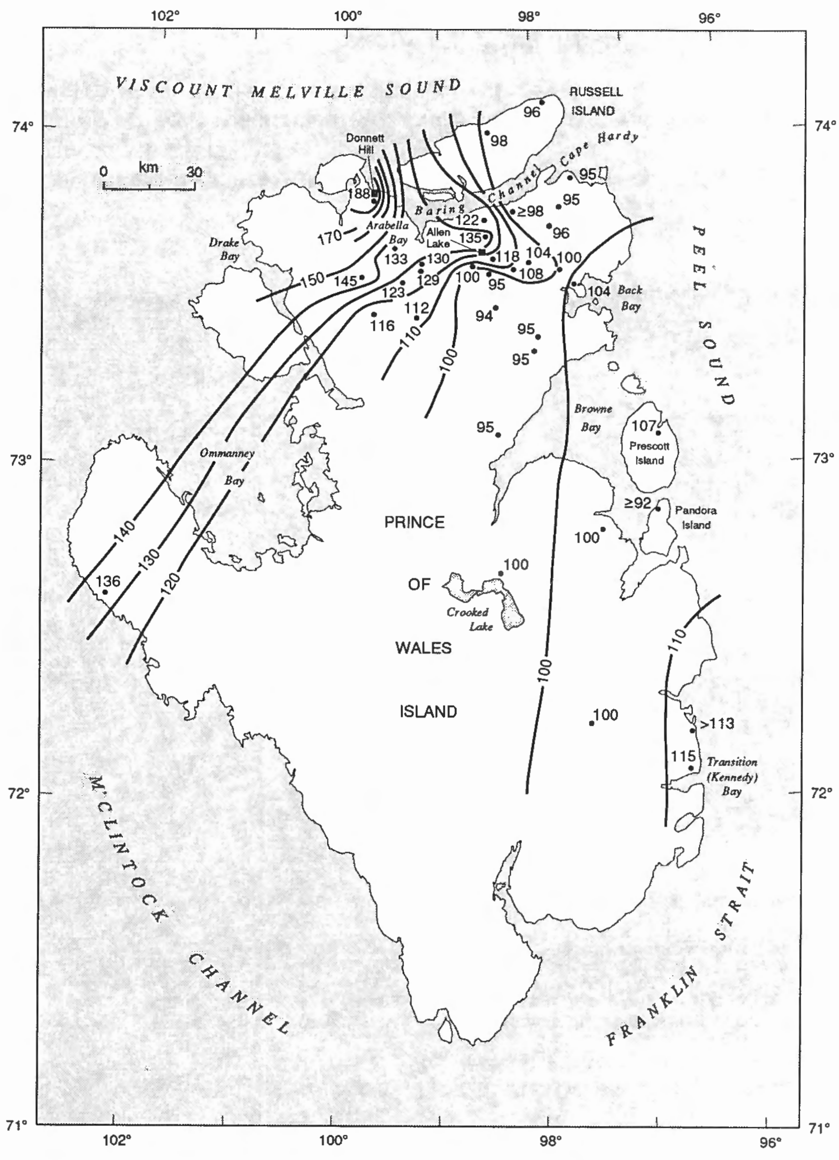

Figure 59. Contours on surveyed marine limit elevations, Prince of Wales Island.

Emergence curves and shoreline deformation

The history of postglacial emergence of Prince of Wales Island is controlled by 130 radiocarbon dates, which are discussed in the context of a synthesis of the sea level history of a larger area by Dyke et al. (1991). They constructed 14 emergence curves for sites scattered around the area, constructed or reviewed 14 more curves from adjacent areas, and, from these and other data, constructed a sequence of isobase maps showing the regional pattern of shoreline deformation. Key conclusions from their summary are reiterated here.

"The isobase patterns suggest that during and just after deglaciation of the Somerset – Boothia – Prince of Wales region, the Boothia Arch (or Horst) was reactivated and produced 60-120 m of local relief, increasing southward, on the 9.3 ka shoreline" (Fig. 60A). "This deformation could have the form of a symmetrical ridge or of a ridge with a steep, faulted, western side along Peel Sound" (Fig. 60B). "The ridge trends north-south across Boothia Peninsula and western Somerset Island. On the west, in the area of Prince of Wales Island, the ridge is flanked by a large isobase plateau wherein the emerged 9.3 ka shoreline has very little tilt. The Boothia – Somerset isobase ridge dampened quickly following deglaciation and the 8 ka shoreline is not affected by it. The Prince of Wales Island isobase plateau, on the other hand, persisted as the most prominent regional isobase feature throughout postglacial time and had lost any measurable gradient by 8 ka. Thus, since 8 ka the entire region of Prince of Wales and adjacent smaller islands, and possibly a larger area, has rebounded without tilting.

This is glacioisostatically abnormal and we are not aware of any similar feature elsewhere.

"The possible correlation between the Boothia – Somerset isobase ridge and the structural Boothia Arch is obvious, but there is no obvious crustal structure that accounts for the Prince of Wales Island isobase plateau. Starting from Kerr's (1980) tectonic model of the Arctic Archipelago, which proposes that the archipelago is a continental subplate severely fragmented by rifting, with the inter island channels occupying large Tertiary rift valleys, we propose a hypothesis of Holocene *block tectonics*, which is that postglacial isostatic rebound of the archipelago has proceeded by movement of a mosaic of blocks, some blocks rebounding and tilting, some rebounding without tilting....

"The fact that shorelines dating from about 8 ka and younger on Prince of Wales Island have not been delevelled means that the last 8000 years of emergence history of the entire island can be described by a single curve. We present such a curve based on 41 driftwood dates"... extended "before 8 ka by addition of 2 marine limit shell dates from the first part of Prince of Wales Island to be deglaciated...." This curve (Fig. 61) has simple exponential form and a half response time of 2000 years.

POSTGLACIAL CLIMATE AND OCEANOGRAPHIC CHANGE

Dyke and Morris (1990) summarized the frequency distribution of postglacial driftwood and bowhead whale remains in the central Arctic and inferred changes in oceanographic circulation and climate. The remains of 112 bowheads have been recovered as have a similar number of pieces of driftwood. Fifty-three samples of each have been radiocarbon dated. Both show abrupt changes in abundance. Because the bowhead is highly adapted to an ice-edge environment, changes in its abundance likely reflect changes in sea ice regime.

Bowheads were abundant in the central Arctic from time of deglaciation to 8.5 ka (Fig. 62). They were largely excluded between 8.5 and 5 ka, reoccupied the area between 5 and 3 ka, and were excluded again during most of the last 3000 years. Driftwood did not arrive until 8.6 ka (Fig. 63), so there is a negative correlation between driftwood and bowhead abundance in the early Holocene. Driftwood arrived in maximum abundance during the last 3000 years, so there is also a negative correlation between driftwood and bowhead abundance in the late Holocene, but the relationship between the two is the reverse of that during the early Holocene. During the middle Holocene both wood and whales occurred in moderate abundance.

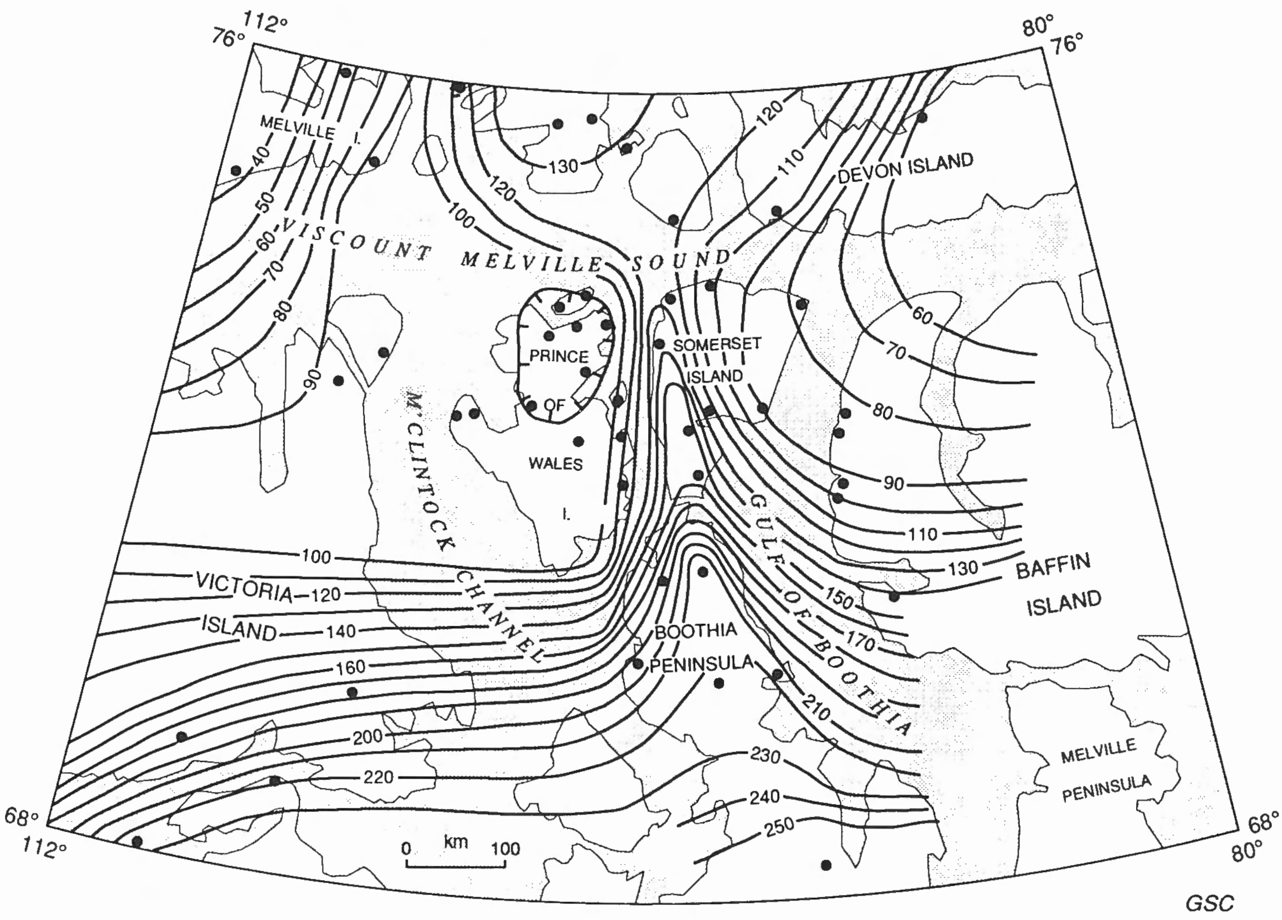

Figure 60A. Isobases on the 9.3 ka shoreline in the central Arctic, from Dyke et al., 1991.

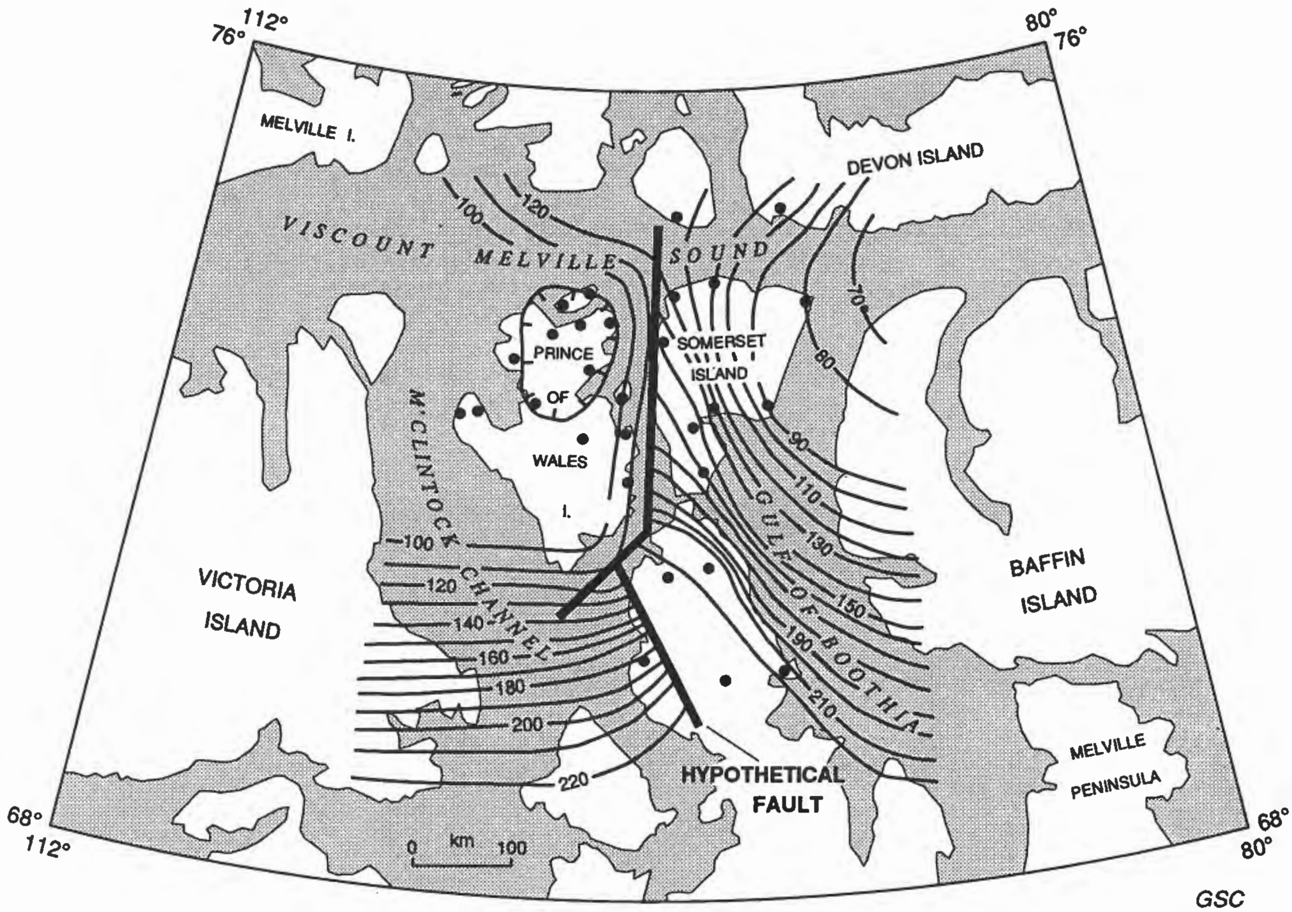

Figure 60B. Isobases on the 9.3 ka shoreline with hypothetical fault zone along Peel Sound, from Dyke et al., 1991.

Dyke and Morris (1990) concluded that the early Holocene oceanographic circulation in the Arctic Archipelago was driven in the summers by glacial meltwater outflow, which exported sea ice from the channels, allowed whales relatively unrestricted access, and prevented driftwood from filtering through the archipelago from the Arctic Ocean. Suddenly diminished meltwater input at 8.5 ka, when Keewatin Ice retreated onto the mainland, allowed establishment of an oceanographic circulation pattern similar to the present one, bringing from the Arctic Ocean driftwood and a sea ice congestion of the central Arctic channels sufficient to exclude the whales. The re-expansion of whale summer habitat between 5 and 3 ka was probably caused by warmer summers because no mechanism was available for a major change in the pattern of ocean circulation. Re-exclusion of the whales at 3 ka records the Neoglacial climatic deterioration. Continuing research in the eastern Arctic shows that these changes were widespread and nearly synchronous (Dyke et al., 1989).

PERMAFROST HISTORY

The history of permafrost on Prince of Wales Island is inferred from the history of basal ice thermal zones as interpreted from morphostratigraphy and from the history of submergence and emergence, all described in earlier sections.

The area of residuum and colluvium (map unit C) on the northern plateau has a simple history of ground temperatures. It had a cold-based ice cover throughout the last glaciation, remained above the postglacial sea, and probably was not submerged after the penultimate glaciation. Therefore, that area likely has been underlain by permafrost since Illinoian time. Since the surface bears no signs of glacial erosion, all glaciations were likely cold based and the ground may have remained frozen throughout the Quaternary. Ground temperatures likely increased during glaciations, even though the ice was cold based. A comparable thermal history is inferred for a larger similar terrain on Somerset Island (Dyke, 1983).

The permafrost history of eastern and northern Prince of Wales Island is also simple. The entire area remoulded by ice flow phase 3 and later deglacial flows (the area of map unit T^3b) had a warm-based ice cover and, hence, lacked subglacial permafrost. Existing permafrost is of postglacial age.

In contrast, the permafrost history of Prince of Wales Lowland is more complex. The lowland was covered by warm-based ice during phase 1, tentatively inferred to date from the Early Wisconsinan. Ice over the western half of the lowland changed to cold based at the start of phase 2, which may also date from the Early Wisconsinan. At that time, the

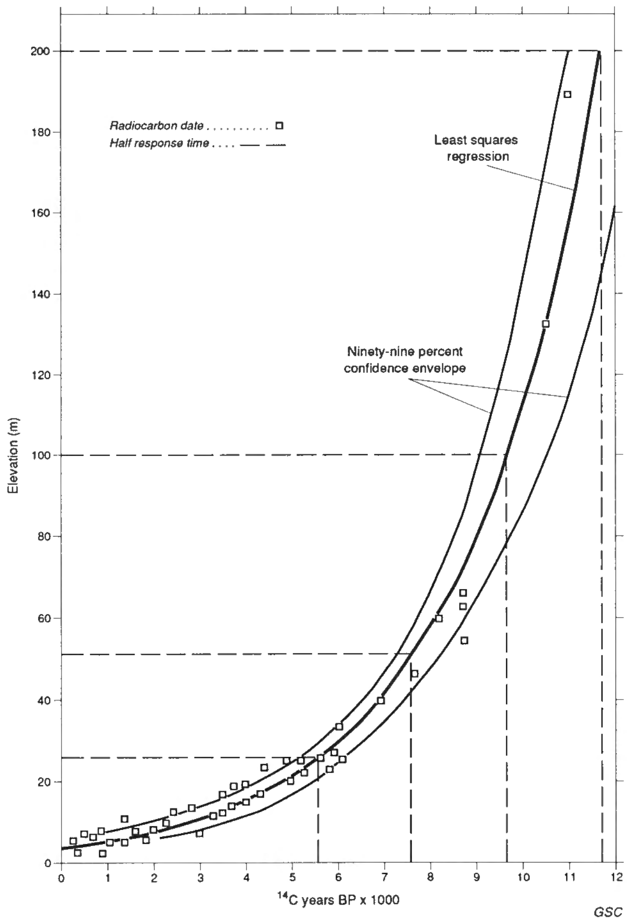

Figure 61. Least squares regression emergence curve for Prince of Wales Island based on 41 driftwood and 2 shell dates; shell dates are highest elevation samples; from Dyke and Morris, 1990.

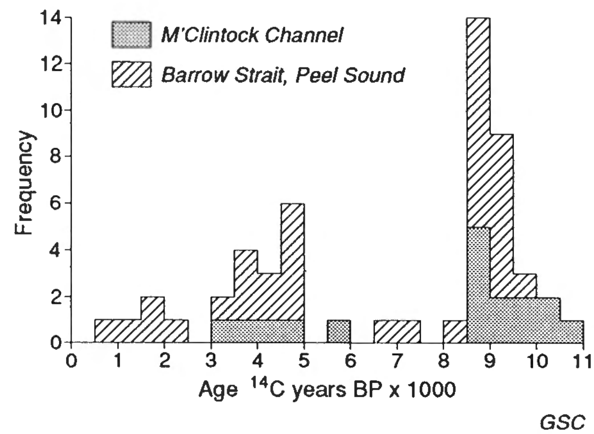

Figure 62. Frequency distribution of 53 radiocarbon-dated bowhead whale specimens with age, central Canadian Arctic, from Dyke and Morris,1990.

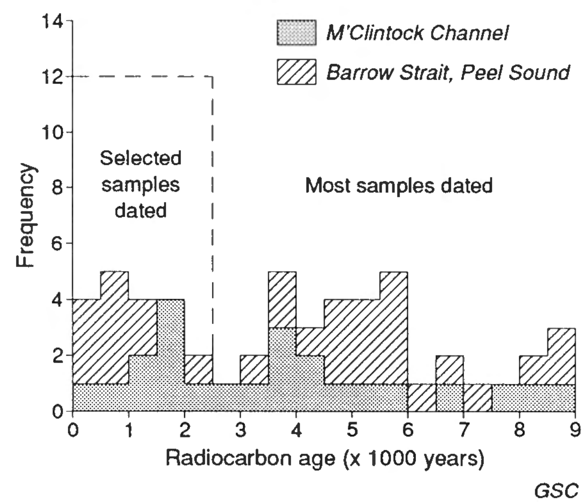

Figure 63. Frequency distribution of 53 radiocarbon-dated driftwood specimens with age, central Canadian Arctic, from Dyke and Morris, 1990.

0°C isotherm shifted below the glacier bed and subglacial permafrost formed. At the start of phase 3, the cold-based ice zone expanded to encompass the rest of Prince of Wales Lowland and possibly a larger area. This expansion is tentatively inferred to date from close to the Late Wisconsinan maximum. It occurred well before 11 ka, perhaps by 25 ka or earlier. The entire area of the lowlands that bears unremoulded glacial bedforms dating from phases 1 and 2 remained covered by cold-based ice until deglaciation about 9.2 ka. Inundation by the postglacial sea may not have lasted long enough to completely degrade the relict subglacial permafrost; extensive submarine permafrost survives on the Beaufort continental shelf after thousands of years of marine submergence. Hence, permafrost on Prince of Wales Lowland originated early in the last glaciation in the western part, later in the glaciation in the eastern part, and likely experienced changes in temperature both subglacially and during marine submergence. The present thermal variation with depth may reflect some or all of that history.

In summary, the permafrost history is complex because glaciations juxtaposed warm- and cold-based ice across broad areas and because the boundaries between the two shifted in response to changing ice flow dynamics. Permafrost likely ranges in age from Illinoian or older to Holocene.

The thickness of subglacial permafrost that formed under cold-based ice was proportional to the temperature depression of basal ice below pressure melting point. Once ice over Prince of Wales Lowland became cold based, it stayed that way, apparently for thousands of years. This long-term stability suggests that temperature was depressed significantly below pressure melting point rather than hovering close to it. In dolomite, about 100 m of subglacial permafrost forms for each 1°C of temperature depression (Judge, 1973).

ENVIRONMENTAL GEOLOGY

INTRODUCTION

Surficial geological maps are fundamental resource documents for planning land use and for predicting and assessing environmental impacts; they inventory and describe the character and composition of the terrain. Although terrain attributes basically restrain all land uses, maps provide a starting point for planning strategies to minimize environmental damage and for planning resource exploration programs. Descriptions and inferences provided thus far should enhance the usefulness of Maps 1689A and 1690A as planning documents.

In this section, we summarize information of particular relevance to land use concerns (material – vegetation – wildlife relationships, granular resource distribution, coastal dynamics and environments, and current and recent seismicity). We present ancillary information on permafrost and on the activity status of geomorphological processes operating on different surface materials. We highlight the importance of these observations to land use planning by providing recommendations to minimize environmental damage. Several of these recommendations are generally applicable to the central Arctic Islands.

LAND USE CONCERNS

Surface material – vegetation – wildlife relationships

In the Arctic, nowhere more than on Prince of Wales Island, the relationship between materials and extent and composition of vegetation is so intimate that surficial geology maps provide the best starting point for an inventory of vegetation. In the absence of vegetation inventories, geological maps provide a sound basis for inferring vegetation cover and composition by those familiar with vegetation – material relationships. For Prince of Wales and Somerset islands, these relationships are elucidated by Woo and Zoltai (1977).

Plant biomass and extreme winter weather define the capacity to support wildlife, particularly ungulates that occupy the area year-round. Prince of Wales Island supports herds of caribou (*Rangifer tarandus*) and muskoxen (*Ovibos moschatus*). The muskox herd is the easternmost large herd in the Arctic Islands south of Parry Channel (Russell and Edmonds, 1977). Farther east they were eliminated by overhunting during the period of British whaling in the nineteenth century. Thus, this herd is vital if this species is to reoccupy its former range. Reoccupation of Somerset Island by a herd of nine muskoxen from Prince of Wales Island occurred during the winter of 1975 (Russell and Edmonds, 1977). The Prince of Wales Island caribou herd, along with herds on Somerset, Victoria, and Banks islands, constitute an intergrade population between Barren Ground caribou of the mainland and Peary caribou of the Queen Elizabeth Islands. Little, if any, interbreeding is thought to occur between the intergrade population and either neighbour even though winter ranges overlap (F. Miller, Canadian Wildlife Service, personal communication, 1989).

Vegetation cover on bedrock varies with lithology. Calcareous rocks are barren but shield rocks have extensive covers of foliose and fruticose lichens. The uneven topography of shield rock promotes exposure of the surface by wind drifting of snow during the nine or ten winter months, which enables foraging by caribou (Russell and Edmonds, 1977). The limited extent of this type of winter caribou habitat, the one most reliably swept free of snow and restricted to the high eastern plateau, suggests that it is nevertheless important to viability of the local herd, although many migrate across Peel Sound to more extensive Precambrian rock terrains there for winter foraging. Russell and Edmonds (1977) "consider availability of winter range to be the most critical factor in evaluating caribou and muskoxen habitats."

Till covers about 70% of the island. About 80% of the till cover is highly calcareous and is either toxic to plant growth or is lacking essential nutrients (Woo and Zoltai, 1977). Plant cover there is <10%, commonly <5% (Fig. 4). Along the eastern side of the island, where till was derived more from clastic and shield rocks, vegetation cover increases to 30-100%. The better-vegetated, sandstone-derived till on the plateau between Browne Bay and Le Feuvre Inlet and on lower terrain on northeastern Prince of Wales and Russell islands constitute the largest caribou winter ranges and are also grazed by muskoxen year round (Russell and Edmonds, 1977; their Fig. 8 and 9). In summer, caribou forage on mesic to xeric sites, mostly on till, which are so widespread that the animals "can not possibly utilize all available summer range" (ibid., p. 6).

Glaciolacustrine and glaciomarine sediments provide substrates for all wetlands on the island that are larger than a hectare or so. These wetlands have continuous vegetation covers and are widespread. They are used extensively by muskoxen for summer and winter foraging (ibid., p. 49). Because the closure relief of wetland basins is only a few metres (see *Organic sediments and landforms*), they are sensitive to slight erosion of sills, a sensitivity heightened by ubiquitous, easily eroded, ice-wedge polygons. Because of highly effective insulation by peat, the tops of ice wedges are only 10-30 cm below the surface. Stripping, compaction, or erosion of peat could trigger ice-wedge degradation, sill erosion, and degeneration of entire peatlands. Even light overland traffic during winter on well vegetated marine sediments can result in extensive scalping of vegetation, exposing the mineral substrate and lowering the permafrost table in subsequent summers. Woo and Zoltai (1977, p. 77) illustrate such a result of winter road use on Russell Island in 1975.

The vegetation cover on marine deposits, as on till, appears to rely on carbonate content. Beaches derived from erosion of highly calcareous till consist mostly of platy clasts of limestone and dolomite and are essentially barren. But some swales between beaches expose moist till that supports mesic plant communities known to be important summer grazing sites for caribou, particularly in the Guillemard Bay – Coningham Bay area. Similar terrain on southeastern Somerset Island is grazed by caribou in the winter, where even the meagre plants on beach ridges are important because wind drifting makes them accessible. Beaches derived from sandstone along Peel Sound are much better vegetated than are others. In the flat lowland south of Back Bay, impeded drainage further boosts vegetation cover and creates enough small hydric sites to support muskoxen.

Granular resources

The surficial geology maps locate and classify granular materials that may prove vital to some future land uses, if only through limitations of supply. In most areas of Laurentide glaciation, sand and gravel deposits are widespread and economically valuable resources. These deposits are normally of glaciofluvial, fluvial, or deltaic origin. On Prince of Wales Island, these sediments collectively account for only about 1% of surface materials and most occurrences are <10 m thick. Raised beach gravels and sands are more widespread but qualitative constraints and environmental concerns limit their potential use. Large areas of the island have exceedingly limited or no sand and gravel.

Glaciofluvial and fluvial sediments in the area are mostly gravel. The thickest deposits occur as alluvial fans but these are coarse, commonly bouldery, particularly near the apex. Many fluvial deposits are currently active, or else occur as terraces along modern streams. Extractive activities at such sites could have a damaging effect on stream and lake biota, particular during the thaw season.

Beach gravel derived from highly calcareous till is about 1 m thick or less in most places. Where cryoturbation and diapirism in the active layer have mixed till with the capping gravel over much of its extent, it no longer constitutes clean aggregate. Beach sand and gravel derived from sandy till is much less modified in this way because they are mostly thicker than the active layer, and even where thin, the underlying till is less frost susceptible and less prone to plastic flow. Hence, sand and sandy gravel raised beaches along Peel Sound, from Young Bay north, constitute a substantial resource of clean aggregate. These beaches, however, are much better vegetated than are the highly calcareous beaches, so future industrial requirements will have to be balanced against wildlife habitat destruction.

Permafrost

Prince of Wales Island lies within continuous permafrost, being about 1000 km north of the continuous permafrost boundary. No direct measurements of permafrost thickness (depth to the 0°C isotherm) have been made on the island, but geophysical profiles at two exploration wells (KMG Decalta well F-62 at Young Bay and Sun Panarctic well E-82 on Russell Island) indicate the location of the base of rock containing frozen pore water (Hardy and Associates Ltd., 1984). In the Russell Island well at 114 m asl, the base of ice-bearing rock is at 305-349 m depth; this well is either above marine limit or it emerged about 10 000 years ago. In the Young Bay well at 21 m asl, the base of ice-bearing rock is at 253-277 m depth; the site emerged about 5000 years ago, which probably accounts for the shallower ice.

Measurements on neighbouring islands show similar depths of permafrost. At the Panarctic Garnier well near the northeast coast of Somerset Island, Taylor and Judge (1974) determined a permafrost thickness of about 500 m, but technical problems limit the accuracy of this measurement (A.E. Taylor, personal communication, 1989). At Resolute Bay on Cornwallis Island, permafrost extends down 396 m (Brown, 1967). On northwestern Bathurst Island it extends to 660 m at a site that emerged about 5000 years ago and to 720 m at a site that emerged about 7000 years ago (A.E. Taylor, personal communication, 1989).

The extent of permafrost offshore has not been mapped. It can be seen to extend off from shore where sea ice has removed sediment in shallow water and exposed the tops of ice wedges. However, in these places the sea freezes to the bottom in winter so permafrost is to be expected. Collier and Judge (1977) measured subzero temperatures in bottom water in Barrow Strait but saline pore water in sea bed materials probably prevents freezing.

In areas of permafrost degradation in raised marine sediments on Prince of Wales Island and in the central Arctic in general, thawing ground ice is normally saline; upon thawing it leaves a temporary salt efflorescence on the surface. This evidence suggests that the sediments froze as they emerged, but it does not preclude the possibility that the sediments were deposited over offshore permafrost.

Where permafrost is of postglacial age, its thickness and thermal gradient are related to ground elevation at sites that emerged too recently to be in equilibrium with mean annual air temperature, as indicated by measurements already discussed. The more recent the emergence, the greater the disequilibrium. Because most of the island is below marine limit, much of it a gently inclined lowland that slowly emerged over 9000 years (Dyke et al., 1991), permafrost thickness may be quite variable. But much of the permafrost, particularly on the lowland, may date from well within the interval of Wisconsin Glaciation, for the ice sheets were cold-based over large areas (see *Permafrost history*). Thus, the present thermal profile under Prince of Wales Lowland may retain features relict from a Wisconsinan subglacial environment and from a Holocene marine submergence, as well as features in equilibrium with present air temperature.

Ground ice

Apart from brief investigations near Back Bay in 1975 (Kurfurst and Veillette, 1977), our research was not designed to determine ground-ice characteristics. Research on Somerset Island (Dyke, 1983) may provide guidance as to what to expect in similar terrains on Prince of Wales Island, although the two islands differ much in Quaternary history and surficial materials.

Buried glacier ice is thought to comprise the bulk of the northwestern end moraine belt and large parts of other end moraines (unit T^3m; see *End moraines*). Ice-cored areas have tell-tale, oversized, ice-wedge polygons. Although the core is rarely exposed, numerous stabilized flow-slide scars suggest that occasionally thaw penetrates to the ice. The top of the ice likely occurs just below the active layer and the relief of the moraines suggests that as much as 60 m of ice is present. The till mantle remains saturated throughout the summer in many places, even on ridges. It has little bearing strength and can be exceedingly unctuous. The moraines have high local relief and steep slopes, so any activity that disturbs the cores will trigger extensive slope failure. These terrains cover hundreds of square kilometres in local occurrences; collectively they cover several thousand.

Segregation and wedge ice are widespread in fine grained marine deposits. Massive ice, likely segregation ice, is exposed in large thermokarst areas on proglacial silt west of Ommanney Bay. This deposit is eroding because of ice exposure, water release, and slumping. Other occurrences of proglacial silt are scattered across the island. Although exposures are rare, segregated ice is likely common in them. Most are low, wet occurrences that invariably contain ice wedges as well. Once exposed, wedges erode quickly to form rills that grow headward.

Wetlands on fine grained sediments have numerous palsa-like mounds about 1 m high and 3-15 m wide. They are common around and in shallow ponds and likely are cored by segregated ice. Similar mounds seem to contain both segregation and wedge ice. Both types are evidence of heaving due to ground ice growth.

Wedge ice is also widespread in deltaic, fluvial, glaciofluvial, and beach deposits that are thicker than the active layer. Wedges extend up to active layer and can be <1 m wide at the top. They generally are not subject to thaw except where slopes are failing and where the troughs are exploited by rill erosion on moderately to steeply sloping raised beach terrains. The latter is common where beaches are sandy; it has lead to a network of parallel, 2-3 m deep gullies on parts of Prescott Island, for example. Diversion of water into ice-wedge troughs by artificial structures would trigger erosion of ice wedges to the detriment of both the terrain and the structures.

Active geomorphological processes

Active geomorphological processes, in addition to those associated with ground ice, differ with materials. Process – material associations allow us to draw inferences about slope stability, bearing strength, and trafficability.

The only surface materials that approach a static state are bedrock and sands and gravels of marine, alluvial, and glaciofluvial origin. These account for only about 20% of the terrain. Even they are subject to metre-scale displacements by frost heaving and to seasonal thermal contraction cracking followed by heaving and folding of materials adjacent to expanding ice wedges.

Frost heaving of crystalline rock thrusts up joint blocks and, along with terrain roughness of tens of metres produced by glacial scouring, limits trafficability. In thin-bedded carbonate rocks, frost heaving disintegrates the active layer and buckles strata along vertical joints, producing striking trenches with raised shoulders (see Dyke, 1984, Fig. 5).

Long term deformation of sand and gravel caused by ice-wedge expansion results in tilting of strata and eventually in overfolding as seen where sediments containing ice wedges are exposed in section. So artificial structures on or in so-called "static cryosols" must withstand considerable stress.

Till exhibits a range of patterned ground, varying with topographic position and with texture. These patterns indicate different kinds of active layer movement. They cover 100% of fine grained till, so movement is pervasive; they are less dense on excessively sandy till, but such till is of minor extent.

At flat sites on summits and in basins, till is patterned with nets and circles that occur in optimum density with diameters of about 1 m. Degree of sorting of stones, diameter, and relief of the forms vary with moisture conditions and stoniness. At wet sites forms are wide, well sorted, and flat. At well drained sites they are smaller, less sorted or unsorted, and domed. We infer that lack of relief at wet sites results from low strength. Indeed, the active layer at these sites remains in a liquid state throughout the summer and is difficult to traverse. At sites not saturated continuously, cell relief is highest on stoniest till (Fig. 64), which suggests that stones support the raised forms.

Nets lengthen as slope angle increases and grade into stripes that run the length of slopes. Gelifluction steps and lobes occur on coarse till with sandy matrix but are uncommon on fine till. They occur where thin sheets of till advance across coarser material. The edges become dry as water drains from the base and front and become stronger than wet material upslope; they impede flow and material aggrades behind them. Elsewhere on fine grained slopes, till is saturated enough during parts of the thaw season that it cannot support the steep slopes that constitute gelifluction risers.

In summary, during thaw and freeze-back, the active layer of till moves in patterns and at rates that depend on moisture regime and slope angle. Uncertainty remains about the mechanics of movement that lead to patterned ground forms, but there seems to be consensus that each results from a sequential concert of processes (Washburn, 1980). Hence, frost or desiccation cracking may imprint a pattern whereas frost heaving on freeze-back imparts relief that allows frost creep and microgelifluction to move stones to the margin. Structures of sorted cells indicate diapiric movement of fines at the centre. Till becomes fluid at low moisture, typically 10-30% by weight, and has a narrow range of plasticity, mostly <10% (Dyke, 1983, p. 13; 1984, p. 10). Disturbance by mechanical vibration can change its state from solid to liquid (Woo and Zoltai, 1977, p. 78).

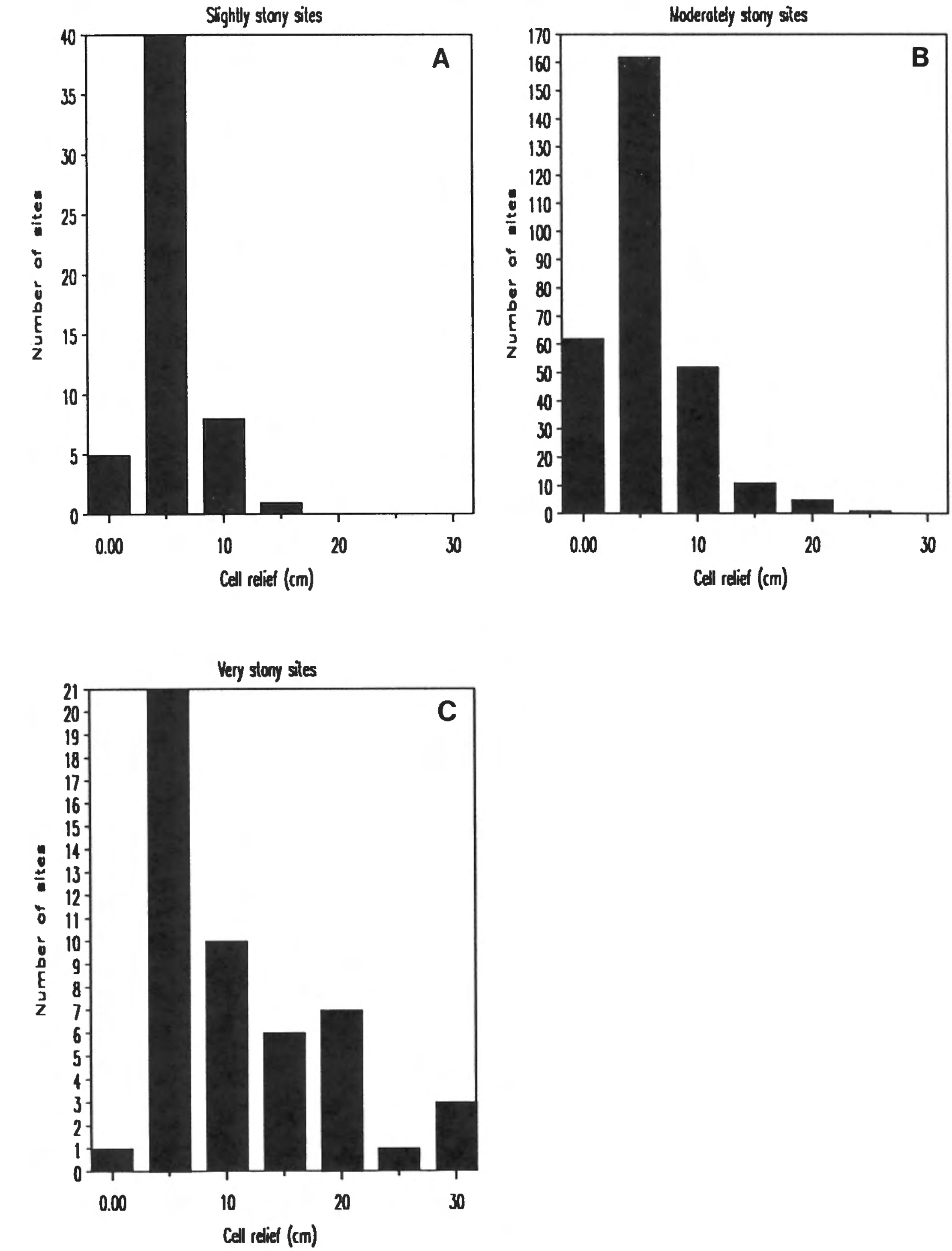

Figure 64. Histograms of patterned ground relief on till of various stoniness on Prince of Wales Island: **A**, slightly stony sites; **B**, moderately stony sites; **C**, very stony sites.

For geotechnical purposes, periglacial processes need to be better understood. No linear artificial structure can avoid terrain on which they operate. Structures locally will alter active layer processes, likely in detrimental ways, if not designed with the processes in mind. Structures that cross slopes may interfere with downslope soil movement, especially if they cause aggradation of permafrost. Interference will result in piling of material against upslope sides of structures and removal of supporting material from downslope sides.

Coastal zone dynamics

Central Arctic coasts are low wave-energy, mesotidal, sea-ice dominated environments. The shore is protected from waves at least 10 months of the year by immobile pack ice, and shorefast ice often persists after pack ice becomes mobile. Peel Sound normally clears for less than a month and M'Clintock Channel often remains ice bound. Even at ice-free times, only waves generated by local winds hit the shore because fetch is short. The beach and shallow water are underlain by permafrost, which limits erosion. Yet waves expend enough energy to produce thin gravel and sand beaches, mostly by reworking of till. Little longshore transport of sediment occurs.

Disturbance by sea ice is the most conspicuous coastal process. Ice rafts erode the shoreface and beach, scraping to the frost table. In places, they push landward and erode raised beaches. Parts of the rafts become buried by debris they carry and by beach gravel. Melting of buried sea ice produces distinct, small, circular pits but some possibly survives as ground ice. The major net result of ice push, however, is deposition on the beach. As suggested above (see *Beach sediments*), the loose, wet material delivered by ice push and deposited in small, steep hummocks is vulnerable to attack and beach formation by even small waves.

Over the course of years the entire coastline seemingly is reworked by sea ice. Ice push features are largest around headlands, so the process is most effective there. On Somerset Island, Taylor (1978) noted shore ice pilings and grounded ice ridges up to 30 m high, one lasting several seasons. Ice piling occurs >100 m landward of the modern beach. Coastal facilities could be damaged or destroyed by massive ice that occasionally thrusts ashore with enormous force.

The coast of this area is now emerging about 40 cm per century, 1 cm every 2.5 years. The effect of this emergence on the shoreline varies with slope. Arrowsmith Plains have coastal segments sloping as little as 1 m per km, which could experience 4 m of shoreline regression per year.

Coastal environments

Seven coastal environments, following the classification of Taylor (1980) for Somerset Island, are distinguished in the area (Fig. 65). To know the nature of the shore and shoreface is essential in planning environmental protection from oil spills and in designing shoreline facilities.

High rock cliffs comprise much of the Peel Sound coast between Transition Bay and northeast Russell Island. Shorter segments of cliffed coast occur along the north shores of Drake and Smith bays. These coasts, backed by cliffs as high as 300 m, some with talus aprons and fans, form barriers to travel by foot or by overland vehicle.

Low rock shores with pocket beaches provide accessible reaches that punctuate cliffed coasts. The moderately steep backshores have a discontinuous mantle of coarse gravel beaches.

Sand and gravel plain coasts extend intermittently between Young and Back bays. Backshores consist of low-gradient flights of raised beaches. The sand and gravel are subject to wind erosion over much of their extent although deflation appears to be slow. Beaches are derived from erosion of sandy till, which becomes visible at low tide, scoured by sea ice, and are augmented by alluvial sand recycled from raised beaches. The intertidal and shallow subtidal areas are extensive. Parts of the modern beach and of the raised beach sequence are separated from the till substrate by organic-rich intertidal sand and mud. These coasts have the only extensive, low gradient sandy beaches in the area. Similar coasts occur in the Cape Anne area of Somerset Island and on western Bathurst Island (Taylor, 1980).

Gravel beaches are the most extensive shore type in the area, as in the central Arctic generally. They are backed by gently to moderately sloping flights of raised beaches of the same composition. The beaches are invariably developed by erosion of till and are rarely >1 m thick. The shoreface consists mostly of till scoured by sea ice.

Till plain coasts occur along much of M'Clintock Channel and Ommanney Bay where land slopes so gently that water is not deep enough at the shoreface to allow beach building. The shore consists of saturated, soupy till with a discontinuous, clast-thick armour of platy stones.

Alluvial coasts are minor elements, the largest being about 3 km long. They occur where active alluvial plains and fans reach the shore. The alluvial sediment is commonly reworked into a low gravel beach ridge at the coast during summer stages of low river flow when coastal processes dominate. In spring, freshwater input leads to breakup of adjacent sea ice and hence, creates a special shallow water habitat. Most alluvium is not underlain by foreset or bottomset deltaic sediment although some bay-head coasts may be true deltaic environments.

Estuarine coasts have significant active deltaic sedimentation at Arabella and Back bays and at Dolphin River in Browne Bay, the first by far the largest. Mud flats, partly exposed at low tide, nearly fill the inner two-thirds of Arabella Bay. Here vigour of coastal processes is restricted by the sheltered embayment and shallow water. Estuarine sediment derive

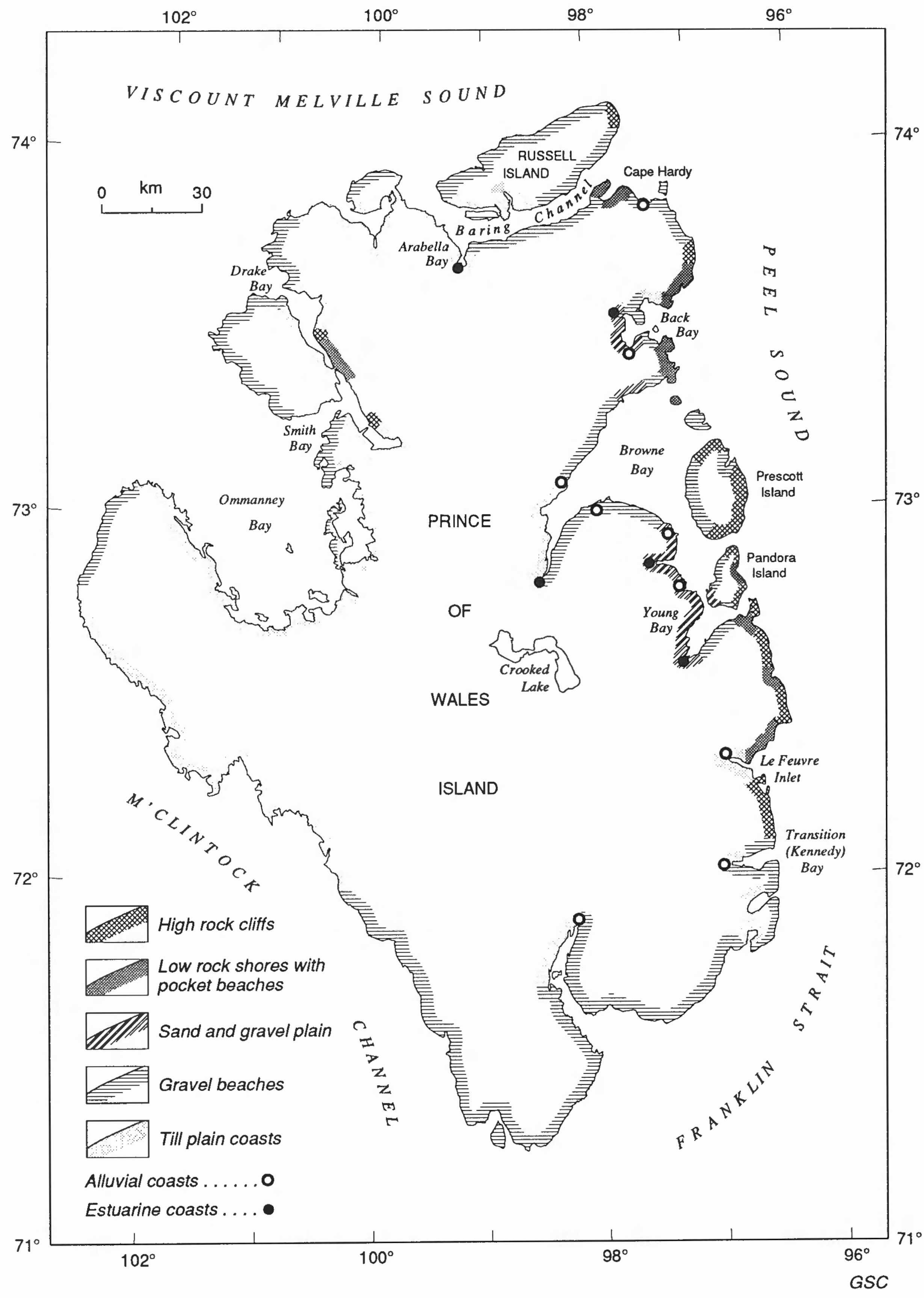

Figure 65. Coastal environments of Prince of Wales Island.

from fluvial erosion of raised glaciomarine and deltaic sediments. A raised estuarine delta southwest of the bay exposes sediment that is likely analogous to that now accumulating. The sediment contains a variety of molluscs, which indicates the ecological value of estuarine coasts.

Current and postglacial seismicity

Eastern Prince of Wales Island is underlain by the western side of Boothia Arch and a narrow belt of steeply dipping sedimentary rock, part of Cornwallis Fold Belt. Peel Sound is a cliff-bound trough within the otherwise positive relief of the arch and fold belt. Its origin has not been investigated but it could be a graben of Tertiary age (Kerr, 1980; Okulitch et al., 1986). The arch and fold belt were intermittently active in several pulses of uplift and faulting from Late Precambrian to Tertiary time.

Recorded seismic activity shows the structure to be active (Basham et al., 1977); it is one of few areas of moderately high seismicity in Canada east of the Cordillera. The largest recorded earthquakes associated with it approach magnitude six. A recent 5.6 magnitude event in Barrow Strait was felt from northern Baffin Island to Polaris Mine on Little Cornwallis Island (J. Adams, personal communication, 1989).

During and just after deglaciation, about 10-8 ka, glacioisostatic stresses reactivated the structure and resulted in a ridge-like deformation of paleoshore levels with 60-120 m of tectonic relief superimposed on the general pattern of glacioisostatic deformation (Dyke et al., 1991). The ridge can be interpreted as a symmetrical arch or an arch bounded by a fault zone along Peel Sound. Either indicates tectonic activity of large amplitude in very recent times. Rock-seated fracture lineaments that affect raised beaches along Peel Sound may be of tectonic origin and hence may indicate, as do recorded earthquakes, continued activity.

Paleo-sea level data also indicate that Prince of Wales Island recovered glacioisostatically as a block that uplifted without tilting. Because normal recovery involves tilting, it appears that some structural configuration, presumably high-angle faults bordering a block, prevented tilting.

LAND USE RECOMMENDATIONS

1. Use of bedrock and vegetated till terrains in the eastern parts of the study area should accommodate these areas as important winter habitat for caribou.
2. Disturbance of vegetation in wetlands on glaciomarine and glaciolacustrine sediments should be avoided because of danger of ice-wedge degradation and thermokarst erosion due to melting of segregated ice in special muskox habitat.
3. Resource use should be planned knowing that areas of sand and gravel are small and scattered; the largest are the vegetated raised beaches between Young and Back bays. Their extraction would require extensive scraping, which would destroy vegetation in important winter habitat for caribou.
4. Extraction of sand and gravel from glaciofluvial and fluvial sediments should be planned to minimize damage to adjacent streams and aquatic life.
5. Trenching, stripping of the active layer, or extensive use by overland vehicles in the large end moraine belts that are extensively ice cored should be avoided.
6. Disturbance of areas of thermokarst erosion underlain by massive ice should be avoided. Further disturbance could result in several metres of ground settlement.
7. Diversion of water into ice-wedge troughs should be avoided. It would lead to erosion of wedges and to extensive erosion of material from slopes, even on "stable" sand and gravel.
8. Design of structures in or crossing bedrock should withstand or accommodate frost heaving of rock masses, the nature of which varies with lithology and moisture regime.
9. Design of structures in or crossing material with ice-wedge polygons should withstand or accommodate thermal contraction cracking, heaving that occurs adjacent to ice-wedge troughs, and frozen sediment deformation in the upper few metres of permafrost on either side of growing wedges.
10. Design of linear structures should take into account mass movement processes; slopes are ubiquitously affected by various of these processes, the nature and rates of which are difficult to predict because the processes are poorly understood.
11. Design of coastal facilities should take into account the pervasive nature of sea ice disturbance and large magnitude of extreme recorded ice-piling events.
12. Plans for coastal zone cleanup of oil spills should be established and should take into account the types of coastline, the brief time available for effective action, and special habitats.
13. Design of any structure crossing the straits around Prince of Wales Island should incorporate an assessment of current seismic risk.

ECONOMIC GEOLOGY

INTRODUCTION

On Prince of Wales Island, most bedrock is obscured by thick drift. Mineral exploration could be economic if glacial deposits were used as a prospecting medium. This approach requires knowledge of local Quaternary stratigraphy, ice flow history, flow dynamics, till lithology, and the relationship between ice-flow dynamics and patterns of drift dispersion, as already described.

This section deals with base metal and uranium concentrations in till, measured in the clay fraction of about 800 samples. The sampling program, like others conducted as parts of regional mapping projects, was designed to characterize bulk properties of the regional till (see *Till composition and glacial dispersion*) rather than to prospect for ore bodies. Thus, the data constitute a regional orientation survey. As such, they establish, for the first time, background levels for trace elements and identify sites and areas that may warrant further attention.

Data are presented as frequency distributions and shaded contour maps. Data are treated similarly to those for adjacent areas (Dyke 1983, 1984; Nixon, 1988). A computer interpolation program generates shaded contour maps (Bélanger, 1978) as presented for Victoria Island till data (Nixon, 1988). The program contours an interpolated grid rather than actual sample sites and values. The algorithm removes some effects of spotty and clustered data and thus produces a more conservative surface than would result from hand contouring. For this reason, the highest interpolated values are generally somewhat, though not seriously, lower than the highest measurements.

Raw data and sample localities are listed in Appendix 2. The data can be reinterpolated readily as more results become available. Brief comments are given on distributions of copper, lead, zinc, cobalt, nickel, chromium, iron, manganese, arsenic, and uranium. Aspects of the distributions can be readily related to bedrock geology and to glacial transport; others remain unexplained though apparently significant.

COPPER

Copper levels in the sampled till range from 4 to 571 ppm, with an average of 34 ppm and standard deviation of 31 (Fig. 66A). Over most of the island copper background is <50 ppm (Fig. 67A). Background seems to be elevated to 50-100 ppm in places, particularly where till was derived primarily from Peel Sound sandstone and conglomerate. Samples with levels in excess of 100 ppm are concentrated in the Back Bay area and near Muskox Hill. Granule lithology of till samples in these areas indicates derivation from local bedrock.

LEAD

Lead levels range from 3 to 163 ppm, with an average of 16 ppm and standard deviation of 10 (Fig. 66B). Over most of the island lead levels define a background at <20 ppm (Fig. 67B). Background is elevated to 20-40 ppm over certain areas of dolomite and sandstone. Anomalous levels exceeding 60 ppm occur in till derived from dolomite near the northwest corner of the island and in till derived from the carbonate to sandstone transition belt on either side of central Baring Channel.

ZINC

Zinc levels range from 14 to 925 ppm, with an average of 78 ppm and standard deviation of 43 (Fig. 66C). Zinc background is at <100 ppm over most of the island but is slightly elevated in the northwest to 100-150 ppm (Fig. 67C). Anomalous levels exceeding 200 ppm occur in till derived from carbonate bedrock at a half-dozen widely scattered sites. Zinc distribution in till closely reflects neither bedrock geology nor glacial transport. In contrast, on Boothia Peninsula zinc reflects bedrock type and glacial transport more faithfully than any other element. All anomalous zinc concentrations overlie carbonate bedrock.

COBALT

Cobalt levels range from 1 to 35 ppm, with an average of 14 ppm and standard deviation of 6 (Fig. 66D). Over most limestone subcrop, cobalt concentrations are <10 ppm (Fig. 67D). Background levels rise to 10-20 ppm over clastic and most dolomite bedrock and further to 20-30 ppm over much of the clastic bedrock in the northeast. Cobalt levels are depressed along a corridor trending across clastic bedrock and into Transition Bay, which likely marks the Transition Bay dispersal plume. Cobalt levels reflect introduction from the west of limestone debris with its lower background. Cobalt also brings out large glacial dispersion patterns on Boothia Peninsula (Dyke, 1984). However, neither here nor on Boothia Peninsula could those elements of the distribution patterns that result from glacial transport be identified without more straightforward evidence of dispersion.

NICKEL

Nickel levels range from 5 to 125 ppm, with an average of 42 ppm and standard deviation of 17 (Fig. 66E). Concentrations of <40 ppm occur over most of the carbonate bedrock, although that rock on the northern plateau is overlain

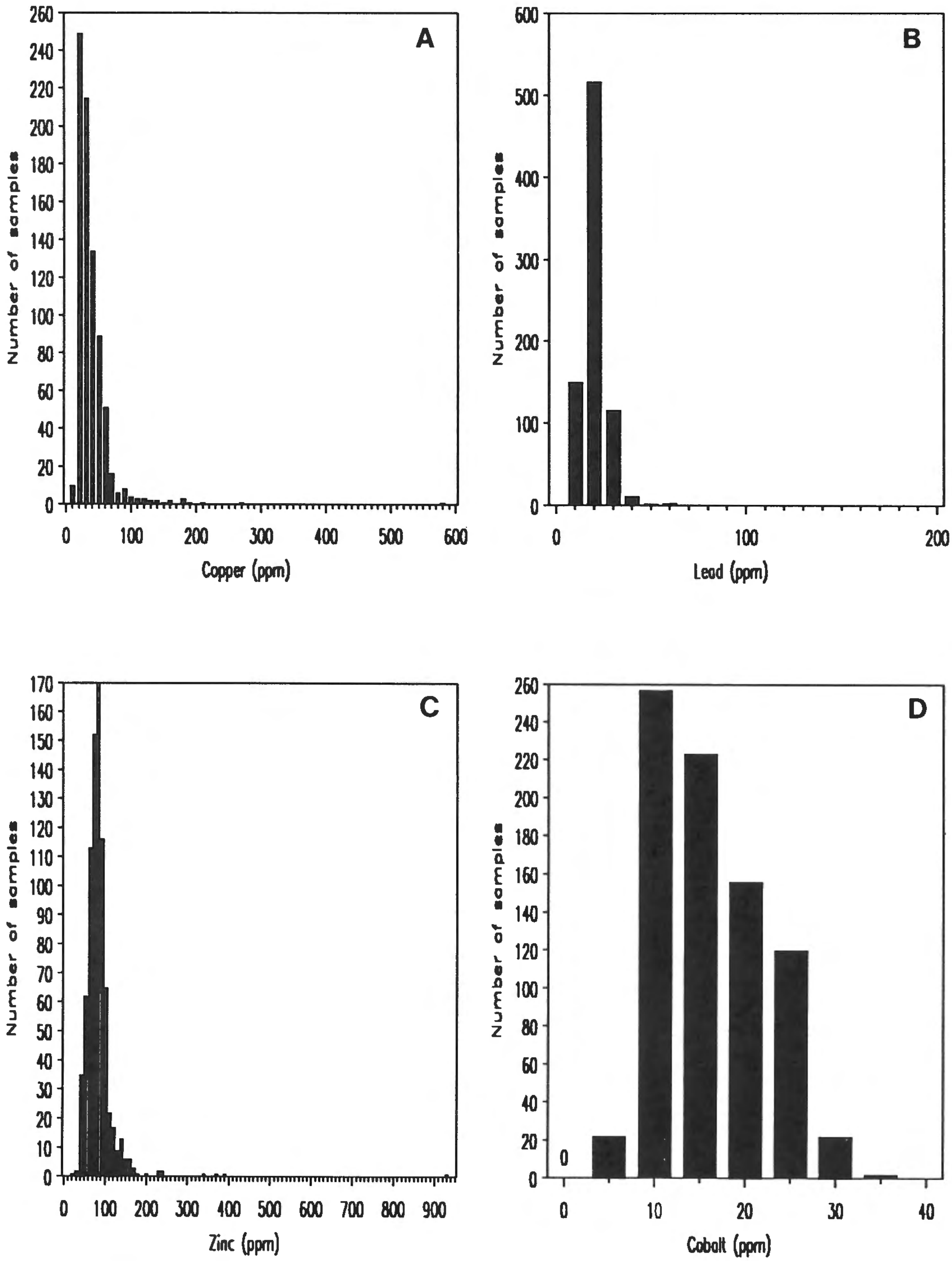

Figure 66. Frequency distributions of trace element concentrations in till samples from Prince of Wales Island: **A**, copper; **B**, lead; **C**, zinc; **D**, cobalt; **E**, nickel; **F**, chromium; **G**, iron; **H**, manganese; **I**, arsenic; **J**, uranium.

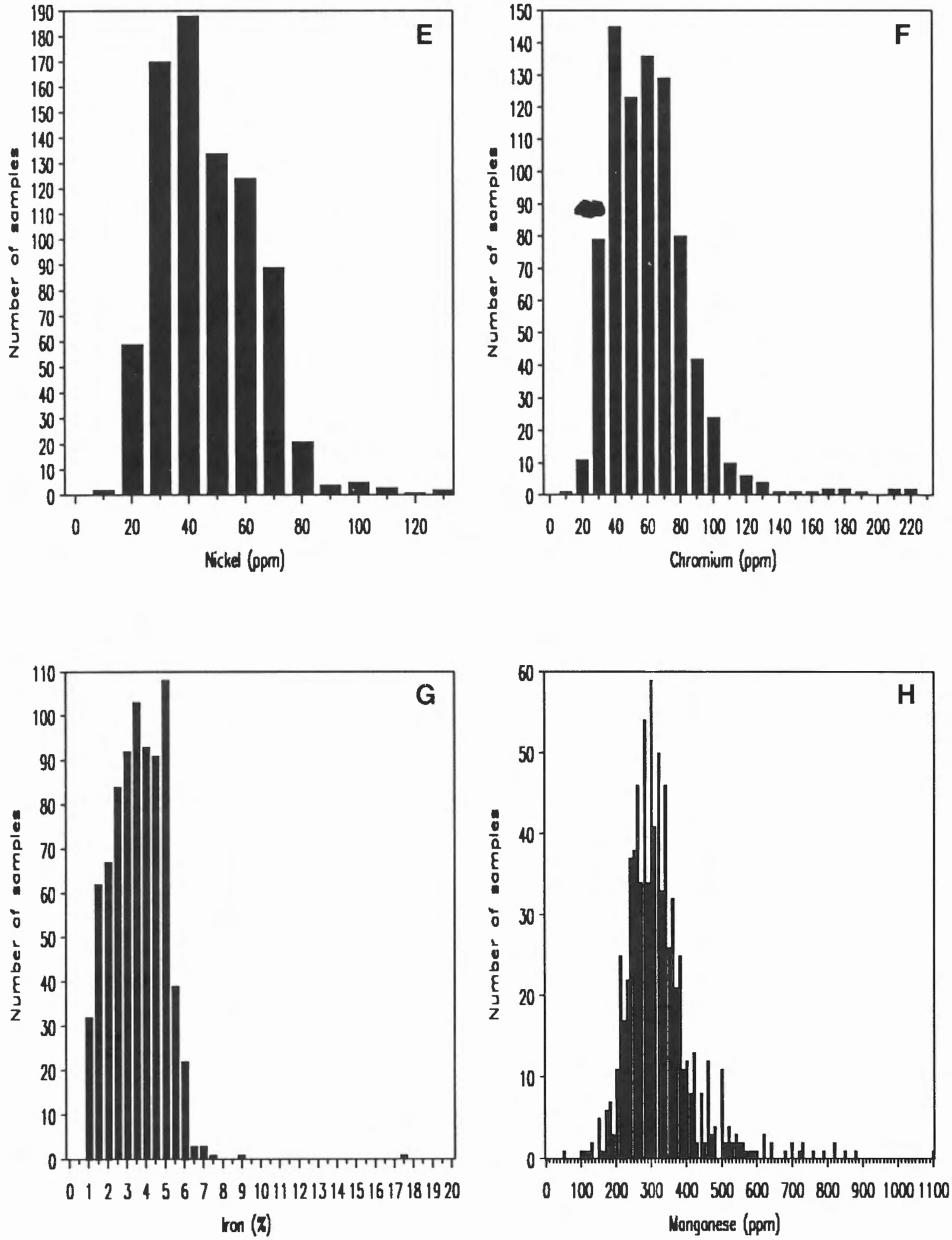

Figure 66 (cont.)

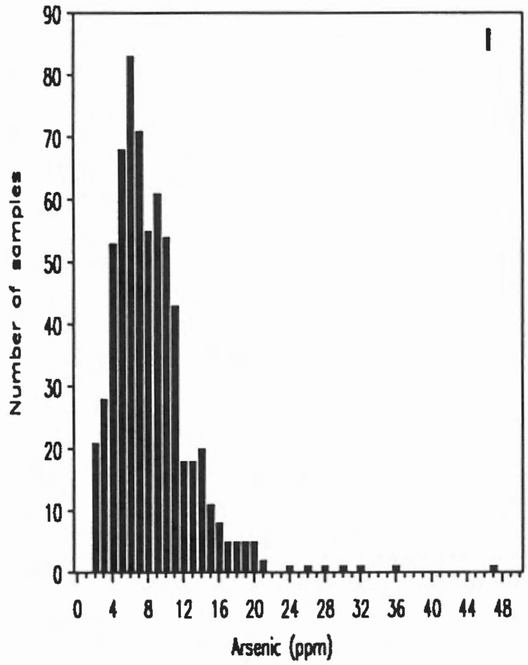

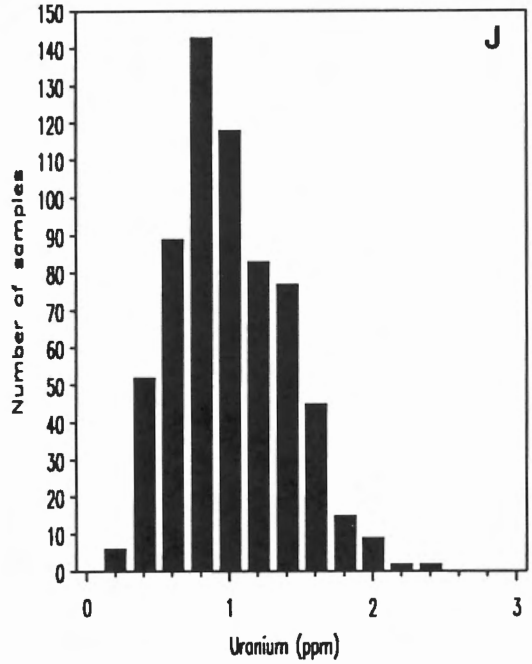

Figure 66 (cont.)

by till with 40-80 ppm nickel. This elevated background extends also across most clastic bedrock, except on the southeastern part of the island where levels are suppressed by introduction of limestone debris with low nickel levels from the west. Highest concentrations occur in till derived from conglomerate on Russell Island and may be recycled from clasts of Precambrian rock in that formation.

CHROMIUM

Chromium ranges from 2 to 220 ppm, with an average of 57 ppm and standard deviation of 26 (Fig. 66F). In general, background is lower over the carbonate rocks of the southern and western part of the island than over clastic rocks and the carbonate rocks of the northern part (Fig. 67F). Low background over clastic rocks in the southeast likely results from eastward glacial transport of limestone debris. Highest concentrations occur in till overlying Peel Sound conglomerate on northeastern Prince of Wales Island and on eastern Russell Island where nickel concentrations are also high.

IRON

Iron content ranges from 0.6 to 17.2%, with an average of 3.4% and standard deviation of 1.4 (Fig. 66G). Background levels are <4% on the southern and western parts of the island and 4-6% in most other places; they are, thus, higher over clastic bedrock and over flanking carbonates in the north. Background levels are suppressed over the southern part of the clastic rock belt by the high erratic component of the till there; the Transition Bay dispersal plume is picked out by an eastward protrusion of the 2% contour. The single sample with >10% iron was brownish red till derived from an underlying gossanous bed <1 m thick in carbonate bedrock. This sample does not contain anomalous levels of other elements measured.

MANGANESE

Manganese, as usual, shows the widest spread of concentrations of any of the elements measured. It ranges from 42 to 1100 ppm, with an average of 319 ppm and standard deviation of 102 (Fig. 66H). Although locally there appear to be relationships between manganese levels and bedrock, such as lower levels over dolomite than over limestone on the peninsula west of Ommanney Bay, these relationships do not hold over the larger area (Fig. 67H). Background levels are quite variable over limestone, over dolomite, and over clastic rocks. Highest levels occur in till derived from conglomerate on the northeastern part of the island, in till derived from dolomite in the same vicinity, and in till derived from carbonate on the north-central part. Because it is difficult to link the broad aspects of manganese distribution to the distribution of bedrock lithologies, it is not possible to identify aspects that might result from glacial transport.

ARSENIC

Arsenic levels range from 2 to 47 ppm, with an average of 8 ppm and standard deviation of 5 (Fig. 66I). Background is at <10 ppm over much of the island and at <20 ppm over most

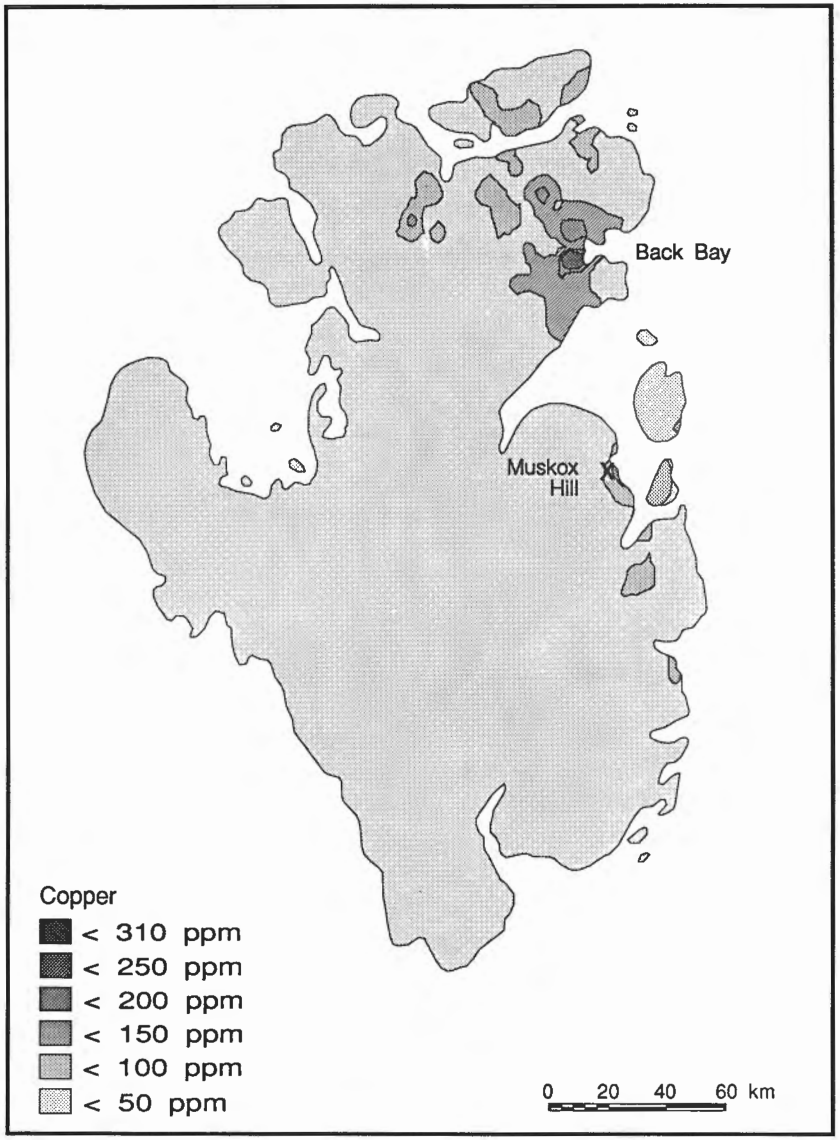

Figure 67A. Copper concentration in till, Prince of Wales Island.

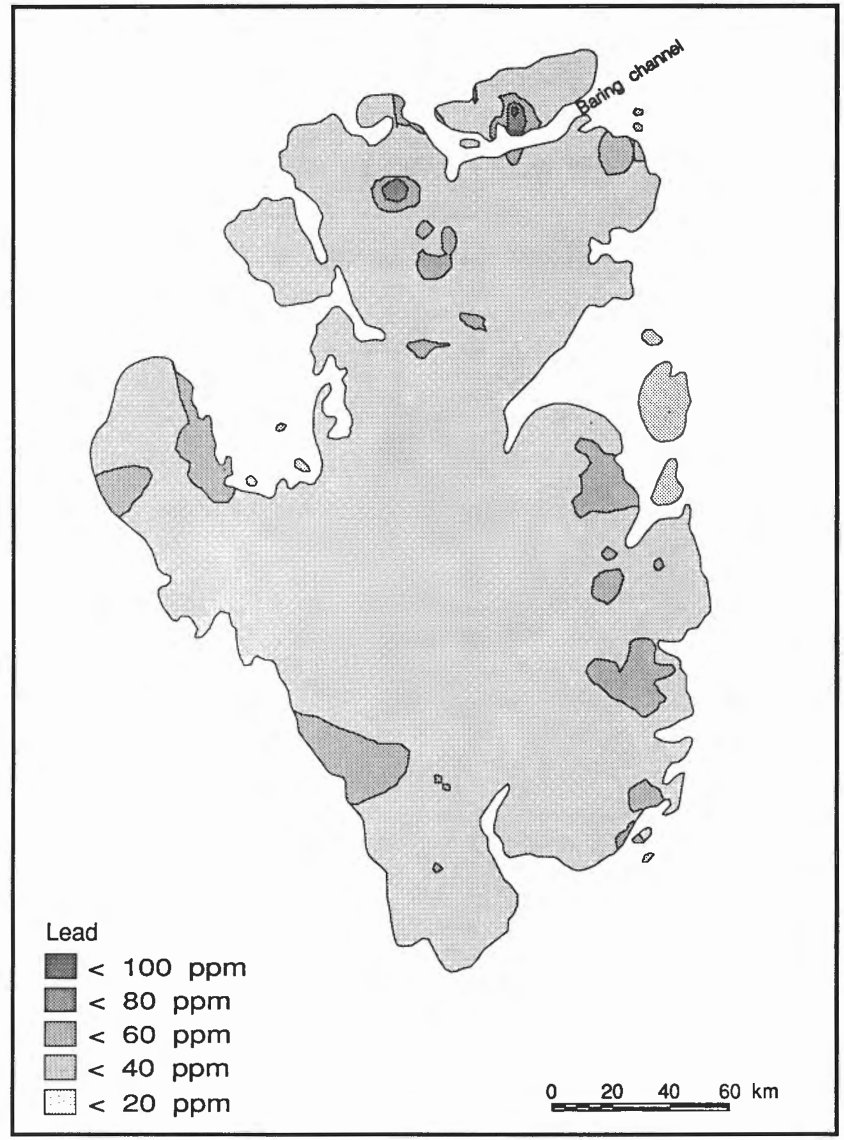

Figure 67B. Lead concentration in till, Prince of Wales Island.

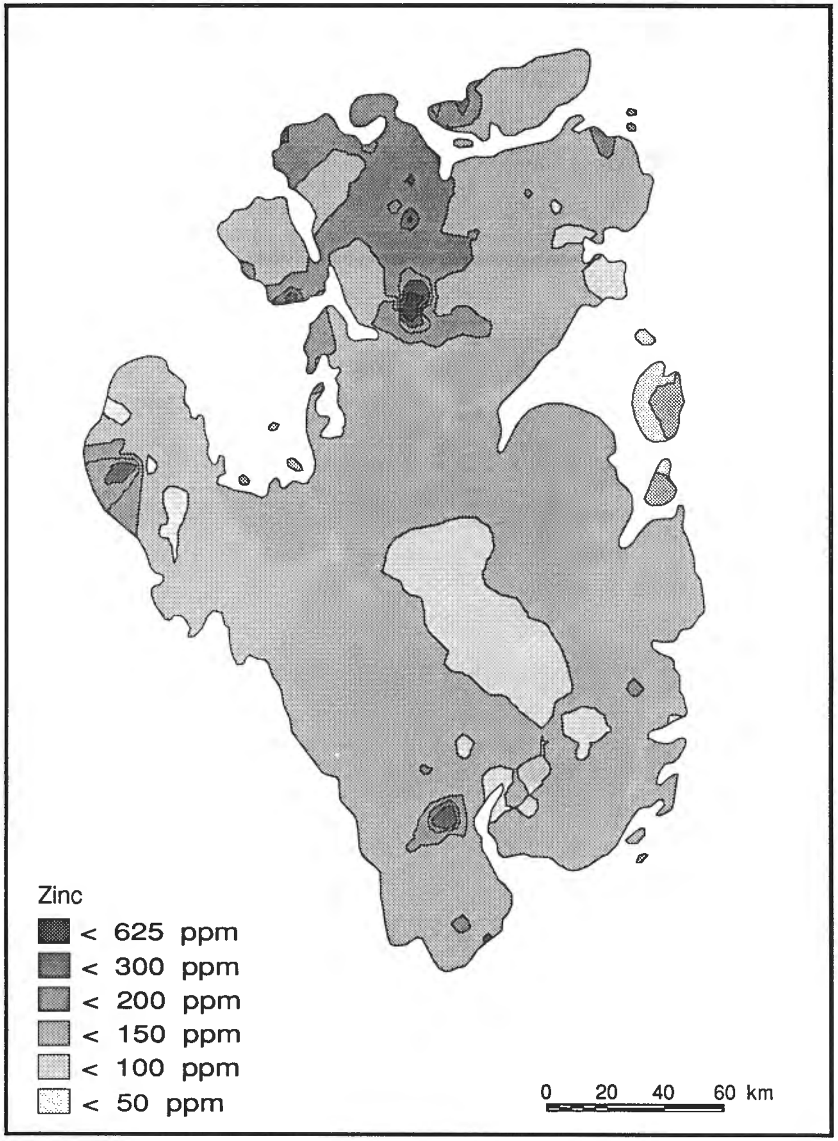

Figure 67C. Zinc concentration in till, Prince of Wales Island.

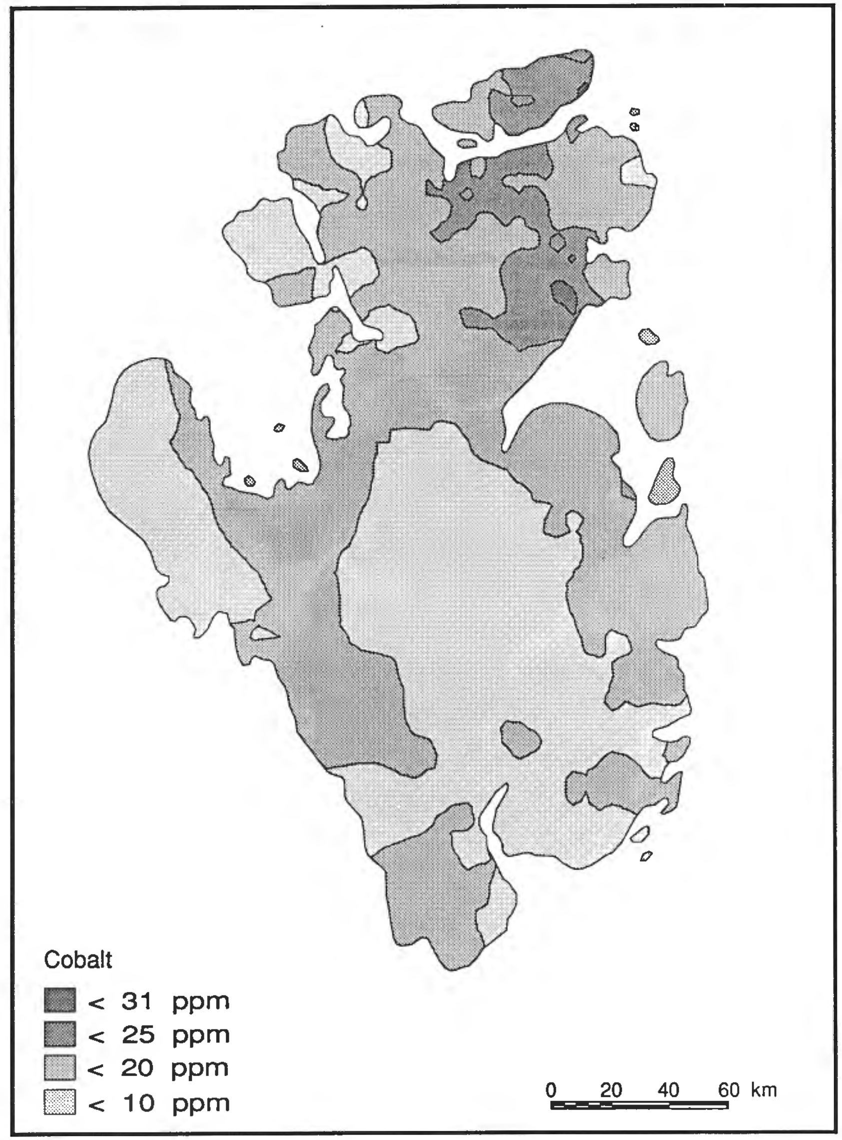

Figure 67D. Cobalt concentration in till, Prince of Wales Island.

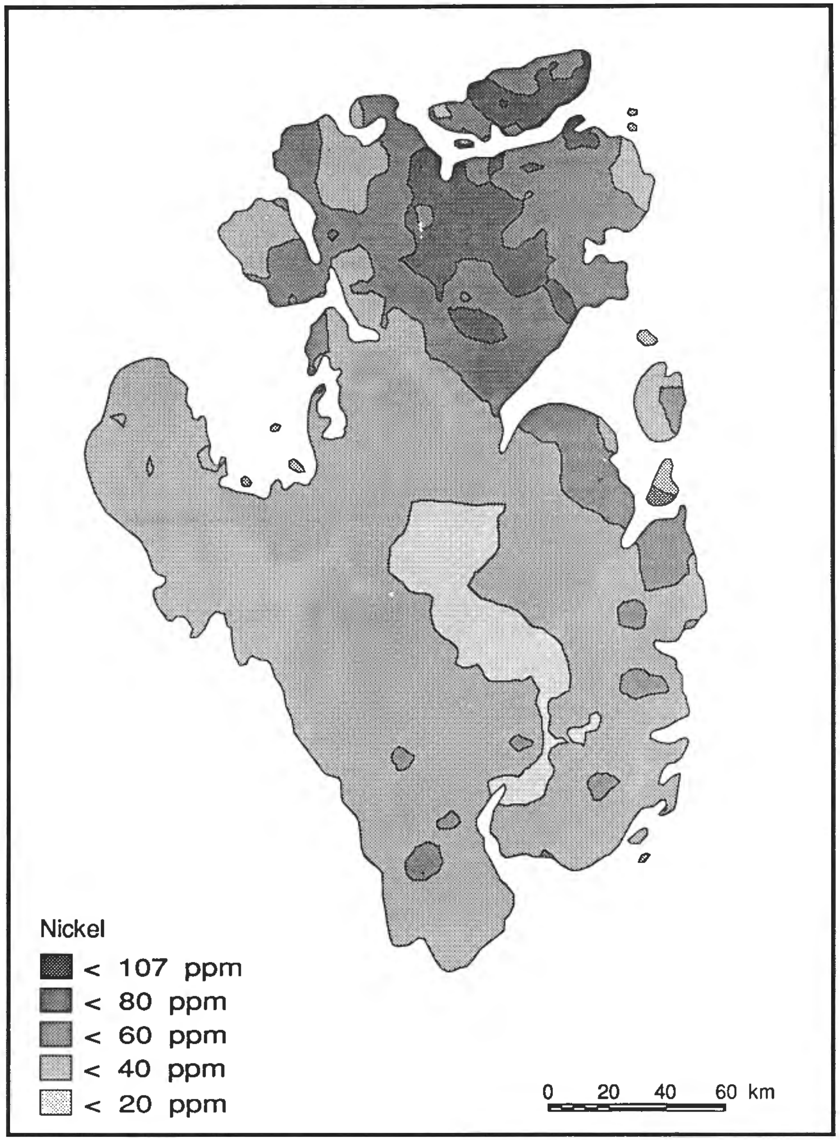

Figure 67E. Nickel concentration in till, Prince of Wales Island.

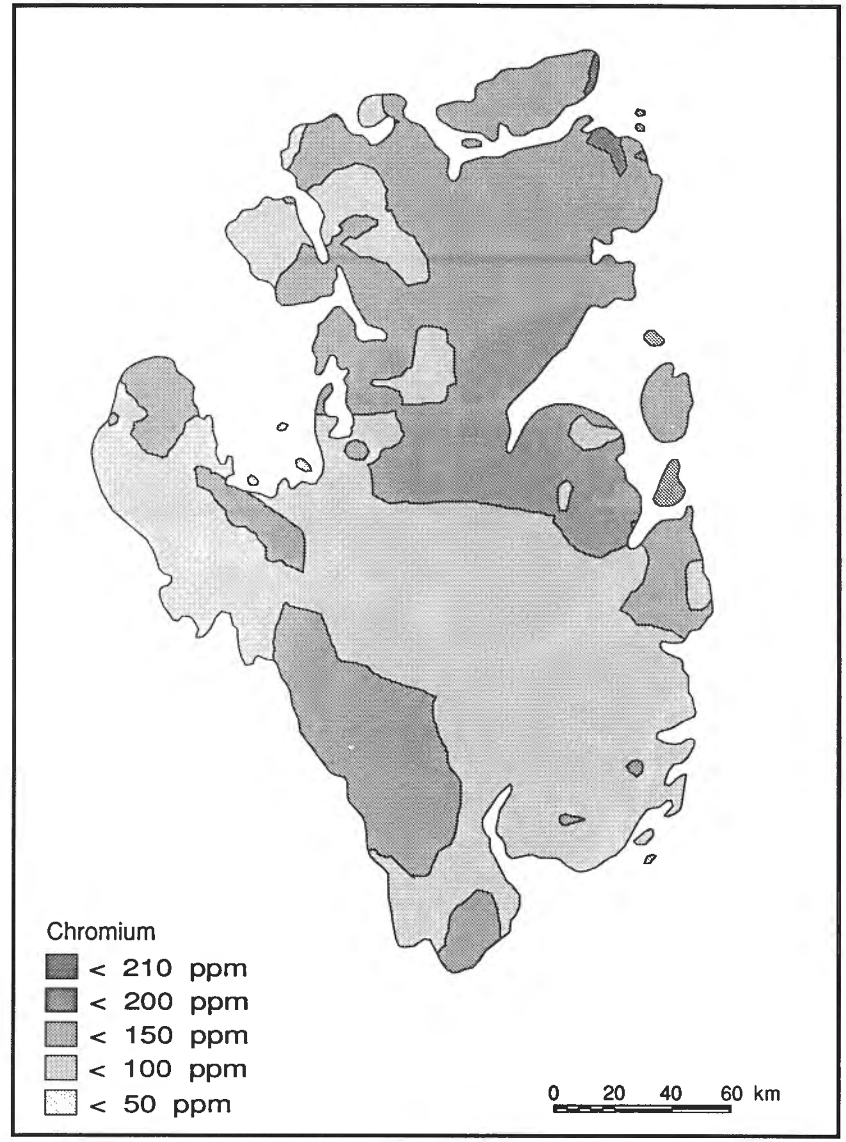

Figure 67F. Chromium concentration in till, Prince of Wales Island.

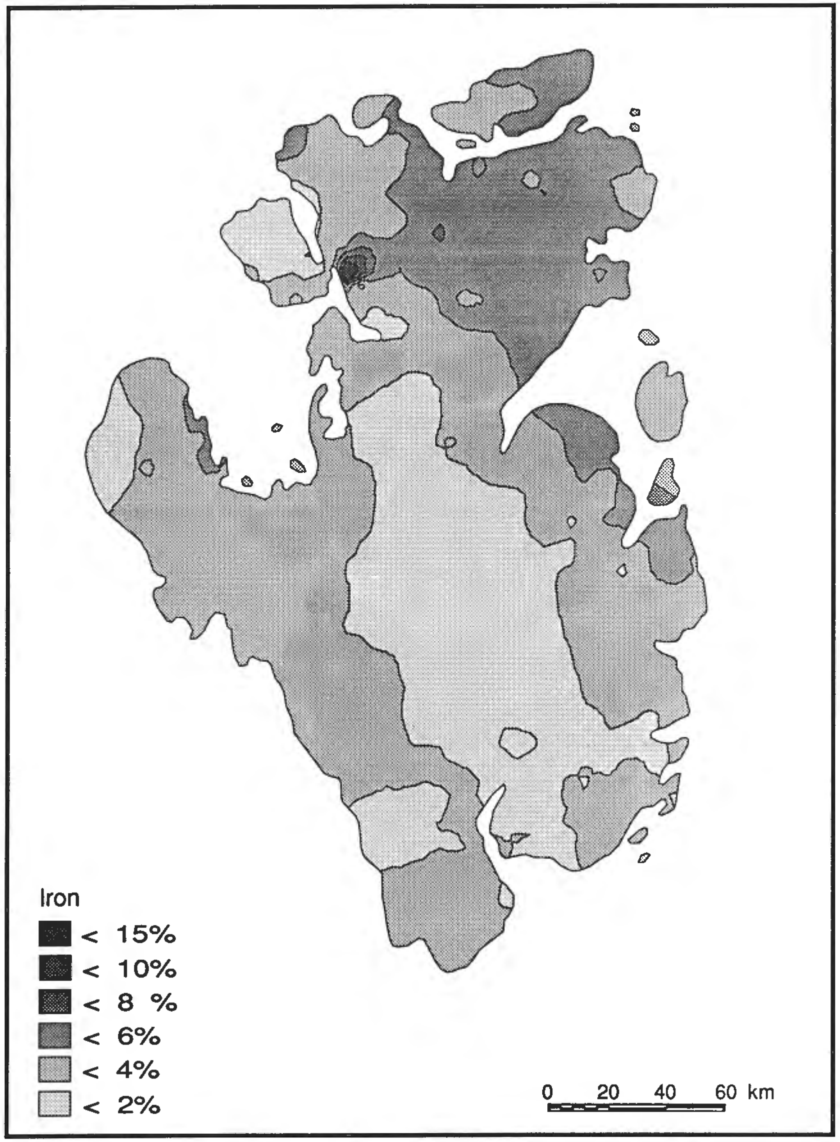

Figure 67G. Iron concentration in till, Prince of Wales Island.

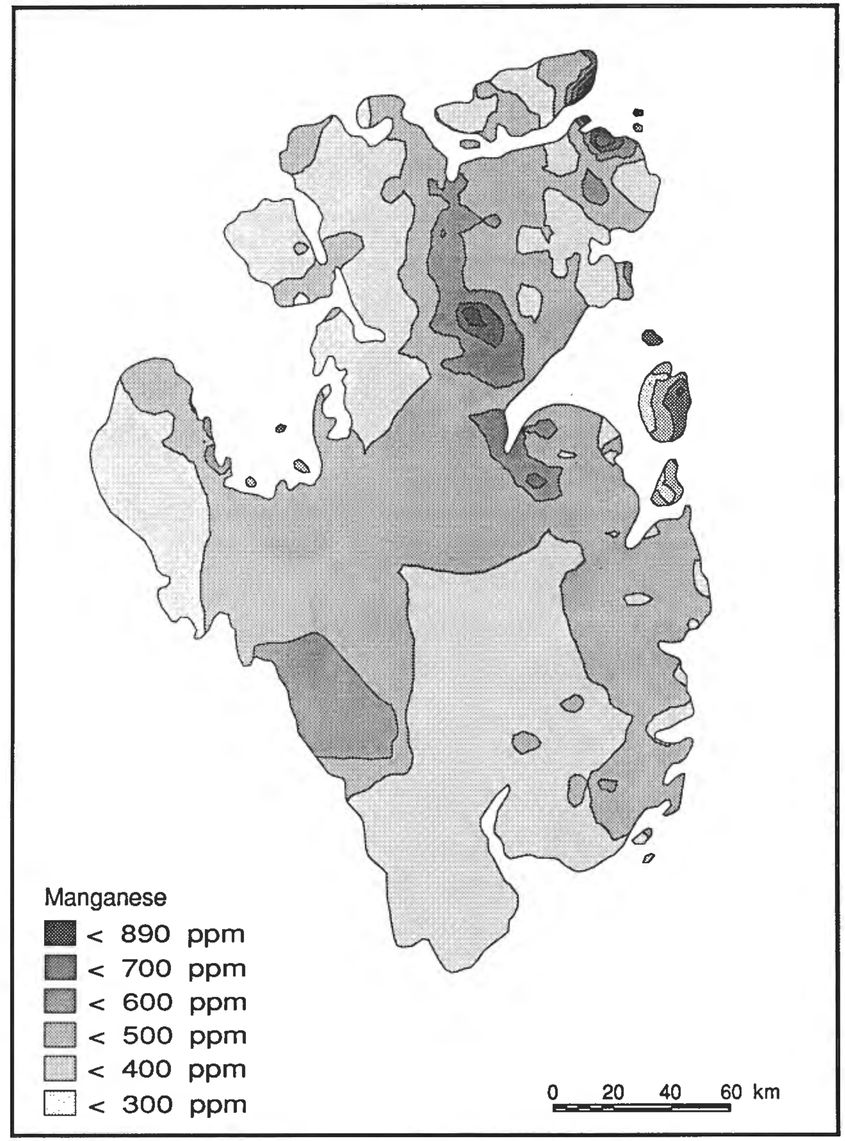

Figure 67H. Manganese concentration in till, Prince of Wales Island.

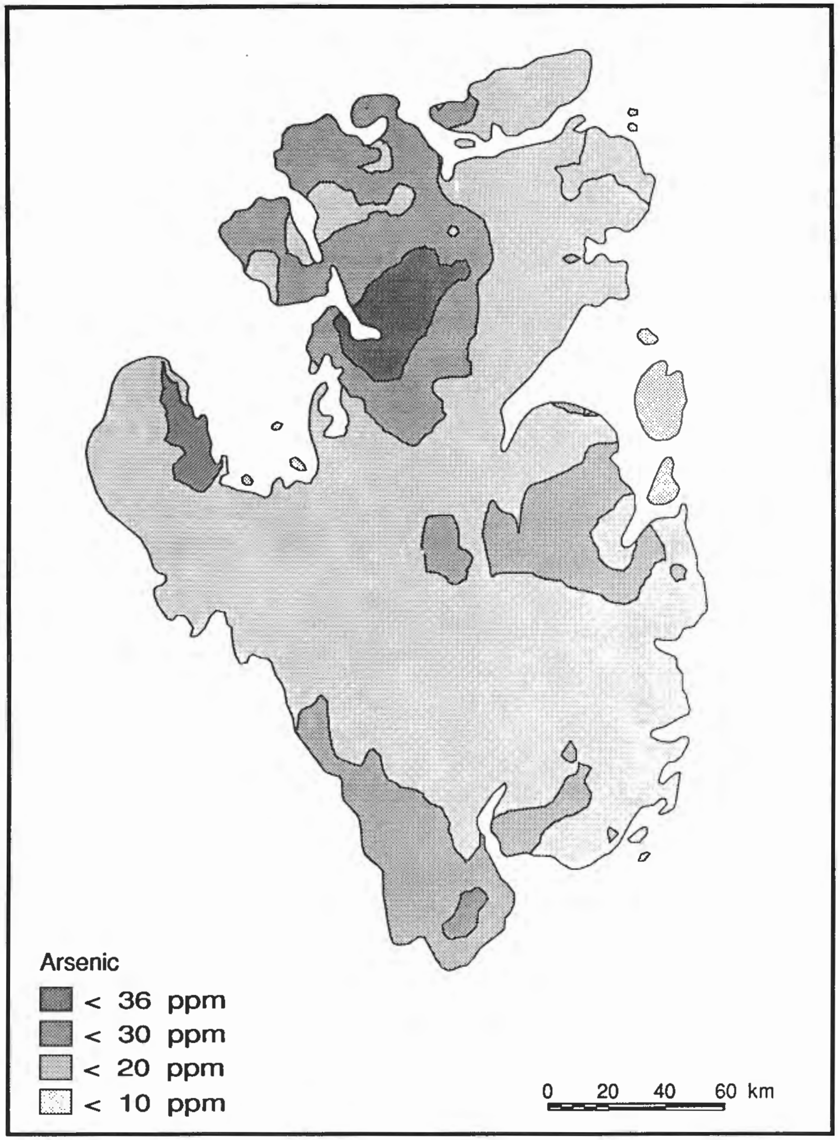

Figure 67I. Arsenic concentration in till, Prince of Wales Island.

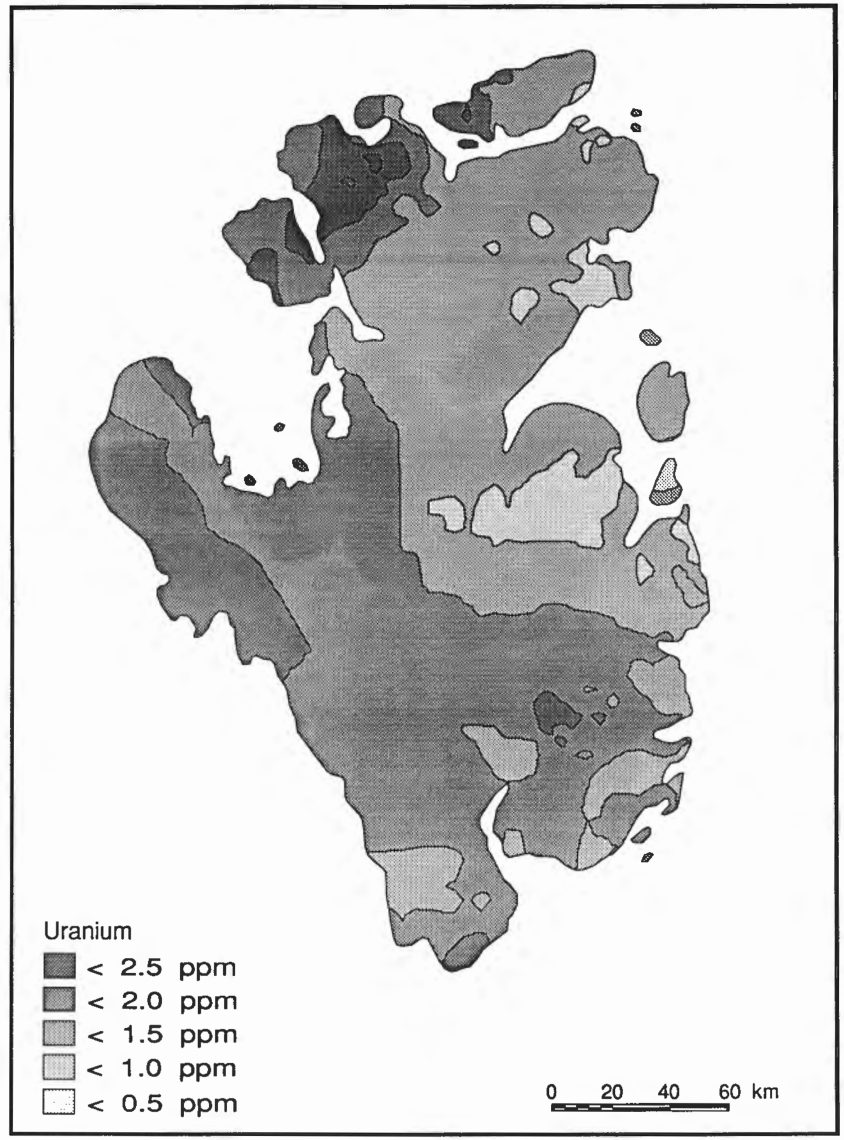

Figure 67J. Uranium concentration in till, Prince of Wales Island.

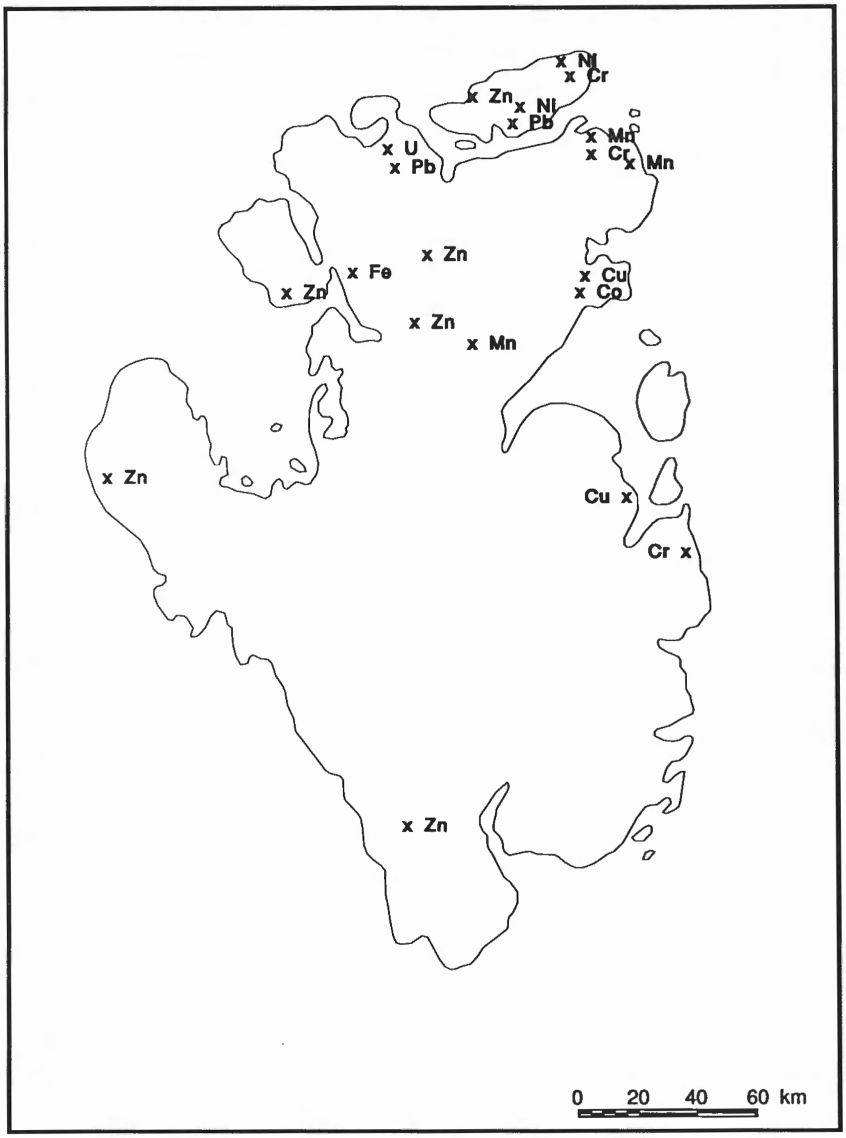

Figure 68. Distribution of high trace element concentrations, Prince of Wales Island.

(Fig. 67I). Variations in background can not be convincingly tied to either bedrock type or to glacial transport. Although dolomites on the northern part of the island appear to have higher background than other rocks there, this relationship does not hold farther south.

URANIUM

Uranium levels range from 0.1 to 2.4 ppm, with an average of 1 ppm and standard deviation of 0.4 (Fig. 66J). Background levels vary systematically, generally increasing from east to west (Fig. 67J). This pattern can not be explained in terms of distribution of bedrock lithologies or of till lithology. Possibly it reflects a gradual enrichment in uranium toward the centre of the Lower Paleozoic sedimentary basin (Victoria Basin) or away from the Boothia Arch.

SUMMARY OF ELEMENT TO ROCK RELATIONSHIPS

Of the elements discussed here, cobalt, nickel, chromium, and iron have similar distributional patterns. All exhibit higher background levels over clastic bedrock, except in the southeast where levels are suppressed by glacial transport. All exhibit higher backgrounds over the carbonate rocks of the northern plateau than over the same formations on the central and southern parts of the island. All except iron attain anomalous levels (see below) over Peel Sound conglomerate and sandstone; the single iron anomaly occurs over carbonate.

Copper, lead, zinc, manganese, arsenic, and uranium distributions show no consistent relationships with the bedrock geology, which precludes recognition of any aspects of the distributions that may be glacigenic. All display geographically persistent variabilities that remain unexplained.

Element to rock relationships apparently are not reliable from region to region. On Boothia Peninsula copper, zinc, nickel, and cobalt are related to bedrock and to glacial transport (Dyke, 1984). On western Victoria Island, copper, lead, zinc, nickel, and chromium show strong regional variabilities that reflect bedrock, whereas cobalt, manganese, arsenic, iron, and uranium do not. Thus, across the central Arctic, nickel and chromium concentrations in till, sampled at a reconnaissance level, appear to reflect bedrock patterns faithfully, whereas manganese and uranium do not, and copper, lead, zinc, cobalt and iron do in some areas but not in others.

Table 4. Maximum concentrations of trace elements encountered in till samples from Prince of Wales, Somerset, and Victoria islands and from Boothia Peninsula

Element	Prince of Wales Island	Boothia Peninsula	Somerset Island	Victoria Island
Cu	571	325	580	469
Pb	163	136	420	84
Zn	925	1400	580	2950
Co	35	92	140	43
Ni	125	370	268	138
Cr	220	350	323	127
Mn	1100	2600	3425	2770
U	2.4	16.3	3.7	2.9
Fe	17.2	10.0	14.0	9.7

DITRIBUTION OF HIGH ELEMENT CONCENTRATIONS

Samples and sample clusters with anomalously high concentrations of trace elements (2 standard deviations above the mean) are not randomly distributed (Fig. 68). Most are from the northern plateau of Prince of Wales Island and from Russell Island.

Till derived mostly from Peel Sound Formation in that area accounts for eight anomalies; two other anomalies occur in till derived from that formation on the eastern part of the island. Three sites have anomalous levels of chromium, two of nickel, two of copper, and one each of lead, cobalt, and manganese.

Till over carbonate rock in the north contains a further eight anomalies and two others occur in till over carbonate rock in the south and west. Six sites have anomalous levels of zinc, two of manganese, and one each of lead, iron, and uranium.

The highest concentrations of trace elements encountered in the till sampling program on Prince of Wales Island are comparable to the maxima encountered in similar sampling programs on Somerset Island, Boothia Peninsula, and western Victoria Island (Table 4). The sparse sampling makes it highly unlikely that the areas of greatest enrichment have been encountered, so closer sampling may yield more provocative results.

ACKNOWLEDGMENTS

This report is the final contribution to GSC Project 810044. The field phases were made possible by logistical support from Polar Continental Shelf Project of GSC out of their Resolute Bay base camp, managed by Mr. Barry Hough. Laboratory phases relied heavily on expertise of the GSC Radiocarbon Dating Laboratory, directed by Dr. Roger McNeely; the GSC Sedimentology Laboratories, directed by Ms. Patty Higgins; and the Saskatchewan Research Council Radiocarbon Dating Laboratory, directed by Mr. Jurgen Wittenberg. Most work was funded by Terrain Sciences Division of GSC but additional support was provided to Thomas Morris and David Green by the Boreal Institute for Northern Studies at the University of Alberta, which funded some of the field assistants' salaries and many radiocarbon dates. Some other dates were purchased out of John England's grant from Natural Sciences and Engineering Research Council of Canada. Daryl Krupa, Alan Minty, Christy Taylor, and David Ness each assisted in fieldwork for one summer, and James Hooper assisted for all three. The Geography Department at the University of Alberta contributed significantly to the project through their support of Morris and Green as graduate students and through their support of the senior author during a sabbatical at the start of the project. In many ways, the scope of the project reflects the opportunities for recruitment of graduate students and continued interaction that would not have been possible without that sabbatical. Dr. Donald Lemmen of GSC sacrificed 2 weeks of his career to a careful review, which helped sharpen our interpretations. Dr. Robert Bélanger, Mr. Steve Courtney, Mr. Mark Nixon, Mr. André Prégent, and Ms. Tracy Barry assisted with computer files and graphics.

REFERENCES

Andrews, J.T.

1970: A geomorphological study of postglacial uplift, with particular reference to Arctic Canada; Institute of British Geographers, Special Publication No. 2, 156 p.

1985: Quaternary Environments: Eastern Canadian Arctic, Baffin Bay and Western Greenland; Allen and Unwin, London, 774 p.

1989: Quaternary geology of the northeastern Canadian Shield; in Chapter 3 of Quaternary Geology of Canada and Greenland, ed. R.J. Fulton; Geological Survey of Canada, Geology of Canada, no. 1, p. 276-301.

Balkwill, H.R., Cook, D.G., Detterman, R.L., Embry, A.F., Hakansson, E., Miall, A.D., Poulton, T.P., and Young, F.G.

1983: Arctic North America and northern Greenland; Chapter 1 of The Phanerozoic Geology of the world, II. The Mesozoic; Elsevier Science Publishers B.V., The Nederlands, p. 1-31.

Basham, P.W., Forsyth, D.A., and Wetmiller, F.J.

1977: The seismicity of northern Canada; Canadian Journal of Earth Sciences, v. 14, p. 1646-1667.

Bélanger, J.R.

1978: URBIS5 user's reference manual; Geological Survey of Canada, Paper 78-21, 27 p.

Berkhout, A.J.W.

1973: Gravity in the Prince of Wales, Somerset, and northern Baffin islands region; in Proceedings of the symposium of the geology of the Canadian Arctic, ed. J.D. Aitken and D.J. Glass; Geological Association of Canada, p. 63-80.

Bird, J.B.

1959: Contributions to the physiography of northern Canada; Zeitschrift fur Geomorphology, band 3, heft 2, p. 151-174.

Bird, J.B. (cont.)

1967: The Physiography of Arctic Canada (With Special Reference to the Area South of Parry Channel); John Hopkins Press, Baltimore, 336 p.

Blackadar, R.G.

1967: Precambrian geology of Boothia Peninsula, Somerset Island, and Prince of Wales Island, District of Franklin; Geological Survey of Canada, Bulletin 151, 61 p.

Blackadar, R.G. and Christie, R.L.

1963: Geological reconnaissance, Boothia Peninsula, and Somerset, King William, and Prince of Wales islands, District of Franklin; Geological Survey of Canada, Paper 63-19, 15 p.

Blake, W., Jr.

1970: Studies of glacial history in Arctic Canada I: pumice, radiocarbon dates, and differential postglacial uplift in the eastern Queen Elizabeth Islands; Canadian Journal of Earth Sciences, v. 7, p. 634-664.

Blake, W., Jr. and Lewis, C.F.M.

1975: Marine surficial geology: observations in the high Arctic, 1974; in Report of Activities, Part A, Geological Survey of Canada, Paper 75-1A, p. 383-387.

Bornhold, B.D., Finlayson, N.M. and Monahan, D.

1976: Submerged drainage patterns in Barrow Strait, Canadian Arctic; Canadian Journal of Earth Sciences, v. 13, p. 305-311.

Bostock, H.S.

1970: Physiography of Canada; Geological Survey of Canada, Map 1254A, scale 1:5 000 000.

Brown, R.J.E.

1967: Permafrost in Canada; Geological Survey of Canada, Map 1246A.

Christie, R.L., Thorsteinsson, R., and Kerr, J.W.

1966: Geology of Prince of Wales Island; Geological Survey of Canada, Open File 66, scale 1:125 000.

Clark, P.U.

1987: Subglacial sediment dispersal and till composition; Journal of Geology, v. 95, p. 527-541.

Collier, J. and Judge, A.S.

1977: Survey of seabottom temperatures and salinities in Barrow Strait; Earth Physics Branch, Open File 77-24.

Craig, B.G.

1964: Surficial geology of Boothia Peninsula and Somerset, King William, and Prince of Wales islands, District of Franklin; Geological Survey of Canada, Paper 63-44, 10 p.

Craig, B.G. and Fyles, J.G.

1960: Pleistocene geology of Arctic Canada; Geological Survey of Canada, Paper 60-12, 21 p.

Dietrich, R.V.

1977: Impact abrasion of harder by softer materials; Journal of Geology, v. 85, p. 242-246.

Dyke, A.S.

1983: Quaternary geology of Somerset Island, District of Franklin; Geological Survey of Canada, Memoir 404, 32 p.

1984: Quaternary geology of Boothia Peninsula and northern District of Keewatin, central Canadian Arctic; Geological Survey of Canada, Memoir 407, 26 p.

1987: A reinterpretation of the ages of glacial and marine limits around the northwestern Laurentide Ice Sheet; Canadian Journal of Earth Sciences, v. 24, p. 591-601.

Dyke, A.S. and Dredge, L.A.

1989: Quaternary geology of the northwestern Canadian Shield; in Chapter 3 of Quaternary Geology of Canada and Greenland, ed. R.J. Fulton; Geological Survey of Canada, Geology of Canada, no. 1, p. 189-214.

Dyke, A.S. and Matthews, J.V., Jr.

1987: Stratigraphy of Quaternary sediments along Pasley River, Boothia Peninsula, central Canadian Arctic; Géographie physique et Quaternaire, v. 41, p. 323-344.

Dyke, A.S. and Morris, T.F.

1988: Drumlin fields, dispersal trains and ice streams in Arctic Canada; Canadian Geographer, v. 32, p. 86-90.

1990: Postglacial history of the bowhead whale and of driftwood penetration, central Canadian Arctic: implications for paleoclimate; Geological Survey of Canada, Paper 89-24.

Dyke, A.S., Morris, T.F. and Green, D.E.C.

1991: Postglacial tectonic and sea level history of the central Canadian Arctic; Geological Survey of Canada, Bulletin 397.

Dyke, A.S., Morris, T.F., and Hooper, J.

1989: Postglacial history of the bowhead whale and driftwood penetration, central and eastern Canadian Arctic (abstract); Abstracts of the 18th Arctic Workshop, Lethbridge.

Dyke, A.S. and Prest, V.K.

1987: Late Wisconsinan and Holocene history of the Laurentide Ice Sheet; Géographie physique et Quaternaire, v. 41, p. 237-263.

1987: Late Wisconsinan and Holocene retreat of the Laurentide Ice Sheet; Geological Survey of Canada, Map 1702A, scale 1:5 000 000.

1987: Paleogeography of northern North America, 18 000 - 5000 years ago; Geological Survey of Canada, Map 1703A, 11 maps, scale 1:12 500 000.

England, J.

1987: Glaciation and the evolution of the Canadian High Arctic landscape; Geology, v. 15, p. 419-424.

Falconer, G., Mathews, W.H., Prest, V.K., and Wilson, J.T.

1958: Glacial Map of Canada; Geological Association of Canada, scale 1:3 801 600.

Fortier, Y.

1948: Flights in 1947 over the region of the north magnetic pole and the mainland between the Arctic coast, Great Slave Lake, and Hudson Bay, Northwest Territories; Geological Survey of Canada, Paper 48-23.

Fortier, Y. and Morley, L.
1956: Geological unity of the Arctic Islands; Transactions of the Royal Society of Canada, v. 50, p. 3-12.

Fortier, Y. et al.
1963: Geology of the north-central part of the Arctic Archipelago, Northwest Territories (Operation Franklin); Geological Survey of Canada, Memoir 320, 671 p.

Green, D.E.C.
1986: The Late Quaternary history of Russell Island, N.W.T.; unpublished M.Sc. thesis, University of Alberta, Edmonton, 131 p.

Hardy and Associates Ltd.
1984: Study of well logs in the Arctic Islands to outline permafrost thickness and/or gas hydrate occurrence; Earth Physics Branch, Open File no. 84-8, 215 + 159 p.

Harington, C.R.
1966: Extralimital occurrences of walruses in the Canadian Arctic; Journal of Mammalogy, v. 47, p. 506-513.

Hasegawa, H.S.
1988: Neotectonics and inferred movements in Canada; Bulletin of the Geological Society of Finland, v. 60, Part 1, p. 3-25.

Hodgson, D.A.
1982: Surficial materials and geomorphological processes, western Sverdrup and adjacent islands, District of Franklin; Geological Survey of Canada, Paper 81-9, 34 p.
1987: Episodic retreat of the Late Wisconsinan Laurentide Ice Sheet over northeast Victoria Island (Storkerson Peninsula and Stefansson Island) (abstract); Abstracts of the 16th Arctic Workshop, Boreal Institute for Northern Studies, University of Alberta, Edmonton, p. 60.

Hooper, J.
1986: Pollen analysis of a peat profile and a buried soil from the Cape Hardy area, northern Prince of Wales Island, N.W.T.; unpublished B.Sc. thesis, University of Alberta, Edmonton, 28 p.

Jenness, J.L.
1952: Problem of glaciation in the western islands of Arctic Canada; Geological Society of America Bulletin, v. 63, p. 939-952.

Judge, A.
1973: The prediction of permafrost thickness; Canadian Geotechnical Journal, v. 10, p. 1-11.

Kerr, J.W.
1977: Cornwallis Fold Belt and the mechanism of basement uplift; Canadian Journal of Earth Sciences, v. 14, p. 1374-1401.
1980: Structural framework of the Lancaster aulacogen, Arctic Canada; Geological Survey of Canada, Bulletin 319, 24 p.

Kerr, J.W. and Christie, R.L.
1965: Tectonic history of Boothia Uplift and Cornwallis Fold Belt, Arctic Canada; American Association of Petroleum Geologists, Bulletin 49, p. 905-926.

Klassen, R.A.
1989: Quaternary geology of Bylot Island; Geological Survey of Canada, Memoir 429.

Klassen, R.A. and Fisher, D.A.
1988: Basal-flow conditions at the northeastern margin of the Laurentide Ice Sheet, Lancaster Sound; Canadian Journal of Earth Sciences, v. 25, p. 1740-1750.

Kurfurst, P.J. and Veillette, J.J.
1977: Geotechnical characterization of terrain units, Bathurst, Cornwallis, Somerset, Prince of Wales and adjacent islands; Geological Survey of Canada, Open File 471.

MacLean, B., Sonnichsen, G., Vilks, G., Powell, C., Moran, K., Jennings, A., Hodgson, D., and Deonarine, B.
1989: Marine geological and geotechnical investigations in Wellington, Byam Martin, Austin, and adjacent channels, Canadian Arctic Archipelago; Geological Survey of Canada, Paper 89-11, 69 p.

Mayewski, P.A., Denton, G.H., and Hughes, T.J.
1981: Late Wisconsin ice sheets in North America; in The Last Great Ice Sheets, ed. G.H. Denton and T.J. Hughes, John Wiley and Sons, New York, p. 67-178.

Miall, A.D.
1970a: Devonian alluvial fans, Prince of Wales Island, Arctic Canada; Journal of Sedimentary Petrology, v. 40, p. 556-571.
1970b: Continental marine transition in the Devonian of Prince of Wales Island, Northwest Territories; Canadian Journal of Earth Sciences, v. 7, p. 125-144.
1983: Stratigraphy and tectonics of the Peel Sound Formation, Somerset and Prince of Wales islands: discussion; in Current Research, Part A, Geological Survey of Canada, Paper 83-1A, p. 493-495.

McKenna-Neuman, C. and Gilbert, R.
1986: Aeolian processes and landforms in glaciofluvial environments of southeastern Baffin Island, N.W.T., Canada; in Aeolian Geomorphology, ed. W.G. Nickling;Allen and Unwin, Boston.

Mörner, N-A.
1974: Relations between shoreline gradients, uplift and ice recession; Norsk Geografisk Tidsskrift, v. 28, p. 273-276.

Morris, T.F.
1988: Quaternary geology of southern Prince of Wales Island, N.W.T., Canada; unpublished Ph.D. thesis, University of Alberta, Edmonton, 200 p.

Mortensen, P.S.
1985: Stratigraphy and sedimentology of the Upper Silurian strata on eastern Prince of Wales Island, Arctic Canada; unpublished Ph.D. thesis, University of Alberta, Edmonton, 335 p.

Mortensen, P.S. and Jones, B.
1986: The role of contemporaneous faulting on Late Silurian sedimentation in the eastern M'Clintock Basin, Prince of Wales Island, Arctic Canada; Canadian Journal of Earth Sciences, v. 23, p. 1401-1411.

National Research Council Permafrost Subcommittee
1988: Glossary of permafrost and related ground-ice terms; National Research Council of Canada, Technical Memorandum 142, 156 p.

Netterville, J.A., Dyke, A.S., and Thomas, R.D.
1976: Surficial geology and geomorphology, Somerset, northern Prince of Wales and adjacent islands; Geological Survey of Canada, Open File 357, scale 1:125 000.

Netterville, J.A., Dyke, A.S., Thomas, R.D., and Drabinsky, K.A.
1976: Terrain inventory and Quaternary geology, Somerset, Prince of Wales, and adjacent islands; in Report of Activities, Part A, Geological Survey of Canada, Paper 76-1A, p. 145-154.

Nixon, F.M.
1988: Till sampling program and presentation of physical and geochemical data from western Victoria Island, Northwest Territories; Geological Survey of Canada, Paper 88-15, 36 p.

Okulitch, A.V., Packard, J.J., and Zolnai, A.I.
1986: Evolution of the Boothia Uplift; Canadian Journal of Earth Sciences, v. 23, p. 350-358.

Ovenden, L.
1988: Holocene proxy-climate data from the Canadian Arctic; Geological Survey of Canada, Paper 88-22, 11 p.

Paterson, W.S.B.
1981: The Physics of Glaciers; Pergamon Press Ltd., Headington Hill Hall, Oxford, 380 p.

Pelletier, B.R.
1966: Development of submarine physiography in the Canadian Arctic and its relation to crustal movements; Royal Society of Canada, Special Publication 9, p. 77-101.

Prest, V.K.
1957: Pleistocene geology and surficial deposits; in Geology and Economic Minerals of Canada, C.H. Stockwell, ed.; Geological Survey of Canada, Economic Geology Report 1, p. 443-495.
1969: Retreat of Wisconsin and Recent ice in North America; Geological Survey of Canada, Map 1257A, scale 1:5 000 000.

Prest, V.K., Grant, D.R., and Rampton, V.N.
1968: Glacial Map of Canada; Geological Survey of Canada, Map 1253A, scale 1:5 000 000.

Ricketts, B.D.
1987: Evolution of the eastern Arctic landscape and the Tertiary-Quaternary transition, Queen Elizabeth Islands (abstract); in Programme with Abstracts, International Union for Quaternary Research, XII International Congress, p. 252.

Russell, R.H. and Edmonds, E.J.
1977: Caribou and muskoxen habitat – Prince of Wales and Somerset islands and Boothia Peninsula, preliminary report; Indian and Northern Affairs Canada, Environmental-Social Program, Northern Pipelines, ESCOM no. A1-11, 83 p.

Shaw, J. and Sharpe, D.R.
1987: Drumlin formation by subglacial meltwater erosion; Canadian Journal of Earth Sciences, v. 24, p. 2316-2322.

Sugden, D.E.
1977: Reconstruction of the morphology, dynamics, and thermal characteristics of the Laurentide Ice Sheet at its maximum; Arctic and Alpine Research, v. 9, p. 21-47.

Taylor, A.E. and Judge, A.S.
1974: Canadian geotechnical data collection, northern wells, 1955 to February 1974; Earth Physics Branch, Geothermal Series, no. 1, 171 p.

Taylor, R.B.
1978: The occurrence of grounded ice ridges and shore ice piling along the northern coast of Somerset Island, N.W.T.; Arctic, v. 31, p. 133-149.

Taylor, R.B. (cont.)
1980: Coastal environments along the northern shore of Somerset Island, District of Franklin; in The Coastline of Canada, ed. S.B. McCann; Geological Survey of Canada, Paper 80-10, p. 239-250.

Thorsteinsson, R. and Mayr, U.
1987: The sedimentary rocks of Devon Island; Geological Survey of Canada, Memoir 411, 181 p.

Tozer, T. and Thorsteinsson, R.
1964: Western Queen Elizabeth Islands, Arctic Archipelago; Geological Survey of Canada, Memoir 332, 242 p.

Trettin, H.
in press: Middle and Late Tertiary tectonic and physiographic developments; in Chapter 18 of Innuitian Orogen and Arctic Platform; ed. H.P. Trettin; Geological Survey of Canada, Geology of Canada, no. 3.

Washburn, A.L.
1980: Geocryology, A Survey of Periglacial Processes and Environments; Halsted Press, John Wiley and Sons, Inc., New York, 406 p.
1983: What is a palsa?; in Mesoformen des reliefs im heutigen periglazialraum, ed. H. Poser and E. Schunke; Gottingen, Abhandlungen der Akademie der Wissenschaften in Gottingen, Mathematisch – Physikalische Klasse, Dritte Folge Nr. 35, p. 34-47.

Woo,V. and Zoltai, S.C.
1977: Reconnaissance of the soils and vegetation of Somerset and Prince of Wales islands, Northwest Territories; Fisheries and Environment Canada, Information Report NORX-186, 127 p.

APPENDIX 1

Sedimentological, lithological, and environmental characteristics of till, Prince of Wales Island

Sample	Z[1]	East	North	Lit Fac	%S	%$	%C	%Pc	%Ss	%Ls	%Veg	%B	Er	Sto	Patterned Ground	Drain	Cell Rel	FT (cm)	%Ca	%Do	%Car
84DCA0003	14	528200	7979700	C[2]	34	55	11	1	7	92	5			Sli[4]	Net,S[5]	Good[6]	3	38	31	27	58
84DCA0004	14	528000	7981300	C	41	47	12	4	3	93	6		Pg[3]	Mod	Net,Ns	Good	3	32	34	26	60
84DCA0005	14	527900	7983500	C	30	58	12	4	0	96	5		Pg	Mod	Net,Ns	Good	2	42	20	31	51
84DCA0007	14	529200	7986200	C	29	49	22	2	4	94	5		Pg	Mod	Net,Ns	Good	3	50	21	30	51
84DCA0010	14	531600	7986900	C	74	26	0	4	0	96	5			Mod		Good		52	33	23	56
84DCA0012	14	532100	7983900	C	35	49	16	0	0	100	1					Good			51	20	71
84DCA0015	14	530500	7974000	C	76	61	13	0	0	100	5		Pg	Mod	Net,Ns	Good		21	21	26	47
84DCA0016	14	535500	7972700	C	24	61	15	1	1	98	5		Pg	Mod	Net,Ns	Good		40	36	28	64
84DCA0017	14	535300	7971000	C	22	71	7	1	0	99	3			Mod	Net,Ns	Good	2	33	23	28	51
84DCA0019	14	538700	7974000	C	45	44	11	2	0	98	1			Mod	Net,Ns	Good		55	46	10	56
84DCA0020	14	537700	7974100	C	29	64	7	2	0	98	2			Mod	Net,Ns	Good	2	33	27	23	50
84DCA0021	14	537000	7975500	C	38	54	8	0	0	100	2			Mod	Net,Ns	Good	2	40	35	9	44
84DCA0022	14	536000	7976000	C	37	50	13	0	3	97	1			Sli	Stripe,Ns	Good		48	39	22	61
84DCA0023	14	535100	7976800	C	34	54	12	3	2	95	1			Mod	DesPolys	Good		50	25	23	48
84DCA0024	14	534100	7977100	C	22	62	16	2	4	94	1			Mod	Net,Ns	Good			24	24	48
84DCA0025	14	534000	7977100	C	41	47	12	2	0	98	1		Pg	Mod	Net,Ns	Good			43	23	66
84DCA0027	14	528600	7986600	C				2	1	97	15		Pg	Mod	Net,Ns	Good			33	25	58
84DCA0029	14	528000	7985800	C	36	48	16	4	0	96	10		Pg	Mod	Net,Ns	Good		56	39	23	62
84DCA0030	14	527100	7984600	C	50	43	7	2	0	98	5		Pg	Mod	Net,Ns	Good	2	32	34	23	57
84DCA0031	14	526900	7983900	C	64	36	0	0	0	100	7		Pg	Mod	Net,Ns	Good	4	38	41	21	62
84DCA0032	14	528600	7984400	C	40	54	6	1	1	98	7		Pg	Mod	Net,Ns	Good	1	50	33	24	57
84DCA0033	14	530100	7983500	C	42	53	5	4	2	94	7		Pg	Mod	Net,Ns	Good	2	50	27	24	51
84DCA0034	14	531800	7982200	C	10	73	17	6	2	92	3		Pg	Mod		Good		55	29	24	53
84DCA0035	14	525900	7984700	C	28	69	3	4	2	94	10		Pg	Mod	Net,Ns	Good	2	37	22	26	48
84DCA0036	14	525000	7984100	C	36	53	11	0	1	99	5		Pg	Mod	Net,Ns	Good	3	36	39	23	62
84DCA0037	14	524800	7982800	C				3	5	92				Mod					31	26	57
84DCA0041	14	523400	7981900	C	36	55	9	1	1	98	2		Pg	Mod	Net,Ns	Good		40	28	26	54
84DCA0043	14	521600	7979900	C	41	52	7	2	2	96	1		Pg	Mod	Net,Ns	Good		46	34	24	58
84DCA0044	14	520100	7981300	C	36	51	13	1	6	93	2		Pg	Mod	Net,Ns	Good		48	41	21	62
84DCA0045	14	520200	7984100	C	56	43	1	1	1	98	3		Pg	Mod	Net,Ns	Good		32	34	24	58
84DCA0046	14	521800	7983000	C	48	50	2	1	0	99	3		Pg	Mod	Net,Ns	Good		37	37	21	58
84DCA0047	14	523800	7984400	C	34	56	10	1	0	99	1		Pg	Mod		Good		55	31	25	56
84DCA0048	14	524600	7986100	C	75	25	0	1	1	98	5			Mod	Net,Ns	Good		40	29	26	55
84DCA0049	14	526000	7986000	C	33	74	3	0	0	100	3		Pg	Mod		Good		47	30	23	53
84DCA0051	14	528000	7986000	C				1	0	99				Mod					32	24	56
84DCA0055	14	527000	7988200	C	36	57	7	1	1	98	7		Pg	Mod	Net,Ns	Good	3	48	32	24	56
84DCA0056	14	525500	7988400	C	35	51	14	3	2	95	7			Mod	Net,Ns	Good	4		34	24	58
84DCA0057	14	524200	7988100	C	43	51	6	1	0	99	7		Pg	Mod	Net,Ns	Good		47	30	26	56
84DCA0058	14	525000	7989000	C	43	51	6	4	0	96	7		Pg	Mod	Net,Ns	Good	4		31	27	58
84DCA0059	14	525800	7990900	C	46	51	3	1	0	99	5		Pg	Mod	Stripe,Ns	Good		42	34	24	58
84DCA0060	14	525700	7992600	C	58	34	8	2	0	98	3		Pg	Mod	Net,Ns	Good			41	21	62
84DCA0061	14	525800	7993900	C	35	48	17	1	3	96	3		Pg	Mod	Net,Ns	Good	4		39	19	58

Appendix 1 (cont.)

Sample	Z[1]	East	North	Lit Fac	%S	%$	%C	%Pc	%Ss	%Ls	%Veg	%B	Er	Sto	Patterned Ground	Drain	Cell Rel	FT (cm)	%Ca	%Do	%Car
84DCA0062	14	526500	7990400	C	58	35	7	1	5	94	3		Pg	Mod	Net,Ns	Good			39	26	65
84DCA0064	14	529300	7988800	C	67	30	3	2	0	98	7		Pg	Mod	Net,Ns	Good	3		32	23	55
84DCA0065	14	530300	7981200	C	50	49	1	1	4	95	1			Mod	DesPolys	Mod	0	29	23	31	54
84DCA0066	14	531900	7977300	C	47	45	8	2	1	97	1		Pg	Mod		Good		36	27	27	54
84DCA0067	14	533800	7978400	C	37	43	20	2	3	95	1		Pg	Mod	Net,Ns	Good	1		43	16	59
84DCA0068	14	534300	7980700	C	18	59	23	1	2	97	1			Mod	Net,Ns	Good	3		25	23	48
84DCA0069	14	535000	7983300	C	40	45	15	2	5	93	1		Pg	Mod	Net,Ns	Good	4	31	39	20	59
84DCA0070	14	534900	7984200	C	38	43	19	2	1	97	5		Pg	Mod	Net,Ns	Good		41	42	20	62
84DCA0071	14	533000	7982500	C	36	45	19	1	0	99	1		Pg	Mod	DesPolys	Good	1		34	20	54
84DCA0072	14	531900	7982500	C	14	43	43	6	1	93	3		Pg	Mod	Net,Ns	Good	1	35	32	16	48
84DCA0077	14	549100	8015000	C	35	54	11	3	0	97	2		Pg	Mod		Good			31	21	52
84DCA0078	14	548600	8017600	C	34	53	13	2	2	96	4		Pg	Mod		Good			32	22	54
84DCA0079	14	548600	8017000	C	34	56	10	1	0	99	5		Pg	Mod	Net,Ns	Good	3	19	31	22	53
84DCA0080	14	550200	8017500	C	40	57	3	4	3	93	40		Pg,Rs	Mod	DesPolys	Poor		39	17	25	42
84DCA0081	14	551200	8018100	MCC	50	42	8	9	8	83	30		Pg,Rs	Mod		Poor		61	25	22	47
84DCA0082	14	551500	8019200	MCC	44	43	13	8	7	85	7		Pg	Mod	Net,Ns	Poor		62	26	21	47
84DCA0083	14	551800	8020000	MCC	38	47	15	6	8	86	15		Pg,Rs	Mod	Net,Ns	Good	1		25	21	46
84DCA0084	14	552100	8019600	C	38	48	14	7	1	92	15		Pg,Rs	Mod	DesPolys	Good	1		28	20	48
84DCA0085	14	552000	8018200	C	56	38	6	5	3	92	30			Mod		Good		73	21	23	44
84DCA0086	14	552300	8017500	MCC	54	42	4	8	9	83	40		Pg,Rs	Mod	DesPolys	Good	0		18	23	41
84DCA0087	14	552100	8016600	C	12	64	24	2	6	92	20		Pg,Rs	Mod	Net,Ns	Good	1	53	22	20	42
84DCA0088	14	550200	8015700	C	36	53	11	0	2	98	3		Pg,Rs	Mod		Good			32	22	54
84DCA0090	14	550900	8015200	C				1	1	98	0		Pg,Rs	Mod		Good			42	15	57
84DCA0091	14	550800	8015900	MCC				6	6	88	50		Pg	Mod	DesPolys	Poor	0	69	29	21	50
84DCA0092	14	552600	8015600	C				0	0	100	0		Pg,Rs	Mod		Good			45	17	62
84DCA0093	14	553700	8015000	MCC	36	51	13	5	7	88	20		Pg,Rs	Mod	Net,Ns	Good	2		20	23	43
84DCA0095	14	555700	8015500	MCC	45	42	13	7	12	81	20		Pg,Rs	Mod	Net,Ns	Good	0	47	25	21	46
84DCA0096	14	556500	8015000	MCC	18	57	25	10	5	85	30		Pg,Rs	Mod		Good		42	22	21	43
84DCA0097	14	557800	8014700	C	20	56	24	2	2	96	15		Pg	Sli	Net,Ns	Good		39	23	21	44
84DCA0099	14	559500	8014000	MCC	36	47	17	1	12	87	30		Pg,Rs	Mod	Net,Ns	Good	1	46	15	22	37
84DCA0100	14	560400	8014300	MCC	37	48	15	7	10	83	15		Pg,Rs	Mod		Good			19	25	44
84DCA0101	14	561500	8015200	C	41	42	17	2	3	95	20		Pg,Rs	Mod		Good		42	13	23	36
84DCA0102	14	563700	8016500	MCC	56	40	4	3	8	89	20		Pg,Rs	Mod	Net,Ns	Good		44	7	26	33
84DCA0103	14	562000	8017100	C	40	46	14	3	3	94	70		Pg,Rs	Mod	DesPolys	Mod	0	39	13	26	39
84DCA0104	14	560800	8016900	MCC	40	46	14	10	10	80	10		Pg,Rs	Mod		Good		72	15	22	37
84DCA0105	14	558500	8017100	MCC	45	47	8	5	11	84	60		Pg,Rs	Mod	Net,Ns	Mod	2	53	16	22	38
84DCA0106	14	556500	8017000	MCC	37	45	18	11	7	82	55		Pg,Rs	Mod		Mod			14	25	39
84DCA0107	14	554400	8016200	MCC	43	43	14	11	3	86	10		Pg,Rs	Mod	Net,Ns	Good	2	39	22	22	44
84DCA0108	14	546900	8016000	C	61	33	6	1	0	99	0		Pg,Rs	Mod	Net,Ns	Good	2		35	25	60
84DCA0109	14	543600	8013400	C	37	48	15	7	3	90	1		Pg,Rs	Mod	DesPolys	Poor	0	44	25	23	48
84DCA0110	14	541800	8012400	C	35	41	24	3	1	96	10		Pg,Rs	Mod	Circle,S	Mod		34	38	17	55
84DCA0111	14	541000	8012000	C	35	47	18	2	0	98	1		Pg,Rs	Mod	DesPolys	Poor		60	32	19	51
84DCA0112	14	539900	8010700	C	62	32	6	0	0	100	1		Pg,Rs	Mod	DesPolys	Poor	0		40	18	58
84DCA0114	14	538100	8018000	C	41	45	14	3	1	96	5		Pg,Rs	Sli	Net,Ns	Good	2	37	19	31	50
84DCA0115	14	540200	8018500	C	54	33	13	7	0	93	10		Pg	Mod	Net,PS	Good			28	21	49

Sample	Z[1]	East	North	Lit Fac	%S	%$	%C	%Pc	%Ss	%Ls	%Veg	%B	Er	Sto	Patterned Ground	Drain	Cell Rel	FT (cm)	%Ca	%Do	%Car
84DCA0116	14	542500	8018800	C	39	41	20	7	0	93	2		Pg,Rs	Mod	Net,PS	Good	1	42	26	21	47
84DCA0117	14	544000	8018700	C	30	46	24	4	0	96	10		Pg,Rs	Mod	DesPolys	Good		41	26	21	47
84DCA0118	14	547600	8018200	C	49	47	4	6	3	91	15		Pg,Rs	Sli		Good		60	16	27	43
84DCA0119	14	546200	8014400	C	45	28	17	4	4	92	1		Pg,Rs	Mod	Net,Ns	Poor	2	40	30	20	50
84DCA0120	14	537000	8003700	C	28	48	24	1	0	99	10		Pg,Rs	Mod	Net,Ns	Mod	1	46	30	21	51
84DCA0121	14	537900	8001500	C	28	50	22	3	1	96	10		Pg,Rs	Mod	Net,S	Good	5	43	32	22	54
84DCA0122	14	538100	7998500	C	39	43	18	0	0	100	12		Pg,Rs	Mod	Net,Ns	Good			35	22	57
84DCA0124	14	542600	7998600	C	18	62	20	5	1	94	10		Pg,Rs	Mod	Net,Ns	Good		42	36	21	57
84DCA0125	14	546100	7999000	C	32	49	19	1	1	98	30		Pg,Rs	Mod	DesPolys	Good		42	28	23	51
84DCA0126	14	546500	8001400	C	45	40	15	6	1	93	20		Pg,Rs	Mod	DesPolys	Good			24	21	45
84DCA0127	14	547100	8003300	C	38	44	18	1	2	97	1		Pg	Mod	Net,Ns	Good	5		40	18	58
84DCA0128	14	551600	8006300	MCC	49	38	13	4	15	81	22		Pg,Rs	Mod	Net,Ns	Good			21	24	45
84DCA0129	14	551300	8011100	C	29	47	24	2	5	93	0		Pg,Rs	Mod		Good		30	31	19	50
84DCA0130	14	550800	8014000	MC	39	42	19	9	14	77	3		Pg	Mod	Net,Ns	Good		37	27	21	48
84DCA0134	14	556100	8018600	MC	32	46	22	6	18	76	10		Pg,Rs	Mod	Net,Ns	Good	4	59	15	21	36
84DCA0135	14	555500	8019400	MCC	33	49	18	6	8	86	22		Pg,Rs	Mod	Net,Ns	Good	1	53	17	22	39
84DCA0136	14	555600	8020400	MC	19	62	19	3	21	76	20		Pg,Rs	Sli	Stripe,Ns	Good		63	11	23	34
84DCA0137	14	555700	8021600	M	45	32	13	2	33	65	30		Pg,Rs	Mod	Net,Ns	Mod	2	56	17	23	40
84DCA0138	14	555300	8022400	MC	38	45	17	5	17	78	30		Pg,Rs	Mod	Net,Ns	Mod	2		22	19	41
84DCA0142	14	570500	7994200	MCC	36	50	14	2	12	86	50		Pg,C,Rs	Mod	DesPolys	Good	0	50	19	26	45
84DCA0145	14	568000	7992100	M	51	41	8	1	56	43	20		Pg,C	Mod	Net,Ns	Good	1		12	24	36
84DCA0148	14	564600	7991500	MC	41	42	17	2	23	75	60		Pg,C	Mod	Net,Ns	Good	2	58	28	22	50
84DCA0150	14	562100	7990500	MCC	36	43	21	4	9	87	5		Pg,Rs,C	Mod		Mod		61	35	21	56
84DCA0151	14	562700	7991500	MCC	62	29	9	1	13	86	5		Pg.Rs,C	Mod	Net,Ns	Good			31	23	54
84DCA0152	14	562700	7993300	MCC	32	47	21	2	10	88	10		Pg,Rs,C	Mod	Net,Ns	Good		38	33	21	54
84DCA0153	14	562300	7994600	C	33	47	20	0	10	90	20		Pg	Mod	DesPolys	Good			29	23	52
84DCA0154	14	564800	7996000	MCC	36	49	15	5	10	85	15		Pg	Sli		Good		37	28	23	51
84DCA0155	14	567800	7996000	MCC	31	49	20	2	9	89	30		Pg,C	Mod	Net,Ns	Good		65	31	23	54
84DCA0156	14	573400	7997000	MCC	40	45	15	0	17	83	80		Pg,C	Mod	Net,Ns	Good	2	69	19	25	44
84DCA0157	14	575800	7997200	M	45	42	13	22	21	57	20		Pg,Rs,C	Mod		Good			7	28	35
84DCA0158	14	571000	7992500	MC	45	40	15	3	20	77	30		Pg,C	Mod	Net,Ns	Good	1		15	25	40
84DCA0159	14	570200	7991500	MCC	33	43	24	2	9	89	2		Pg,C	Mod	Net,Ns	Good		60	43	20	63
84DCA0160	14	569400	7990500	MC	39	42	19	3	19	78	15		Pg,C	Mod	Net,Ns	Good	1		35	19	54
84DCA0162	14	571500	7988700	M	54	42	4	2	36	62	10		Pg,C	Mod		Mod			16	25	41
84DCA0164	14	516400	7987400	M	39	48	13	4	59	37	90		Pg,C	Sli		Poor		51	4	29	33
84DCA0165	14	570300	7984200	M	54	40	6	6	53	41	90		Pg,C	Sli	DesPolys	Poor		43	6	28	34
84DCA0166	14	572000	7982800	MC	39	46	15	2	19	79	85		C	Sli	DesPolys	Poor	1	73	12	28	40
84DCA0168	14	573200	7981000	M	41	49	10	8	39	53	90		C	Sli	DesPolys	Poor		50	4	28	32
84DCA0169	14	574700	7981300	M	48	39	13	3	61	36	90		C	Sli	Net,Ns	Poor		43	7	27	34
84DCA0170	14	575600	7983900	M	48	43	9	3	37	60	90		C	Sli	DesPolys	Poor	0	43	6	29	35
84DCA0171	14	573900	7984800	M	36	50	14	1	37	62	90			Sli		Poor			6	29	35
84DCA0172	14	573700	7986400	M	43	46	11	3	41	56	90		C	Sli	Net,Ns	Mod		63	3	26	29
84DCA0173	14	574000	7989600	MSS	40	49	11	1	82	17	80			Sli	DesPolys	Mod	0	52	4	26	30
84DCA0175	14	574800	7991200	MCC	34	46	20	2	18	80	10		Pg,C	Mod	Net,Ns	Good			28	21	49
84DCA0176	14	572900	7992700	C	35	43	22	1	8	91	10		Pg,C	Mod	Net,Ns	Good		56	27	22	49

Appendix 1 (cont.)

Sample	Z[1]	East	North	Lit Fac	%S	%$	%C	%Pc	%Ss	%Ls	%Veg	%B	Er	Sto	Patterned Ground	Drain	Cell Rel	FT (cm)	%Ca	%Do	%Car
84DCA0177	14	571000	7996000	MCC	27	46	27	6	9	85	7		Pg,C	Sli		Good			37	20	57
84DCA0178	14	570900	7997800	C	31	44	24	1	2	97	10		Pg,C	Mod	Net,Ns	Good	1	59	36	19	55
84DCA0179	14	570500	8001500	MCC	30	46	24	1	13	86	12		Pg,C	Sli	DesPolys	Good		64	32	21	53
84DCA0180	14	570300	8004200	MCC	48	32	20	5	14	81	10		Pg,C	Mod	Net,Ns	Good			35	17	52
84DCA0181	14	569500	8009500	S	44	46	10	2	96	2	85		Sli	DesPolys	Good			66	1	17	18
84DCA0182	14	565200	8011200	MSS	45	46	9	2	88	10	90		C	Sli	Net,Ns	Mod	3	71	5	21	26
84DCA0183	14	557000	8012200	M	41	43	16	2	34	64	30		Pg,C	Mod	Net,Ns	Good		53	13	26	39
84DCA0184	14	558100	8010000	M	44	48	8	4	63	33	90		Pg,C	Sli	DesPolys	Poor		63	2	20	22
84DCA0185	14	560400	8006700	M	36	50	14	6	39	55	100			Sli	Net,Ns	Poor	4	54	5	25	30
84DCA0186	14	561000	8004500	M	39	47	14	2	65	33	95		Pg,C	Mod	Net,Ns	Mod		66	7	24	31
84DCA0187	14	563300	8001500	M	30	53	17	4	34	62	80		Sli	Net,Ns	Poor			62	7	22	29
84DCA0189	14	565800	7998000	C	34	46	20	2	1	97	10		Pg,C	Mod	Net,Ns	Good			32	1	33
84DCA0193	14	576500	8006600	M	52	41	7	12	28	60	2		Pg,C	Mod	DesPolys	Good		71	6	23	29
84DCA0194	14	581000	8004500	MC	32	48	20	7	17	76	1		Pg,C	Mod	Net,Ns	Good	0	47	23	22	45
84DCA0195	14	582700	8003300	MC	33	48	19	3	19	78	30		Pg,C	Sli	DesPolys	Mod	0	56	18	22	40
84DCA0197	14	581800	8000600	M	19	63	18	26	13	61	80			Sli	DesPolys	Mod	0	58	7	22	29
84DCA0198	14	580300	7900000	MC	48	44	8	6	17	76	40		Pg,C	Mod	Stripe,Ns	Mod		58	19	24	43
84DCA0199	14	577100	7993600	MC	48	43	9	0	27	73	20		Pg,C	Mod	Net,Ns	Good	2	40	15	26	41
84DCA0200	14	579700	7991600	MC	41	44	15	4	17	79	10		Pg,C	Mod	DesPolys	Good	0		30	22	52
84DCA0203	14	586100	7993500	MCC	49	44	7	0	19	81	20		Pg,C	Mod	Stripe,Ns	Good		36	9	27	36
84DCA0204	14	585600	7991000	M	51	39	10	23	27	50	10		Pg,C	Mod		Good			9	27	36
84DCA0205	14	585100	7989000	MPP	69	23	8	85	15	0	40		Pg,C	Mod	DesPolys	Mod		50	4	23	27
84DCA0206	14	583000	7990300	M	41	52	7	2	29	69	40		Pg,C	Mod		Good			0	26	26
84DCA0212	14	557100	7953800	C	35	45	20	2	0	97	1		Pg,Rs	Mod	Net,Ns	Good	2		21	20	41
84DCA0214	14	557800	7956500	MC	38	47	15	0	30	70	3		Pg,Rs	Mod	Net,Ns	Mod	1	49	25	25	50
84DCA0215	14	560300	7958200	MCC	37	44	19	2	14	83	4		Pg,Rs	Mod	Net,Ns	Mod		57	23	24	47
84DCA0216	14	562700	7961900	C	33	48	19	0	1	99	6		Pg,Rs	Mod	DesPolys	Mod		37	20	26	46
84DCA0217	14	566000	7964000	MCC	39	45	16	6	8	86	8		Pg,Rs	Mod		Good			25	24	49
84DCA0218	14	567000	7966200	C	38	44	18	7	2	91	12		Pg,Rs	Mod	DesPolys	Good		59	24	23	47
84DCA0219	14	567900	7968900	C	36	48	16	4	1	95	15		Pg,Rs,C	Mod	DesPolys	Good			21	26	47
84DCA0220	14	569400	7975500	MCC	44	40	16	3	16	81	30		Pg,Rs	Mod	DesPolys	Mod	0	65	22	25	47
84DCA0221	14	563600	7975000	C	45	42	13	4	4	92	45		Pg,Rs	Mod	DesPolys	Good		54	15	24	39
84DCA0222	14	562100	7971500	MCC	36	42	22	10	2	88	5		Pg,Rs	Mod	Net,Ns	Good	1		40	20	60
84DCA0223	14	561500	7969100	MCC	35	50	15	3	10	87	1		Pg,Rs	Mod	Net,Ns	Good			26	28	54
84DCA0224	14	560300	7969600	MCC	35	43	22	2	16	82	15		Pg,Rs	Mod	Net,Ns	Good	1	50	41	21	62
84DCA0225	14	559100	7968100	C	38	38	24	1	2	97	2		Pg,Rs	Mod	Net,Ns	Good	2		42	15	57
84DCA0226	14	557700	7963100	MCC	37	46	17	8	5	87	1		Pg,Rs	Mod	DesPolys	Mod	0		26	23	49
84DCA0228	14	554800	7957700	C	35	45	20	0	9	91	1		Pg,Rs	Mod	DesPolys	Good	0	49	30	22	52
84DCA0233	14	556600	7952300	MCC	52	23	25	2	9	89	2		Pg,Rs	Mod	Net,Ns	Good	1	32	42	19	61
84DCA0234	14	553700	7951500	MCC	39	49	12	3	12	85	1		Pg,Rs	Mod	DesPolys	Mod	0	47	23	26	49
84DCA0235	14	551000	7951800	MCC	45	44	11	4	7	89	1		Pg,Rs	Mod	DesPolys	Mod	0	48	14	29	43
84DCA0237	14	550500	7952900	C	28	50	22	0	10	90	1		Pg,Rs	Mod	DesPolys	Good		52	23	27	50
84DCA0238	14	550500	7953800	MCC	18	61	21	9	5	86	2		Pg,Rs	Sli	DesPolys	Mod		43	19	27	46
84DCA0239	14	551700	7956000	MCC	34	47	19	4	9	87	1		Pg,Rs	Mod	DesPolys	Good		51	23	25	48
84DCA0240	14	552100	7954500	C	50	36	14	3	3	94	2		Pg,Rs	Mod		Good			30	24	54

Sample	Z[1]	East	North	Lit Fac	%S	%$	%C	%Pc	%Ss	%Ls	%Veg	%B	Er	Sto	Patterned Ground	Drain	Cell Rel	FT (cm)	%Ca	%Do	%Car
84DCA0241	14	553000	7953000	C	43	38	19	1	6	93	1		Pg,Rs	Mod		Good			37	21	58
84DCA0242	14	555100	7954600	C	36	45	19	1	4	95	1		Pg,Rs	Mod	Net,PS	Good	1	58	30	22	52
84DCA0243	14	555100	7953200	C	35	41	24	1	0	99	1		Pg,Rs	Mod	Net,PS	Good	2		49	21	70
84DCA0246	14	555100	7961800	MC	34	47	19	17	4	79	1		Pg,Rs	Mod	DesPolys	Mod		55	22	23	45
84DCA0247	14	555700	7965800	MCC	30	51	19	4	12	84	1		Pg,Rs	Sli	DesPolys	Mod	0	53	21	25	46
84DCA0248	14	555100	7968500	C	60	37	3	3	1	96	1		Pg,Rs	Mod	Net,PS	Good	2		36	24	60
84DCA0249	14	552600	7970000	C	32	49	19	1	2	97	5		Pg,Rs	Mod	DesPolys	Good	0	44	28	23	51
84DCA0250	14	553000	7972200	C	43	41	16	7	2	91	2		Pg,Rs	Mod	Net,PS	Mod	2	53	30	21	51
84DCA0251	14	551800	7975800	C	58	31	11	0	0	100	1		Pg,Rs	Mod	Net,PS	Good	4		41	19	60
84DCA0252	14	549800	7974000	MCC	43	34	23	6	5	89	1		Pg,Rs	Mod	Net,PS	Good	5	26	32	18	50
84DCA0253	14	549800	7970700	MCC	46	37	17	5	8	87	1		Pg,Rs	Mod	Net,PS	Poor	3	59	26	20	46
84DCA0254	14	551000	7964000	C	36	40	24	6	2	92	2		Pg,Rs	Mod	DesPolys	Mod	0	43	27	19	46
84DCA0255	14	552000	7959800	C	36	48	16	5	4	91	1		Pg,Rs	Mod	DesPolys	Mod	0	46	28	23	51
84DCA0256	14	549600	7954400	C	35	45	20	4	2	94	1		Pg,Rs	Ver	Stripe,S	Poor		55	25	25	50
84DCA0257	14	548000	7955400	C	38	43	19	3	0	97	2		Pg,Rs	Mod	Net,Ns	Mod		57	30	24	54
84DCA0258	14	544400	7957000	C	62	31	7	5	3	92	17		Pg,Rs	Mod	Net,S	Mod	1	69	17	29	46
84DCA0259	14	545300	7960200	C	30	49	21	3	1	96	10		Pg,Rs	Mod	Net,Ns	Poor	5		24	26	50
84DCA0260	14	544500	7963500	MCC	31	43	26	12	0	88	12		Pg,Rs	Mod	Net,PS	Mod		48	18	22	40
84DCA0261	14	542000	7963800	C	20	55	25	3	1	96	20		Pg	Mod	DesPolys	Mod	0	51	19	24	43
84DCA0262	14	540300	7963000	C	28	52	20	4	3	93	5		Pg,Rs	Mod	Net,Ns	Mod	5	43	24	23	47
84DCA0263	14	539500	7960300	C	16	68	16	4	0	96	40		Pg,Rs	Mod	Net,Ns	Poor		49	11	28	39
84DCA0264	14	539500	7957100	C	40	41	19	0	1	99	10		Pg,Rs	Mod	Net,Ns	Good	1		38	21	59
84DCA0265	14	539300	7954800	C	38	43	19	0	0	100	2		Pg	Mod	DesPolys	Mod	0	37	39	21	60
84DCA0403	14	506000	8211200	MSS	45			2	79	19	5			Sli		Poor		42	11	19	30
84DCA0407	14	521000	8215000	M	43			4	25	66			Rs,C	Mod		Good			10	24	34
84DCA0408	14	521200	8214200		39								Rs,C	Mod		Good					0
84DCA0410	14	520000	8213800	S	37			0	99	1	10		C	Ver		Good			3	18	21
84DCA0411	14	519800	8213600	S	37			0	100	0	25		C	Ver		Good			7	19	26
84DCA0412	14	519500	8213200	MSS	38			0	85	15	40		C	Ver		Good			11	19	30
84DCA0413	14	518700	8213000	S	36			0	100	0	20		C	Ver		Good			3	21	24
84DCA0414	14	518000	8213000	MSS	38			0	86	14			C	Ver		Good			6	17	23
84DCA0415	14	517000	8213100	S	38			0	97	3	20		C	Ver		Good			3	15	18
84DCA0416	14	516200	8213200	MSS	37			1	87	12	1		C	Ver		Good			8	15	23
84DCA0417	14	515600	8213200	MS	36			1	76	23	1		C	Ver		Good			5	16	21
84DCA0421	14	512500	8213500	MCC	40			3	19	78	20		Rs	Ver		Good			13	21	34
84DCA0422	14	514900	8211500	C	29			0	0	100	1		Rs	Mod		Good			10	11	21
84DCA0423	14	514800	8210700	C	29			0	0	100	1		Rs	Ver		Good			18	16	34
84DCA0424	14	515300	8209500	S	30			0	98	2	1		C	Ver		Good			5	13	18
84DCA0425	14	512600	8207600	C	31			0	0	100	1			Ver		Good			9	17	26
84DCA0426	14	513300	8208000	C	33			0	0	100	1			Ver		Good			10	23	33
84DCA0427	14	511000	8207600	C	35			0	0	100	10			Mod		Good			7	26	33
84DCA0428	14	510800	8206000	C	35			0	0	100	10		Rs	Mod		Mod		52	15	14	29
84DCA0431	14	524000	8214800	S	38			0	91	9	10		C	Mod		Good			1	12	13
84DCA0432	14	522800	8214700	S	38			0	99	1	10		C	Ver		Good			4	16	20
84DCA0433	14	523400	8214300	S	37			0	100	0	10		C	Mod		Good		57	0	9	9

Appendix 1 (cont.)

Sample	Z'	East	North	Lit Fac	%S	%$	%C	%Pc	%Ss	%Ls	%Veg	%B	Er	Sto	Patterned Ground	Drain	Cell Rel	FT (cm)	%Ca	%Do	%Car
84DCA0434	14	522400	8214300	S	38			0	92	8	10		C	Mod		Good			3	15	18
84DCA0435	14	521700	8214200	S	37			0	96	4	10		C	Mod		Good			2	16	18
84DCA0436	14	521400	8215000	S	39			0	98	2	20		C	Mod		Mod			3	18	21
84DCA0437	14	524800	8216000	S	38			0	99	1	10		C	Ver		Good			1	13	14
84DCA0438	14	527600	8217000	S	44			1	98	1	10		C	Mod		Good			2	25	27
84DCA0439	14	528200	8216900	S	46			0	99	1	10		Pg	Ver		Good		58	1	13	14
84DCA0440	14	529000	8216800	MSS	52			1	81	18	10			Mod		Good			1	12	13
84DCA0441	14	528500	8217500	S	52			0	98	2	10			Mod		Good			2	16	18
84DCA0442	14	525200	8217300	S	45			0	98	2	10			Mod		Good			3	14	17
84DCA0443	14	524200	8217400	S	45			0	97	3	10		Pg,C	Ver		Good			1	14	15
84DCA0444	14	524800	8215000	S	39			.0	97	3	10		C	Mod		Good			3	18	21
84DCA0445	14	523700	8216400	S	42			0	100	0	10		C	Mod		Good			0	14	14
84DCA0446	14	523900	8216000	S	39			0	97	3	10		C	Mod		Good			3	21	24
84DCA0485	14	527400	8220000	S	49			1	96	3	5		C	Mod		Good			3	18	21
84DCA0486	14	528000	8219800	S	50			0	98	2	10		C	Mod		Mod			4	20	24
84DCA0487	14	528500	8219800	S	52			0	93	7	10		C	Mod		Mod			2	17	19
84DCA0488	14	529200	8220200	S	56			0	97	3	5		C	Mod		Good			2	17	19
84DCA0489	14	529000	8220700	S	55			0	96	4	5		C	Mod		Good			4	17	21
84DCA0490	14	528400	8220500	S	51			0	97	3	5		C	Mod		Good			1	16	17
84DCA0491	14	529500	8220800	S	64			0	99	1	5		C	Mod		Good			4	19	23
84DCA0492	14	529500	8221200	S	63			0	99	1	5		C	Mod		Good			2	21	23
84DCA0493	14	530300	8220800	S	67			1	96	3	5		C	Ver		Good			2	17	19
84DCA0494	14	530200	8221200	S	65			1	99	0	5		C	Ver		Good			1	18	19
84DCA0495	14	530700	8221100	S	70			0	98	2	5		C	Ver		Good			3	19	22
84DCA0496	14	539400	8222000	MSS	62			0	87	13	5		C	Ver		Good			1	20	21
84DCA0528	14	541300	8220900	MSS	80			1	88	11	5		C	Ver		Good			2	21	23
84DCA0529	14	541200	8220100	S 83					0 95	5	5		C	Ver		Good			1	27	28
84DCA0530	14	539800	8221300	MS	81			0	76	24	5		Pg,C	Ver		Good			6	15	21
84DCA0531	14	523000	8202400	S	73			3	93	4	40		C	Sli		Mod		68	1	7	8
84DCA0534	14	522800	8204900	MSS	70			3	89	8	10		C	Mod		Good			1	7	8
84DCA0535	14	522700	8205700	MSS	64			3	83	14	10		C	Mod		Good			2	11	13
84DCA0536	14	520200	8207200	S	47			0	97	3	5		C	Ver		Good			5	15	20
84DCA0537	14	521200	8208000	S	45			2	94	4	5		C	Ver		Good			1	11	12
84DCA0538	14	521400	8209700	S	44			0	100	0	30		C	Mod		Mod		53	1	15	16
84DCA0539	14	525400	8211100	MS	65			5	72	23	10		Pg,C	Ver		Mod			1	13	14
84DCA0540	14	526400	8208300	S	81			2	97	1	10		C	Ver		Good			0	7	7
84DCA0541	14	527300	8213800	M	47			5	56	39	10		Pg,C	Ver		Good			2	15	17
84DCA0542	14	528000	8215500	S	52			0	99	1	10		Rc,C	Ver		Good			1	11	12
84DCA0543	14	530600	8215600	MS	47			3	77	20	3		C	Ver		Good			1	12	13
84DCA0544	14	537000	8223100	MSS	45			5	80	15	10		C	Mod		Good			6	30	36
84DCA0545	14	535500	8221200	M	48			3	69	28	10		Pg,C	Mod		Good			5	28	33
84DCA0546	14	533600	8220500	M	85			10	40	50	10		Pg,C	Mod		Good		58	6	29	35
84DCA0547	14	527500	8212500	M	49			4	68	28	20		C	Ver		Good			2	15	17
84DCA0555	14	527500	8207000	S	83			1	93	6	80		C	Ver		Poor			1	8	9
84DCA0557	14	517400	8197800	S	46			2	95	3	10			Mod		Mod		54	2	13	15

Sample	Z[1]	East	North	Lit Fac	%S	%$	%C	%Pc	%Ss	%Ls	%Veg	%B	Er	Sto	Patterned Ground	Drain	Cell Rel	FT (cm)	%Ca	%Do	%Car
84DCA0559	14	513000	8196900	MCC	45			0	20	80	10			Mod		Good					0
84DCA0560	14	513600	8197500	M	44			0	36	64	30			Mod		Mod			5	12	17
84DCA0561	14	521700	8204400	S	62			0	100	0	3		C	Ver		Good			1	7	8
84DCA0562	14	518100	8205600	MSS	46			2	84	14	10		C	Mod		Mod		55	8	13	21
84DCA0563	14	518500	8206900	S	48			0	94	6	20		C	Ver		Mod		56	4	13	17
84DCA0564	14	516100	8207200	MC	40			0	29	71	10		Rs	Mod		Good		56	6	13	19
84DCA0566	14	516300	8204300	C	45			0	0	100	5			Mod		Good			3	15	18
84DCA0567	14	513700	8204800	C	35			1	2	97	10			Mod		Good		55	7	14	21
84DCA0568	14	513000	8202200	M	28			1	63	36	30		Pg,Rs	Mod		Mod		52	5	15	20
84DCA0569	14	515000	8202300	C	43			0	0	100	10		Rs	Mod		Good		50	11	13	24
84DCA0570	14	520200	8201000	MS	47			0	78	22	10		C	Mod		Good			1	9	10
84DCA0571	14	521000	8200500	M	49			0	38	62	10		Pg,C	Ver		Good		46	4	12	16
84DCA0582	14	491700	8198600	C	44			0	10	90	10			Mod		Good		57	23	17	40
84DCA0583	14	491300	8198800	C	42			0	0	100	10			Mod		Good		55	23	19	42
84DCA0584	14	490200	8199800	C	40			0	0	100	10			Mod		Good			23	19	42
84DCA0585	14	490700	8199100	C	41			0	0	100	10			Mod		Good			26	18	44
84DCA0586	14	491000	8198400	C	44			0	0	100	10			Mod		Good		57	26	15	41
84DCA0587	14	492300	8197700	C	46			0	0	100	10			Mod		Good			23	17	40
84DCA0589	14	489100	8200700	C	38			0	0	100	10			Mod		Mod		58	24	20	44
84DCA0590	14	493200	8203100	C	42			0	0	100	10		Pg	Mod		Good			19	36	55
84DCA0591	14	495300	8201200	C	39			0	0	100	5			Mod		Good			35	25	60
84DCA0592	14	492200	8194400	C	38			0	0	100	10			Mod		Good			22	23	45
84DCA0594	14	495100	8195700	C	53			0	0	100	20			Mod		Mod			28	29	57
84DCA0596	14	506900	8195800	C	51			0	0	100	10			Mod		Good		55	18	20	38
84DCA0597	14	502600	8200600	C	37			0	0	100	10			Mod		Good			28	13	41
84DCA0598	14	498000	8201500	C	37			0	0	100	10			Ver		Good			24	25	49
84DCA0599	14	497300	8202800	C	41			0	0	100	10			Mod		Good			33	19	52
84DCA0600	14	496100	8204500	C	43			0	0	100	20			Mod		Good			25	23	48
84DCA0601	14	494800	8198200	C	48			0	0	100	10			Mod		Good			24	24	48
84DCA0602	14	497300	8199500	C	45			1	0	99	5			Ver		Good		57	27	27	54
84DCA0603	14	500500	8198000	C	47			0	0	100	20			Ver		Good			19	30	49
84DCA0701	14	415700	8093300	C	54	33	13	0	0	100	3	1	Pg	Mod	Circle,PS				25	29	54
84DCA0708	14	418200	8086400	C	40	39	21	0	0	100	10	3	Pg	Mod	Circle,PS	Mod			21	34	55
84DCA0709	14	416000	8087400	C	40	36	23	0	0	100	10	1	Pg	Ver	Circle,PS	Good			16	42	58
84DCA0710	14	413200	8088600	C	67	24	9	0	0	100	10			Mod	Circle,Ns	Good			18	43	61
84DCA0712	14	407000	8093500	C	63	25	12	1	0	99	8	3	Pg	Mod	Circle,Ns	Good			15	55	70
84DCA0713	14	407500	8098500	C	50	28	22	0	0	100	3		Pg	Mod	Circle,WS	Poor			15	44	59
84DCA0714	14	404700	8096600	C	32	43	26	1	0	99	5	3		Mod	Circle,Ns	Mod			15	54	69
84DCA0715	14	402000	8092200	C	30	49	21	0	0	100	1			Mod	Stripe,Ns	Good			19	59	78
84DCA0720	14	419500	8081200	C	49	35	16	0	0	100	10	3	Pg	Mod	Circle,Ns	Good			25	35	60
84DCA0722	14	415200	8083000	C	17	54	29	0	0	100	3	1	Pg	Mod	Net,Ns	Good			7	16	23
84DCA0723	14	416500	8081100	C	40	45	15	0	0	100	5	1		Mod		Good			22	44	66
84DCA0724	14	419200	8077500	C	35	45	20	1	0	99	5	1		Mod	Circle,Ns	Good			16	50	66
84DCA0725	14	421900	8075200	C	34	42	25	0	0	100	20	1		Mod	Circle,Ns	Mod			26	26	52
84DCA0726	14	425000	8073500	C	40	36	24	0	0	100	5	1		Mod	Circle,Ns	Good			28	35	63

Appendix 1 (cont.)

Sample	Z[1]	East	North	Lit Fac	%S	%$	%C	%Pc	%Ss	%Ls	%Veg	%B	Er	Sto	Patterned Ground	Drain	Cell Rel	FT (cm)	%Ca	%Do	%Car
84DCA0728	14	423900	8079300	C	65	25	10	0	0	100	3	1		Mod	Circle,Ns	Mod			27	34	61
84DCA0729	14	404500	8090000	C	65	26	9	0	0	100	5	1		Ver	Circle,Ns	Good			24	42	66
84DCA0730	13	595400	8086700	C	45	40	15	2	0	98	1	5	Pg	Mod	Circle,S	Good	5		5	70	75
84DCA0731	13	591000	8083500		30	50	20				3	3	Pg	Mod	Circle,S	Poor			17	68	85
84DCA0732	13	589600	8082800	C	27	45	28	1	0	99	3	8	Pg	Mod	Circle,Ns	Good			15	60	75
84DCA0733	13	590700	8079000	C	21	54	25	0	0	100	10	20		Mod	Circle,S	Good			4	71	75
84DCA0734	13	593200	8077800	C	34	49	17	0	0	100	1	10	Pg	Mod	Circle,Ns	Good			14	70	84
84DCA0737	14	410300	8088000	C	43	44	13	0	0	100	1	1		Mod	DesPolys	Good	3		13	67	80
84DCA0738	14	408400	8088500	C	34	44	23	0	0	100	8	1	Pg	Mod	Circle,Ns	Good	8		7	61	68
84DCA0739	14	404700	8085400	C	46	37	18	0	0	100	1	5		Mod	Circle,PS	Good			7	65	72
84DCA0740	14	402200	8080500	C	15	44	41	0	0	100	1	5		Mod	Net,PS	Mod			17	53	70
84DCA0741	14	402700	8077500		24	48	28				1	1	Pg	Mod	Net,PS	Good	5		9	60	69
84DCA0742	14	404700	8071200	C	29	50	21	1	0	99	1	1	Pg	Sli	DesPolys	Good	3		11	59	70
84DCA0743	14	406600	8072300	C	46	41	13	2	0	98	3	1	Pg	Mod	Net,PS	Good	3		13	65	78
84DCA0744	14	405600	8078800	C	50	40	10	0	0	100	1	1		Ver	Net,PS	Good	15		8	73	81
84DCA0745	14	416000	8089500	C	46	34	20	0	0	100	8	3	Pg	Ver	Circle,PS	Good			18	35	53
84DCA0750	14	469300	8178200	C	29	44	28	0	0	100	5	3	Pg	Mod	Net,Ns	Good	8		26	37	63
84DCA0751	14	470700	8177000	C	31	45	24	0	0	100	8	8		Mod	Net,PS	Poor			16	46	62
84DCA0752	14	474200	8176200	C	29	46	26	0	0	100	3	10	Pg	Sli	Net,S	Poor			19	44	63
84DCA0753	14	468500	8183000	C	25	52	24	1	0	99	3	3	Pg,Rs	Mod	Net,Ns	Mod			12	51	63
84DCA0754	14	468500	8185700	C	45	35	20	1	0	99	5	1	Pg	Mod	Stripe,Ns	Good			16	41	57
84DCA0756	14	469400	8187500	C	63	25	12	0	0	100	3	5	Pg,Rs	Ver	Stripe,PS	Mod			7	42	49
84DCA0758	14	479900	8190600	C	24	56	21	0	0	100	10	3	Pg,Rs	Mod	Stripe,Ns	Good			3	45	48
84DCA0759	14	482900	8193600	C	55	34	11	0	0	100	70			Mod	Circle,Ns	Poor			9	37	46
84DCA0761	14	467000	8180000	C	40	40	21	0	0	100	3	3	Pg	Mod	Net,Ns	Good			22	43	65
84DCA0762	14	466500	8177800	C	24	46	30	1	0	99	3	3	Pg,Rs	Mod	Net,Ns	Good	8		21	38	59
84DCA0763	14	463700	8175200	C	26	47	27	0	0	100			Pg,Rs	Mod	Net,Ns	Good	8		22	36	58
84DCA0764	14	461000	8173000	C	28	46	26	0	0	100	3	1	Rs	Sli	Net,Ns	Good	5		16	45	61
84DCA0765	14	459000	8171100	C	63	24	13	2	0	98			Pg,Rs	Mod	Net,Ns	Good			15	49	64
84DCA0767	14	457300	8168000	C	22	55	24	0	0	100			Pg,Rs	Sli					13	56	69
84DCA0768	14	463000	8166800	C	34	52	15	0	0	100	5	3	Pg,Rs	Sli	Circle,Ns	Good			11	51	62
84DCA0769	14	466600	8165800	C	34	43	24	0	0	100	1	12	Pg,Rs	Sli	Net,S	Poor			19	46	65
84DCA0770	14	471700	8169400	C	21	57	22	0	3	97	3	1	Pg,Rs	Sli	Net,PS	Poor			6	53	59
84DCA0771	14	471400	8166700	C	39	46	15	0	1	99	1	1		Mod	Net,Ns	Good			6	47	53
84DCA0774	14	463800	8189500	C	41	39	20	2	0	98	10	5		Mod	Net,Ns	Good			16	51	67
84DCA0775	14	453000	8195400	C	62	32	6	1	0	99				Ver					6	70	76
84DCA0776	14	456000	8191200	C	42	37	22	0	0	100	5	1	Pg,Rs	Mod	Stripe,Ns	Good	12		21	39	60
84DCA0777	14	458700	8188300	C	29	45	26	0	1	99	3	3	Pg,Rs	Sli	Stripe,Ns	Good			23	43	66
84DCA0778	14	477100	8176200	C	32	50	18	0	0	100	30	3	Pg,Rs	Ver	Net,Ns	Poor	20		7	38	45
84DCA0780	14	515000	8172100	C	43	39	18	0	1	99			Rs,Rc	Ver	Circle,Ns	Good			2	25	27
84DCA0781	14	515500	8173600	S	46	38	17	0	97	3	50	0	Rs,GC,Pg	Sli	Net,Ns	Poor			0	20	20
84DCA0782	14	517200	8173500	S	53	32	16	0	97	3	30	1	Rs,Rc,GC	Mod	Circle,Ns	Good			0	22	22
84DCA0783	14	518600	8171300	MSS	41	46	13	0	80	20	55	3	Rs	Sli	Stripe,Ns	Mod			0	14	14
84DCA0786	14	519900	8171700	S	57	31	12	0	100	0	70	5		Sli	Stripe,S	Good	10		0	20	20
84DCA0787	14	522500	8171200	S	37	40	23	0	100	0	60	1		Sli	Stripe,Ns	Good			0	15	15

Sample	Z'	East	North	Lit Fac	%S	%$	%C	%Pc	%Ss	%Ls	%Veg	%B	Er	Sto	Patterned Ground	Drain	Cell Rel	FT (cm)	%Ca	%Do	%Car
84DCA0788	14	521700	8173500	S	61	24	16	1	98	1	10	1		Mod	Net,Ns	Good			0	18	18
84DCA0789	14	519200	8173400	S	65	21	14	0	100	0	50	1	Pg	Mod	Net,Ns	Poor			0	31	31
84DCA0790	14	513000	8171700	C	36	44	20	0	4	96	70	1	Rs	Mod	Net,Ns	Good	10		9	25	34
84DCA0791	14	513200	8173500	MSS	50	33	17	0	84	16	20	1	Rs	Mod	Net,Ns	Good	15		1	28	29
84DCA0792	14	513600	8175000	S	46	38	16	0	91	9	40	1	Rs	Mod	Net,Ns	Good			1	25	26
84DCA0793	14	516300	8175800	S	57	28	14	0	95	5	60	1		Mod	Net,Ns	Mod			0	22	22
84DCA0794	14	518000	8180600	MSS	52	30	17	0	80	20	1	1	Rs	Sli	DesPolys	Good			3	23	26
84DCA0795	14	514500	8170500	C	33	43	24	0	0	100	20	1	Rs	Mod	Net,Ns	Good	10		13	21	34
84DCA0796	14	519000	8166500	C	50	33	17	0	2	98	30	1	Rs	Ver	Circle,Ns	Good			3	28	31
84DCA0797	14	515000	8167200	MSS	42	39	19	0	83	17	10	5	Rs	Mod	Net,Ns	Good	8		1	20	21
84DCA0798	14	516600	8166500	MCC	45	37	18	0	16	84	50	1	Rs	Mod	Stripe,Ns	Good			1	21	22
84DCA0799	14	517500	8168200	MCC	44	38	17	0	11	89	80	1	Rs	Mod	Net,Ns	Good			6	20	26
84DCA0800	14	516000	8169600	C	38	39	23	0	4	96	50	1	Rs	Mod	Stripe,Ns	Good	20		12	18	30
84DCA0801	14	511400	8172800	C	33	49	18	0	0	100	10	1	Rs	Mod	Net,Ns	Good	10		10	24	34
84DCA0802	14	510300	8175600	MCC	41	38	21	0	12	88	5	1	Pg,Rs	Ver	Net,Ns	Good			2	27	29
84DCA0803	14	511800	8176000	C	37	42	21	0	9	91	20	1	Rs	Mod	Net,Ns	Good	15		0	28	28
84DCA0805	14	515000	8179700	M	47	35	18	0	37	63	50	1	Rs	Sli	DesPolys	Poor	2		5	30	35
84DCA0808	14	517100	8188000	M	67	23	10	1	32	67	60	1	Rs	Mod	Net,Ns	Poor			1	30	31
84DCA0809	14	515200	8185200	M	41	39	19	1	52	47	95	1	Rs	Sli	Stripe,Ns	Mod	5		1	23	24
84DCA0811	14	520000	8168500	M	38	41	21	0	37	63	10	1	Rs	Mod	Circle,Ns	Good			4	23	27
84DCA0812	14	512000	8170500	C	37	43	20	0	0	100	60	1	Rs	Sli	Circle,Ns	Good	15		5	21	26
84DCA0813	14	511500	8169400	MCC	39	41	20	0	14	86	80	1	Rs	Mod	Circle,Ns	Good			2	23	25
84DCA0815	14	510500	8172500	C	43	38	19	0	4	96	20	1	Pg,Rs	Mod	Net,Ns	Good	15		9	25	34
84DCA0816	14	508000	8171500	C	41	40	19	0	2	98	10	1	Pg,Rs	Mod	Net,Ns	Good	10		6	30	36
84DCA0817	14	507000	8174500	MCC	33	45	22	0	17	83	5	1	Rs	Mod	Circle,Ns	Good			9	28	37
84DCA0819	14	506400	8169500	MCC	39	40	21	0	13	87	30	1	Rs	Sli	Net,Ns	Good	10		5	24	29
84DCA0820	14	508600	8168000	MC	40	41	19	0	22	78	10	1	Rs	Mod	Net,Ns	Good			6	23	29
84DCA0821	14	511000	8167700	M	40	43	17	0	53	47	30	1	Rs	Mod	DesPolys	Mod	2		1	20	21
84DCA0822	14	513200	8167400	C	35	46	19	0	10	90	70	1	Rs	Mod	Stripe,Ns	Mod			1	22	23
84DCA0823	14	505400	8175700	MCC	40	39	21	0	11	89	20	1	Pg,Rs	Ver	Net,Ns	Good	15		6	33	39
84DCA0824	14	503000	8175700	C	20	47	33	0	1	99	8	1	Rs	Mod	Net,Ns	Good	10		10	35	45
84DCA0825	14	500900	8176200	MCC	50	35	15	0	14	85	10	1	Pg,Rs	Mod	Net,Ns	Good	15		10	33	43
84DCA0826	14	499000	8177400	C	53	30	17	0	4	96	10	1	Rs	Ver	Circle,Ns	Good	10		8	28	36
84DCA0828	14	495800	8177000		27	48	26				8	1	Rs	Ver	Circle,Ns	Good	15		9	34	43
84DCA0830	14	495900	8181100	C	50	38	12	0	3	97	50	1	Rs	Mod	Net,Ns	Good			8	28	36
84DCA0831	14	499000	8183700	C	17	51	31	2	0	98			Rs						13	42	55
84DCA0832	14	506200	8184300	C	38	46	16	1	1	99	60	3	Rs	Mod	Circle,Ns	Good	8		5	37	42
84DCA0833	14	506400	8181800	C	42	39	18	0	1	99	10	1	Pg,Rs	Ver	Net,Ns	Good	10		10	34	44
84DCA0834	14	506700	8178800	M	36	44	20	0	51	49	50	1	Rs	Mod	Circle,Ns	Good	10		3	25	28
84DCA0835	14	509500	8177000	C	33	45	23	0	4	96	20	1	Pg,Rs	Mod	Circle,Ns	Good	20		8	29	37
84DCA0836	14	509000	8178700	C	57	32	12	0	3	97	1	1	Pg,Rs	Ver		Good	3		4	33	37
84DCA0837	14	511000	8180300	MC	44	38	18	0	21	79	60	1	Rs	Sli	DesPolys	Poor	2		4	25	29
84DCA0838	14	510900	8182500	C	38	41	21	0	1	99	10	1	Rs	Mod	Net,Ns	Good	5		13	32	45
84DCA0839	14	508400	8183100	C	46	39	16	1	2	97	5	1	Rs	Ver	Net,Ns	Good	8		9	25	34
84DCA0840	14	509200	8185700	C	45	42	13	1	2	97	5	1	Rs	Mod	Net,Ns	Good	8		9	25	34

Appendix 1 (cont.)

Sample	Z1	East	North	Lit Fac	%S	%$	%C	%Pc	%Ss	%Ls	%Veg	%B	Er	Sto	Patterned Ground	Drain	Cell Rel	FT (cm)	%Ca	%Do	%Car
84DCA0842	14	512500	8187700	C	45	44	11	1	1	98	8	1	Pg,Rs	Ver	Net,Ns	Good	20		13	29	42
84DCA0843	14	518300	8188600	MCC	52	33	14	1	12	86	70	1	Rs	Ver	Stripe,Ns	Mod	15		0	33	33
84DCA0845	14	521200	8184600	S	52	35	13	3	93	5	70	0		Sli	DesPolys	Mod	5		1	21	22
84DCA0846	14	519500	8169000	C	55	31	14	0	10	90	20	1	Rs	Mod	Net,Ns	Mod	8		4	20	24
84DCA0847	14	524000	8166200	M	60	26	14	0	55	45	50	1	Rs	Mod	Net,Ns	Good	8		1	24	25
84DCA0848	14	525000	8168200	MSS	66	23	11	0	82	18	30	5	Rs	Mod	Net,Ns	Mod	5		0	22	22
84DCA0849	14	523100	8169500	MSS	64	26	10	0	89	11	40	1	Rs	Ver	Net,Ns	Good	5		0	21	21
84DCA0850	14	511500	8166100	MCC	31	47	22	0	18	82	5	1	Rs	Mod	Net,PS	Good	5		10	20	30
84DCA0851	14	513000	8163600	M	40	40	20	0	48	52	3	1	Rs	Mod	Net,PS	Mod	3		2	24	26
84DCA0852	14	511200	8161700	MCC	40	42	18	0	17	83	80	1	Rs	Mod	Net,Ns	Good	8		5	25	30
84DCA0853	14	514000	8158700	MC	32	50	18	0	22	78	70	1	Rs	Sli	Net,PS	Poor	3		5	24	29
84DCA0854	14	515600	8157400	C	34	45	21	0	1	99	10	1		Sli	Net,Ns	Poor	3		7	18	25
84DCA0855	14	514500	8165700	MC	36	45	17	0	25	75	30	1	Rs	Mod	Net,PS	Good			2	22	24
84DCA0858	14	531700	8139900	MSS	64	23	13	0	88	12	80	1	Rs,C	Mod	Net,Ns	Good	3		0	9	9
84DCA0859	14	532500	8140500	S	46	39	15	0	100	0	60	1		Mod	Net,Ns	Good	5		0	9	9
84DCA0860	14	532500	8142100	S	71	18	11	0	98	1	50	10		Mod	Net,Ns	Good	10		1	31	32
84DCA0862	14	530900	8144000	S	57	28	15	0	98	2	20	10		Sli	Net,Ns	Good	8		0	14	14
84DCA0863	14	528800	8142700	MC	41	41	18	0	27	73	30	1	C	Mod	Net,Ns	Good	10		1	18	19
84DCA0864	14	526700	8140700	C	40	39	21	0	2	98	60	1	Rs,C	Ver	Net,Ns	Good	20		1	32	33
84DCA0865	14	527500	8138500	C	37	43	20	0	5	95	50	5	Rs	Mod	Circle,Ns	Good	20		1	17	18
84DCA0866	14	528400	8135000	C	37	37	26	0	7	93	10	1	Rs	Sli	Stripe,Ns	Good	3		1	20	21
84DCA0867	14	531400	8135400	MSS	49	33	18	0	88	12	20	1	Rs	Mod	Stripe,Ns	Good	8		0	17	17
84DCA0868	14	532800	8144700	S	59	25	16	0	90	10	70	1		Mod	Stripe,Ns	Good	5		1	17	18
84DCA0869	14	533400	8148200	S	70	19	11	0	100	0	5	1		Mod	Net,Ns	Good	8		1	26	27
84DCA0870	14	532800	8150500	S	63	25	12	0	100	0	30	1		Mod	Net,Ns	Good	5		1	10	11
84DCA0871	14	532100	8155000	MS	71	17	12	0	78	22	20	1	C	Mod	DesPolys	Good			0	12	12
84DCA0872	14	529400	8153100	MSS	54	30	16	0	87	13	90	1		Mod	DesPolys	Mod	3		0	19	19
84DCA0873	14	527000	8150700	M	40	38	21	0	60	40	50	1		Mod	Stripe,Ns	Good	3		1	23	24
84DCA0874	14	526300	8148200	C	34	43	23	0	9	91	20	1	Rs	Mod	Net,Ns	Good	8		2	20	22
84DCA0875	14	529000	8146500	S	44	37	19	0	93	7				Sli	DesPolys				0	14	14
84DCA0876	14	530200	8160300		67	23	10				30	1	C	Sli	Net,Ns	Good	10		1	22	23
84DCA0877	14	528000	8162500	S	71	19	10	0	99	1	90	1	C	Mod	Net,Ns	Good			0	16	16
84DCA0879	14	521200	8165000	C	38	41	21	0	0	100	30	1	Rs	Ver	Circle,Ns	Good	20		4	26	30
84DCA0880	14	519700	8162100	MCC	48	34	18	0	18	82	30	1	Rs,C	Mod	Net,Ns	Mod	8		2	23	25
84DCA0881	14	518500	8159800	MC	33	44	22	0	29	71	5	1	Rs	Mod	Net,Ns	Good	20		8	22	30
84DCA0882	14	518100	8156800	C	30	45	25	1	0	99	10	1	Rs	Mod	Stripe,Ns	Good			8	29	37
84DCA0884	14	517600	8152300	C	34	43	23	0	6	94	5	1	Rs	Mod	Net,Ns	Good	3		9	21	30
84DCA0886	14	519500	8149100	MCC	37	41	23	0	13	87	30	1	Rs	Mod	Net,Ns	Good	10		6	19	25
84DCA0887	14	522600	8151000	C	28	47	25	0	3	97	10	1	Rs	Mod	Net,Ns	Good	12		14	20	34
84DCA0888	14	525600	8151700	S	44	40	16	0	100	0	20	0		Mod	Net,Ns	Good	3		0	13	13
84DCA0889	14	527500	8144600	MS	35	42	23	0	73	27	40	1	C	Sli	Net,Ns	Good	3		0	16	16
84DCA0890	14	521400	8147800	C	30	44	26	0	0	100	10	1	Rs	Mod	Circle,Ns	Good	25		7	18	25
84DCA0891	14	520100	8144500	C	39	40	22	0	0	100	20	1	Rs	Mod	Circle,Ns	Good	20		2	22	24
84DCA0892	14	518000	8142100	C	29	47	24	0	0	100	5	1	Rs	Mod	Net,Ns	Good	5		12	15	27
84DCA0893	14	518600	8139100	C	25	50	25	0	0	100	5	1		Mod	Net,Ns	Good	3		16	26	42

Sample	Z[1]	East	North	Lit Fac	%S	%$	%C	%Pc	%Ss	%Ls	%Veg	%B	Er	Sto	Patterned Ground	Drain	Cell Rel	FT (cm)	%Ca	%Do	%Car
84DCA0894	14	518200	8134900	MC	30	42	28	0	26	74	30	1	Rs	Mod	Net,Ns	Good	3		10	12	22
84DCA0895	14	520200	8131700	C	27	47	26	0	0	100	5	1		Sli	Net,Ns	Good	3		2	18	20
84DCA0897	14	523600	8130600	MS	32	46	22	0	70	30	80	1	C	Sli	DesPolys	Good	3		1	13	14
84DCA0898	14	527200	8131200	S	41	35	25	0	98	2	50	1	C	Sli	Circle,Ns	Good	3		1	17	18
84DCA0899	14	538000	8140500	S	68	17	15	0	100	0	80	1		Mod	Circle,Ns	Good	5		0	9	9
84DCA0905	14	539000	8143200	S	65	21	14	0	100	0	70	1		Mod	Circle,Ns	Good	12		0	11	11
84DCA0906	14	551400	8141600	MSS	84	9	7	0	86	14	0	15	Pg,C	Mod		Good	0		0	12	12
85DCA0002	14	555800	8082300	S	87	11	2	0	96	4	100		Pg	Sli	Net,Ns	Good	2	58	4	15	19
85DCA0004	14	555800	8079000	S	82	14	4	1	91	8	80		Pg	Mod	Net,Ns	Good	1	64	2	11	13
85DCA0007	14	550200	8071000	S	47	36	17	3	94	3	90		C	Sli	Net,Ns	Good		51	3	30	33
85DCA0008	14	549800	8063400	MSS	43	36	21	3	81	16	90		C	Mod	Net,Ns	Good	2	58	4	33	37
85DCA0009	14	553500	8057000	S	60	32	8	3	93	4	90		Pg,C	Mod	DesPolys	Good	0	46	2	31	33
85DCA0010	14	543800	8060000	MSS	52	34	14	4	81	15	95		Pg	Mod	DesPolys	Good	0	56	3	34	37
85DCA0011	14	540500	8066000	MC	60	32	8	5	17	78	50		Pg,C	Ver	Net,Ns	Good	4	36	5	41	46
85DCA0012	14	541200	8075300	MC	50	37	13	1	28	71	80		Pg,C	Mod	Net,Ns	Good		66	5	35	40
85DCA0013	14	548400	8094700	S	71	18	11	4	96	0	70		Pg	Mod	Circle,Ns	Good	0	54	3	5	8
85DCA0015	14	547800	8091100	MSS	48	38	14	0	83	17	80		Pg,C	Mod	DesPolys	Good		49	0	30	30
85DCA0016	14	540600	8082100	M	45	55	0	3	52	45	95		Pg	Mod	Net,Ns	Good	4	68	2	30	32
85DCA0017	14	539500	8085200	MS	43	38	19	0	70	30	41		Pg,C	Mod	Net,Ns	Good	4	80	1	26	27
85DCA0018	14	537500	8089500	MSS	43	38	19	0	89	11	100		C	Sli	Net,Ns	Poor	6	37	1	19	20
85DCA0019	14	533500	8086200	MS	38	42	20	0	74	26	40		C	Mod	Net,Ns	Good	2	51	4	26	30
85DCA0020	14	530200	8084500	MCC	37	44	19	2	12	86	30		C	Mod	Net,Ns	Good	6	41	12	30	42
85DCA0021	14	531400	8080600	M	37	39	24	1	69	30	80		C	Mod	Net,Ns	Good	1	55	3	23	26
85DCA0022	14	530400	8077200	C	56	30	14	4	6	90	20		Pg,C	Mod	Net,Ns	Good	2	62	14	39	53
85DCA0023	14	533500	8079000	MS	32	48	20	1	72	27	70		Pg,C	Mod	Net,Ns	Good	0	52	7	36	43
85DCA0024	14	538200	8080000	M	43	43	14	2	64	34	70		C	Mod	Net,Ns	Good	6	46	2	28	30
85DCA0025	14	544000	8082700	M	45	39	16	1	52	47	60		Pg,C	Mod	Net,Ns	Good	3	69	2	35	37
85DCA0026	14	551800	8080300	S	64	25	11	0	99	1	100		Pg,C	Mod	DesPolys	Good	0	53	6	23	29
85DCA0028	14	543800	8084400	S	70	23	7	0	98	2	60			Mod	Net,Ns	Good	2	61	0	24	24
85DCA0029	14	540600	8089100	S	54	31	15	1	99	0	70		Pg,C	Mod	Net,Ns	Good	0	65	2	22	24
85DCA0030	14	539400	8093000	M	52	32	16	0	60	40	60		Pg,C	Mod	Net,Ns	Good	6	46	1	23	24
85DCA0031	14	535600	8095000	MSS	51	32	17	0	87	13	90		Pg	Mod	Net,Ns	Good		46	1	20	21
85DCA0032	14	533500	8097500	MSS	44	38	18	0	84	16	30			Mod	DesPolys	Good	0	51	1	20	21
85DCA0033	14	531800	8101500	M	54	35	11	0	66	34	80		Pg,C	Mod	Net,Ns	Good	3	58	15	24	39
85DCA0034	14	535800	8103000	M	59	22	19	1	37	62	10		Pg,C	Mod	Stripe,Ns	Good		60	14	28	42
85DCA0036	14	544200	8000000	S	49	36	15	0	92	8	100			Mod	Net,Ns	Poor	0	59	0	22	22
85DCA0037	14	544200	8094400	S	58	26	16	0	100	0	100		C	Sli	Net,Ns	Poor	3	42	1	19	20
85DCA0038	14	544300	8088100	S	68	17	15	0	96	4	100			Mod	DesPolys	Good	0	42	1	9	10
85DCA0039	14	550500	8088000	S	69	22	9	0	100	0	80		Pg	Mod	Net,Ns	Good	0	62	1	28	29
85DCA0041	14	551800	8090500	S	65	24	11	0	90	10	100			Mod	Net,Ns	Mod	10	36	1	12	13
85DCA0043	14	501300	7944000	C	56	32	12	1	0	99	30		Pg	Ver	Net,Ns	Good	2		43	19	62
85DCA0044	14	498000	7941200	C	31	53	16	0	3	97	50			Mod	DesPolys	Good	0	52	42	28	70
85DCA0045	14	498000	7935200	C	34	53	13	1	0	99	30			Mod	Net,Ns	Mod	5		26	41	67
85DCA0046	14	496800	7930000	C	33	54	13	0	0	100	10			Ver	Net,Ns	Good	8		28	35	63
85DCA0048	14	491800	7936300	C	29	58	13	1	0	99	40			Mod	DesPolys	Poor	0		62	17	79

Appendix 1 (cont.)

Sample	Z'	East	North	Lit Fac	%S	%$	%C	%Pc	%Ss	%Ls	%Veg	%B	Er	Sto	Patterned Ground	Drain	Cell Rel	FT (cm)	%Ca	%Do	%Car
85DCA0049	14	490300	7948000	C	59	31	10	0	4	96	20		Pg	Mod	Net,Ns	Good	6		27	48	75
85DCA0050	14	497000	7947000	C	40	43	17	3	1	96	20		Pg	Mod	DesPolys	Good	0	65	22	49	71
85DCA0054	14	507100	7947800	C	36	56	18	0	0	100	10		Pg	Ver	Net,Ns	Good	1		25	50	75
85DCA0055	14	511200	7952100	C	37	48	15	2	0	98	10		Pg	Ver	Net,Ns	Good	2		37	41	78
85DCA0056	14	515000	7958600	C	42	42	16	0	0	100	45			Ver	Net,Ns	Good	1		33	45	78
85DCA0057	14	519700	7956500	C	45	41	14	5	0	95	40		Pg	Mod	Net,Ns	Good	2	70	15	60	75
85DCA0059	14	520000	7950000	C	46	37	17	0	0	100	10		Pg	Mod	Net,Ns	Good	3	61	41	39	80
85DCA0060	14	515000	7946500	C	44	38	18	1	1	98	10			Mod	Net,Ns	Good	2		41	40	81
85DCA0061	14	509700	7943800	C	48	38	14	0	0	100	5		Pg	Ver	Net,Ns	Good	1		45	37	82
85DCA0062	14	509100	7938000	C	35	45	20	0	0	100	10		Pg	Mod	Net,Ns	Good	2	16	25	48	73
85DCA0063	14	508200	7931400	C	31	53	16	3	2	95	15		Pg	Mod	DesPolys	Good	0		18	26	44
85DCA0064	14	513000	7930800	C	35	45	20	2	0	98	10			Ver	Net,Ns	Good	1		40	37	77
85DCA0065	14	520300	7933000	C	35	45	20	0	0	100	10		Pg	Ver	Net,Ns	Good			32	49	81
85DCA0066	14	522600	7938000	C	42	33	25	2	0	98	10		Pg	Ver	Net,Ns	Good	4		50	40	90
85DCA0067	14	514800	7939700	C	30	47	23	1	2	97	10		Pg	Ver	Net,Ns	Good	1		35	46	81
85DCA0068	14	508000	7941600	C	31	47	22	4	2	94	2		Pg	Ver	Net,Ns	Good			20	55	75
85DCA0069	14	497500	7953000	C	44	45	11	4	2	94	25		Pg	Mod	Net,Ns	Good	1		34	45	79
85DCA0070	14	497400	7965100	C	47	47	6	1	7	92	40		Pg	Mod	DesPolys	Poor	2	52	15	54	69
85DCA0071	14	506600	7974500	C	39	35	26	1	0	99	0		Pg	Mod	Net,Ns	Good	1		64	39	103
85DCA0072	14	504000	7968600	C	29	45	26	3	2	95	1		Pg	Mod	DesPolys	Good	0	55	39	41	80
85DCA0073	14	504200	7962000	C	29	47	24	3	1	96	10		Pg	Mod	DesPolys	Good	0	61	35	44	79
85DCA0074	14	503100	7954600	C	35	43	22	2	1	97	20		Pg	Ver	Net,Ns	Good	2		31	33	64
85DCA0076	14	506000	7939000	C	64	29	7	2	0	98	5		Pg	Ver	Net,Ns	Good	1		32	44	76
85DCA0077	14	505800	7930500	C	32	46	22	2	0	98	10		Pg	Ver	Net,Ns	Good	1		47	51	98
85DCA0078	14	504000	7925000	C	52	41	7	0	0	100	10			Mod	Net,Ns	Good	2	50	16	40	56
85DCA0080	14	500000	7923000	C	32	53	15	1	2	97	25			Mod	Net,Ns	Good	2		17	51	68
85DCA0081	14	499500	7932400	C	39	44	17	2	2	96	30		Pg	Mod	Net,Ns	Good	1	65	13	27	40
85DCA0082	14	500200	7938600	C	34	55	11	0	0	100	10		Pg	Ver	DesPolys	Good	2		21	44	65
85DCA0085	14	569800	8047100	MP	62	23	15	84	5	11	90		Pg,C	Mod	Stripe,Ns	Good		77	7	32	39
85DCA0086	14	565200	8048000	S	48	42	10	5	92	3	60		Pg,C	Mod	DesPolys	Good		79	1	25	26
85DCA0089	14	597500	8056700	MSS	63	24	13	15	85	0	90		Pg,C	Mod	Net,Ns	Good	1	73	1	21	22
85DCA0090	14	571500	8061100	M	55	25	20	54	32	14	80		Pg,C	Mod	Stripe,Ns	Good	0	80	5	17	22
85DCA0091	14	576700	8055800	MP	46	32	22	71	20	9	80		Pg,C	Mod	Net,Ns	Poor	0		7	27	34
85DCA0093	14	577800	8045200	MPP	69	22	9	87	12	1	70		Pg,C	Mod	Stripe,Ns	Poor		65	1	4	5
85DCA0094	14	565400	8042600	M	62	28	10	30	30	40	100		Pg,C	Mod		Mod		74	2	44	46
85DCA0095	14	570300	8036000	M	63	26	11	25	51	24	40		Pg,C	Mod	Stripe,Ns	Good	2	66	5	40	45
85DCA0096	14	569600	8025700	MSS	46	45	9	4	89	7	80		Pg,C	Mod	Net,Ns	Good	1	75	2	44	46
85DCA0097	14	573500	8020000	MSS	44	40	16	5	82	13	80		Pg,C	Mod	Stripe,Ns	Good			4	42	46
85DCA0100	14	573500	8029400	S	50	39	11	2	93	5	60		Pg,C	Mod	DesPolys	Good	0	79	9	37	46
85DCA0101	14	573600	8040200	M	55	33	12	55	28	17	90		Pg,C	Mod	Net,Ns	Good		72	7	31	38
85DCA0102	14	562100	8047300	M	71	21	8	57	39	4	80		Pg,C	Mod	DesPolys	Good		76	4	44	48
85DCA0103	14	558100	8048000	MS	55	36	9	6	71	23	90		Pg,C	Mod	DesPolys	Poor	0	66	4	28	32
85DCA0104	14	551800	8047100	M	26	60	14	10	55	35	90		Pg,C,Rs	Mod	DesPolys	Good		63	7	57	64
85DCA0105	14	546500	8048900	M	35	43	22	10	47	43	60		Pg,C,Rs	Mod	Net,Ns	Good	1	82	15	53	68
85DCA0106	14	539100	8053000	MS	43	42	15	7	70	23	40		Pg	Ver	Stripe,Ns	Good			22	52	74

Sample	Z[1]	East	North	Lit Fac	%S	%$	%C	%Pc	%Ss	%Ls	%Veg	%B	Er	Sto	Patterned Ground	Drain	Cell Rel	FT (cm)	%Ca	%Do	%Car
85DCA0107	14	540200	8043300	M	57	31	12	5	64	31	90		Pg	Mod	DesPolys	Good	0	76	9	47	56
85DCA0108	14	547400	8042600	M	36	41	23	9	52	39	60		Pg,C	Mod	Net,Ns		0	74	16	60	76
85DCA0109	14	553700	8041500	S	53	37	10	2	93	5	40		Pg,C	Mod	Net,Ns	Good	3	78	3	52	55
85DCA0110	14	583300	8051100	P	78	14	8	97	2	1	95		Pg,C	Ver		Mod			7	23	30
85DCA0112	14	586500	8049500	P	61	27	12	96	3	1	60		Pg,Rs,C	Ver	Net,Ns	Good			4	20	24
85DCA0113	14	588500	8045300	P	60	28	12	92	5	3	90		Pg,C	Ver	Net,Ns	Poor	2		1	47	48
85DCA0114	14	585500	8043100	M	21	52	27	67	11	22	0		Pg,Rs,C	Mod	DesPolys	Good	0	81	15	52	67
85DCA0115	14	581000	8042500	P	67	21	12	100	0	0	50		Pg,Rs,C	Mod	Stripe,Ns	Good	1		2	17	19
85DCA0116	14	560900	8042600	MSS	71	23	6	7	81	12	80		Pg,C	Mod	Net,Ns	Good	2	82	2	43	45
85DCA0118	14	556000	8035300	MSS	59	28	13	0	83	17	40		Pg,C	Mod	DesPolys	Good	0	77	3	32	35
85DCA0119	14	550200	8033000	M	52	38	10	13	46	41	40		Pg,C	Mod	DesPolys	Good	0	78	7	47	54
85DCA0120	14	550500	8027000	M	36	43	21	5	69	26	20		Pg,C	Mod	Net,Ns	Good	4		6	54	60
85DCA0121	14	559100	8025700	M	39	44	17	6	59	35	40		Pg,C	Mod	Net,Ns	Good	1	63	10	51	61
85DCA0122	14	562800	8034200	M	49	32	19	6	58	36	40		Pg,C	Mod	Stripe,Ns	Good	0	83	10	38	48
85DCA0307	14	539600	8185600	S	68	23	9	0	95	5	8		Rs	Mod	Circle,Ns	Good			1	37	38
85DCA0308	14	539600	8183100	C	43	42	15	0	4	96	5	1	Rs	Mod	DesPolys	Good	2		13	52	65
85DCA0309	14	537400	8182300	M	43	47	11	0	45	55	10	0	Rs	Sli		Good			1	14	15
85DCA0317	14	545300	8191500	MCC	49	36	16	0	20	80			Rs						2	29	31
85DCA0329	14	546800	8192800	MCC	39	45	16	2	9	89	20	3	Pg,Rs	Mod	Net,Ns	Mod			1	26	27
85DCA0338	14	550400	8197000	MCC	66	24	9	0	20	80				Mod	Net,S	Mod			1	35	36
85DCA0339	14	543500	8180000	M	72	22	6	0	33	67	50	1	Rs,C,GS	Mod	DesPolys	Good	5		1	39	40
85DCA0340	14	541500	8176700	MC	54	36	11	0	29	71	10	3	Rs	Ver		Good			1	41	42
85DCA0341	14	542000	8173500	M	40	37	23	0	53	47	95	1	Rs	Mod	Net,Ns	Good			3	36	39
85DCA0342	14	542700	8172000	MSS	49	40	11	0	86	14		1	Rs	Mod	Stripe,Ns	Poor			1	31	32
85DCA0343	14	548400	8166700	MC	51	36	12	0	25	75	20	1	Rs	Mod	Net,Ns	Good			0	24	24
85DCA0344	14	550000	8172000	M	55	32	13	0	42	58	40	3	Rs	Mod	Stripe,Ns	Good			2	36	38
85DCA0345	14	549900	8172400	S	54	24	23	0	91	9			Rs						1	8	9
85DCA0346	14	549100	8176600	MCC	63	27	10	0	19	81	90	1	Rs	Sli	Stripe,PS	Mod			0	47	47
85DCA0347	14	547000	8180300	C	51	41	9	0	4	96	5	5	Rs	Mod	Net,PS	Mod			0	59	59
85DCA0348	14	544900	8186600	C	52	38	10	0	3	97	5	1	Pg,Rs	Mod	Net,S	Good			0	62	62
85DCA0349	14	547800	8188000	C	46	38	16	0	2	98	15	1	Rs	Mod	Stripe,S	Good			3	61	64
85DCA0350	14	548600	8191100	C	42	42	16	0	5	95	10	1	Rs	Mod	Stripe,Ns	Good			7	63	70
85DCA0353	14	556100	8194200	MCC	44	42	14	0	19	81	10	1	Rs	Mod	Net,Ns	Good	15		10	69	79
85DCA0354	14	554500	8187700	MC	58	34	8	0	25	75	5	1	Rs	Ver	Net,PS	Good	8		0	64	64
85DCA0355	14	552900	8184200	C	45	42	13	0	7	93	5	1	Rs	Mod	DesPolys	Good			2	55	57
85DCA0356	14	549500	8184000	MCC	50	40	10	0	15	85	5	1	Rs	Mod	Stripe,S	Good	5		1	65	66
85DCA0358	14	540600	8190300	MCC	50	33	17	0	17	83	5	1	Rs,Rc	Mod	Stripe,S	Poor			7	43	50
85DCA0359	14	541900	8193000	MS	50	30	20	0	77	23	1	1	Rc	Mod	Circle,S	Good			4	22	26
85DCA0360	14	538900	8191200	S	58	21	20	0	100	0	10	40	Rc	Mod	Circle,S	Good			3	15	18
85DCA0361	14	538100	8194000	S	64	18	18	0	100	0	5	30		Mod	Stripe,S	Good			1	1	2
85DCA0362	14	541000	8196100	S	60	22	19	0	91	9	1	30		Mod	Stripe,S	Good			6	7	13
85DCA0365	14	534000	8185500	S	53	35	12	0	98	2		1	GC	Sli	DesPolys		5		0	20	20
85DCA0366	14	532900	8187000	S	48	39	13	0	100	0	20			Mod		Good			3	9	12
85DCA0369	14	529000	8186000	S	29	56	15	0	100	0	10	1		Mod	DesPolys	Good			1	6	7
85DCA0370	14	525900	8186000	S	32	54	14	0	99	1	50	1		Sli	DesPolys	Mod			1	12	13

Appendix 1 (cont.)

Sample	Z[1]	East	North	Lit Fac	%S	%$	%C	%Pc	%Ss	%Ls	%Veg	%B	Er	Sto	Patterned Ground	Drain	Cell Rel	FT (cm)	%Ca	%Do	%Car
85DCA0374	14	532500	8193000	S	63	23	14	0	100	0	5	1		Sli	Stripe,S	Mod			0	14	14
85DCA0375	14	549400	8181500	MCC	52	34	14	0	11	89	60		Rs	Mod	Net,PS	Good	5		1	47	48
85DCA0380	14	560000	8183500	C	46	43	12	0	0	100	10		Rs	Ver	Circle,S	Good			3	70	73
85DCA0382	14	538200	8183000	MSS	36	47	18	0	85	15	10	1	Rs,Rc	Ver	Net,Ns	Good	5		2	21	23
85DCA0384	14	528200	8180200	S	39	48	13	0	92	8	20	1	GS	Mod	Net,Ns	Good			2	14	16
85DCA0385	14	529500	8174900	S	53	29	18	0	97	3	90	1	GS	Sli	Stripe,Ns	Good			2	11	13
85DCA0387	14	530500	8166800	MSS	64	21	15	0	80	20	50	1	C	Mod	Net,Ns	Good	10		2	20	22
85DCA0388	14	539000	8169000	S	64	9	28	0	100	0	80	5	Rc	Mod	Stripe,Ns	Good			1	1	2
85DCA0389	14	537200	8176200	S	73	18	9	0	99	1	50	5	Rc,C	Sli	DesPolys	Mod			1	9	10
85DCA0393	14	494000	8171800	C	25	59	15	0	0	100	8	1	Rs	Ver	Net,PS	Good	5		23	22	45
85DCA0394	14	492300	8174400	C	40	42	18	0	0	100	10	1		Mod	Stripe,Ns	Good			14	26	40
85DCA0395	14	490500	8174600	C	39	44	17	0	0	100	10	1	Rs	Mod	Stripe,Ns	Good	8		15	31	46
85DCA0396	14	485100	8169400	C	30	57	13	0	0	100	5	1	Rs	Ver	Circle,PS	Good	15		1	50	51
85DCA0397	14	483500	8169400	C	25	58	17	0	0	100	5	1		Ver	Net,S	Good	30		18	36	54
85DCA0398	14	479900	8169200	C	33	52	16	0	0	100	30	1		Mod	Net,Ns	Good	8		16	39	55
85DCA0399	14	479900	8173500	C	28	51	21	1	0	99	40	1		Mod	Net,Ns	Good	5		3	39	42
85DCA0400	14	480500	8177700	C	37	45	18	0	0	100	20	1	Pg	Mod	Net,PS	Good	3		6	41	47
85DCA0401	14	440100	8186000	C	27	51	22	0	0	100	50	5	Rs	Mod	Stripe,Ns	Good	8		4	43	47
85DCA0403	14	485500	8164900	C	39	43	18	0	0	100	10	5	Pg,Rs	Mod	Net,Ns	Good	8		5	36	41
85DCA0404	14	484100	8160200	C	22	44	34	0	0	100	10	1	Rs	Sli	Net,Ns	Good	5		11	30	41
85DCA0406	14	478100	8151000	C	26	56	18	1	0	99	10	1		Ver	Net,PS	Good	8		10	45	55
85DCA0407	14	476100	8148000	C	27	58	16	0	0	100	5	1	Rs	Ver	Net,S	Good	30		22	36	58
85DCA0408	14	483800	8146500	C	35	50	15	0	0	100	40	1	Pg,Rs	Mod	Stripe,S	Good			17	21	38
85DCA0409	14	484500	8153100	C	40	42	18	0	0	100	10	1	Pg,Rs	Ver	Net,Ns	Good	10		17	23	40
85DCA0410	14	489500	8162500								10	1	Rs	Ver	Net,PS	Good					0
85DCA0411	14	489600	8155200	C	30	47	23	0	0	100	10	1		Sli	Net,PS	Good	3		17	16	33
85DCA0413	14	490500	8144400	C	31	43	26	0	0	100	5	1	Rs	Ver	Stripe,PS	Good	5		27	17	44
85DCA0414	14	491300	8140600	C	32	45	22	0	0	100	10	1	Pg,Rs	Mod	Net,PS	Good	5		17	27	44
85DCA0415	14	497100	8142000	C	34	49	17	0	0	100	70	1	Rs	Mod	Stripe,Ns	Poor	5		28	8	36
85DCA0416	14	492800	8153900	C	24	45	31	0	0	100	20	1		Mod	Net,Ns	Good	5		26	13	39
85DCA0417	14	497000	8167100	C	28	45	27	0	0	100	10	1	Rs	Mod	Stripe,Ns	Good			15	21	36
85DCA0418	14	498500	8159700	C	42	34	24	0	0	100	5	1	Rs	Mod	Net,Ns	Good	3		13	22	35
85DCA0419	14	502800	8156100	C	27	49	24	0	0	100	20	1		Sli	Net,Ns	Good	5		17	16	33
85DCA0420	14	504900	8150300		29	48	24				30	1	Rs	Sli	Stripe,Ns	Good	5		14	17	31
85DCA0421	14	500800	8139500	C	22	55	23	0	0	100	10	1		Sli	Net,Ns	Good	5		16	14	30
85DCA0422	14	504800	8157800	C	28	46	26	1	0	99	5	1	Pg,Rs	Mod	Net,Ns	Good	5		13	17	30
85DCA0423	14	504800	8162500	C	31	47	22	0	0	100	20	1	Rs	Sli	Stripe,Ns	Good	5		9	20	29
85DCA0427	14	480000	8159500	C	28	53	20	0	0	100	5	1	Rs	Mod	Net,Ns	Good	15		13	37	50
85DCA0428	14	474800	8158500	C	27	47	25	1	1	98	20	1	Pg,Rs	Sli	Stripe,Ns	Good	8		20	36	56
85DCA0429	14	476100	8164000	MS	28	57	15	0	71	29	30	1		Mod	Net,Ns	Poor			2	42	44
85DCA0430	14	479000	8165900	C	26	55	19	0	0	100	10	5		Mod	Net,Ns	Good			4	41	45
86DCA0003	14	482800	7970000	C	38	40	22	0	4	96	20		Pg	Mod	DesPolys	Poor		49	46	34	80
86DCA0004	14	490400	7964600	C	30	48	22	0	0	100	20		Pg	Mod	Circle,PS	Mod	1	37	45	25	70
86DCA0005	14	491700	7956700	C	33	46	21	3	0	97	20		Pg	Ver	Circle,PS	Mod		24	49	37	86
86DCA0006	14	485400	7952200	C	41	41	18	2	1	97	35		Pg	Mod	Circle,S	Good	0	30	42	46	88

Sample	Z[1]	East	North	Lit Fac	%S	%$	%C	%Pc	%Ss	%Ls	%Veg	%B	Er	Sto	Patterned Ground	Drain	Cell Rel	FT (cm)	%Ca	%Do	%Car
86DCA0007	14	479000	7963100	C	46	35	19	1	4	95	30		Pg	Mod	Net,Ns	Good	1	17	34	51	85
86DCA0014	14	477800	7976100	C	42	42	16	1	0	99	20		Pg	Mod	Net,Ns	Good	2	15	56	25	81
86DCA0015	14	476100	7983000	C	40	36	24	3	0	97	10		Pg	Mod	Net,Ns	Mod	1	34	57	23	80
86DCA0016	14	479900	7988200	C	28	50	22	1	0	99	7		Pg	Mod	DesPolys	Mod	0	26	37	51	88
86DCA0017	14	480100	7995500	C	46	39	15	2	0	98	10		Pg,Rs	Mod	Net,PS	Good	3	37	64	29	93
86DCA0018	14	469600	7993500	C	42	38	20	0	0	100	10		Pg	Ver	DesPolys	Good	1	5	47	36	83
86DCA0019	14	471800	7985000	C	28	50	22	0	0	100	20		Pg	Mod	DesPolys	Good	0	19	46	26	72
86DCA0020	14	471900	7975600	C	38	48	14	1	0	99	20			Mod	Net,Ns	Good		17	31	47	78
86DCA0021	14	488500	7970700	C	42	38	20	4	6	90	20		Pg,Rs	Mod	DesPolys	Good	0	32	24	43	67
86DCA0022	14	491200	7973700	C	27	34	39	3	3	94	5		Pg	Mod	Net,Ns	Good		23	48	34	82
86DCA0023	14	498000	7976400	MC	60	29	11	16	9	75	50		Pg	Sli	DesPolys	Good	1	35	13	63	76
86DCA0024	14	502000	7980000	C	48	32	20	7	3	90	10		Pg	Mod	Circle,S	Good		30	25	54	79
86DCA0025	14	494500	7985300	MCC	45	31	24	6	6	88	30		Pg,Rs	Mod	Net,Ns	Good		19	21	57	78
86DCA0026	14	490300	7980500	MCC	35	33	32	7	4	89	60		Pg	Mod	DesPolys	Poor		46	17	50	67
86DCA0027	14	485600	7977200	C	29	43	28	1	0	99	50		Pg	Mod	DesPolys	Poor	0	35	22	51	73
86DCA0028	14	481600	7972800	C	31	47	22	0	0	100	20			Mod	DesPolys	Mod	0	25	38	48	86
86DCA0033	14	532600	7993200	C	36	33	31	2	1	97	15		Pg	Mod	DesPolys	Good	0	18	44	42	86
86DCA0034	14	533000	7997200	C	32	36	32	0	2	98	20		Pg	Sli	Net,Ns	Good	4	14	43	47	90
86DCA0035	14	529300	8001000	C	33	30	37	1	0	99	15		Pg	Sli	Net,Ns	Good	2	12	49	30	79
86DCA0036	14	527500	8006000	C	80	7	13	1	1	98	10		Pg	Mod	Net,Ns	Good	3	15	51	37	88
86DCA0037	14	524600	8014000	C	33	29	38	1	0	99	5		Pg	Sli	Net,Ns	Good	4	15	55	34	89
86DCA0038	14	520000	8007400	C	31	33	36	0	3	97	5		Pg	Mod	Net,Ns	Good		16	43	47	90
86DCA0039	14	522000	7999300	C	41	31	28	0	0	100	10		Pg	Mod	Net,PS	Good	1	18	41	45	86
86DCA0040	14	522800	7974300	C	39	30	31	3	1	96	10		Pg,Rs	Mod	Net,Ns	Good	2	15	39	49	88
86DCA0041	14	517200	7967000	C	65	14	21	2	1	97	12		Pg	Mod	Net,Ns	Good	1	17	44	40	84
86DCA0043	14	512600	7972200	C	50	24	26	3	0	97	7		Pg	Ver	Net,Ns	Good	1	12	39	43	82
86DCA0058	14	525300	8077000	C	28	41	31	1	1	98	10		Pg,Rs	Mod	DesPolys	Good	0	36	33	33	66
86DCA0059	14	525600	8083500	MCC	39	33	28	6	11	83	45		Pg,Rs	Mod	Circle,S	Good	2	41	29	36	65
86DCA0060	14	523900	8088000	C	46	28	26	0	1	99	10		Pg,Rs	Mod	Net,PS	Good	2	23	37	34	71
86DCA0062	14	521000	8083600	C	33	34	33	1	1	98	30		Pg,Rs	Mod	DesPolys	Good	0	15	27	27	54
86DCA0063	14	520400	8078700	C	58	23	19	0	0	100	30		Pg,Rs	Mod	Net,PS	Good	1	17	34	44	78
86DCA0064	14	517000	8075000	C	49	24	27	5	0	95	20		Pg,Rs	Mod	Stripe,S	Good		29	58	19	77
86DCA0065	14	513500	8068100	C	52	26	22	4	0	96	1		Pg,Rs	Mod	DesPolys	Good		19	46	29	75
86DCA0066	14	526500	8059500	MCC	80	8	12	8	8	84	60		Pg,Rs	Mod	Net,Ns	Mod	1	20	25	42	67
86DCA0067	14	530700	8050300	MCC	57	25	18	7	4	89	60		Rs	Mod	Net,Ns	Good	0	47	27	42	69
86DCA0068	14	538100	8048000	C	73	14	13	4	4	92	50		Pg,Rs	Mod	Net,PS	Good	0	20	48	32	80
86DCA0069	14	541500	8055800	MC	47	31	22	12	18	70	100		Pg,Rs	Mod	Circle,S	Mod	0	35	14	46	60
86DCA0070	14	540500	8061700	M	46	26	28	6	32	62	90		Pg,C	Mod	Net,Ns	Good	2	39	15	39	54
86DCA0071	14	537500	8065400	MCC	64	16	20	3	17	80	100		Pg,C	Mod	Net,Ns	Good		40	14	43	57
86DCA0072	14	531800	8061500	MCC	34	35	31	12	5	83	100		Pg,Rs	Mod	DesPolys	Mod		43	25	48	73
86DCA0073	14	530800	8067000	MCC	44	31	25	2	13	86	70		Pg,Rs	Mod	Net,Ns	Good	2	23	29	38	67
86DCA0074	14	537000	8074100	C	41	37	22	1	4	94	30		Pg,Rs,C	Mod	Net,S	Good		30	22	29	51
86DCA0075	14	532200	8075200	C	36	29	35	0	5	95	35		Pg,Rs,C	Mod	Stripe,Ns	Mod		38	18	23	41
86DCA0076	14	528500	8073600	C	49	30	21	1	2	97	20		Pg,Rs,C	Mod	Net,Ns	Good	4	28	22	38	60
86DCA0077	14	524400	8072800	C	53	27	20	0	3	97	20		Pg	Mod	Net,PS	Good	1	15	42	27	69

Appendix 1 (cont.)

Sample	Z[1]	East	North	Lit Fac	%S	%$	%C	%Pc	%Ss	%Ls	%Veg	%B	Er	Sto	Patterned Ground	Drain	Cell Rel	FT (cm)	%Ca	%Do	%Car
86DCA0078	14	523500	8067900	MCC	38	33	29	9	5	86	80		Pg,Rs	Mod	DesPolys	Poor		50	24	40	64
86DCA0079	14	523500	8064200	C	55	26	19	4	1	95	20		Pg,Rs,C	Mod	Net,PS	Good	2	33	24	44	68
86DCA0082	14	501700	8053500	C	38	37	25	0	0	100	0								65	25	90
86DCA0083	14	512000	8041200	C	42	32	26	1	1	98	0								56	31	87
86DCA0084	14	507200	8026300	C	34	31	35	1	0	99	1					Good			46	41	87
86DCA0085	14	556100	7997100	C	27	39	34	0	1	99	2								33	48	81
86DCA0086	14	550600	7990500	C	35	36	29	2	1	97	2								36	44	80
86DCA0087	14	543700	7981100	C	41	36	23	0	0	100	0					Good			50	38	88
86DCA0088	14	530000	7957500	C	46	32	22	1	0	99	2					Good			32	52	84
86DCA0089	14	558000	7979800	C	28	35	37	8	1	91	15								30	47	77
86DCA0090	14	565400	7986700	C	47	36	17	0	10	90	100								20	58	78
86DCA0091	14	580500	7969500	C	47	38	15	2	0	98	5								16	73	89
86DCA0092	14	586000	7983400	C	44	36	20	5	0	95	2								29	58	87
86DCA0093	14	590500	8038100	M	42	28	30	54	1	45	5								19	41	60
86DCA0094	14	578500	8063300	P	59	18	23	99	0	1	95								3	2	5
86DCA0095	14	509500	8067400	C	33	29	38	6	0	94	90		Pg,Rs	Mod	Net,Ns	Good	2	16	36	39	75
86DCA0096	14	509500	8072100	C	69	17	14	6	1	93	80		Pg,Rs	Mod		Good		33	23	44	67
86DCA0112	14	571700	8081500	S	41	11	48	3	96	1	20		Pg	Mod	Net,Ns	Good	0	28	10	11	21
86DCA0113	14	571900	8079400	MPP	72	10	18	80	15	5	20		Rc,Rs,C	Mod	Stripe,S	Poor		58	10	27	37
86DCA0114	14	573500	8076000	P	57	11	32	95	5	0	30		Rc,Rs,C	Mod		Poor		43	12	10	22
86DCA0115	14	576000	8078100	P	59	18	23	92	2	6	50		Rc,Rs		Stripe,Ns	Poor		41	12	29	41
86DCA0116	14	574500	8081200	P	80	4	16	100	0	0	90		Pg,Rc,Rs	Mod		Good		30	17	28	45
86DCA0117	14	573400	8083600	MPP	72	13	15	80	11	14	80		PC,Rc,Rs			Good		39	10	24	34
86DCA0118	14	571400	8084300	MSS	84	3	13	11	83	6	10		Pg,Rc,C		Net,Ns	Good		35	17	50	67
86DCA0119	14	573400	8086400	MS	67	19	14	21	70	9	40		Pg,Rs,C	Mod		Poor		72	11	39	50
86DCA0120	14	575300	8090000	P	57	27	16	100	0	0	40		Pg,Rs,C	Mod	Net	Good			9	34	43
86DCA0412	13	583200	8086800	C	47	43	11	0	0	100	3	5	Pg	Mod	Circle,S	Good			11	67	78
86DCA0416	13	589400	8099900	C	43	40	17	4	0	96	3	3	Pg	Mod	Net,S	Good			5	57	62
86DCA0419	13	585500	8082800	C	33	47	20	0	0	100	1	3		Mod	Stripe,S	Good	5		6	70	76
86DCA0420	13	587800	8079200	C	32	48	20	1	0	99	1	20		Ver	Net,PS	Good	10		14	63	77
86DCA0426	13	582900	8091800	C	33	47	20	1	0	99	1	1	Pg	Sli	Net,S		5		10	63	73
86DCA0430	13	579500	8088100	C	38	53	9	1	0	99	1	1	Pg	Mod	Net,PS	Good			3	69	72
86DCA0433	14	451100	8147000	C	47	35	18	0	0	100	20	1	Pg	Mod	Net,Ns	Good	10		23	23	46
86DCA0435	14	446800	8153600	C	51	33	16	0	0	100	30	1	Pg	Mod	Net,Ns	Good			32	24	56
86DCA0441	14	455300	8137500	C	39	35	26	0	1	99	20	1	Pg	Mod	Net,Ns	Good			19	28	47
86DCA0442	14	452900	8140500	C	30	46	25	0	0	100	30	1	Pg	Mod	Stripe,Ns	Good			20	32	52
86DCA0443	14	451000	8143900	C	33	44	23	0	0	100	10	1	Pg	Mod	Net,Ns	Good	10		29	14	43
86DCA0444	14	446900	8147700	C	29	49	23	0	0	100	30	1	Pg	Mod	Net,Ns	Good			29	18	47
86DCA0445	14	442200	8151000	C	39	42	18	0	0	100	10	1		Ver	Net,Ns	Good	20		32	20	52
86DCA0447	14	438200	8154500	C	35	46	19	0	0	100	1	3	Pg	Mod	Net,PS	Good			22	53	75
86DCA0448	14	440400	8157200	C	38	47	15	1	0	99	1	8	Pg	Mod	Net,S	Good			16	68	84
86DCA0449	14	443100	8161100	C	53	31	16	0	0	100	8	5	Pg	Mod	Net,PS	Good	8		25	33	58
86DCA0450	14	440800	8167000	C	41	38	21	1	0	99	5	1	Pg	Mod	Stripe,Ns	Good	3		29	27	56
86DCA0456	14	449800	8133500	C	50	36	14	1	0	99	60	1	Pg	Mod	Net,Ns	Mod			2	52	54
86DCA0458	14	439400	8137000	C	18	48	34	0	0	100	40	1	Pg	Sli	Stripe,Ns	Mod	8		12	29	41

Sample	Z^1	East	North	Lit Fac	%S	%$	%C	%Pc	%Ss	%Ls	%Veg	%B	Er	Sto	Patterned Ground	Drain	Cell Rel	FT (cm)	%Ca	%Do	%Car
86DCA0459	14	446600	8143600	C	26	41	33	0	0	100	10	1	Pg	Mod	Net,Ns	Good	8		21	26	47
86DCA0460	14	444200	8145000	C	28	45	26	0	0	100	20	1	Pg	Mod	Net,Ns	Good	3		38	11	49
86DCA0461	14	439700	8147100	C	32	43	25	1	0	99	5	1	Pg	Mod	Net,PS	Good	8		32	21	53
86DCA0462	14	436000	8144600		38	40	22				1	5	Pg	Mod	Net,PS	Good	8		30	31	61
86DCA0463	14	428900	8143700	C	51	36	14	0	0	100	10	1	Pg	Sli	DesPolys	Mod			11	49	60
86DCA0464	14	459300	8143300	C	74	22	4	0	0	100					Circle,S	Good			1	2	3
86DCA0465	14	463500	8136800	C	27	47	26	0	0	100	10	1	Pg,Rm	Mod	Net,Ns	Good	8		30	23	53
86DCA0467	14	464800	8132400	C	28	42	30	0	0	100	10	8	Pg,Rm	Ver	Net,Ns	Good	25		10	36	46
86DCA0470	14	456800	8147000	C	38	45	17	0	1	99	10	1	Pg,Rm	Mod	Stripe,PS	Good			18	39	57
86DCA0471	14	456800	8151600	C	32	49	19	0	0	100	20	1	Pg,GC,Rm	Mod	Stripe,Ns	Good			9	37	46
86DCA0472	14	454700	8153200	C	31	53	16	0	0	100	5	1	GC	Ver	Circle,Ns	Good	20		4	44	48
86DCA0474	14	485000	8129500	C	27	50	23	0	1	99	10	1	Pg,Rs,Rm	Sli	Stripe,Ns	Good	8		11	46	57
86DCA0475	14	488500	8126000	C	31	50	19	0	0	100	5	1	Pg,Rs	Ver	Stripe,S	Good	8		18	34	52
86DCA0480	14	489400	8118500	C	44	45	11	0	0	100	20	1	Pg	Mod	Stripe,Ns	Good	12		22	30	52
86DCA0481	14	489600	8122700	C	38	45	17	0	0	100	5	5	Pg	Ver	Net,Ns	Good			23	23	46
86DCA0482	14	480700	8117600	C	34	50	16	0	0	100	5	1	Pg	Mod	Stripe,Ns	Good			16	52	68
86DCA0484	14	480700	8113500	C	45	44	11	0	0	100	5	1	Pg	Mod	Stripe,Ns	Good	3		24	49	73
86DCA0485	14	481100	8110800	C	41	43	16	0	1	99	5	1	Pg,Rs	Ver	Net,PS	Good	30		24	35	59
86DCA0487	14	481700	8107000		33	42	25				1	1	Pg,Rs	Ver	Net,Ns	Good	18		42	27	69
86DCA0488	14	484000	8102400	C	41	43	17	0	1	99	5	1	Pg,Rs	Ver	Net,Ns	Good			27	34	61
86DCA0491	14	481500	8129800	C	36	47	16	0	1	99	10	1	Pg,Rs,Rm	Mod	Net,Ns	Good	10		14	33	47
86DCA0492	14	479400	8130800	C	30	55	15	0	0	100	5	1	Pg,Rm	Mod	Net,Ns	Good	8		9	42	51
86DCA0493	14	479400	8130800		25	58	17				5	1	Pg	Mod	Net,Ns	Good	8		10	47	57
86DCA0494	14	476000	8129200	C	35	50	16	0	1	99	30	1	Pg,Rs,Rm	Mod	Stripe,PS	Good	10		6	47	53
86DCA0495	14	471300	8126800	C	30	52	18	0	0	100	5	1	Pg,Rs	Mod	DesPolys	Good	2		12	49	61
86DCA0496	14	466300	8128500	C	35	51	15	1	0	99	5	20	Pg,Rs	Mod	Net,PS	Good	10		17	50	67
86DCA0503	14	475200	8126300	C	31	48	21	0	4	96	20	1	Pg,Rs	Mod	Stripe,Ns	Good	8		24	46	70
86DCA0506	14	478500	8120800	C	43	43	14	1	4	95	10	1	Pg,Rs	Mod	Net,Ns	Good	3		25	51	76
86DCA0513	14	467500	8120500	C	44	43	13	0	2	98	10	1	Pg	Mod	Net,PS	Good	3		15	58	73
86DCA0514	14	491100	8125800	C	20	54	26	0	0	100	10	1	Pg	Mod	Net,PS	Good	5		17	15	32
86DCA0515	14	492900	8121800	C	33	47	21	0	0	100	5		Pg	Mod	Net,PS	Good	5		37	12	49
86DCA0517	14	496000	8126000	C	35	44	21	0	1	99	5			Ver	Net,Ns	Good			22	12	34
86DCA0518	14	497200	8129000	C	37	43	20	0	1	99	5	1	Pg	Ver	Net,Ns	Good	12		36	7	43
86DCA0519	14	497500	8130600	C	40	42	18	0	0	100	5	1	Pg	Mod	Stripe,Ns	Good			22	12	34
86DCA0520	14	497500	8133900	C	20	53	27	0	0	100	5	1	Pg	Sli	Net,PS	Good	5		20	13	33
86DCA0521	14	495000	8129800	C	35	46	19	0	0	100	10	1	Pg	Mod	Net,PS	Good	5		21	10	31
86DCA0522	14	492900	8130200	C	23	52	25	0	0	100	10	1	Pg	Sli	Stripe,Ns	Poor	5		24	14	38
86DCA0523	14	490200	8131000	C	25	54	20	0	0	100	10	1	Pg	Mod	Stripe,PS	Good	8		20	12	32
86DCA0525	14	490400	8111600	C	47	40	13	0	0	100	20	1	Pg	Mod	Stripe,Ns	Good	8		29	25	54
86DCA0526	14	491300	8115200	C	52	34	14	0	0	100	15	1	Pg	Mod	Stripe,PS	Good	5		34	19	53
86DCA0532	14	563000	8105900	S	69	15	16	4	94	3	50	1	Pg,C	Sli	Net,Ns	Good	3		1	10	11
86DCA0533	14	566100	8104200	M	34	48	18	18	38	44	30	1	Pg,C	Sli	Stripe,Ns	Good	3		3	18	21
86DCA0534	14	568300	8104900	S	77	12	11	0	100	0	50	1		Mod	Stripe,S	Good	8		1	1	2
86DCA0535	14	570300	8106000	S	79	13	7	0	96	4	60	1		Mod	Stripe,PS	Good	5		1	5	6
86DCA0536	14	572600	8102200	S	68	14	18	0	97	3	60	1		Ver	Net,Ns	Mod			1	4	5

Appendix 1 (cont.)

Sample	Z[1]	East	North	Lit Fac	%S	%$	%C	%Pc	%Ss	%Ls	%Veg	%B	Er	Sto	Patterned Ground	Drain	Cell Rel	FT (cm)	%Ca	%Do	%Car
86DCA0537	14	569400	8100800	S	67	20	12	1	91	7	60	1	C	Sli	Stripe,Ns	Good	5		0	3	3
86DCA0538	14	567500	8101800	S	71	15	13	0	100	0	60	1	C	Sli	Stripe,Ns	Good	5		1	0	1
86DCA0541	14	564400	8108100	MSS	67	23	10	0	81	19	60	1	C	Sli	Net,Ns	Good	3		4	3	7
86DCA0542	14	566800	8110500	S	73	13	14	0	100	0	10	1			Net,Ns	Good	8		1	2	3
86DCA0543	14	569500	8109800	S	67	18	16	0	99	1	70			Sli		Good			1	0	1
86DCA0544	14	569800	8111800	S	71	15	14	0	93	7	70	1	C	Mod	Stripe,Ns	Mod	5		1	4	5
86DCA0545	14	567800	8112800	MSS	70	18	12	0	84	16	80	1	C	Sli	Stripe,Ns	Good	3		1	15	16
86DCA0559	14	570800	8115400	S	73	13	14	0	99	1	15	2	C	Mod	Net,Ns	Good	8		0	9	9
86DCA0567	14	572500	8114400	C	50	40	10	3	0	97	10		Pg,Rs	Ver	Circle,PS	Good	8		18	61	79
86DCA0569	14	570200	8109600	S	74	17	10	1	99	1	30		Rc,C	Mod	Stripe,Ns	Good			1	0	1
86DCA0570	14	575100	8110200	MPP	65	21	14	87	6	7			Rc,C,Rs	Mod	Circle,S				0	10	10

[1] Abbreviations used in column headings in order of appearance: Z, universal transverse mercator grid zone; East, UTM easting; North, UTM northing; Lit Fac, lithic facies; S, sand; $, silt; C, clay; Pc, Precambrian rock granules; Ss, sandstone granules; Ls, limestone and dolomite granules; Veg, vegetation cover; B, boulder cover; Er, erratics; Sto, stoniness; Drain, site drainage class; Cell Rel, patterned ground cell relief; FT, depth to frost table; Ca, calcite; Do, dolomite; Car, total carbonate.
[2] See Table 2 for definition of lithic facies.
[3] Erratic lithologies: Pg, Precambrian shield rock; C, limestone and dolomite; Rs, red sandstone and siltstone; Rm, red mudstone; Rc, red conglomerate of Peel Sound Formation.
[4] Stoniness classes: Sli, slightly stony; Mod, moderately stony; Ver, very stony.
[5] S, sorted; Ns, nonsorted; DesPolys, dessication polygons.
[6] Drainage classes: poor, moderate, good.

APPENDIX 2

Geochemistry of till samples from Prince of Wales Island

Sample	East[1]	North	Cu[2]	Pb	Zn	Co	Ni	Cr	Fe	Mn	Ufl	As
84DCA0003	14528200	7979700	13	12	53	8	24	30	1.3	215	1.3	3
84DCA0004	14528000	7981300	18	15	68	7	19	28	1.5	230	1.3	11
84DCA0005	14527900	7983500	15	17	60	7	19	31	1.4	270	1.6	9
84DCA0007	14529200	7986200	17	15	62	8	22	32	1.5	255	1.8	8
84DCA0010	14531600	7986900	13	14	61	9	19	33	1.5	260	1.0	10
84DCA0012	14532100	7983900	13	9	37	6	18	20	0.8	175	1.7	4
84DCA0015	14530500	7974000	24	21	95	13	33	52	3.0	370	1.4	13
84DCA0016	14535500	7972700	33	24	102	18	54	60	3.8	400	1.6	15
84DCA0017	14535300	7971000	17	17	76	8	22	39	1.7	250	0.8	11
84DCA0019	14538700	7974000	25	19	88	14	48	40	2.0	495	0.7	6
84DCA0020	14537700	7974100	20	9	87	18	66	48	2.5	320	0.6	4
84DCA0021	14537000	7975500	24	17	99	15	53	44	2.3	455	0.5	11
84DCA0022	14536000	7976000	16	14	60	8	28	29	1.3	225	0.9	6
84DCA0023	14535100	7976800	18	17	74	10	33	36	1.8	295	0.7	10
84DCA0024	14534100	7977100	22	14	72	9	30	38	1.9	260	1.7	13
84DCA0025	14534000	7977100	30	22	133	11	40	35	1.7	405	1.1	11
84DCA0027	14528600	7986600	15	15	51	7	21	26	1.2	235	1.3	9
84DCA0029	14528000	7985800	15	13	42	6	20	21	1.1	220	1.2	8
84DCA0030	14527100	7984600	16	15	55	8	27	29	1.4	250	1.1	13
84DCA0031	14526900	7983900	18	16	66	10	34	37	1.5	365	1.1	11
84DCA0032	14528600	7984400	16	13	45	6	22	24	1.2	210	1.3	7
84DCA0033	14530100	7983500	21	17	66	7	27	34	1.5	240	1.5	13
84DCA0034	14531800	7982200	18	16	72	7	26	34	1.6	250	1.2	12
84DCA0035	14525900	7984700	10	15	72	9	24	37	1.7	285	1.2	8
84DCA0036	14525000	7984100	14	12	37	5	19	21	1.0	225	1.3	5
84DCA0037	14524800	7982800	14	10	40	7	20	21	0.9	220	1.7	6
84DCA0041	14523400	7981900	17	16	51	8	19	24	1.2	255	1.2	7
84DCA0043	14521600	7979900	13	10	39	7	15	20	1.0	215	1.3	5
84DCA0044	14520100	7981300	11	11	34	5	15	17	0.9	175	0.8	3
84DCA0045	14520200	7984100	14	13	46	7	16	22	1.1	235	1.0	5
84DCA0046	14521800	7983000	13	14	52	7	18	26	1.3	250	1.0	7
84DCA0047	14523800	7984400	12	10	36	6	14	20	1.0	230	1.4	4
84DCA0048	14524600	7986100	17	18	65	9	24	32	1.7	315	1.0	10
84DCA0049	14526000	7986000	19	17	73	10	25	39	2.1	275	0.8	10
84DCA0051	14528000	7986000	14	13	39	7	20	22	1.0	235	2.0	4
84DCA0055	14527000	7988200	17	17	45	7	18	24	1.2	210	1.9	9
84DCA0056	14525500	7988400	18	17	52	7	19	28	1.3	260	1.6	7
84DCA0057	14524200	7988100	13	13	48	7	18	24	1.1	240	1.3	6
84DCA0058	14525000	7989000	14	15	47	6	17	24	1.2	230	1.8	6
84DCA0059	14525800	7990900	14	14	48	7	18	23	1.2	240	2.0	6
84DCA0060	14525700	7992600	16	15	56	8	22	26	1.3	255	1.3	7
84DCA0061	14525800	7993900	18	17	61	6	19	25	1.4	260	1.9	9
84DCA0062	14526500	7990400	15	14	45	6	20	24	1.2	235	1.3	6
84DCA0064	14529300	7988800	17	16	47	7	20	30	1.4	270	1.4	11
84DCA0065	14530300	7981200	17	18	60	10	28	34	1.5	315	1.2	8
84DCA0066	14531900	7977300	17	19	67	11	26	39	2.0	305	1.2	12
84DCA0067	14533800	7978400	16	15	42	8	22	25	1.2	215	1.4	6
84DCA0068	14534300	7980700	21	20	76	10	27	44	2.7	305	1.2	14
84DCA0069	14535000	7983300	17	12	66	12	40	42	2.5	315	1.2	6
84DCA0070	14534900	7984200	16	15	41	6	21	23	1.1	190	1.6	6
84DCA0071	14533000	7982500	24	17	69	12	31	40	2.0	290	1.6	12
84DCA0072	14531900	7982500	21	16	54	10	23	32	1.6	275	1.2	9
84DCA0077	14549100	8015000	21	23	71	11	34	40	3.2	350	0.9	6
84DCA0078	14548600	8017600	22	22	72	12	42	44	3.6	340	1.2	5
84DCA0079	14548600	8017000	20	20	73	14	36	40	3.4	355	1.0	6
84DCA0080	14550200	8017500	18	19	78	12	29	40	3.2	330	0.9	7
84DCA0081	14551200	8018100	24	21	71	9	28	34	3.0	330	1.2	9
84DCA0082	14551500	8019200	23	22	81	8	27	36	3.2	300	1.0	9
84DCA0083	14551800	8020000	21	22	74	12	30	40	3.2	325	1.2	5
84DCA0084	14552100	8019600	23	21	75	10	32	37	3.2	330	1.3	6

Appendix 2 (cont.)

Sample	East[1]	North	Cu[2]	Pb	Zn	Co	Ni	Cr	Fe	Mn	Ufl	As
84DCA0085	14552000	8018200	31	24	83	11	30	39	3.5	325	1.6	11
84DCA0086	14552300	8017500	21	21	84	12	29	43	3.3	375	0.9	9
84DCA0087	14552100	8016600	18	23	92	13	33	54	4.0	345	0.7	10
84DCA0088	14550200	8015700	16	18	48	8	22	29	2.4	285	0.9	4
84DCA0090	14550900	8015200	23	27	77	15	47	50	3.8	370	0.3	5
84DCA0091	14550800	8015900	22	22	76	9	27	40	3.0	300	0.9	6
84DCA0092	14552600	8015600	21	26	103	13	36	55	3.9	815	0.6	7
84DCA0093	14553700	8015000	19	23	86	11	28	41	3.1	335	0.9	6
84DCA0095	14555700	8015500	25	25	83	11	31	46	3.6	360	1.2	9
84DCA0096	14556500	8015000	27	22	86	14	41	51	3.8	370	1.2	9
84DCA0097	14557800	8014700	27	22	83	13	39	48	3.6	345	0.9	5
84DCA0099	14559500	8014000	33	21	80	13	38	50	3.6	335	0.6	8
84DCA0100	14560400	8014300	32	21	60	11	30	41	2.8	320	0.9	8
84DCA0101	14561500	8015200	36	20	82	14	44	54	3.7	335	0.6	11
84DCA0102	14563700	8016500	84	16	74	18	46	54	3.3	325	0.6	6
84DCA0103	14562000	8017100	38	19	70	12	32	44	3.0	365	1.2	7
84DCA0104	14560800	8016900	27	19	72	12	34	42	3.1	390	1.2	6
84DCA0105	14558500	8017100	28	19	73	10	36	47	3.6	345	1.4	8
84DCA0106	14556500	8017000	29	17	65	11	34	41	2.9	360	1.4	6
84DCA0107	14554400	8016200	22	21	81	9	26	38	3.0	310	1.6	10
84DCA0108	14546900	8016000	21	23	84	12	42	50	3.8	425	1.4	7
84DCA0109	14543600	8013400	20	20	77	10	31	47	3.4	340	1.2	5
84DCA0110	14541800	8012400	20	27	80	11	38	46	3.6	360	1.2	6
84DCA0111	14541000	8012000	15	53	58	7	23	34	2.4	285	1.5	5
84DCA0112	14539900	8010700	17	22	75	9	32	42	3.2	335	1.2	8
84DCA0114	14538100	8018000	17	17	73	11	29	41	3.1	355	1.2	6
84DCA0115	14540200	8018500	22	20	78	12	35	44	3.5	375	1.6	7
84DCA0116	14542500	8018800	20	16	63	9	25	35	2.6	340	0.3	2
84DCA0117	14544000	8018700	18	17	64	8	25	36	2.7	305	1.8	6
84DCA0118	14547600	8018200	24	22	71	9	29	39	3.0	325	1.3	8
84DCA0119	14546200	8014400	24	24	76	11	33	43	3.4	340	1.2	7
84DCA0120	14537000	8003700	15	18	61	7	26	34	2.5	270	0.9	9
84DCA0121	14537900	8001500	20	19	63	8	26	35	2.6	275	1.2	8
84DCA0122	14538100	7998500	11	13	36	5	16	21	1.5	165	1.6	5
84DCA0124	14542600	7998600	18	17	48	7	22	27	2.1	225	1.6	7
84DCA0125	14546100	7999000	20	20	57	9	28	37	2.9	290	1.3	8
84DCA0126	14546500	8001400	14	18	76	9	28	40	2.9	360	1.4	5
84DCA0127	14547100	8003300	21	25	70	13	41	45	3.3	350	1.4	5
84DCA0128	14551600	8006300	44	33	131	16	52	53	4.0	340	0.9	8
84DCA0129	14551300	8011100	21	18	84	17	56	56	3.8	360	0.7	4
84DCA0130	14550800	8014000	20	20	59	9	25	35	2.5	305	0.9	5
84DCA0134	14556100	8018600	28	17	72	12	32	47	3.4	375	1.6	5
84DCA0135	14555500	8019400	21	22	80	11	34	45	3.4	310	1.8	7
84DCA0136	14555600	8020400	30	22	84	14	43	54	3.7	305	1.0	9
84DCA0137	14555700	8021600	31	18	64	11	35	41	2.9	370	1.0	6
84DCA0138	14555300	8022400	24	22	89	10	30	44	3.1	325	0.9	5
84DCA0142	14570500	7994200	23	24	86	10	29	45	3.0	300	1.0	13
84DCA0145	14568000	7992100	24	13	60	12	36	54	3.0	295	0.8	5
84DCA0148	14564600	7991500	28	15	48	9	27	46	2.8	285	0.8	5
84DCA0150	14562100	7990500	16	18	46	7	20	24	1.8	210	1.6	7
84DCA0151	14562700	7991500	22	15	50	10	31	33	2.3	280	0.8	4
84DCA0152	14562700	7993300	20	19	54	8	25	31	2.3	275	1.4	8
84DCA0153	14562300	7994600	18	19	56	8	26	32	2.4	280	1.0	7
84DCA0154	14564800	7996000	20	16	45	7	25	29	2.1	250	1.0	6
84DCA0155	14567800	7996000	21	17	49	8	23	31	2.0	270	0.8	5
84DCA0156	14573400	7997000	33	18	60	12	31	43	2.3	330	0.8	5
84DCA0157	14575800	7997200	27	23	76	11	25	56	3.5	315	0.8	14
84DCA0158	14571000	7992500	27	17	66	10	38	45	2.8	300	0.7	6
84DCA0159	14570200	7991500	14	16	36	6	18	21	1.6	200	1.0	7
84DCA0160	14569400	7990500	15	15	48	9	21	31	1.3	260	1.4	5
84DCA0162	14571500	7988700	34	15	64	16	38	49	2.8	400	0.9	4
84DCA0164	14516400	7987400	37	15	84	16	50	57	3.1	360	0.9	9
84DCA0165	14570300	7984200	21	11	78	12	33	47	2.4	305	0.6	9
84DCA0166	14572000	7982800	23	13	79	13	43	54	2.6	370	0.6	8
84DCA0168	14573200	7981000	21	11	82	12	34	48	2.6	250	0.9	6
84DCA0169	14574700	7981300	32	17	90	13	39	52	2.5	295	0.9	10

	East[1]	North	Cu[2]	Pb	Zn	Co	Ni	Cr	Fe	Mn	Ufl	As
84DCA0170	14575600	7983900	41	16	82	15	45	48	2.8	315	0.6	8
84DCA0171	14573900	7984800	37	18	77	17	44	48	3.0	365	0.8	9
84DCA0172	14573700	7986400	30	17	78	16	50	55	3.4	350	0.7	8
84DCA0173	14574000	7989600	28	15	76	15	49	52	3.1	280	0.8	5
84DCA0175	14574800	7991200	27	17	53	10	33	35	2.4	295	0.2	5
84DCA0176	14572900	7992700	20	21	62	9	27	36	2.9	310	1.3	10
84DCA0177	14571000	7996000	18	19	48	7	23	29	2.2	280	1.5	9
84DCA0178	14570900	7997800	21	15	48	8	23	30	2.1	295	0.9	6
84DCA0179	14570500	8001500	17	18	55	8	25	34	2.4	285	1.0	11
84DCA0180	14570300	8004200	23	19	62	10	31	36	2.6	340	0.9	7
84DCA0181	14569500	8009500	13	8	56	12	37	67	3.4	215	0.9	2
84DCA0182	14565200	8011200	101	13	63	13	34	48	2.7	250	0.9	5
84DCA0183	14557000	8012200	34	22	69	12	34	40	2.8	390	0.9	7
84DCA0184	14558100	8010000	25	14	86	13	40	59	3.5	245	0.7	4
84DCA0185	14560400	8006700	24	18	79	16	44	58	3.8	420	0.9	6
84DCA0186	14561000	8004500	37	19	80	14	42	60	4.0	350	0.9	8
84DCA0187	14563300	8001500	24	21	84	12	37	55	3.7	320	0.7	8
84DCA0189	14565800	7998000	18	18	52	7	23	29	2.2	275	1.4	7
84DCA0193	14576500	8006600	23	17	72	11	35	52	3.2	280	0.6	5
84DCA0194	14581000	8004500	19	23	72	10	28	40	2.9	375	1.4	7
84DCA0195	14582700	8003300	22	18	66	10	28	46	3.1	330	1.4	7
84DCA0197	14581800	8000600	19	14	73	12	39	58	3.6	255	0.6	5
84DCA0198	14580300	7900000	27	18	67	11	34	48	3.4	295	0.9	7
84DCA0199	14577100	7993600	32	17	97	11	32	41	2.8	300	0.7	6
84DCA0200	14579700	7991600	24	17	63	10	29	34	2.8	290	0.9	5
84DCA0203	14586100	7993500	36	18	68	11	37	43	3.2	300	0.7	9
84DCA0204	14585600	7991000	32	16	75	12	40	46	3.1	360	0.6	5
84DCA0205	14585100	7989000	98	7	64	11	23	62	2.1	118	0.2	2
84DCA0206	14583000	7990300	25	10	95	10	33	42	2.3	185	0.7	3
84DCA0212	14557100	7953800	19	16	57	10	25	32	1.4	270	1.1	6
84DCA0214	14557800	7956500	17	16	73	10	26	36	1.8	320	1.6	7
84DCA0215	14560300	7958200	16	18	58	7	20	32	1.6	260	1.0	9
84DCA0216	14562700	7961900	17	17	70	9	21	36	1.8	270	1.1	9
84DCA0217	14566000	7964000	19	16	62	9	21	34	1.7	290	0.9	9
84DCA0218	14567000	7966200	18	18	70	8	21	36	1.9	320	1.0	7
84DCA0219	14567900	7968900	17	20	62	8	21	33	1.7	280	0.7	10
84DCA0220	14569400	7975500	27	25	69	11	32	40	2.3	300	0.8	10
84DCA0221	14563600	7975000	19	18	81	12	34	43	2.6	340	0.6	7
84DCA0222	14562100	7971500	16	18	51	8	21	25	1.3	280	1.0	6
84DCA0223	14561500	7969100	22	17	76	15	52	44	2.8	325	0.8	6
84DCA0224	14560300	7969600	19	18	75	10	29	37	2.2	375	1.8	7
84DCA0225	14559100	7968100	25	22	82	15	53	46	2.4	335	1.2	7
84DCA0226	14557700	7963100	19	19	65	9	24	36	1.7	320	1.2	9
84DCA0228	14554800	7957700	21	20	67	11	31	38	2.2	315	1.4	7
84DCA0233	14556600	7952300	18	16	53	8	31	31	1.4	270	1.2	8
84DCA0234	14553700	7951500	17	19	62	7	22	33	1.7	315	1.2	9
84DCA0235	14551000	7951800	15	20	73	7	23	37	2.2	290	1.6	10
84DCA0237	14550500	7952900	16	18	57	7	23	30	1.6	275	1.5	8
84DCA0238	14550500	7953800	16	17	73	10	25	36	2.1	305	1.6	8
84DCA0239	14551700	7956000	19	18	57	8	26	37	1.7	260	1.2	7
84DCA0240	14552100	7954500	17	19	50	8	21	30	1.4	270	1.4	9
84DCA0241	14553000	7953000	21	19	62	9	37	35	1.7	310	1.2	7
84DCA0242	14555100	7954600	20	17	63	9	32	37	1.8	285	1.2	7
84DCA0243	14555100	7953200	18	17	52	8	28	30	1.3	225	1.	4
84DCA0246	14555100	7961800	19	19	73	10	29	40	2.0	390	1.2	4
84DCA0247	14555700	7965800	16	16	67	9	26	37	1.8	320	1.3	4
84DCA0248	14555100	7968500	22	20	87	13	34	40	2.2	495	1.2	4
84DCA0249	14552600	7970000	24	20	68	10	30	40	3.0	295	1.	10
84DCA0250	14553000	7972200	25	24	69	11	32	40	3.2	355	1.	8
84DCA0251	14551800	7975800	20	24	72	11	32	40	3.4	415	0.6	8
84DCA0252	14549800	7974000	25	22	76	12	41	45	3.8	325	0.8	7
84DCA0253	14549800	7970700	22	20	82	13	33	46	3.8	410	1.	6
84DCA0254	14551000	7964000	18	18	66	10	24	36	2.9	360	1.3	5
84DCA0255	14552000	7959800	16	21	60	8	24	34	2.8	295	1.3	7
84DCA0256	14549600	7954400	21	18	58	8	30	34	2.7	275	0.9	7
84DCA0257	14548000	7955400	19	20	64	8	26	35	2.9	265	1.	7

Appendix 2 (cont.)

Sample	East[1]	North	Cu[2]	Pb	Zn	Co	Ni	Cr	Fe	Mn	Ufl	As
84DCA0258	14544400	7957000	25	25	75	10	28	38	3.4	335	1.1	16
84DCA0259	14545300	7960200	23	21	70	10	29	36	3.1	310	1.	8
84DCA0260	14544500	7963500	19	21	68	8	23	36	3.2	400	2.1	7
84DCA0261	14542000	7963800	19	18	72	10	27	42	3.2	340	1.	11
84DCA0262	14540300	7963000	14	21	69	8	23	40	3.0	315	1.	9
84DCA0263	14539500	7960300	15	17	82	12	29	50	3.4	300	1.1	6
84DCA0264	14539500	7957100	14	17	55	8	24	32	2.3	245	1.	7
84DCA0265	14539300	7954800	17	15	62	9	32	36	2.6	240	0.8	5
84DCA0403	14506000	8211200	34	11	70	17	51	67	3.9	290	1.	6
84DCA0407	14521000	8215000	21	15	68	11	29	42	3.2	280	1.4	6
84DCA0408	14521200	8214200	35	11	62	17	43	57	4.0	240	1.5	8
84DCA0410	14520000	8213800	22	11	74	20	61	69	4.5	270	1.	5
84DCA0411	14519800	8213600	20	7	75	20	63	64	4.6	285	1.1	6
84DCA0412	14519500	8213200	67	14	98	21	59	57	4.6	260	1.3	10
84DCA0413	14518700	8213000	29	11	67	23	85	75	5.6	315	1.3	6
84DCA0414	14518000	8213000	48	8	83	18	56	55	4.4	240	1.3	8
84DCA0415	14517000	8213100	24	8	71	19	55	60	4.3	245	1.3	5
84DCA0416	14516200	8213200	32	8	74	19	53	60	4.8	280	1.	5
84DCA0417	14515600	8213200	33	8	69	20	54	54	4.6	235	1.1	7
84DCA0421	14512500	8213500	47	14	86	19	48	56	4.3	255	1.2	12
84DCA0422	14514900	8211500	41	30	60	23	51	40	4.0	230	1.3	8
84DCA0423	14514800	8210700	66	59	137	23	52	49	4.8	500	0.9	19
84DCA0424	14515300	8209500	22	8	61	19	48	51	4.2	280	0.9	3
84DCA0425	14512600	8207600	46	11	71	24	51	52	3.9	340	0.8	3
84DCA0426	14513300	8208000	45	14	104	22	60	52	4.1	270	1.	6
84DCA0427	14511000	8207600	43	14	88	20	55	54	4.3	245	1.1	9
84DCA0428	14510800	8206000	40	12	67	20	55	56	4.3	245	1.1	4
84DCA0431	14524000	8214800	22	11	80	21	61	64	4.6	330	1.	6
84DCA0432	14522800	8214700	16	7	71	21	56	61	4.8	290	0.7	6
84DCA0433	14523400	8214300	17	7	78	23	58	62	4.4	315	1.	5
84DCA0434	14522400	8214300	16	7	69	21	51	55	4.3	230	0.7	5
84DCA0435	14521700	8214200	23	6	73	23	56	52	3.9	240	0.7	6
84DCA0436	14521400	8215000	21	7	71	23	59	56	4.3	255	0.8	4
84DCA0437	14524800	8216000	19	8	79	23	63	67	4.4	335	1.	5
84DCA0438	14527600	8217000	49	16	97	19	49	60	4.8	245	1.3	12
84DCA0439	14528200	8216900	47	11	90	23	65	74	4.1	570	0.6	6
84DCA0440	14529000	8216800	38	12	92	23	62	70	4.7	365	0.9	7
84DCA0441	14528500	8217500	37	8	86	23	72	74	4.4	330	0.9	7
84DCA0442	14525200	8217300	21	8	83	22	63	58	4.3	280	0.9	5
84DCA0443	14524200	8217400	18	8	70	21	59	64	4.2	240	0.7	5
84DCA0444	14524800	8215000	12	7	67	23	59	52	3.9	285	0.9	5
84DCA0445	14523700	8216400	14	4	68	26	67	66	4.2	440	0.9	5
84DCA0446	14523900	8216000	34	6	72	24	61	60	4.6	285	0.9	4
84DCA0485	14527400	8220000	23	9	82	23	69	68	4.3	270	1.1	8
84DCA0486	14528000	8219800	25	9	84	24	79	92	4.8	295	1.4	7
84DCA0487	14528500	8219800	38	13	85	23	83	90	4.7	280	1.3	8
84DCA0488	14529200	8220200	34	12	87	24	79	104	5.1	320	1.4	9
84DCA0489	14529000	8220700	35	10	83	22	78	94	4.8	255	1.2	8
84DCA0490	14528400	8220500	31	11	85	24	85	114	4.9	380	0.5	7
84DCA0491	14529500	8220800	38	9	86	23	93	121	4.7	260	1.2	6
84DCA0492	14529500	8221200	39	9	85	27	123	220	5.1	250	1.2	7
84DCA0493	14530300	8220800	51	9	92	26	98	93	4.6	265	0.6	7
84DCA0494	14530200	8221200	53	9	88	27	97	215	4.2	500	0.9	7
84DCA0495	14530700	8221100	50	8	78	26	102	155	4.8	265	1.	5
84DCA0496	14539400	8222000	47	13	86	26	101	170	4.2	530	0.9	10
84DCA0528	14541300	8220900	30	11	78	20	66	98	4.4	540	1.	8
84DCA0529	14541200	8220100	48	9	80	27	125	172	5.0	785	0.7	11
84DCA0530	14539800	8221300	32	14	76	18	49	50	4.1	375	1.	5
84DCA0531	14523000	8202400	34	10	76	21	61	80	4.2	300	0.9	8
84DCA0534	14522800	8204900	46	11	81	21	61	81	4.3	315	0.9	8
84DCA0535	14522700	8205700	54	10	78	23	68	102	4.7	415	0.9	10
84DCA0536	14520200	8207200	45	10	70	20	55	74	4.6	245	0.6	2
84DCA0537	14521200	8208000	13	7	58	22	50	51	3.7	210	0.7	7
84DCA0538	14521400	8209700	28	12	76	21	56	60	4.0	370	1.	6
84DCA0539	14525400	8211100	34	17	86	20	56	59	4.2	425	1.	9
84DCA0540	14526400	8208300	31	9	73	24	67	64	4.0	340	0.8	7

Sample	East[1]	North	Cu[2]	Pb	Zn	Co	Ni	Cr	Fe	Mn	Ufl	As
84DCA0541	14527300	8213800	33	16	85	18	52	64	4.4	335	1.3	9
84DCA0542	14528000	8215500	37	10	80	21	63	58	4.6	255	0.6	5
84DCA0543	14530600	8215600	31	24	91	19	54	62	4.4	415	0.9	6
84DCA0544	14537000	8223100	29	20	75	13	41	47	3.4	285	0.9	9
84DCA0545	14535500	8221200	29	19	86	14	41	50	4.1	300	1.1	9
84DCA0546	14533600	8220500	35	20	80	14	39	45	3.9	325	0.7	9
84DCA0547	14527500	8212500	45	20	99	19	54	64	5.0	330	1.3	13
84DCA0555	14527500	8207000	43	8	53	21	57	72	3.8	315	0.4	7
84DCA0557	14517400	8197800	59	6	57	19	68	87	3.5	220	0.6	4
84DCA0559	14513000	8196900	41	109	84	21	99	94	3.7	500	0.6	11
84DCA0560	14513600	8197500	38	10	71	18	64	72	3.8	270	0.9	4
84DCA0561	14521700	8204400	37	5	64	24	66	63	4.0	270	0.6	2
84DCA0562	14518100	8205600	20	6	64	23	58	58	4.3	325	0.4	2
84DCA0563	14518500	8206900	25	12	67	18	47	60	4.3	235	0.9	5
84DCA0564	14516100	8207200	31	11	61	19	54	56	4.1	225	0.4	3
84DCA0566	14516300	8204300	68	21	73	21	53	52	4.1	270	0.8	8
84DCA0567	14513700	8204800	60	21	85	23	49	48	4.1	205	1.3	10
84DCA0568	14513000	8202200	51	11	66	19	53	56	4.0	255	0.9	6
84DCA0569	14515000	8202300	50	9	58	22	51	51	3.9	255	0.9	2
84DCA0570	14520200	8201000	43	9	66	20	54	68	4.0	200	1.1	5
84DCA0571	14521000	8200500	33	7	65	22	61	67	4.4	235	1.3	4
84DCA0582	14491700	8198600	38	13	84	13	39	44	2.8	255	1.5	8
84DCA0583	14491300	8198800	42	15	94	13	40	46	3.3	250	1.3	9
84DCA0584	14490200	8199800	48	13	85	13	41	45	3.0	280	1.1	8
84DCA0585	14490700	8199100	43	16	89	13	40	43	2.9	275	1.5	10
84DCA0586	14491000	8198400	37	13	81	12	30	39	2.4	285	1.5	7
84DCA0587	14492300	8197700	44	13	90	14	39	43	3.2	270	1.1	8
84DCA0589	14489100	8200700	46	17	138	13	41	44	2.9	290	1.1	13
84DCA0590	14493200	8203100	38	26	235	16	62	69	2.9	335	0.9	14
84DCA0591	14495300	8201200	39	12	340	15	50	48	3.0	235	1.3	7
84DCA0592	14492200	8194400	41	16	98	13	36	43	3.1	275	1.3	10
84DCA0594	14495100	8195700	41	19	153	13	45	48	2.7	300	1.7	18
84DCA0596	14506900	8195800	59	9	69	21	65	66	3.5	275	0.9	3
84DCA0597	14502600	8200600	56	13	92	20	75	74	4.0	345	0.9	6
84DCA0598	14498000	8201500	44	21	180	17	58	56	3.8	265	1.3	12
84DCA0599	14497300	8202800	46	17	147	17	54	54	3.4	270	1.6	10
84DCA0600	14496100	8204500	53	23	166	19	69	77	4.2	310	1.	10
84DCA0601	14494800	8198200	41	16	155	14	45	51	3.2	300	1.	10
84DCA0602	14497300	8199500	35	15	230	14	49	51	3.1	305	1.6	10
84DCA0603	14500500	8198000	45	24	149	17	62	63	3.8	255	1.6	13
84DCA0701	14415700	8093300	29	20	97	15	35	55	4.2	435	2.	9
84DCA0708	14418200	8086400	26	19	80	14	38	50	3.8	375	1.	7
84DCA0709	14416000	8087400	30	26	103	14	39	58	4.6	395	1.1	15
84DCA0710	14413200	8088600	26	45	98	17	44	60	4.5	500	0.9	17
84DCA0712	14407000	8093500	19	24	90	12	31	53	4.8	405	1.6	19
84DCA0713	14407500	8098500	19	23	106	12	30	53	4.4	420	2.	8
84DCA0714	14404700	8096600	22	19	74	10	30	49	3.4	320	1.3	13
84DCA0715	14402000	8092200	15	14	39	6	19	25	1.8	205	1.	6
84DCA0720	14419500	8081200	25	19	76	14	39	49	3.9	435	1.	10
84DCA0722	14415200	8083000	34	23	108	19	56	67	5.3	495	1.	9
84DCA0723	14416500	8081100	35	30	92	19	49	62	5.1	465	1.	13
84DCA0724	14419200	8077500	23	20	60	11	32	40	3.1	360	1.1	9
84DCA0725	14421900	8075200	25	19	75	13	31	48	3.6	375	1.6	7
84DCA0726	14425000	8073500	24	20	73	13	39	51	3.6	365	1.4	9
84DCA0728	14423900	8079300	24	17	75	15	37	46	3.5	410	1.2	7
84DCA0729	14404500	8090000	29	36	78	14	35	46	4.2	460	1.4	18
84DCA0730	13595400	8086700	17	19	78	9	27	42	3.4	325	1.6	10
84DCA0731	13591000	8083500	13	13	35	6	17	22	1.7	205	1.6	8
84DCA0732	13589600	8082800	15	15	46	6	21	31	2.1	230	1.6	7
84DCA0733	13590700	8079000	18	17	55	8	25	39	2.7	250	2.1	9
84DCA0734	13593200	8077800	17	13	38	6	18	20	1.8	164	1.8	9
84DCA0737	14410300	8088000	19	22	73	8	23	33	2.9	245	1.4	11
84DCA0738	14408400	8088500	20	22	74	10	29	50	3.5	320	1.6	11
84DCA0739	14404700	8085400	24	23	79	13	42	60	3.8	360	1.2	9
84DCA0740	14402200	8080500	16	15	46	8	25	41	2.2	230	1.2	4
84DCA0741	14402700	8077500	19	21	70	10	30	48	3.5	310	1.6	11

Appendix 2 (cont.)

Sample	East[1]	North	Cu[2]	Pb	Zn	Co	Ni	Cr	Fe	Mn	Ufl	As
84DCA0742	14404700	8071200	17	16	42	6	22	24	2.0	245	1.8	8
84DCA0743	14406600	8072300	20	19	51	7	20	25	2.3	235	1.4	10
84DCA0744	14405600	8078800	23	22	72	10	29	39	3.2	265	1.1	16
84DCA0745	14416000	8089500	27	25	104	16	37	52	4.4	450	1.1	14
84DCA0750	14469300	8178200	26	9	97	8	40	29	2.1	235	2.4	9
84DCA0751	14470700	8177000	21	11	115	9	32	31	2.5	230	1.9	9
84DCA0752	14474200	8176200	25	11	112	9	38	31	2.5	240	1.8	9
84DCA0753	14468500	8183000	20	11	94	10	34	34	2.5	255	1.4	6
84DCA0754	14468500	8185700	20	12	91	10	34	38	2.9	260	1.3	11
84DCA0756	14469400	8187500	34	22	133	14	61	65	4.6	390	1.2	14
84DCA0758	14479900	8190600	34	17	107	17	58	63	4.7	335	0.8	12
84DCA0759	14482900	8193600	36	32	127	18	54	60	4.0	340	0.8	21
84DCA0761	14467000	8180000	27	12	101	10	41	30	2.7	260	2.	13
84DCA0762	14466500	8177800	25	10	109	9	39	29	2.4	245	2.4	9
84DCA0763	14463700	8175200	29	11	92	9	36	32	2.5	250	1.8	10
84DCA0764	14461000	8173000	27	12	94	9	35	32	2.6	250	1.6	10
84DCA0765	14459000	8171100	26	13	93	13	43	36	3.0	315	1.4	14
84DCA0767	14457300	8168000	18	13	76	9	29	33	2.2	260	1.7	6
84DCA0768	14463000	8166800	26	14	128	10	37	38	3.2	260	1.5	11
84DCA0769	14466600	8165800	24	11	111	9	35	30	2.4	260	1.6	9
84DCA0770	14471700	8169400	32	152	133	14	48	55	4.0	350	1.3	14
84DCA0771	14471400	8166700	39	16	135	17	57	60	4.1	335	1.6	12
84DCA0774	14463800	8189500	21	14	120	8	31	36	2.5	270	0.8	14
84DCA0775	14453000	8195400	23	16	156	11	39	48	3.3	360	1.6	13
84DCA0776	14456000	8191200	24	10	115	8	38	34	2.7	250	1.5	13
84DCA0777	14458700	8188300	26	11	98	8	37	30	2.4	235	1.6	10
84DCA0778	14477100	8176200	32	16	130	14	50	51	3.6	310	1.8	11
84DCA0780	14515000	8172100	32	8	67	17	54	65	4.2	340	0.8	5
84DCA0781	14515500	8173600	59	10	64	20	66	94	3.8	280	0.3	6
84DCA0782	14517200	8173500	47	7	64	21	63	88	4.0	380	0.5	5
84DCA0783	14518600	8171300	48	6	58	16	52	64	3.0	370	0.8	4
84DCA0786	14519900	8171700	63	7	60	17	52	66	3.7	320	0.8	6
84DCA0787	14522500	8171200	53	12	67	18	47	72	4.0	310	1.2	10
84DCA0788	14521700	8173500	23	10	61	25	63	98	5.4	310	0.6	3
84DCA0789	14519200	8173400	27	5	64	29	73	123	3.6	250	0.6	2
84DCA0790	14513000	8171700	24	15	71	24	60	63	5.1	375	0.6	4
84DCA0791	14513200	8173500	47	14	58	22	51	63	4.5	350	0.8	4
84DCA0792	14513600	8175000	86	10	64	21	55	73	4.4	290	0.7	3
84DCA0793	14516300	8175800	54	12	64	20	58	83	5.0	320	0.8	2
84DCA0794	14518000	8180600	35	10	52	21	45	68	4.4	495	0.6	2
84DCA0795	14514500	8170500	47	10	66	20	47	55	4.1	305	0.8	4
84DCA0796	14519000	8166500	65	21	116	25	62	67	4.8	350	0.8	6
84DCA0797	14515000	8167200	31	11	56	20	56	68	4.7	310	0.8	2
84DCA0798	14516600	8166500	87	16	80	20	60	76	4.6	280	0.6	4
84DCA0799	14517500	8168200	131	11	59	19	53	56	4.4	275	0.8	4
84DCA0800	14516000	8169600	49	11	66	22	48	54	4.1	315	0.8	4
84DCA0801	14511400	8172800	27	11	70	18	54	62	3.8	280	0.3	2
84DCA0802	14510300	8175600	23	10	68	22	60	61	4.6	340	0.6	2
84DCA0803	14511800	8176000	53	12	67	28	70	68	4.6	295	0.8	4
84DCA0805	14515000	8179700	49	14	79	20	46	63	4.4	295	0.8	4
84DCA0808	14517100	8188000	45	16	73	20	47	65	4.1	355	0.6	9
84DCA0809	14515200	8185200	48	13	78	20	55	84	4.9	315	0.4	6
84DCA0811	14520000	8168500	67	15	70	21	60	70	5.0	300	0.6	2
84DCA0812	14512000	8170500	56	13	73	20	52	59	4.4	305	0.7	3
84DCA0813	14511500	8169400	59	23	88	18	56	66	4.6	300	0.8	10
84DCA0815	14510500	8172500	37	14	73	17	46	55	4.1	270	0.6	11
84DCA0816	14508000	8171500	48	19	87	20	53	63	4.6	335	0.6	3
84DCA0817	14507000	8174500	43	15	67	21	52	57	4.1	385	0.8	4
84DCA0819	14506400	8169500	79	13	79	25	70	77	4.8	335	0.8	4
84DCA0820	14508600	8168000	58	11	75	24	69	80	4.6	340	0.8	4
84DCA0821	14511000	8167700	60	13	68	21	60	78	4.5	270	1.3	5
84DCA0822	14513200	8167400	55	11	75	21	61	82	4.3	295	0.8	4
84DCA0823	14505400	8175700	44	15	78	29	69	63	4.6	385	0.8	4
84DCA0824	14503000	8175700	24	18	68	14	30	42	3.1	320	1.1	6
84DCA0825	14500900	8176200	43	16	74	20	50	61	4.1	365	0.8	5
84DCA0826	14499000	8177400	24	7	71	21	76	107	5.2	355	0.3	2

Sample	East[1]	North	Cu[2]	Pb	Zn	Co	Ni	Cr	Fe	Mn	Ufl	As
84DCA0828	14495800	8177000	32	16	82	21	45	56	3.8	325	0.8	7
84DCA0830	14495900	8181100	53	22	91	23	67	71	5.0	330	0.7	11
84DCA0831	14499000	8183700	23	15	66	14	29	38	2.6	300	1.6	3
84DCA0832	14506200	8184300	28	17	65	14	35	47	3.0	295	1.1	5
84DCA0833	14506400	8181800	36	20	66	19	52	55	3.8	340	0.8	6
84DCA0834	14506700	8178800	38	12	60	21	60	64	4.4	350	1.1	3
84DCA0835	14509500	8177000	45	21	80	22	68	72	4.2	345	0.8	5
84DCA0836	14509000	8178700	65	36	71	28	65	80	4.9	520	0.8	17
84DCA0837	14511000	8180300	77	21	72	23	59	68	5.0	335	0.8	6
84DCA0838	14510900	8182500	54	20	77	23	74	65	4.0	300	0.8	6
84DCA0839	14508400	8183100	53	32	72	26	76	90	4.8	305	0.8	8
84DCA0840	14509200	8185700	42	36	73	19	56	70	4.2	345	0.6	11
84DCA0842	14512500	8187700	66	65	74	28	61	73	4.6	400	0.8	11
84DCA0843	14518300	8188600	91	13	72	26	74	89	4.8	325	1.1	10
84DCA0845	14521200	8184600	39	8	60	23	57	78	3.8	230	0.6	3
84DCA0846	14519500	8169000	47	14	58	20	52	58	4.0	285	0.6	6
84DCA0847	14524000	8166200	179	9	52	18	55	51	3.5	225	0.8	10
84DCA0848	14525000	8168200	18	7	48	19	50	54	3.9	330	0.8	3
84DCA0849	14523100	8169500	142	17	79	25	55	81	6.2	420	0.7	13
84DCA0850	14511500	8166100	51	10	77	23	68	82	4.8	345	0.7	4
84DCA0851	14513000	8163600	52	10	72	24	70	98	5.0	350	0.7	2
84DCA0852	14511200	8161700	67	21	86	23	63	74	4.7	320	0.8	7
84DCA0853	14514000	8158700	56	18	75	19	62	72	5.0	315	0.8	4
84DCA0854	14515600	8157400	53	20	84	19	52	63	5.4	280	0.8	9
84DCA0855	14514500	8165700	46	9	68	21	69	81	5.0	310	0.8	3
84DCA0858	14531700	8139900	123	16	62	22	44	85	6.3	285	0.6	5
84DCA0859	14532500	8140500	107	18	76	25	60	88	5.4	360	0.6	8
84DCA0860	14532500	8142100	64	12	56	21	48	79	4.7	305	0.8	4
84DCA0862	14530900	8144000	153	24	68	24	56	86	5.3	390	0.4	9
84DCA0863	14528800	8142700	58	21	81	27	66	73	5.5	370	0.8	3
84DCA0864	14526700	8140700	115	11	52	20	53	78	5.1	260	0.8	6
84DCA0865	14527500	8138500	59	12	57	24	62	77	4.4	295	0.3	3
84DCA0866	14528400	8135000	65	24	80	35	67	82	6.0	475	0.5	9
84DCA0867	14531400	8135400	59	14	60	24	58	88	5.4	280	0.4	3
84DCA0868	14532800	8144700	571	20	91	30	58	95	5.2	250	0.3	20
84DCA0869	14533400	8148200	31	9	51	21	51	115	5.7	400	0.3	3
84DCA0870	14532800	8150500	42	8	48	21	47	104	5.7	240	0.6	3
84DCA0871	14532100	8154000	172	7	44	21	50	94	5.5	260	0.6	4
84DCA0872	14529400	8153100	107	14	55	22	54	89	5.1	335	0.6	4
84DCA0873	14527000	8150700	8	6	32	15	43	94	4.6	141	0.6	2
84DCA0874	14526300	8148200	37	15	66	29	69	59	4.8	300	0.8	5
84DCA0875	14529000	8146500	94	18	78	26	63	81	5.4	335	0.6	7
84DCA0876	14530200	8160300	81	15	58	17	42	80	4.8	215	0.6	6
84DCA0877	14528000	8162500	43	10	44	16	41	80	5.1	195	0.7	5
84DCA0880	14519700	8162100	34	15	69	26	54	76	5.8	355	0.6	4
84DCA0881	14518500	8159800	38	15	60	21	53	67	4.4	330	0.3	4
84DCA0882	14518100	8156800	41	15	68	22	53	69	4.6	305	0.3	5
84DCA0884	14517600	8152300	40	17	69	18	54	62	4.2	270	0.6	4
84DCA0886	14519500	8149100	55	19	81	19	66	72	4.7	275	0.5	9
84DCA0887	14522600	8151000	54	14	91	20	64	75	4.6	305	0.6	6
84DCA0888	14525600	8151700	18	5	47	21	68	80	3.6	330	0.3	2
84DCA0889	14527500	8144600	55	15	73	19	58	86	4.8	270	0.6	8
84DCA0890	14521400	8147800	36	7	60	22	62	72	4.3	290	0.6	3
84DCA0891	14520100	8144500	55	15	64	24	64	80	4.8	360	0.6	4
84DCA0892	14518000	8142100	46	14	67	23	66	78	4.8	315	0.6	4
84DCA0893	14518600	8139100	52	13	67	24	65	80	4.6	330	0.6	4
84DCA0894	14518200	8134900	59	14	64	22	61	80	4.6	260	0.4	4
84DCA0895	14520200	8131700	25	9	80	21	55	70	4.6	280	0.5	2
84DCA0897	14523600	8130600	49	16	72	22	50	67	5.7	325	0.6	4
84DCA0898	14527200	8131200	69	13	61	23	64	65	4.3	380	0.6	7
84DCA0899	14538000	8140500	15	5	31	15	43	67	3.4	110	0.2	2
84DCA0905	14539000	8143200	19	9	47	15	38	65	4.2	215	0.6	6
84DCA0906	14551400	8141600	18	10	50	18	47	74	4.7	495	0.7	5
85DCA0002	14555800	8082300	43	11	32	11	24	55	3.6	410	0.4	8
85DCA0004	14555800	8079000	82	5	33	12	28	54	2.8	150	0.1	5
85DCA0007	14550200	8071000	95	26	110	24	52	89	5.1	360	0.7	11

Appendix 2 (cont.)

Sample	East[1]	North	Cu[2]	Pb	Zn	Co	Ni	Cr	Fe	Mn	Ufl	As
85DCA0008	14549800	8063400	42	14	69	18	46	85	4.8	340	0.6	6
85DCA0009	14553500	8057000	65	13	65	16	45	72	5.0	280	0.7	11
85DCA0010	14543800	8060000	40	13	68	17	42	74	5.0	325	0.6	7
85DCA0011	14540500	8066000	32	23	86	16	43	67	2.8	415	0.3	16
85DCA0012	14541200	8075300	41	26	83	17	50	65	2.8	310	0.2	16
85DCA0013	14548400	8094700	6	8	40	16	26	54	4.0	150	0.7	4
85DCA0015	14547800	8091100	33	13	80	16	41	66	5.0	260	0.6	10
85DCA0016	14540600	8082100	38	26	82	16	42	70	5.3	310	0.6	24
85DCA0017	14539500	8085200	37	18	92	16	46	64	4.6	280	0.8	6
85DCA0018	14537500	8089500	33	17	80	17	51	70	4.9	300	0.8	10
85DCA0019	14533500	8086200	51	26	88	22	56	70	5.7	390	0.8	4
85DCA0020	14530200	8084500	30	22	85	17	49	60	4.7	310	0.7	8
85DCA0021	14531400	8080600	16	9	74	17	49	71	4.8	290	0.3	6
85DCA0022	14530400	8077200	28	21	82	13	45	53	3.6	300	0.5	10
85DCA0023	14533500	8079000	52	30	84	16	49	65	5.3	370	0.6	10
85DCA0024	14538200	8080000	33	20	73	15	45	65	5.2	270	0.8	11
85DCA0025	14544000	8082700	41	29	87	13	41	63	4.6	265	0.3	17
85DCA0026	14551800	8080300	268	19	74	18	37	66	4.4	390	0.3	12
85DCA0028	14543800	8084400	40	17	60	18	40	68	4.6	550	0.6	10
85DCA0029	14540600	8089100	27	15	56	15	37	60	4.3	300	0.8	7
85DCA0030	14539400	8093000	59	18	96	22	42	70	4.8	310	0.3	11
85DCA0031	14535600	8095000	43	18	88	18	45	72	5.1	330	0.6	10
85DCA0032	14533500	8097500	49	15	80	16	48	78	6.0	330	0.8	11
85DCA0033	14531800	8101500	27	17	78	13	39	62	4.1	310	0.8	11
85DCA0034	14535800	8103000	41	14	76	14	49	65	4.4	340	0.8	7
85DCA0036	14544200	8000000	54	14	76	16	45	74	4.7	350	0.3	8
85DCA0037	14544200	8094400	31	13	52	13	34	68	4.4	210	0.8	5
85DCA0038	14544300	8088100	13	7	36	10	24	54	3.5	130	0.8	3
85DCA0039	14550500	8088000	58	18	84	22	46	75	5.0	260	0.7	14
85DCA0041	14551800	8090500	13	7	40	13	28	55	3.4	260	0.8	3
85DCA0043	14501300	7944000	29	20	92	12	39	42	3.8	280	1.1	28
85DCA0044	14498000	7941200	23	18	83	13	33	54	3.4	235	1.3	14
85DCA0045	14498000	7935200	30	23	102	12	36	52	4.8	250	1.1	47
85DCA0046	14496800	7930000	30	16	114	11	36	50	3.9	235	1.3	30
85DCA0048	14491800	7936300	25	13	84	11	37	46	2.2	265	0.9	7
85DCA0049	14490300	7948000	21	19	80	11	39	37	3.3	235	0.9	15
85DCA0050	14497000	7947000	16	16	68	10	28	36	2.5	250	1.1	11
85DCA0054	14507100	7947800	19	16	56	10	25	28	2.0	220	1.1	12
85DCA0055	14511200	7952100	23	22	58	10	32	35	2.0	260	0.8	15
85DCA0056	14515000	7958600	23	15	66	8	29	37	2.1	210	1.	15
85DCA0057	14519700	7956500	16	17	56	8	21	34	2.0	310	1.5	9
85DCA0059	14520000	7950000	12	13	56	7	17	21	1.4	180	1.	7
85DCA0060	14515000	7946500	17	15	47	8	25	30	1.7	205	1.	11
85DCA0061	14509700	7943800	19	14	55	9	22	22	2.2	225	1.3	11
85DCA0062	14509100	7938000	14	11	49	9	21	24	1.7	210	1.5	11
85DCA0063	14508200	7931400	24	19	60	9	26	39	2.4	230	1.5	21
85DCA0064	14513000	7930800	22	16	55	9	30	35	2.1	210	1.3	14
85DCA0065	14520300	7933000	16	14	56	6	25	28	1.5	215	1.	15
85DCA0066	14522600	7938000	13	10	34	6	19	17	1.2	165	1.	7
85DCA0067	14514800	7939700	16	16	47	6	24	26	1.9	210	1.1	11
85DCA0068	14508000	7941600	18	13	52	7	21	28	1.8	205	1.	11
85DCA0069	14497500	7953000	17	13	67	7	25	43	1.9	210	1.	6
85DCA0070	14497400	7965100	25	17	85	12	37	50	3.3	250	1.3	10
85DCA0071	14506600	7974500	12	11	33	5	17	17	1.1	170	1.	5
85DCA0072	14504000	7968600	15	13	41	5	20	20	1.5	200	1.1	9
85DCA0073	14504200	7962000	17	15	47	6	20	21	1.7	220	1.	10
85DCA0074	14503100	7954600	19	16	90	11	34	40	2.4	260	1.1	12
85DCA0076	14506000	7939000	19	18	60	7	23	35	1.8	290	1.	18
85DCA0077	14505800	7930500	17	16	52	8	22	25	1.8	250	1.3	9
85DCA0078	14504000	7925000	17	13	116	7	32	35	3.5	230	1.3	10
85DCA0080	14500000	7923000	26	18	70	11	34	35	2.6	265	1.9	13
85DCA0081	14499500	7932400	19	16	80	9	26	39	2.9	240	1.	17
85DCA0082	14500200	7938600	23	18	85	12	34	48	3.4	290	0.8	20
85DCA0085	14569800	8047100	54	17	74	13	39	75	4.0	300	0.3	6
85DCA0086	14565200	8048000	10	10	62	18	50	68	4.6	365	0.8	7
85DCA0089	14597500	8056700	11	8	52	16	44	92	4.5	290	0.3	6

Sample	East[1]	North	Cu[2]	Pb	Zn	Co	Ni	Cr	Fe	Mn	Ufl	As
85DCA0090	14571500	8061100	36	13	72	18	48	110	4.8	350	0.8	6
85DCA0091	14576700	8055800	34	13	84	22	45	106	4.2	540	0.3	7
85DCA0093	14577800	8045200	35	8	70	11	25	48	2.8	300	0.3	4
85DCA0094	14565400	8042600	36	18	87	16	43	86	4.8	310	1.3	14
85DCA0095	14570300	8036000	26	16	66	13	34	61	3.2	340	1.5	11
85DCA0096	14569600	8025700	11	8	58	14	41	55	2.8	280	0.7	6
85DCA0097	14573500	8020000	47	12	65	17	45	66	3.5	370	0.6	9
85DCA0100	14573500	8029400	12	8	56	15	39	58	3.5	340	0.8	6
85DCA0101	14573600	8040200	22	11	60	13	37	62	3.6	210	0.6	6
85DCA0102	14562100	8047300	27	12	68	15	42	93	4.9	250	0.7	10
85DCA0103	14558100	8048000	53	25	90	16	53	68	4.2	380	0.6	13
85DCA0104	14551800	8047100	27	17	67	21	37	54	3.0	295	0.4	11
85DCA0105	14546500	8048900	27	19	60	9	26	40	2.0	350	1.1	6
85DCA0106	14539100	8053000	25	22	74	14	43	57	3.3	340	0.4	10
85DCA0107	14540200	8043300	32	24	87	13	36	56	2.6	350	0.8	12
85DCA0108	14547400	8042600	30	18	52	9	22	39	1.6	320	0.8	10
85DCA0109	14553700	8041500	136	15	67	18	42	69	4.0	320	0.2	12
85DCA0110	14583300	8051100	24	11	49	8	21	42	2.1	160	0.3	3
85DCA0112	14586500	8049500	172	8	124	35	118	170	7.4	675	0.3	6
85DCA0113	14588500	8045300	208	11	132	30	106	210	8.6	725	0.6	9
85DCA0114	14585500	8043100	35	16	65	12	38	50	2.3	380	1.3	6
85DCA0115	14581000	8042500	37	13	76	13	27	55	3.1	210	0.3	5
85DCA0116	14560900	8042600	14	8	54	14	42	86	4.2	310	0.8	5
85DCA0118	14556000	8035300	16	10	54	13	39	68	4.0	300	0.8	8
85DCA0119	14550200	8033000	44	17	74	12	41	58	3.6	280	1.	11
85DCA0120	14550500	8027000	34	18	96	14	49	56	3.5	350	0.6	7
85DCA0121	14559100	8025700	28	18	67	12	37	54	2.6	325	0.8	9
85DCA0122	14562800	8034200	18	14	56	10	36	49	2.6	315	0.7	5
85DCA0307	14539600	8185600	33	17	84	18	68	95	6.9	880	0.4	16
85DCA0308	14539600	8183100	51	43	104	18	63	65	5.2	715	0.4	16
85DCA0309	14537400	8182300	71	11	74	17	58	100	5.4	270	0.4	10
85DCA0317	14545300	8191500	38	25	95	13	36	54	3.2	300	0.8	13
85DCA0329	14546800	8192800	32	34	94	16	49	52	4.0	300	0.6	14
85DCA0338	14550400	8197000	34	22	90	13	36	56	5.0	620	1.3	19
85DCA0339	14543500	8180000	39	32	115	16	60	63	3.5	370	0.6	11
85DCA0340	14541500	8176700	72	24	84	15	44	70	4.8	365	0.8	20
85DCA0341	14542000	8173500	37	19	73	12	39	72	4.6	290	0.9	19
85DCA0342	14542700	8172000	23	8	63	17	52	96	3.9	285	0.5	4
85DCA0343	14548400	8166700	42	17	98	14	41	70	3.5	285	0.8	5
85DCA0344	14550000	8172000	42	18	74	10	36	60	4.2	280	0.7	18
85DCA0345	14549900	8172400	4	7	14	1	5	45	2.5	42	0.4	4
85DCA0346	14549100	8176600	34	16	82	10	34	70	4.8	240	1.1	14
85DCA0347	14547000	8180300	31	26	96	12	36	62	4.2	620	0.6	15
85DCA0348	14544900	8186600	43	28	140	17	55	84	6.4	725	0.6	15
85DCA0349	14547800	8188000	43	16	80	14	41	50	4.2	390	0.6	11
85DCA0350	14548600	8191100	25	19	65	11	32	34	3.6	580	0.5	12
85DCA0353	14556100	8194200	26	32	70	9	24	29	2.8	460	0.6	10
85DCA0354	14554500	8187700	29	39	90	9	30	45	3.3	310	0.4	10
85DCA0355	14552900	8184200	32	25	85	11	32	55	4.8	380	0.8	17
85DCA0358	14540600	8190300	74	29	140	17	50	78	5.9	520	0.9	16
85DCA0359	14541900	8193000	53	15	74	16	48	84	4.8	400	0.4	10
85DCA0360	14538900	8191200	64	10	58	18	59	130	4.0	250	0.4	7
85DCA0361	14538100	8194000	60	7	85	27	79	183	5.8	1100	0.4	3
85DCA0362	14541000	8196100	123	11	122	30	87	210	5.4	850	0.3	6
85DCA0365	14534000	8185500	89	9	70	22	61	135	5.7	360	0.4	4
85DCA0366	14532900	8187000	21	5	68	23	74	143	5.4	325	0.5	3
85DCA0369	14529000	8186000	14	7	50	17	52	88	4.0	280	0.8	5
85DCA0370	14525900	8186000	19	6	55	15	45	74	4.0	250	0.4	6
85DCA0374	14532500	8193000	58	5	58	23	79	118	5.8	440	0.4	3
85DCA0375	14549400	8181500	43	15	82	13	39	64	5.8	420	0.4	12
85DCA0380	14560000	8183500	44	31	78	9	35	34	3.4	320	1.3	36
85DCA0382	14538200	8183000	47	13	82	17	65	103	5.9	560	0.8	8
85DCA0384	14528200	8180200	20	7	70	18	61	100	4.6	200	0.6	5
85DCA0385	14529500	8174900	39	15	76	17	56	90	5.6	240	0.6	12
85DCA0387	14530500	8166800	33	10	65	13	43	65	5.3	360	0.7	14
85DCA0388	14539000	8169000	25	10	64	18	58	118	6.7	600	1.1	7

Appendix 2 (cont.)

Sample	East[1]	North	Cu[2]	Pb	Zn	Co	Ni	Cr	Fe	Mn	Ufl	As
85DCA0389	14537200	8176200	30	11	60	18	57	110	6.0	400	0.4	10
85DCA0393	14494000	8171800	44	18	106	24	77	128	5.3	500	0.8	5
85DCA0394	14492300	8174400	51	13	96	20	63	75	3.4	360	0.6	8
85DCA0395	14490500	8174600	45	14	105	15	61	70	4.6	320	0.7	10
85DCA0396	14485100	8169400	64	13	105	22	80	75	5.9	460	0.8	14
85DCA0397	14483500	8169400	54	23	198	19	67	75	6.0	380	0.8	14
85DCA0398	14479900	8169200	45	17	150	18	56	58	4.6	310	1.1	11
85DCA0399	14479900	8173500	46	14	145	19	64	68	5.0	320	1.3	10
85DCA0400	14480500	8177700	38	14	145	16	61	62	4.8	360	1.3	16
85DCA0401	14440100	8186000	37	18	155	20	58	64	5.6	380	1.1	20
85DCA0403	14485500	8164900	57	15	112	20	63	58	5.0	375	1.3	13
85DCA0404	14484100	8160200	26	19	115	13	43	50	4.6	320	1.	15
85DCA0406	14478100	8151000	39	21	160	15	50	68	5.0	300	0.7	15
85DCA0407	14476100	8148000	38	17	120	15	60	58	4.1	280	0.6	18
85DCA0408	14483800	8146500	46	25	115	17	66	74	5.4	410	0.6	32
85DCA0409	14484500	8153100	43	15	100	20	67	75	5.5	380	0.6	14
85DCA0411	14489600	8155200	60	25	100	22	69	85	6.8	540	0.7	15
85DCA0413	14490500	8144400	39	20	150	18	56	70	5.4	460	0.8	19
85DCA0414	14491300	8140600	46	17	96	21	69	66	5.3	415	0.8	20
85DCA0415	14497100	8142000	34	18	100	15	56	64	5.0	380	0.8	26
85DCA0416	14492800	8153900	45	17	98	20	80	92	5.0	400	0.6	8
85DCA0417	14497000	8167100	40	14	98	19	74	77	5.0	360	0.6	7
85DCA0418	14498500	8159700	43	16	87	22	71	84	5.3	420	0.7	12
85DCA0419	14502800	8156100	45	18	105	18	63	77	5.3	360	0.7	11
85DCA0420	14504900	8150300	43	17	95	18	61	79	5.1	340	0.4	10
85DCA0421	14500800	8139500	40	13	93	18	58	81	5.6	360	0.7	9
85DCA0422	14504800	8157800	47	18	86	19	66	78	5.2	460	0.7	10
85DCA0423	14504800	8162500	46	18	80	20	66	74	4.9	360	0.8	8
85DCA0427	14480000	8159500	151	25	230	21	76	70	4.7	310	0.8	14
85DCA0428	14474800	8158500	25	15	95	8	38	44	2.4	250	1.3	11
85DCA0429	14476100	8164000	16	7	70	13	59	70	4.0	240	0.4	6
85DCA0430	14479000	8165900	35	15	115	16	57	72	5.2	300	1.1	14
86DCA0003	14482800	7970000	16	13	55	8	29	39	1.3	300		
86DCA0004	14490400	7964600	24	17	384	13	50	100	2.5	300		
86DCA0005	14491700	7956700	22	16	68	9	33	71	1.6	260		
86DCA0006	14485400	7952200	20	21	87	15	45	64	1.9	240		
86DCA0007	14479000	7963100	22	19	55	7	26	48	1.4	270		
86DCA0014	14477800	7976100	22	13	73	8	30	2	1.6	270		
86DCA0015	14476100	7983000	23	14	83	10	35	61	2.4	280		
86DCA0016	14479900	7988200	23	16	94	15	49	68	3.2	320		
86DCA0017	14480100	7995500	23	16	79	11	34	73	1.9	240		
86DCA0018	14469600	7993500	17	14	60	8	25	53	1.4	200		
86DCA0019	14471800	7985000	23	17	85	13	40	63	3.1	510		
86DCA0020	14471900	7975600	20	29	79	11	37	50	2.6	410		
86DCA0021	14488500	7970700	17	19	69	6	26	40	2.0	260		
86DCA0022	14491200	7973700	13	12	41	6	17	26	1.0	220		
86DCA0023	14498000	7976400	31	17	90	8	31	56	2.5	200		
86DCA0024	14502000	7980000	21	20	64	7	23	38	2.3	250		
86DCA0025	14494500	7985300	16	17	52	7	24	30	1.8	240		
86DCA0026	14490300	7980500	14	9	42	6	19	22	0.8	210		
86DCA0027	14485600	7977200	20	17	82	10	31	50	3.0	260		
86DCA0028	14481600	7972800	22	26	136	10	40	37	2.6	290		
86DCA0033	14532600	7993200	14	9	43	6	22	42	0.9	230		
86DCA0034	14533000	7997200	14	14	38	6	19	41	0.9	220		
86DCA0035	14529300	8001000	13	13	41	7	23	46	0.9	210		
86DCA0036	14527500	8006000	18	17	63	10	31	63	1.3	420		
86DCA0037	14524600	8014000	11	9	34	4	14	27	0.7	180		
86DCA0038	14520000	8007400	13	10	37	6	15	23	0.8	220		
86DCA0039	14522000	7999300	15	13	49	6	21	30	1.0	260		
86DCA0040	14522800	7974300	12	11	34	7	18	21	0.7	210		
86DCA0041	14517200	7967000	15	13	51	5	19	30	0.9	210		
86DCA0043	14512600	7972200	14	12	42	6	20	23	0.9	210		
86DCA0058	14525300	8077000	22	12	68	15	44	48	2.7	300		
86DCA0059	14525600	8083500	26	12	57	13	33	66	2.1	460		
86DCA0060	14523900	8088000	19	10	53	9	28	35	1.9	240		
86DCA0062	14521000	8083600	35	14	79	14	51	81	3.7	460		

Sample	East[1]	North	Cu[2]	Pb	Zn	Co	Ni	Cr	Fe	Mn	Ufl	As
86DCA0063	14520400	8078700	22	12	66	11	30	37	2.1	340		
86DCA0064	14517000	8075000	26	13	66	13	39	43	2.7	360		
86DCA0065	14513500	8068100	25	14	84	15	43	62	3.2	640		
86DCA0066	14526500	8059500	14	12	73	6	25	40	1.6	300		
86DCA0067	14530700	8050300	21	10	77	12	34	60	2.7	300		
86DCA0068	14538100	8048000	14	14	48	7	22	39	1.5	280		
86DCA0069	14541500	8055800	35	18	73	11	39	64	3.1	300		
86DCA0070	14540500	8061700	37	12	58	13	37	68	3.3	400		
86DCA0071	14537500	8065400	45	17	95	11	44	72	3.0	280		
86DCA0072	14531800	8061500	18	16	51	8	21	44	1.6	380		
86DCA0073	14530800	8067000	33	26	62	12	41	105	3.3	320		
86DCA0074	14537000	8074100	38	51	95	15	62	106	4.0	410		
86DCA0075	14532200	8075200	37	12	75	22	58	111	4.6	420		
86DCA0076	14528500	8073600	23	16	63	12	39	66	2.4	300		
86DCA0077	14524400	8072800	18	15	57	12	34	61	2.2	510		
86DCA0078	14523500	8067900	29	15	58	12	34	86	2.7	460		
86DCA0079	14523500	8064200	23	18	64	9	28	63	2.3	300		
86DCA0082	14501700	8053500	15	11	44	5	15	32	0.9	330		
86DCA0083	14512000	8041200	19	12	55	8	28	45	1.2	280		
86DCA0084	14507200	8026300	12	11	39	5	15	37	0.9	240		
86DCA0085	14556100	7997100	14	14	51	6	19	36	1.4	300		
86DCA0086	14550600	7990500	13	13	50	7	20	33	1.1	320		
86DCA0087	14543700	7981100	19	12	65	11	36	38	1.5	320		
86DCA0088	14530000	7957500	19	15	57	8	23	36	1.6	260		
86DCA0089	14558000	7979800	15	9	56	8	22	39	1.4	380		
86DCA0090	14565400	7986700	42	15	93	16	44	52	2.3	450		
86DCA0091	14580500	7969500	22	14	90	11	41	71	2.0	200		
86DCA0092	14586000	7983400	25	19	67	9	32	67	1.9	310		
86DCA0093	14590500	8038100	37	16	78	14	43	85	3.0	500		
86DCA0094	14578500	8063300	34	9	77	15	44	80	2.8	480		
86DCA0095	14509500	8067400	15	14	53	8	18	54	1.3	340		
86DCA0096	14509500	8072100	25	19	73	8	29	75	2.3	320		
86DCA0112	14571700	8081500	17	7	51	12	41	116	3.8	820		
86DCA0113	14571900	8079400	61	15	64	15	40	88	3.8	460		
86DCA0114	14573500	8076000	16	7	43	8	24	63	2.3	150		
86DCA0115	14576000	8078100	44	12	61	14	39	86	3.5	480		
86DCA0116	14574500	8081200	17	7	45	11	21	48	2.1	280		
86DCA0117	14573400	8083600	81	17	72	15	37	70	3.3	360		
86DCA0118	14571400	8084300	19	8	41	11	25	92	2.9	460		
86DCA0119	14573400	8086400	82	15	71	12	40	54	2.9	240		
86DCA0120	14575300	8090000	118	19	168	21	99	176	5.0	700		
86DCA0412	13583200	8086800	23	17	118	8	29	24	1.5	210		
86DCA0416	13589400	8099900	19	19	74	9	37	55	2.4	360		
86DCA0419	13585500	8082800	14	17	50	6	24	40	1.8	260		
86DCA0420	13587800	8079200	27	29	368	7	32	52	1.6	260		
86DCA0426	13582900	8091800	13	13	31	5	17	26	1.1	200		
86DCA0430	13579500	8088100	16	14	50	5	19	39	1.8	230		
86DCA0433	14451100	8147000	29	15	139	11	58	50	2.5	350		
86DCA0435	14446800	8153600	21	9	89	8	38	31	1.1	250		
86DCA0441	14455300	8137500	25	13	100	9	40	50	2.8	345		
86DCA0442	14452900	8140500	29	14	101	8	40	48	2.5	300		
86DCA0443	14451000	8143900	32	11	170	9	62	52	2.4	300		
86DCA0444	14446900	8147700	17	8	83	8	45	52	2.2	280		
86DCA0445	14442200	8151000	21	12	84	10	51	59	2.1	340		
86DCA0447	14438200	8154500	18	9	49	5	23	22	1.0	180		
86DCA0448	14440400	8157200	11	10	30	3	16	20	0.9	130		
86DCA0449	14443100	8161100	27	10	89	10	46	48	1.9	340		
86DCA0450	14440800	8167000	23	13	101	8	48	34	1.3	280		
86DCA0456	14449800	8133500	19	17	94	10	38	50	2.5	320		
86DCA0458	14439400	8137000	23	13	100	14	39	52	3.2	370		
86DCA0459	14446600	8143600	20	13	91	11	44	54	2.5	320		
86DCA0460	14444200	8145000	16	7	84	9	46	42	1.4	260		
86DCA0461	14439700	8147100	23	10	95	8	53	40	1.4	260		
86DCA0462	14436000	8144600	18	10	66	8	39	25	0.9	200		
86DCA0463	14428900	8143700	27	15	105	9	40	40	2.1	280		

Appendix 2 (cont.)

Sample	East[1]	North	Cu[2]	Pb	Zn	Co	Ni	Cr	Fe	Mn	Ufl	As
86DCA0464	14459300	8143300	16	10	58	2	10	16	17.2	100		
86DCA0465	14463500	8136800	25	12	82	10	47	43	1.3	300		
86DCA0467	14464800	8132400	18	18	92	13	34	65	3.3	280		
86DCA0470	14456800	8147000	23	12	69	10	31	65	3.3	470		
86DCA0471	14456800	8151600	32	19	122	15	57	77	3.0	310		
86DCA0472	14454700	8153200	38	17	112	16	67	70	3.2	300		
86DCA0474	14485000	8129500	27	18	90	11	43	59	2.8	350		
86DCA0475	14488500	8126000	19	17	87	14	42	62	3.4	550		
86DCA0480	14489400	8118500	29	25	121	13	46	75	3.6	350		
86DCA0481	14489600	8122700	24	17	151	11	40	73	3.1	400		
86DCA0482	14480700	8117600	24	22	90	10	35	57	2.6	340		
86DCA0484	14480700	8113500	17	14	51	13	38	70	4.1	300		
86DCA0485	14481100	8110800	18	14	137	10	35	45	2.0	250		
86DCA0487	14481700	8107000	15	10	60	10	39	48	1.3	280		
86DCA0488	14484000	8102400	19	18	63	10	38	49	1.8	320		
86DCA0491	14481500	8129800	20	16	925	10	38	53	2.9	280		
86DCA0492	14479400	8130800	14	9	80	13	51	71	3.5	320		
86DCA0493	14479400	8130800	23	13	102	13	59	75	3.5	320		
86DCA0494	14476000	8129200	21	12	99	10	38	42	2.4	260		
86DCA0495	14471300	8126800	26	16	125	10	46	40	2.2	280		
86DCA0496	14466300	8128500	23	17	85	9	33	30	1.5	210		
86DCA0503	14475200	8126300	18	17	74	7	31	30	1.1	280		
86DCA0506	14478500	8120800	21	22	95	9	33	41	1.9	290		
86DCA0513	14467500	8120500	29	18	91	10	37	93	2.0	285		
86DCA0514	14491100	8125800	36	19	119	17	58	80	4.4	440		
86DCA0515	14492900	8121800	33	8	99	16	61	66	2.7	390		
86DCA0517	14496000	8126000	41	20	103	22	64	83	4.7	620		
86DCA0518	14497200	8129000	43	25	121	22	68	80	4.4	700		
86DCA0519	14497500	8130600	33	15	89	21	65	76	4.2	520		
86DCA0520	14497500	8133900	29	8	50	9	27	55	2.9	400		
86DCA0521	14495000	8129800	32	15	84	19	72	89	4.5	440		
86DCA0522	14492900	8130200	35	23	95	17	56	76	4.5	520		
86DCA0523	14490200	8131000	40	12	84	21	67	80	4.5	420		
86DCA0525	14490400	8111600	38	11	67	11	35	58	3.0	440		
86DCA0526	14491300	8115200	17	10	71	13	53	63	2.4	380		
86DCA0532	14563000	8105900	9	8	49	15	40	71	4.2	250		
86DCA0533	14566100	8104200	13	11	46	11	37	100	3.6	640		
86DCA0534	14568300	8104900	19	16	78	9	36	50	2.4	320		
86DCA0535	14570300	8106000	25	15	96	11	49	54	2.6	340		
86DCA0536	14572600	8102200	22	12	42	8	27	62	2.7	320		
86DCA0537	14569400	8100800	22	13	65	13	38	71	3.5	440		
86DCA0538	14567500	8101800	30	20	70	17	51	75	4.0	460		
86DCA0541	14564400	8108100	10	6	39	11	27	51	2.5	340		
86DCA0542	14566800	8110500	14	14	44	9	26	59	3.1	560		
86DCA0543	14569500	8109800	19	10	45	8	26	47	2.4	240		
86DCA0544	14569800	8111800	22	11	53	12	33	68	3.1	480		
86DCA0545	14567800	8112800	24	12	56	12	37	61	3.5	380		
86DCA0559	14570800	8115400	31	15	57	14	37	60	3.5	760		
86DCA0567	14572500	8114400	14	28	93	5	21	27	1.2	280		
86DCA0569	14570200	8109600	8	3	29	9	28	44	2.5	360		
86DCA0570	14575100	8110200	71	17	77	17	47	92	5.0	530		

[1]The first two digits give the UTM grid zone, the following six give the easting.
[2]All values are ppm except for iron, given in %.